

Sources, drivers and sedimentology of Icelandic dust events

By

Tom Mockford

A Doctoral thesis submitted in partial fulfilment of the requirements for
the award of Doctor of Philosophy of Loughborough University

December 2017

© by Tom Mockford (2017)

Abstract

There is increasing evidence for high magnitude dust storms in High latitude environments. Yet, aeolian processes in these areas have been largely understudied and therefore our knowledge of these systems is limited. Understanding dust emission processes from the high latitudes regions is of increasing importance because future climate scenarios indicate a reduction in terrestrial ice masses and an expansion in glacial outwash plains which are the main dust sources in high latitude environments. Of these regions, Iceland is the most researched high latitude dust source region, however our understanding of processes which lead to dust events are still poorly understood.

This thesis examines the interlinking relationship between dust source and dust particle sedimentology and the physical and meteorological drivers which promote or inhibit dust emission in Iceland. This is achieved through active aeolian monitoring at source during two monitoring periods at Markarfljot, South Iceland. These measurements are complimented using secondary data sources (e.g. meteorological and satellite data), sedimentological mapping and particle analysis and laboratory abrasion experiments.

This thesis is the first high resolution multi event record of dust emissions in the high latitudes and concludes by showing that potential dust concentrations and dust particle size are driven by the interlinking relationship between wind speed, sediment texture and surface moisture. Factors that affect the potential sediment availability for dust events are more important in the high latitudes than in the subtropics in driving spatial and temporal variabilities in dust emission.

Measurements presented in this thesis are required to verify and tune regional and global modelling attempts to quantify the potential contribution of high latitude dust in the Earth system. However, further measurements are required to fully understand seasonal changes in dust emissions, across a variety of dust source units within all high latitude dust source regions.

Acknowledgments

After four years in Loughborough completing this PhD, there are too many people to thank. Firstly, I would like to thank my supervisors Professor Joanna Bullard, Dr Dave Graham and Dr Rene Wackrow for their mentorship, guidance and support throughout this process. Professor Throstur Thorsteinsson (University of Iceland) also deserves special praise as without him, I would have never been able to conduct the two field seasons which underpin the results of this thesis.

I'd particularly like to thank Jo as she has allowed me to be at the forefront of the field of High Latitude Cold Climate dust research. The opportunity to travel all around the world and work with some of the most renowned scientists within our discipline has given me an opportunity that most PhD students do not get. I'd like thank Dr Kevin White and Dr Richard Hodgkins for examining this thesis; I hope you enjoy reading it as much as I have enjoyed writing it.

I would like to thank everybody in the Geography department who have made me a part of the Loughborough family for the past four years. I'd particularly like to thank Matt Baddock for his academic support and friendship; Mark Szegner, Richard Harland and Sue Clarke for their administrative support; Paul Wood for his everyday concern of my well-being and Kate Mathers, Clay Prater and Davide Vettori for dealing with my office antics over the past 6 months.

Loughborough Geography has one of the friendliest, funniest and most cohesive group of PhD students I have ever come across. Without the support of other PhD students, it can be a very lonely and difficult task completing a PhD. My special thanks go to Kate Mathers, Andreás Culora, Avi Baruch, Milly Bulcock, Chris Jones and Peny Sotiropoulou for keeping me on track and making every day at work memorable.

I wouldn't be where I am today without my family. When I told my parents that I was moving to Lubbock, Texas to conduct an MSc at Texas Tech focusing on dust storms, I could see how happy they were that I had found something that challenged me and made me happy. It has been five years since I returned from the USA, and I am so happy I can now share this work with you. Thank you for everything you have done for me; I dedicate this work to you and I hope it fills you with the utmost pride.

And finally, I would like to thank my fiancée Charlotte who has supported me greatly in the last 6 months to get me over the finish line. I look forward to finishing this chapter in my life and moving on to our next adventure together. Unfortunately, you will have to read it first!

Table of contents

Abstract	i
Acknowledgments	ii
Table of contents	iv
List of Tables	ix
List of Figures	xi
1. Dust emissions in the Earth system	1
1.0 Introduction	1
1.1 Dust, climate and Earth's environmental system	2
1.2 Focuses in aeolian research	5
1.3 High latitude dust emissions	6
1.3.1 Glacial-fluvial-aeolian system	7
1.3.2 Types of glacial system	9
1.3.3 Glacio-fluvial suspended sediment	10
1.3.4 Aeolian Processes	12
1.3.4.1 Transport Capacity	13
1.3.4.2 Sediment Availability	14
1.4 High Latitude Cold Climate dust source regions	17
1.4.1 Alaska.....	17
1.4.2 Greenland	22
1.4.3 Canada	25
1.4.4 Iceland	26
1.4.5 Patagonia.....	26
1.4.6 New Zealand.....	28
1.4.7 Antarctica.....	30
1.4.8 Eurasia.....	31
1.5 Summary.....	32
1.6 Thesis justification.....	33
2. The Icelandic dust cycle	36
2.1 Introduction	36
2.2 Background.....	36

2.3 Dust source geomorphology	38
2.4 Dust emission at the field scale.....	42
2.5 Dust event seasonality	45
2.6 Remote sensing observations.....	48
2.7 Modelling of Icelandic dust.....	51
2.8 The impact of dust deposition	53
2.9 Summary.....	56
3. Sedimentological characteristics of Icelandic dust sources	57
3.1 Introduction	57
3.2 Aims and Objectives	63
3.3 Methods	64
3.3.1 Study Site	64
3.3.2 Aerial mapping.....	65
3.3.3 Sediment sampling	68
3.3.4 Particle size distribution analysis	68
3.3.5 Scanning Electron Microscope	71
3.4 Results.....	73
3.4.1 Aerial mapping.....	73
3.4.2 Site 1 – Ephemeral Channel System	76
3.4.2.1 Particle sediment size.....	76
3.4.2.2 Particle characteristics.....	81
3.4.3 Site 2 - Relict Sandur system.....	84
3.4.3.1 Particle sediment size.....	84
3.4.3.2 Particle characteristics.....	86
3.5 Discussion.....	90
3.5.1. Aerial mapping of high latitude dust sources	90
3.5.2 Variations in particle characteristics.....	92
3.5.3 Variations in particle size	95
3.5.4 Can particle size indicate the mode of aeolian transport?	97
3.6 Conclusion	99
4. Icelandic dust event magnitudes, characteristics and pathways at the event-scale.....	101
4.1 Introduction	101
4.2 Dust storm classification	105

4.2.1 Transport-Capacity Limited.....	105
4.2.2 Sediment-Availability Limited	107
4.2.3 Sediment-Supply (un)Limited.....	107
4.2.4 Wind speed PM ₁₀ relationship	108
4.3 Aims and Objectives	109
4.4 Methods	110
4.4.1 Field measurements	110
4.4.2 Meteorological data	111
4.4.3 WMO meteorological weather codes	112
4.4.4 HYSPLIT air parcel trajectory modelling	112
4.4.5 CALIPSO	114
4.5 Results	115
4.5.1 Section 1 – Field measurements of dust events	115
4.5.1.1 Frequency and Magnitude.....	115
4.5.1.2 Event classification	116
4.5.1.3 Selected examples of each event type	120
4.5.1.3.1 Transport capacity limited events	120
4.5.1.3.2 Sediment availability limited events.....	122
4.5.2 Section 2 – Secondary data sources for measured dust events	125
4.5.2.1 Dust Transport Pathways	125
4.5.2.2 Dust transport to Reykjavik.....	126
4.5.2.3 Meteorological dust codes.....	128
4.5.2.4 MODIS/AOD/CALIPSO	128
4.5.3: Section 3 – Expanded secondary dust measurements.....	128
4.5.3.1 Transport pathways	128
4.5.3.2 MODIS/AOD/CALIPSO	133
4.6 Discussion.....	133
4.6.1 Dust storm characteristics.....	133
4.6.2 Temporal controls of dust events.....	137
4.6.3 Conceptual framework for event scale variations in dust emissions	141
4.6.4 Transport pathways and heights.....	143
4.6.5 Use of satellite remote sensing in the high latitudes	146
4.6.6 Use of meteorological weather codes for defining dust events	147

4.7 Conclusions	148
5. The role of aeolian abrasion in creating dust sized sediments for high latitude dust events.....	150
5.1 Introduction	150
5.2 The process of aeolian abrasion	152
5.3 Dust particle creation in high latitude environments	155
5.4 Aim and Objectives	157
5.5 Methods	157
5.5.1 Parent sediments	157
5.5.2 Abrasion Chamber	159
5.5.3 Particle Size Distribution	162
5.5.4 Temperature/Humidity	163
5.6 Results	164
5.6.1 Total dust production as a function of soil texture	164
5.6.2 Total dust production as a function of temperature and humidity	166
5.6.3 Impact on parent sediments.....	170
5.6.3.1 Markarfljotsandur.....	170
5.6.3.2 Markarfljot ephemeral channel system	172
5.6.3.3 Mýrdalssandur	172
5.6.4 Dust particle size distributions	175
5.6.4.1 Markarfljotsandur.....	175
5.6.3.2 Markarfljot ephemeral channel system	177
5.6.3.3 Mýrdalssandur	179
5.7 Discussion.....	181
5.7.1 The impact of sediment texture on total dust production and aeolian abrasion.....	181
5.7.2 The impact of temperature and humidity on total dust production and aeolian abrasion	185
5.7.3 A comparison of total dust production.....	188
5.8 Conclusion	190
6. Summary, future research and concluding remarks	192
6.1 Field measurements of dust events in the high latitudes	192
6.2 The creation of ultra-fine sediments at source	195

6.3 The relationship between soil texture, soil moisture and wind speed in driving dust emissions in Iceland.....	197
6.4 The impact of temperature on dust production.....	200
6.5 High latitude dust in a warming earth?	200
6.6 Concluding remarks	201
References.....	203

List of Tables

Table 1.1: The dominant characteristics of High latitude dust sources (Bullard et al., 2016).....	18
Table 2.1: Different Icelandic dust source units and their total area (km ²) based on the severity index proposed by Arnalds (2001)	40
Table 2.2: World Meteorological Organisation (WMO) weather codes relating to dust events. Codes are assigned every 3 hours in manned WMO weather stations	45
Table 3.1: Preferential Dust Source Classification from Bullard et al. (2011)	59
Table 3.2: Classification accuracy (Figure 3.8) produced from a confusion Matrix (using 100 random points).....	75
Table 3.3: Mean and skewness statistics of SEDIMETRICS surveys from Figure 3.12	80
Table 3.4: Dominant sediment size (from particle laser sizer) and characteristics (from SEM micrographs) for the ephemeral channel system and the relict sandur system.....	93
Table 4.1: Dust storm characteristics for 9 dust events at the Markarfljot relict sandur. Bold represents values used for population of Figure 4	117
Table 4.2: Horizontal mass flux (kg m ⁻¹ day ⁻¹) and maximum dust concentration (µg m ⁻³) comparison with other field calculated aeolian transport rates from subtropical and high latitude dust sources.....	135
Table 5.1: Experiment sediment source locations and PDS classification (Bullard et al., 2011)	158
Table 5.2: Summary of average total dust produced in 8 hours (g), total dust as a % of the initial sample weight, % of dust produced in first 1 hour and % of dust produced in first 2 hours for all samples at 26 - 29°C (W) and 8 - 12°C (C)	164
Table 5.3: Summary of combined average temperature (°C) and average relative humidity (%) during abrasion experiments in warm (W) and cold (C) conditions ...	166

Table 5.4: Differences in total dust production from warm and cold abrasion runs from all sediment types. Statistically significant P-values are displayed in red ($P < 0.05$)	169
Table 5.5: Particle size fraction breakdown of surface sediments from Markarfljotsandur before and after abrasion experiments	171
Table 5.6: Particle size fraction breakdown of surface sediments from Markarfljot Ephemeral Channel System before and after abrasion experiments	173
Table 5.7: Particle size fraction breakdown of surface sediments from M Mýrdalssandur before and after abrasion experiments	174
Table 5.8: Particle size fraction breakdown (%) of created dust particles from the Markarfljotsandur sediments for all time periods	176
Table 5.9: Particle size fraction breakdown of created dust particles from the Markarfljot ephemeral channel system sediments for all time periods	178
Table 5.10: Particle size fraction breakdown of created dust particles from the Mýrdalssandur sediments for all time periods	180

List of Figures

Figure 1.1: The global dust cycle in the Earth system (adapted from Shao et al., 2011).....	4
Figure 1.2: The interlinking glacial, fluvial, lacustrine and aeolian sediment linkages. The model was specifically designed for understanding the nature of high latitude dust events (Bullard, 2013)	8
Figure 1.3: Jökulhlaup and non-Jökulhlaup samples from Southern Iceland (1964-1998) (Old et al., 2005). (right) Dust record recorded at Storhöfði	11
Figure 1.4: (top) Average monthly wind speed for 1984 and 1985. Bars show average wind speed and standard deviation for all days; X indicates average wind speed for dust events only. (bottom) Total dust event days per month for 1984 and 1985 (Bullard and Mockford, 2018).	12
Figure 1.5: Observations of high-latitude dust storm frequency based on visibility data (circles) and peer-reviewed publications (triangles). Areas where the precipitation: potential evapotranspiration ratio <0.65 (aridity index) (United Nations Environment Programme,1997) and subtropical dust emission zones are included for reference (Bullard et al., 2016).....	19
Figure 1.6: MODIS Terra/Aqua Level 1b of Alaskan dust plumes from Copper River (November 2017)	21
Figure 1.7: Dust storm at Copper River, Alaska. Photo courtesy of Santiago Gassó	22
Figure 1.8: Seasonal variation in dust observations and meteorological factors from Kangerlussuaq, West Greenland (Bullard and Mockford, 2018).	23
Figure 1.9: HYSPLIT air parcel trajectory model outputs indicating potential dust transport pathways for associated dust days from Kangerlussuaq West, Greenland (Bullard and Mockford, 2018).	24
Figure 1.10: Dust storm at Slims Valley, Yukon. Photo courtesy of James King	25
Figure 1.11: MODIS Terra Level 1b (19/11/16) image of a Patagonian dust storm..	28

Figure 1.12: Potential dust deposition locations from New Zealand (pink) from 5-day HYSPLIT air parcel trajectory model outputs (Bullard et al., 2016; adapted from Neff and Bertler, 2015).....	29
Figure 2.1: a) Icelandic dust source map based on Arnalds (2001) aeolian susceptibility index (Table 2.1). Major dust source units labelled in bold. Major glacial systems labelled in italics. Met stations used for Figure 2.5 labelled with triangles. b) Landsat 8 Thematic Mapper mosaic of Iceland showing dominant land cover types. Blue areas indicate ice/snow (Arnalds, 2001; Baddock et al., 2017)	37
Figure 2.2: Dust event at a sandy field in Iceland (June 2015).....	39
Figure 2.3: The Markarfljot ephemeral channel system, June 2014. Image acquired from a UAV survey flown at 100m altitude. As river stage in the main channel increases, floodwater enters the outer sections of the floodplain	41
Figure 2.4: The Markarfljot ephemeral channel system, May 2014. Large areas of silt are left unarmoured and unvegetated after river water has retreated.	43
Figure 2.5: Seasonal dust day record for Storhöfði (South Iceland) and Grímsstaðir (North Iceland) based on a 20-year WMO meteorological data set (Bullard et al. 2016).....	46
Figure 2.6: 6-year daily dust concentration ($\mu\text{g m}^3$) from Heimaey, Iceland (Prospero et al., 2012). The sensor was placed in a well-defined dust transport pathway (Arnalds, 2014; Baddock et al. 2017)	47
Figure 2.7: Top: Landsat 8 RGB image from South Iceland (17/09/2013). A) Dust storm at Landeyjsandur/Markarfljotsandur B) Dust storm at Mýrdalssandur. Figure courtesy of Matt Baddock.....	50
Figure 2.8: Seasonal variation in trajectory line density for 72-hour HYSPLIT air parcel trajectory model outputs started at 100 m height originating from Vatnsskarðshólar on days of observed dust 1992–2012. Input data is the 2.5 ° NCEP/NCAR Reanalysis data (Baddock et al., 2017).....	52
Figure 3.1: Landsat 8 image (19/09/2013) from Markarfljot, South Iceland. The two identified dust source regions are marked with triangles. Dust can be seen being entrained from both source regions. The ice cap is Eyjafjallajökull	64
Figure 3.2: Loughborough University Delta Fixed Wing Unmanned Aerial Vehicle..	66

Figure 3.3: Sampling strategy for UAV, sediment sampling and aeolian monitoring at the Ephemeral Channel system and the Relict Sandur system.....	67
Figure 3.4: Monitoring wind erosion using BSNE Traps on the relict sandur system at Markarfljot (June 2015)	69
Figure 3.5: Conceptual diagram for SEDIMETRICS surveys at the ephemeral channel system	70
Figure 3.6: Automated sediment sizing using technique described in Graham et al., (2005a, 2005b).....	71
Figure 3.7: UAV Orthophoto of the ephemeral channel system in May 2014. The orthophoto was generated using Agisoft Photoscan.	73
Figure 3.8: Supervised Classification of orthophoto from Figure 3.7 using texture analysis in ArcGIS	74
Figure 3.9: Segment of a) orthophoto and b) supervised classification indicating areas of misclassification in Figure 3.8.....	75
Figure 3.10: Digital Elevation Model of the ephemeral channel system created using UAV images in Agisoft Photoscan. Arrows represent the location of the ground control points and the proportional errors of height measurements in comparison to known heights at the surface. Blue represents low elevations	76
Figure 3.11: Particle Size Distribution of 3 dust events from the ephemeral channel system (2014). The size distributions of surface sediments from the lag deposit (i.e. gravel bars) and Ephemeral channel (i.e. unarmoured silt drapes) are drawn for comparison.....	77
Figure 3.12: SEDIMETRICS particle size distributions for all sites at the ephemeral channel system (all) and singular sites with decreasing distance to the main river channel (a-g)	79
Figure 3.13: Markarfljot ephemeral channel system in June 2015. Channel inundation across the floodplain inhibited potential dust emission during this period	80
Figure 3.14: SEM Micrographs showing source sediments from the ephemeral channel system at Markarfljot (a-d). e is the geochemical fingerprint.....	82

Figure 3.15: SEM Micrographs showing airborne dust sediments caught in suspension from the ephemeral channel system at Markarfljot (a-d). e is the geochemical fingerprint	83
Figure 3.16: Particle size distribution of 5 dust events from relict sandur system (2015) at 0.3, 0.6, 1.4 and 2.4m. Surface sediments are overlaid for comparison. ..	85
Figure 3.17: SEM Micrographs showing surface sediments from the relict sandur system at Markarfljot (a-d). e is the geochemical fingerprint	87
Figure 3.18: SEM Micrographs showing airborne sediments in saltation (0.3m and 0.6m BSNE traps) from the relict sandur system at Markarfljot (a-d). e is the geochemical fingerprint	88
Figure 3.19: SEM Micrographs showing airborne dust sediments caught in suspension (1.4 and 2.4 m BSNE traps) from the relict sandur system at Markarfljot (a-d). e is the geochemical fingerprint	89
Figure 4.1: Conceptual model for event-scale dust emissions: a) Transport-Capacity Limited (TCL), b) Sediment-Availability Limited (SAL), c) Sediment-Supply Limited (SSL), d) Wind speed-PM10 relationship. T0-T1 is the potential saltation lag impact for aeolian activity. BF is the best-fit mathematical function for the wind speed-PM10 relationship. 95L and 95H are the 95% confidence bounds of BF	106
Figure 4.2: Field equipment set-up, Markarfljot, May/June 2015. DustTrak DRX, BSNE traps, cup anemometers	110
Figure 4.3: Relationship between dust event average PM10 ($\mu\text{g m}^{-3}$) and horizontal mass flux for 9 dust events at Markarfljot	115
Figure 4.4: a) 5-minute averaged wind speed and PM10 relationship for 3 TCL events b) 10 second average wind speed and PM10 relationships for same events (including 95% confidence intervals)	116
Figure 4.5: Wind speed PM10 relationships for events listed in Table 1. Black dots represent points inside the mathematical relationship from Fig.2b, whereas red and blue dots represent points outside	119
Figure 4.6: Event 8, 27th June 2015, a) Surface wind speed b) wind direction c) PM10 concentration	120

Figure 4.7: Event 3, 02nd June 2015, a) Surface wind speed b) PM10 concentration	121
Figure 4.8: Event 5, 15th June 2015, a) Surface wind speed b) wind direction c) PM10 concentration	123
Figure 4.9: Event 1, 30th May 2015, a) Surface wind speed b) wind direction c) PM10 concentration. Black arrows indicate periods of low intensity rainfall (<0.2mm)	124
Figure 4.10: 72hr HYSPLIT forward trajectories for 9 dust events recorded at Markarfljot	125
Figure 4.11: Reykjavik aerosol monitoring stations (GRE, FHG) on 15th June 2015. a) PM10 concentration b) 15-min average wind speed c) 15-min averaged wind direction. Figure courtesy of Throstur Thorsteinsson	126
Figure 4.12: NOAA HYSPLIT Dispersion model 2 hourly plume model for Markarfljot on 15/06/15 (Event 5). Reykjavik is located with star	127
Figure 4.13: Seasonal dust day record for Storhöfði (South Iceland) from northerly wind directions from 2010 - 2015	129
Figure 4.14: Trajectory line density (% of trajectories per 1°x1° cell) for 72h forward HYSPLIT simulations at a 100m start height for all northerly wind direction days from Markarfljot where a dust observation was recorded at Storhöfði (1995-2015)	130
Figure 4.15: Trajectory line density (% of trajectories per 1°x1° cell) for 72h forward HYSPLIT simulations at a 100m start height for all northerly wind direction days from Markarfljot where a dust observation was recorded at Storhöfði (2010-2015) split by season.....	131
Figure 4.16: Trajectory point density (% of trajectories per 1°x1° cell) for 72h forward HYSPLIT simulations at a 100m start height for all northerly wind direction days from Markarfljot where a dust observation was recorded at Storhöfði (2010-2015) split by altitude.....	132
Figure 4.17: Dust event from South Iceland on 17/09/13 identified by a) MODIS 250km level terra 1b data (at 12:50) b) terra level 1b aerosol optical depth c) CALIOP 532nm total attenuated backscatter (at 14:12) d) corresponding CALIOP vertical feature mask. Dotted line in a and b is CALIOP transect	134

Figure 4.18: Markarfljot sandur after a) 1 hour of dust emissions and b) 14+ hour of dust emissions during event 5 (15/06/15). Spacing between ripples is approximately a) 10-20cm b) 50cm-1m	139
Figure 4.19: PM10 concentration ($\mu\text{g m}^{-3}$) and hourly relative humidity (%) at Markarfljot during event 5 (15/06/15).....	139
Figure 4.20: Wind direction ($^{\circ}$) and wind speed (m s^{-1}) at Markarfljot Automated weather station between 01/05/15 – 30/06/15.....	144
Figure 5.1: Conceptual diagram indicating mechanisms which lead to the creation of silt and clay sized particles from sands travelling in aeolian transport (Wright, 1988)	153
Figure 5.2: Parent soil material particle size distribution for the three sediment groups used in the abrasion chamber experiments.....	159
Figure 5.3: Laboratory set up of aeolian abrasion chamber (Bullard et al., 2004) ..	160
Figure 5.4: Total dust % produced as a function of initial sample weight during 8-hour abrasion experiments at 26 - 29 $^{\circ}\text{C}$ with error bar	165
Figure 5.5: Total dust % produced as a function of initial sample weight during 8-hour abrasion experiments at 26 - 29 $^{\circ}\text{C}$ (solid line) and 8-12 $^{\circ}\text{C}$ for all sediments (dashed lines).....	167
Figure 5.6: Particle size distribution of surface sediments from Markarfljotsandur: Surface sediments (0hr) (black), 8-hour abraded sediments in warm conditions (26 – 29 $^{\circ}\text{C}$) and 8-hour abraded sediments in cold conditions (8 - 12 $^{\circ}\text{C}$).....	171
Figure 5.7: Particle size distribution of surface sediments from Markarfljot ephemeral channel system: Surface sediments (0hr) (black), 8-hour abraded sediments in warm conditions (26 – 29 $^{\circ}\text{C}$) and 8-hour abraded sediments in cold conditions (8 - 12 $^{\circ}\text{C}$).	173
Figure 5.8: Particle size distribution of surface sediments from Mýrdalssandur: Surface sediments (0hr) (black), 8-hour abraded sediments in warm conditions (26 – 29 $^{\circ}\text{C}$) and 8-hour abraded sediments in cold conditions (8 - 12 $^{\circ}\text{C}$).....	174

Figure 5.9: Particle size distribution of created dust particles from Markarfljotsandur sediments for 1,2,4 and 8hrs of abrasion at warm (dashed) and cold temperatures 176

Figure 5.10: Particle size distribution of created dust particles from the Markarfljot ephemeral channel system sediments for 1,2,4 and 8hrs of abrasion at warm (dashed) and cold temperatures (solid)..... 178

Figure 5.11: Particle size distribution of created dust particles from the Mýrdalssandur sediments for 1,2,4 and 8hrs of abrasion at warm (dashed) and cold temperatures (solid) 180

Figure 5.12: Total dust concentration from an aeolian abrasion chamber comparison between three Icelandic sediment types (this thesis) and other sediment types from the literature (Smith et al., 1991; Bullard et al., 2004) 189

Figure 6.1: The underlying importance of continuous source measurements for high latitude dust research 195

Figure 6.2: The interlinking relationship between wind speed, moisture and soil texture and how it impacts on dust emissions from the high latitudes 198

1. Dust emissions in the Earth system

1.0 Introduction

Dust emissions have long been associated with the hot desert regions within the subtropics (Prospero et al., 2002; Washington et al., 2003). Research focused on dust emissions from the high latitudes has increased in the past decade as it has become recognised as an important part of the global dust cycle (Prospero et al., 2012; Bullard, 2013; Arnalds et al., 2016; Bullard et al., 2016; Bullard, 2017). However, due to sparse measurements, our understanding of the processes which drive high latitude dust events is limited (McKenna Neuman, 1993; 2003). There is a need for active measurements of high latitude dust events to verify and tune regional and global dust models (e.g. Groot Zwaaftink et al., 2017).

The main aim of this thesis is:

To assess sources, drivers and sedimentology of Icelandic dust events

This will be achieved by answering the following three research questions:

- 1) To compare the sedimentological characteristics of two Icelandic dust sources and assess the impact these sediments have on dust particle characteristics
- 2) To determine the dominant drivers and characteristics of Icelandic dust events through field and secondary meteorological data
- 3) To examine the susceptibility of three different Icelandic dust source sediments to aeolian abrasion

The specific objectives of each of these aims will be presented at the end of Chapter 1. The aim of Chapter 1 is to set out the role of dust in the Earths system and our current understanding of dust emissions in the high latitudes.

1.1 Dust, climate and Earth's environmental system

Mineral aerosols (termed dust) are soil particles suspended in the air by wind. Wind erosion processes detach particles from the surface and eject them into the atmosphere (McTainsh and Strong, 2007). Dependent on soil surface characteristics, dust particles can be transported either locally or over significant distances (Prospero, 1999). Current estimates for global emission rates vary from $1060 \pm 194 \text{ Tg yr}^{-1}$ (Werner et al. 2002) to 3321 Tg yr^{-1} (Takemura et al., 2000), with the amount of material in the atmosphere at any one time ranging from 8 Tg yr^{-1} to 35.9 Tg yr^{-1} (Ginoux et al. 2001; Miller et al. 2004; Zender et al. 2004; Tegen et al. 2004). It is also expected that these values will continue to increase due to global climate warming (IPCC, 2007) as new areas become prone to wind erosion due to desertification and changes in atmospheric weather patterns (Woodward et al., 2005; Romm, 2011). McConnell et al. (2007) found that aluminosilicate dust deposition more than doubled through the 20th century from ice core data from the Antarctic Peninsula. This was associated with a $+1^\circ\text{C}$ temperature increase in the Southern Hemisphere, decreasing relative humidity and increasing levels of desertification in Patagonia and Argentina.

This potential increase in emissions teamed with a recognition of the importance of dust particles in the land-atmosphere-ocean system has caused an increased interest in dust emissions in recent years (e.g. Stout et al., 2009; Okin et al. 2011; Ravi et al., 2011; Bryant, 2013). Dust emissions occur at a variety of spatial scales (Ravi et al. 2011). Locally, this will be the re-distribution of soil particles (e.g. between agricultural fields: Goosens et al. 2001; Sharratt et al., 2007). On a regional and global scale, particles may travel within the upper atmosphere for several days, travelling thousands of kilometres across continents and oceans (Prospero et al. 2002; Washington et al. 2003; Okin et al, 2011; Ravi et al. 2011; Shao et al., 2011).

The emission, transport, transformation and deposition of dust particles and how they impact atmospheric, oceanic and terrestrial processes is usefully summarised by Shao et al., (2011) (Figure 1.1). During emission, dust is ejected at the micro scale due to spatial and temporal variations in wind speed and turbulence in environments where suitable sediment is available for transport (Mahowald et al., 1999; Zender and Kwon, 2005; Bullard et al., 2008). The supply and availability of these sediments will be influenced by the spatial and temporal variation in vegetation cover (Tegen et al., 2002;

Engelstaedter et al., 2003; Cowie et al., 2013), surface soil moisture content (Fécan et al., 1998; Ishizkua et al., 2008; Ravi et al., 2006; Mockford et al., 2018), surface lag deposits (Sutton and McKenna Neuman, 2008) and surface soil crusts (Cahill et al., 1996; Belnap and Gillette, 1997; 1998; Houser and Nickling, 2001; Reynolds et al., 2007; Sweeney et al., 2008). Temporally, these factors will vary from the hertz scale to the geological time scale (Kocurek, 1998; Kocurek and Lancaster, 1999). Once material has been emitted, it is transported initially by local turbulent wind systems. If not deposited locally, particles can be transported into the upper atmosphere and transported via synoptic and global circulation systems (Shao et al., 2011). During transport, material is transformed as it reacts with other atmospheric pollutants (DeMott et al., 2003; Dall'Osto et al., 2010; Pandolfi et al., 2014) and thus has a significant impact on the atmospheric radiation budget via the direct scattering and absorption of incoming and outgoing solar radiation (Tegen, 2003; Satheesh and Moorthy, 2005; Prospero et al. 2012). The impact of this will be dependent on the mineral optical properties of the particles (e.g. particle shape; Kalashnikova and Sokolik, 2002; Shao et al., 2011), the vertical distribution of dust within the boundary layer (DeMott et al., 2003) and the albedo of the surface layer (Sokolik and Toon, 1996; Tegen et al., 1996).

Deposition of dust particles provide a major source of particulates to global biomes which have a significant effect in forcing earth system processes (Ravi et al., 2006). This is because dust does not just include a mineralogical component but also includes the transportation of organic material which is rich in N, P, C, Fe, bacteria etc. (Herut et al., 2002; Okin et al. 2004). For example, dust from the Sahara, the world's biggest contributor to the global dust budget, has been shown to be the main supplier of Fe and P to the Amazon rainforest (Prospero, 1996; Prospero et al., 1996; Bristow et al., 2010). This has been shown to increase primary productivity in the Amazon as well as in the North Atlantic (Bristow et al., 2010). Dust deposition plays a fundamental role in oceanic biogeochemical cycles (Mahowald et al. 2005), and it is generally recognised that dust particles are the largest input of iron into oceanic ecosystems (Jickells et al. 2005). This iron can be utilised in the growth of algae, and in turn, phytoplankton. An increased dust loading into oceanic ecosystems has therefore been linked with increased carbon dioxide sequestration (Mahowald et al. 2005; Propsero et al. 2012).

Dust particles transported into urban areas have been shown to create serious public health issues (Griffin and Kellogg, 2004). This is due to dust storms carrying sizeable levels of bacteria, fungi and virus particles (Griffin and Kellogg, 2004). These effects are concentrated around large cities. Some places suggested to be severely affected include: Iceland (Gudmundsson, 2011); China (Meng and Lu, 2007) and the Caribbean (Prospero and Lamb, 2003). A single major dust storm that impacted the major cities of eastern Australia in 2009 is estimated to have an economic cost of at least A\$299 million, which included clean-up costs, medical treatments and days lost from work due to dust induced health problems (Tozer and Leys, 2013).

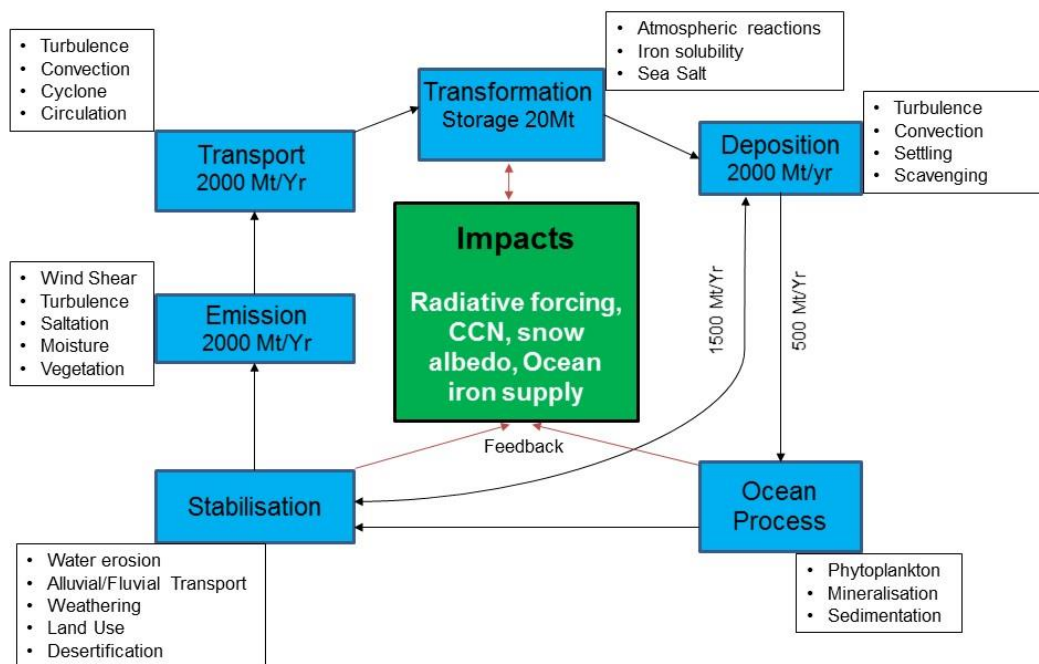


Figure 1.1: The global dust cycle in the Earth system (adapted from Shao et al., 2011)

1.2 Focuses in aeolian research

Much of the literature cited already has been related to dust storms that originate from sub-tropical dryland environments (warm deserts). The majority of research on aeolian processes has occurred in these environments. The reason for this is simple: the largest known dust sources in the world are in hot arid desert environments. Some of the largest areas include the Bodélé depression, North Africa (Washington et al. 2006; Todd et al. 2008); the Lake Eyre Basin, Australia (Bullard et al. 2008; Baddock et al. 2009) and the Taklamakan desert, China (Iwasaka et al. 1983; Xuan et al. 2004).

However, sources located outside the sub-tropical dust belt also contribute to the total atmospheric dust load. These sources are found in high-latitude environments (e.g. McKenna Neuman, 2003; Prospero et al. 2012; Bullard, 2013). These areas have often previously been glaciated but are now predominately ice free (Bullard, 2013). However, the processes which govern dust events are currently poorly understood (Bullard et al., 2016). There are several reasons why dust emission research has focused on the sub-tropical dust belt:

1. Hot desert dust sources are much larger contributors to the total atmospheric dust load than high latitude, cold climate dust sources (Prospero et al., 2012; Bullard et al., 2016)
2. In the high latitudes, low population densities lead to sparse levels of observation. Many hot desert regions also have low population densities; however, many more highly populated areas are within prominent dust transport pathways (e.g. West Africa). In the high latitudes, it is possible that dust is transported preferentially over oceanic environments and therefore the ability to observe these events are further limited.
3. Major advances in our understanding of the dust cycle in the subtropics have been made since an increase in the availability of satellite sensors which can detect dust. In high latitudes, the use of these sensors is often confounded because of persistent cloud cover, winter darkness and the inability of current remote sensing techniques to distinguish dust from the surface (e.g. brightness temperature; Ackerman et al., 1997).

Although dust sourced from the high latitudes has been relatively under researched it has been suggested that the relative contribution of high latitude dust to the total

atmospheric dust budget may increase under contemporary climate conditions due to influence warming might have on retreating glaciers/ice caps (Cannone et al. 2008; Thorsteinsson et al., 2012). Retreating ice will likely provide greater volumes of sediment to deposited in terrestrial landscapes which in the short term (e.g. 50 – 100 years) could increase total dust fluxes once this material has been made available for aeolian transport (Bullard et al. 2013). In the longer term, it is unclear how glacial retreat will impact dust emission as drastic changes in surface sedimentology, changes in localised wind patterns and the revegetation of previously glaciated landscapes may in turn decrease the likelihood that particles could be entrained in the aeolian system.

It has been reported that dust storms in high latitude environments can be some of the most intense events in the world (Arnalds, 2010; Arnalds et al., 2016). Arnalds (2010) reported dust emissions from a single dust event in Iceland to be 5000 g m^{-2} . This is comparable to rates recorded at the Bodélé depression, which is known to be one of the dustiest places in the world (Warren et al. 2007). However, this statement and value is somewhat misleading as the total dust mass is also related to the size of the source region.

The study of dust events in the high latitudes is somewhat in its infancy and because of this, researchers have not yet been able to establish a clear understanding of the basic principles of aeolian processes within these environments. The following sections will introduce sources and processes which lead to dust emissions at the high latitudes.

1.3 High latitude dust emissions

High latitude dust sources are defined in this thesis as dust sources which are located $\geq 50^\circ\text{N}$ and $\geq 40^\circ\text{S}$ (Bullard et al., 2016). The difference in latitude between hemispheres is due to the low density of land masses in the southern hemisphere (Bullard et al., 2016). These sources vary from hyper-arid environments to super humid environments (Bullard, 2013). Bullard et al. (2016) identified 9 high latitude dust source areas, which include: Iceland (e.g. Arnalds et al. 2012, 2013; Dagsson-Waldhauserova et al. 2013, 2014; Prospero et al. 2012; Groot Zwaaftink et al., 2017; Wittman et al., 2017); Greenland (e.g. Bullard and Austin, 2011, Anderson et al., 2017; Bullard and Mockford, 2018); Alaska (Crusius et al. 2011); Canada (Nickling, 1978),

Eurasia (Bullard et al., 2016); Patagonia (Gasso and Stein, 2007; Gaiero et al., 2007; Gasso et al., 2010); New Zealand (e.g. McGowan et al. 1996) and Antarctica (Atkins and Dunbar, 2009; Bhattachan et al., 2015). The total contribution of dust sourced from the high latitudes is approximately 5% of the total atmospheric dust budget (Bullard et al., 2016), with approximately 3% of this being sourced from sources >60°N (Groot Zwaaftink et al., 2016). Although this is relatively small in comparison to the total contribution from the sub-tropics, this contribution is comparable to that from Australia or Southern Africa (Prospero et al., 2002; Ginoux et al., 2012).

1.3.1 Glacial-fluvial-aeolian system

As summarised by Bullard (2013), Figure 1.2 shows the interlinking relationships between the glacial, fluvial, aeolian and lacustrine systems within a high latitude environment. It was identified that the principal factor controlling aeolian activity in the high latitudes is the sorting/abundance of fine sediment (Bullard, 2013; Bullard et al., 2016). These sediments often have a glacial origin (Bullard et al., 2016) and the amount of material available is dependent on the sedimentological makeup of the subglacial substrate (Bullard et al., 2013) and the ability of ice to transport sediment (Boulton, 1996).

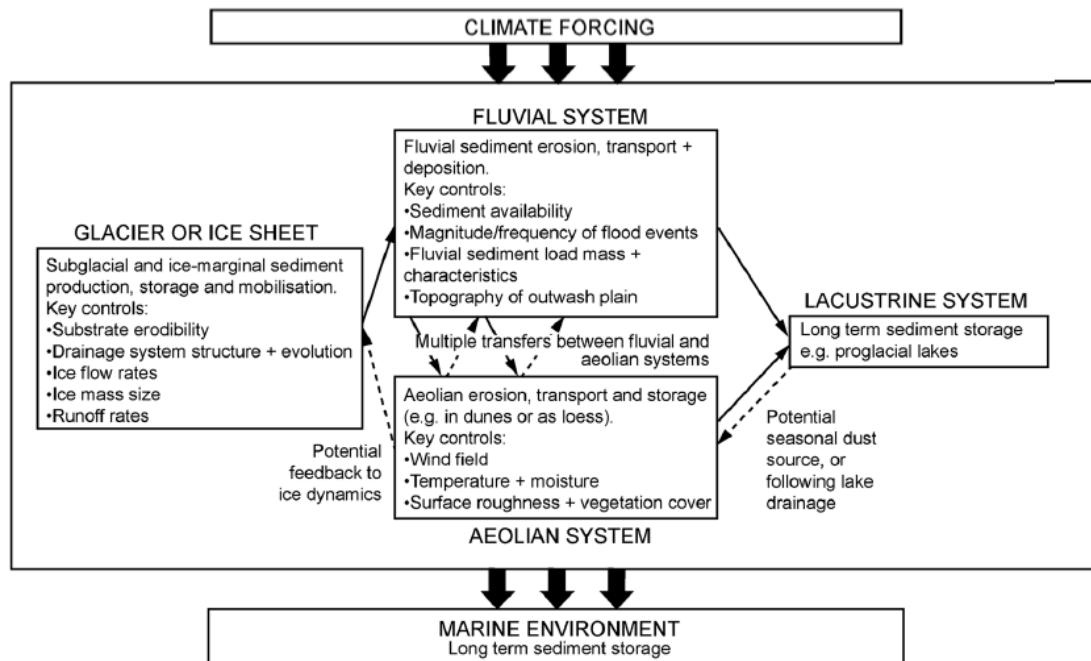


Figure 1.2: The interlinking glacial, fluvial, lacustrine and aeolian sediment linkages. The model was specifically designed for understanding the nature of high latitude dust events (Bullard, 2013)

Particles are transported within the glacio-fluvial environment before being deposited on proglacial floodplains (Richards, 1984). The size of particles is controlled by the distance from the original source (Arnalds, 2001; Gisladottir et al., 2005) and the transport capacity of the corresponding glacio-fluvial meltwater channels (Wainwright et al., 2015). Particles associated with dust storms are created via the abrasion between the glacier bed and grains in glacial transport are termed glacial/rock flour (Wentworth, 1922; Jackson et al., 1948; Dowdeswell, 1982). Glacial flour is the finest material created in the glacial system. Sand sized (63-2000 μm) particles carried in suspension are often deposited on glacial outwash plains (Gisladottir et al. 2005) whereas the silt (2-63 μm) and clay (<2 μm) sized particles are deposited in ephemeral outwash channel networks (Bullard, 2013).

Sediments, from sand sized (63 – 2000 μm) to clay sized (<2 μm) are transported through the glacio-fluvial channel network and are deposited within the active channel systems when changes in river flow occur. These deposits are often left draped along the landscape, and once desiccated, are available for transportation in the aeolian system (Dijkmans and Törnqvist, 1991; Bullard and Austin, 2011). However, during major flood events, sediments can be deposited on the entire floodplain. The

characteristics of these sediments will be governed by the transport capacity properties of the flow and the settling velocity. For example, in Iceland, the formation of large scale sand deposits has been linked to Holocene jökulhlaup activity (Maizels, 1989; 1991; 1993).

The re-distribution of these sediments can lead to the formation of dune fields and sandur regions which act as local storages for aeolian sediments (Mountney and Russell, 2004; Hugenholtz and Wolfe, 2007; Barchyn and Hugenholtz, 2012). These landforms are unlikely to represent contemporary processes and may also represent the location of paleo ice margins (Bateman and Murton, 2006).

1.3.2 Types of glacial system

Whether a glacial system is predominately warm or cold based will have a significant impact on the timing, magnitude and frequency of the delivery of fine sediment to the aeolian system (Gurnell et al., 1996; Hodson and Ferguson, 1999; Cuffey et al., 2000; Waller, 2001; Atkins et al., 2002). The differences in sediment yields between warm- and cold-based glaciers has been widely researched (e.g. Hodgson and Ferguson, 1999; Hodgkins et al. 2003). Warm based glaciers often have large quantities of sub glacial water as the entire ice mass is above/at the pressure melting point (Swift et al., 2005). Meltwater is routed to the bed of the glacier which promotes rapid basal sliding, which in turn provides a mechanism for the creation of fine sediments (Iversen and Semmens, 1995). Sediment supply is directly linked to subglacial reservoirs which evolve on a temporal scale based around local climatic conditions. Sediment pulses are seasonally-driven by increases in temperature during summer months and sediments often become exhausted after initial high-volume flushes (Hodgson and Ferguson, 1999). In contrast, it is assumed that cold based glaciers, which are not at the pressure melting point, do not produce large quantities of seasonal sediment because there is a lack of meltwater routing to the base of the glacier. Without this input of water, basal sliding is unlikely to occur, and erosion is likely to be limited (Boulton, 1979). Whilst, observations from Antarctica (e.g. Atkins et al., 2002) have shown that cold glaciers can erode and deposit fine sediments, the rates at which this occurs is much slower for warm based glaciers.

However, caution should be taken as the lack of research into cold-based glacier basal processes limits a full understanding about the complexity of the system. Waller (2001)

suggests that the 'zero basal velocity' suggested for cold-based glacier systems is overly simplistic and that work is required to understand the conditions in which cold-based glaciers incur basal motion processes and how this process affects glacial motion and glacial sediment availability.

1.3.3 Glacio-fluvial suspended sediment

Particles sourced from glacial systems will be entrained and transported in proglacial meltwater channels (Maizels, 1989; Richards, 1984, Ashworth and Ferguson, 1986), where channel size is a function of seasonal discharge. These systems often have clearly defined seasonal and diurnal patterns (e.g. increased sediment fluxes during warmer periods; Stott and Grove, 2001), however it has been shown that the volume of meltwater is not linearly correlated with sediment flux (Hodgkins, 1999).

Under normal flow regimes, the main control on sediment concentrations is short term sediment availability (Stott and Grove, 2001). Stott and Grove (2001) explored the relationship between summer short-term discharge patterns and suspended sediment fluctuation in Skeldal River, North East Greenland. Even though they found that suspended sediment concentration was primarily a function of discharge fluctuations, other events (known as transient flushes; Fountain, 1996) were observed during periods of low flow. These flushes may be a function of other sediment inputs which are not controlled by changes in glacial hydrology. For example, in Iceland, significant tephra deposits are often found adjacent to glacial masses and could become entrained in proglacial channels through overland flow during precipitation events. These proglacial/extra-glacial sediments have been reported to significantly affect suspended sediment concentrations globally (e.g. Orwin and Smart, 2004). Other inputs include sediment deposition from bank erosion/collapses (Orwin and Smart, 2004) and the impact of channel reworking (Retelle and Child, 1996).

High concentrations of suspended sediment can also be triggered during high magnitude low frequency glacial outburst floods (e.g. jökulhlaups). Jökulhlaups occur after volcanic material (from eruptions) interacts with glacial snow/ice (Maizels, 1997; Tweed and Russell, 1999) and/or when subglacial or proglacial lake dams fail (Bennett and Bullard, 1991; Russell, 2007). It has been suggested that due to continued glacial thinning and retreat under current climate conditions will lead to further jökulhlaups (Pagli and Sigmundsson, 2008).

These catastrophic flood events have the potential to transport extremely large volumes of sediment. Dunning et al. (2013) studied the evolution of proglacial sediments during/after the 2010 Eyjafjallajökull eruption in the Markarfljot catchment, South Iceland. Discharge during the jökulhlaup peaked several times (Dunning et al. 2013), with 67% of the total sediment being deposited during the initial flush, with much of the material being re-worked by meltwater events post-eruption. Old et al. (2005) found that suspended sediment flux increased from 190 kg s^{-1} to 4650 kg s^{-1} during two jökulhlaups in southern Iceland. It was estimated that 61% of all sediments transported during this event were $<63 \mu\text{m}$.

Silt is extremely important for dust events in both subtropical (Gill et al. 2006) and high latitude environments (Thorarinsdottir and Arnalds, 2012). Figure 1.3 (Old et al. 2005) shows the total percentage of silt in jökulhlaup and non-jökulhlaup suspended sediment samples with the corresponding dust record at Storhöfði, Iceland (Prospero, personal communication). The 1997 jökulhlaup delivered a significant proportion of silt to proglacial aeolian environment potentially increase dust concentrations following these events.

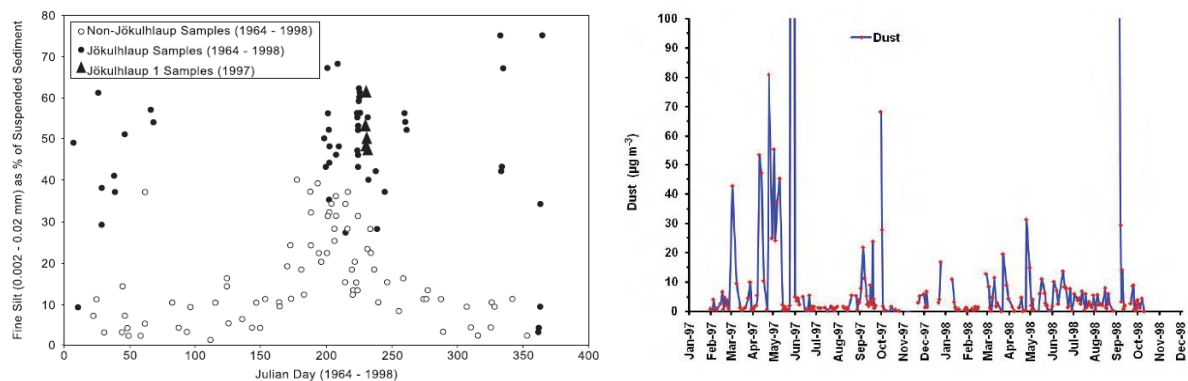


Figure 1.3: Jökulhlaup and non-Jökulhlaup samples from Southern Iceland (1964-1998) (Old et al., 2005). (right) Dust record recorded at Storhöfði

The relationship between dust storm frequency and jökulhlaup activity is however complicated (Bullard and Mockford, 2018). Bullard and Mockford (2018) showed using a 70-year WMO weather code data set from Kangerlussuaq, West Greenland that it was difficult to discern whether known jökulhlaups were causing increases in dust storm frequency. From their record, only the 1984 jökulhlaup was followed by a significant increase in dust events in the following year (Figure 1.4), whereas other noted jökulhlaups (e.g. Russell, 1993; Mernild and Hasholt, 2009) did not seem to

increase dust storm frequency. Large pulses of sediment are likely to be deposited during jökulhlaups, however factors affecting its ability to be available for aeolian entrainment may restrict emissions for a considerable period following large scale flood events (Bullard and Mockford, 2018). It should also be noted that dust storm frequency is only likely to increase if jökulhlaup frequency increases and that the effect of a single jökulhlaup on dust storm frequency may be short lived.

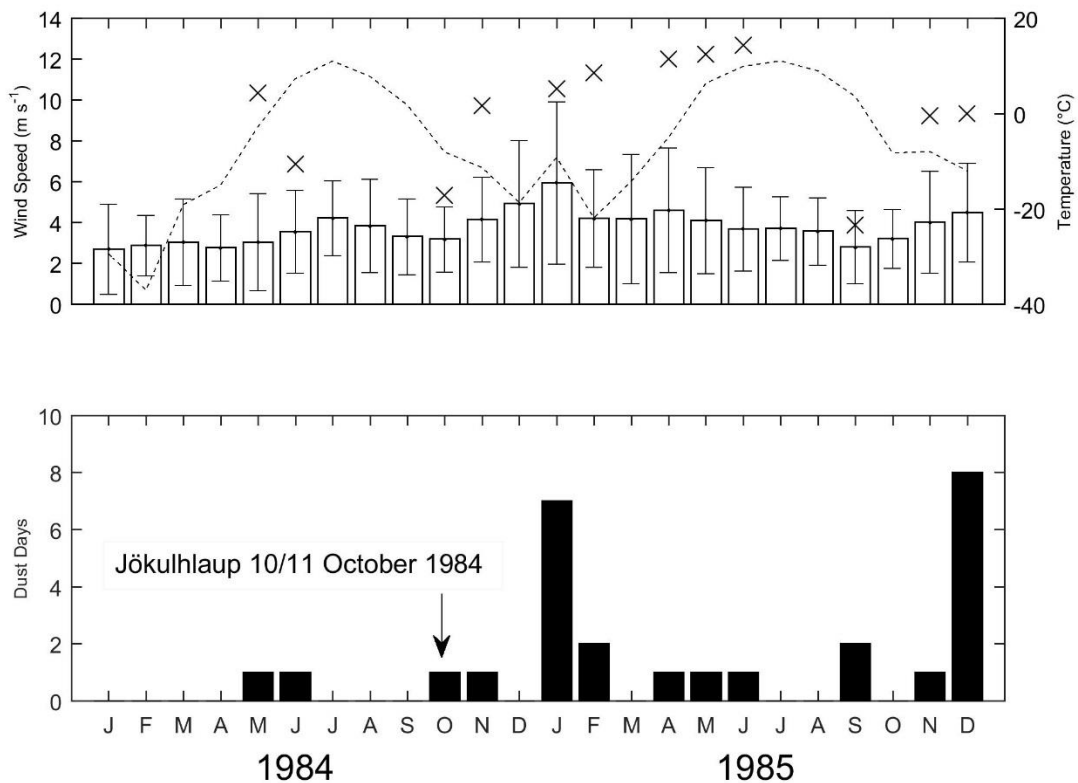


Figure 1.4: (top) Average monthly wind speed for 1984 and 1985. Bars show average wind speed and standard deviation for all days; X indicates average wind speed for dust events only. (bottom) Total dust event days per month for 1984 and 1985 (Bullard and Mockford, 2018).

1.3.4 Aeolian Processes

Once sediment has been supplied by the glacial system and has been suitably deposited, material can be entrained by the wind as dust storms (Bullard et al., 2016). Bullard et al. (2011) identified 3 key controls on the temporal availability of sediments which in turn control aeolian activity: transport capacity, sediment availability and sediment supply (Kocurek and Lancaster, 1999). As sediment supply has been addressed in sections 1.3.1 – 1.3.3, this will not be discussed further in this section.

1.3.4.1 Transport Capacity

Transport capacity is the amount of sediment which can be transported by a given wind shear (Wainwright et al., 2015). In simpler terms, it is the effective wind speed to entrain particles from a surface. Wind speed has been shown to be the major control on dust emission frequency and magnitude in sub-tropical environments (Gillette, 1978; Grini et al., 2005). However, our understanding of the importance of wind speed for controlling dust emissions in cold climates is limited. Although it has been suggested that aeolian processes operating at high latitudes are similar to those in the sub tropics, there are key differences which modify potential total mass fluxes (McKenna Neuman, 1993; Bullard, 2013; Bullard et al., 2016).

Surface wind speeds in high latitude environments are some of the strongest in the world (Mitchell et al., 2005; NASA, 2014), and in certain locations have been estimated to be approximately 150% higher than those from the sub tropics (NASA, 2014). Synoptic weather patterns which drive surface winds differ between the hemispheres (Cassano et al., 2006; Lynch et al., 2006), however the majority of dust raising winds at high latitudes are frontal and katabatic wind regimes (Wolfe, 2013).

In the northern hemisphere, the polar cell is often dominant and due to its atmospheric stability, wind speeds are often low (Einarsson, 1984). When depressions move across the Arctic, often sourced from the sub tropics, surface wind speed increases significantly due to large disruptions in atmospheric stability (Einarsson, 1984). Wind speed in Iceland during the most intense storms has reached 45 m s^{-1} (Arnalds et al., 2016). In Greenland, Hedegaard (1982) recorded surface wind speeds up to 50 m s^{-1} . In the southern hemisphere, the Antarctic ice sheet produces interior levels of atmospheric instability causing strong katabatic winds to form (Parish, 1984; Parish and Cassano, 2003). Wind speeds in the Antarctic have been shown to average 29 m s^{-1} over a 24-hour period; thus, making it the windiest place on Earth (Periard and Pettre, 1993). Although synoptic scale atmospheric patterns have a major influence on surface wind speed, local factors are also critical, and these vary between the source environments. These factors will be addressed in more detail in section 1.4.

Air density has been shown to change the threshold shear velocity required for entrainment of sediments. Air density decreases with temperature (McKenna Neuman and Nickling, 1989; Davis, 1992; McKenna Neuman, 1993), therefore in colder air,

flows can apply higher drag force coefficients on particles at the surface (McKenna Neuman, 1993; 2003). McKenna Neuman (2003), using wind tunnel experiments, showed that that approximately 70% more sand can be transported in saltation at -40°C than at $+40^{\circ}\text{C}$, which was attributed to increase turbidity at the surface in cold air masses. This means that sediment transport in cold environments should produce higher rates of sediment transport at the same wind speed than under the same conditions in warm environments (McKenna Neuman, 2003). This is potentially important for dust emissions as it has been shown that saltation of sand sized grains is the dominant process for emitting fine particles (Gillette, 1978; Shao et al., 1993; Grini and Zender, 2004).

The threshold shear velocity for motion (e.g. fluid threshold, Bagnold, 1942) in high latitude regions (as in the sub-tropics) varies, but most report threshold values between $4\text{-}10\text{ m s}^{-1}$ at surface level (Gisladottir et al., 2005; Bullard and Austin, 2011). This is not dissimilar to those recorded for sub-tropical environments (e.g. Grini and Zender, 2004).

1.3.4.2 Sediment Availability

As noted, the wind speed required to entrain sediments will vary between sources and at the same source between events because of the spatial and temporal variability in factors that affect sediment availability. In this thesis, the concept of sediment availability refers to when suitable sediments are exposed/present at the surface but factors other than wind speed are preventing aeolian entrainment. For dust events in all environments, several factors have been shown to significantly affect sediment availability. These include precipitation, relative humidity, vegetation, temperature (e.g. air density) and surface sediment lags.

Precipitation has been shown to inhibit dust emissions globally (e.g. Bergametti et al., 2015). In the high latitudes, rainfall varies from $<50\text{ mm}$ a year in Antarctica to $>1500\text{ mm}$ a year in south Iceland and New Zealand (Bullard et al., 2016). Even in areas where rainfall is low, the impact of precipitation on surface soil moisture will be greater than at the sub-tropics due to low evapotranspiration rates (Mitchell et al., 2005). The amount of rainfall required to suppress dust emissions is highly debated and will most likely be a function of the amount and intensity of the rainfall, the strength of the wind speed following the rainfall event and the parent surface soil sedimentology (Nickling

and McKenna Neuman, 1989). The threshold moisture content to suppress aeolian entrainment is agreed to be somewhere between 5% to 25% soil moisture content at the surface (McKenna Neuman, 1993). The time in which emissions will be suppressed is a function of rainfall magnitude and intensity, surface soil sedimentology, vegetation density and evapotranspiration rates (Wiggs et al., 2004; Bergametti et al., 2016). No study has been conducted testing this hypothesis as in reality it is extremely difficult to measure surface soil moisture content in real time. This is because only the top 1mm of soil needs to dry before entrainment can occur.

Another factor affecting soil moisture is the high relative humidity found in high latitude environments (Mitchell et al., 2005; Wolfe, 2013). For example, it is common in South Iceland that average spring/summer relative humidity will be between 50-70% (Einarsson, 1984). Marx et al. (2005) showed that the relative humidity during New Zealand dust events was often >70%. The ability of the surface soil to lower high levels of moisture without high rates of evapotranspiration in low temperatures in high latitude environments is most likely only achieved by wind desiccation.

Temperature can affect dust emissions through changes in air density (as stated above). In high latitude regions, where temperatures are on average < -9°C during winter months (Wolfe, 2013), the development of permafrost will affect surface soil properties. Where permafrost does exist, the surface soil will likely be frozen and therefore aeolian entrainment will be significantly diminished (McKenna Neuman, 1993; 2003). At these temperatures, sublimation will play a key role in releasing particles which are bonded together in pore ice (McKenna Neuman, 1993). Once melting has occurred during periods of warmer temperatures, a thin active layer of soil is often ice-free and could potentially be entrained by the wind. However, these soils are often waterlogged as drainage is impeded by a continuous blanket of pore ice (McKenna Neuman, 1993). The ability of these soils to drain, and therefore dry out, will be a function of the surface soil texture (Fécan et al., 1998) and the depth of surface permafrost (Walvoord and Striegl, 2007). If the water is unable to drain, this may also promote seasonal vegetation growth which would further bind and protect the soil from deflation via the wind (Wolfe, 2013).

Vegetation is likely to suppress dust emissions at high latitudes in a similar way to the sub-tropics. Vegetation provides a roughness element which inhibits dust emission by

disrupting air flow and increasing the fluid threshold for motion (Raupach, 1992; Okin and Gillette, 2001; Tegen et al., 2002; Engelstaedter et al., 2003; Okin, 2008; Webb et al. 2014). This concept is often referred to as shear stress partitioning (Raupach, 1992; Wolfe and Nicking, 1993; 1996; Shao, 2008). Sediment transport has been shown to increase in vegetated landscapes if the type, density and spatial patterns of vegetation promotes the channelling of flow (Okin et al., 2001; 2006) or where there are isolated roughness elements (Mayaud et al., 2017). In reality, dust sized particles are likely to be trapped on the leaves of vegetation (Hope et al., 1991).

As vegetation densities are often altered seasonally due to changes in temperature, the period in which vegetation can grow in high latitudes is likely to be a lot shorter than that in the sub tropics. This means that the impact of vegetation on dust emissions in high latitude regions may be short lived and confined to short growing seasons during summer months (Hugenholtz et al., 2009).

Our understanding of the impact on vegetation on dust emissions has mainly focused on grasses and shrubs (Tegen et al., 2002; Okin and Gillette, 2004; Munson et al., 2011). In the high latitudes, the most recent deglaciated landscapes were first colonised by biological soil crusts which have been shown to provide landscape stability in both sub-tropical (Belnap and Gillette, 1998) and high latitude environments (Belnap and Gardner, 1993).

The interplay between transport capacity, sediment availability and sediment supply are critical to understanding the spatial and temporal patterns of high latitude cold climate dust emissions. Most research has shown that dust events can occur all year round in the high latitudes (Crusius et al., 2011; Dagsson-Waldhauserova et al., 2014a; Bullard et al., 2016; Bullard and Mockford, 2018), however significant differences in the seasonal timings of dust emission peaks occur between source regions. This is because the factors which govern transport capacity, sediment availability and sediment supply vary between source regions.

The next section (1.4) will focus on source areas singularly and present the current understanding of dust emissions within that region, focusing fundamentally on the factors which drive the spatial and temporal patterns of dust emission from these regions.

1.4 High Latitude Cold Climate dust source regions

Figure 1.6 (Bullard et al., 2016) shows the global distribution of observations and peer reviewed literature of high latitude dust emissions. Our current understanding of dust emission from these regions is shown in Table 1.1 (Bullard et al., 2016). Although it seems from Table 1.1 that for most high latitude dust source regions we have a solid understanding of dust emission and the processes associated with it, many of these assertions are based on a limited body of research (Figure 1.6). In this next section, each of the regions shown in Table 1.1 and Figure 1.6 will be discussed in further detail, highlighting the seasonal patterns of dust activity and the gaps in our understanding of these systems. This will lead to a detailed structure for research conducted in this thesis.

1.4.1 Alaska

Most of our understanding of dust emissions from Alaska are drawn from loess research in central Alaska (Muhs et al., 2013; 2016). However, the first observation of dust events was documented over 100 years ago (Tarr and Martin, 1913). The first empirical study to assess contemporary dust emissions was carried out by Dust emission occurs all year round but are most frequent during autumn (Figure 1.6). The timing is related to the seasonal flushing of suitable sediments from glacial systems coinciding with down valley wind directions. Sediments are transported in complex proglacial channel networks (Schroth, 2011; Crusius et al., 2011). After discharge levels decrease, fine sediment is deposited across large proglacial floodplains where the material is available for entrainment in the aeolian system (Figure 1.7). Strong surface wind speeds coincide with this period due to the persistence of high pressure system over Alaska (Bullard et al., 2016); these pressure systems drive strong northerly katabatic winds which are channelled along south-facing valleys which coincides with a very prominent southern dust transport pathway (Figure 1.6). The largest source in the region is Copper River (Figure 1.6) (Schroth et al., 2009; 2011; Crusius et al. 2011; Bullard et al., 2016).

Table 1.1: The dominant characteristics of High latitude dust sources (Bullard et al., 2016)

	Alaska	Canada	Greenland	Iceland	Antarctica	New Zealand
Area of active dust emission	No data available	No data available	No data available	20,000 km ² (area with active aeolian processes)	4,800 km ² (area of Dry Valleys)	34,300 km ² (area susceptible to wind erosion)
Key known locations	South central and south west including Copper River and Matanuska-Susitna Valley	Isolated locations in the Yukon, Baffin Island, and Ellesmere Island	Kangerlussuaq Fjord region and ice-free northern land mass	Southern coast and North East	McMurdo Dry Valleys	Lake Tekapo region, South Island
Geomorphology of dust sources	Glacial outwash plains, braided river systems, and reworked loess	River floodplains and glacial outwash	Glacial outwash plains and reworked loess	Glacial outwash plains	Dry river valleys and lake beds and debris bands in ice	Braided river systems and reworked loess
Key dust-raising wind systems	Katabatic winds	Chinook/föhn winds and katabatic winds	Katabatic winds	Low-pressure systems and katabatic winds	Katabatic winds	Föhn winds
Threshold wind speed	>14 m s ⁻¹ at 2 m	2.5 m s ⁻¹ at <0.5 m	6 m s ⁻¹ at 2 m	5–10 m s ⁻¹ at 2 m	Unknown	7.5 m s ⁻¹ at 2.65 m
Seasonality of emissions	Primarily autumn	Late winter/early spring and autumn	Spring and autumn/winter	Year round but dominate in spring and early summer	Winter (all aeolian activity)	Early spring (September and October) and late Autumn (April and May)
Quantity of emissions	>0.06 × 10 ⁶ t yr ⁻¹	No data available	No data Available	35 ± 5 × 10 ⁶ t yr ⁻¹	No data available	No data available
Mean annual rainfall at dust sources	200–450 mm yr ⁻¹	No data available	<200 mm yr ⁻¹	1500–2500 mm yr ⁻¹	3–50 mm yr ⁻¹	600 mm yr ⁻¹

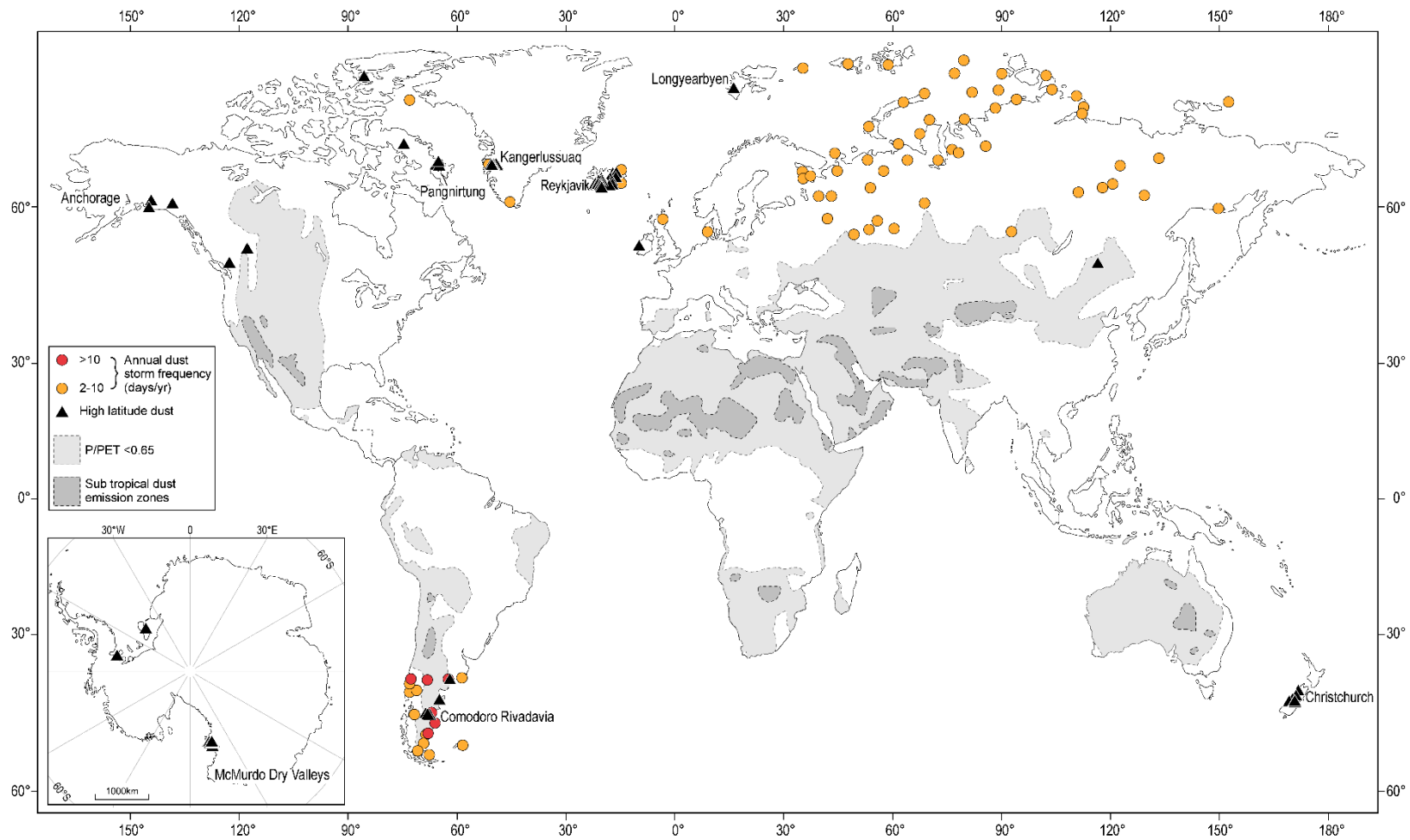


Figure 1.5: Observations of high-latitude dust storm frequency based on visibility data (circles) and peer-reviewed publications (triangles). Areas where the precipitation: potential evapotranspiration ratio <0.65 (aridity index) (United Nations Environment Programme, 1997) and subtropical dust emission zones are included for reference (Bullard et al., 2016)

Dust deposition has been linked to potential phytoplankton blooms in the Gulf of Alaska. Schroth et al. (2009) showed that Alaskan dust particles have a relatively high proportion of iron and Crusius et al. (2011) estimated that the iron from dust which is bioavailable, and therefore contributes to potential increases in oceanic productivity is of the same order of magnitude as material deposited by the glacio-fluvial systems. However, as dust events are concentrated in Autumn, the impact that dust deposition may have on oceanic productivity is debatable. This is because during these periods, light levels are still low and therefore oceanic productivity is low. Crusius et al., (2011) suggests that the material most likely is still available when light levels increase in the spring/summer, however further work linking dust deposition and oceanic productivity in the Gulf of Alaska is required.

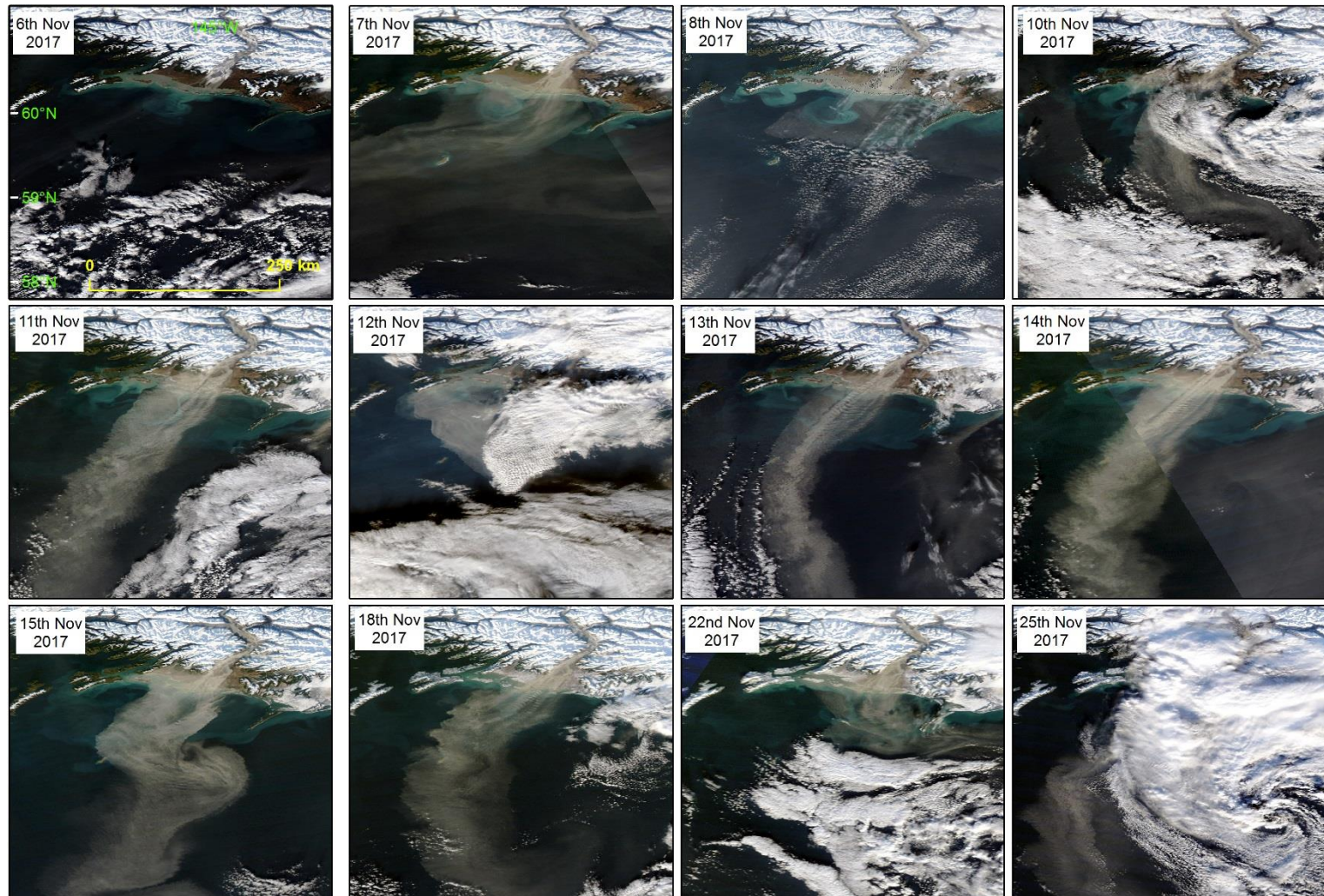


Figure 1.6: MODIS Terra/Aqua Level 1b of Alaskan dust plumes from Copper River (November 2017)



Figure 1.7: Dust storm at Copper River, Alaska. Photo courtesy of Santiago Gassó

1.4.2 Greenland

Dust emissions in Greenland have been significantly understudied in comparison to other Arctic dust sources. Observations of dust events in Greenland have often been ad-hoc, sporadic and limited to summer months (Bullard and Austin, 2011; Bullard and Mockford, 2018, Figure 1.8). The first known recorded observation of a dust event in Greenland was by Hobbs (1931, 1942) who reported fierce winds and sediment transport from ice-free proglacial environments. Dijkmans and Tornqvist (1991) showed that dust storms in Kangerlussuaq, SW Greenland occurred during wind speeds between $14-18 \text{ m s}^{-1}$, travelling down the valley and extending to 100m altitude. Bullard and Austin (2011) showed that there was a clear relationship between the glacio-fluvial meltwater system and the deposition of fine sediments ($<100 \mu\text{m}$) in proglacial environments.

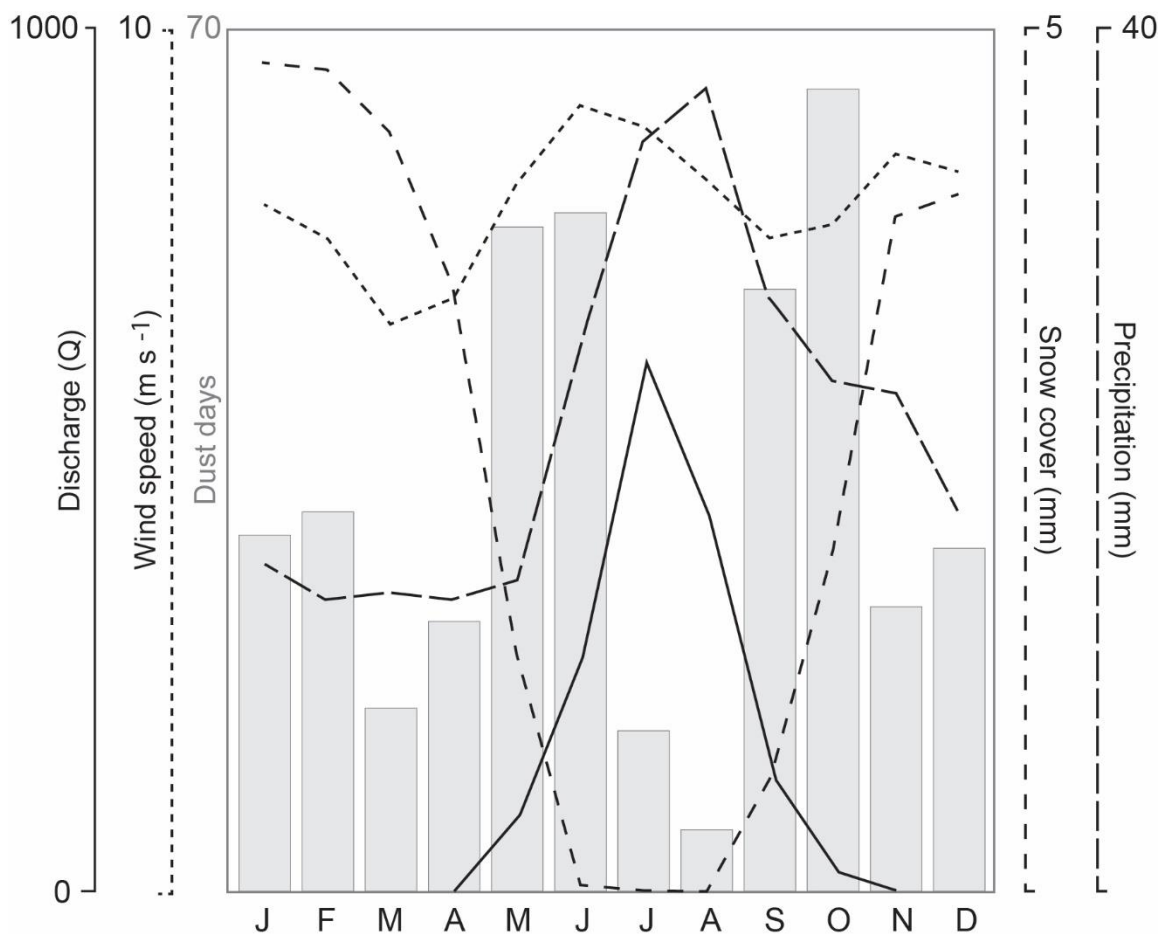


Figure 1.8: Seasonal variation in dust observations and meteorological factors from Kangerlussuaq, West Greenland (Bullard and Mockford, 2018).

The first systematic study to assess dust emissions from Greenland was conducted by Bullard and Mockford (2018). This study used a 70-year WMO meteorological data set which utilised 3 hourly weather observations. Of the 90+ weather codes which can be assigned, 9 of these indicate dust emissions (WMO, 2015). Figure 1.8 shows the seasonal pattern of dust event days (e.g. a day in which any dust code is recorded) and associated meteorological variables from 1945 – 2015. Dust emissions do occur all year round, however two clear peaks of heightened dust emissions occur during early spring and autumn. Dust emissions seem to decrease significantly during the summer months. The two peaks of heightened concentration occur when temperatures are increasing, causing snow cover to decrease. Snow cover will inhibit dust emissions by protecting sediments, therefore once this has been removed, dust can be entrained. During the summer months, precipitation increases, which will

increase surface soil moisture levels, which have been shown to significantly inhibit dust emission. This is also teamed with peak glacio-fluvial discharge levels; the sandur systems which are associated with dust emission are most likely inundated by meltwater streams and therefore sediment is not available for dust entrainment.

Bullard and Mockford (2018) also assessed the potential transport pathways of dust from Kangerlussuaq, SW Greenland. Using HYSPLIT forward trajectories on days which had been identified as dust days from the WMO meteorological data set (e.g. Baddock et al. 2017), Bullard and Mockford (2018) showed that many pathways

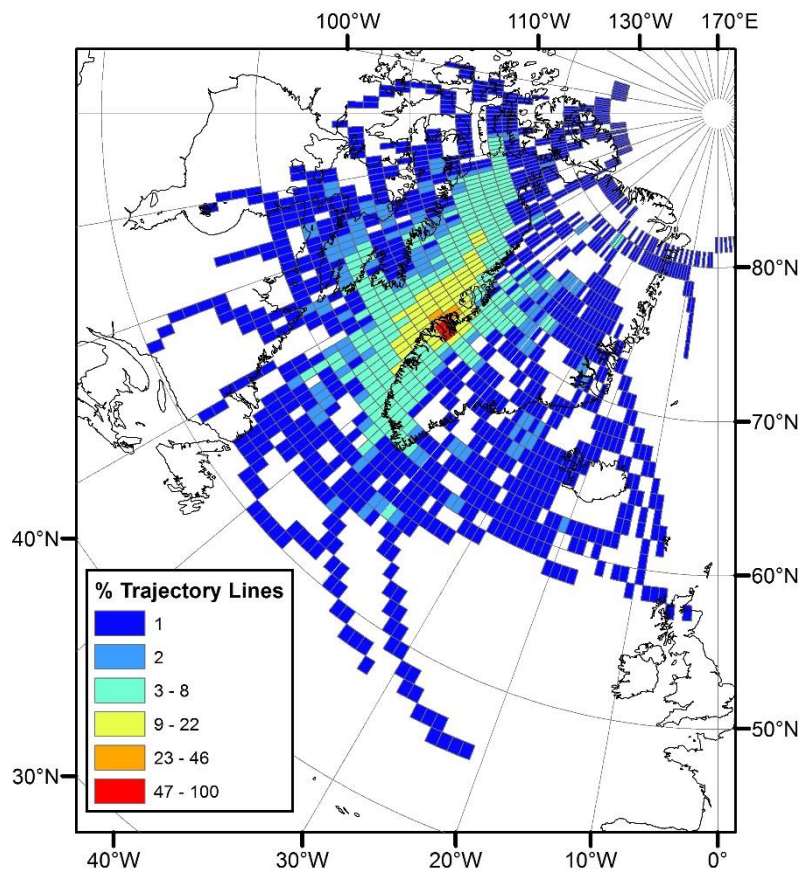


Figure 1.9: HYSPLIT air parcel trajectory model outputs indicating potential dust transport pathways for associated dust days from Kangerlussuaq West, Greenland (Bullard and Mockford, 2018).

associated with dust transport material away from the Greenland Ice Sheet (Figure 1.9). Dust deposition is therefore more likely to impact terrestrial and oceanic ecosystems (e.g. Anderson et al., 2017) rather than cryospheric environments (Painter et al., 2012).

1.4.3 Canada

Canada, like Greenland, is relatively understudied in comparison to other Arctic dust source regions. This is probably because it is assumed that dust events in the Canadian Arctic are relatively uncommon or are very small in terms of magnitude. Source geomorphologies are associated with periglacial environments such as ephemeral lakes and glacio-fluvial outwash plains (Bullard et al., 2016). Nickling (1978) measured the vertical dust flux from Slims Valley, Yukon (Figure 1.10). It was shown that dust was emitted from glacial outwash deposits under strong katabatic winds. Other ad hoc observations have been made showing dust deposition in snow packs and that large quantities of dust can be observed above 1m from the surface (Church, 1972).



Figure 1.10: Dust storm at Slims Valley, Yukon. Photo courtesy of James King

Meteorological conditions in Canada are expected to promote large scale dust emissions. Katabatic winds, which are often channelled by mountain topography, have been reported to reach 28 m s^{-1} (Bullard et al., 2016). However, dust emissions are often limited by factors that affect sediment availability. Surfaces are often protected by vegetation until autumn where large scale frost removes it. During the same period,

a synoptic meteorological shift increases wind speed in line with changes in the jet stream (Bullard et al., 2016). This then leads to the promotion of dust events.

Our lack of understanding of the spatial and temporal scale of dust emissions in Canada is confounded by poor observation in the region. Most areas in arctic Canada have very low population density, very few meteorological stations and events are often missed within the satellite record. This teamed with semi continuous snow cover and low temperatures which help to cement surface sediments (e.g. permafrost) possibly lead to a reported low dust emission potential for this region.

Most dust has been shown to be deposited locally and therefore may have an impact on local cryospheric systems. For example, Edlund and Woo (1992) showed that dust deposition at Ellesmere Island accelerated snow pack melt by more than a week. However, disentangling the impact of local dust deposition and long-range transport (e.g. Asia, Zdanowicz et al., 2000) is difficult.

1.4.4 Iceland

Iceland is the most researched high latitude dust source region in the world (Arnalds et al., 2016). However, the Iceland literature will be discussed in Chapter 2, as Iceland is the setting for the research conducted in this thesis.

1.4.5 Patagonia

In the southern hemisphere, Patagonia (and southern South America) has been shown to be a major dust source region in the high latitudes (Gaiero, 2007; Gaiero et al., 2004; 2007; McConnell et al., 2007; Gasso and Stein, 2007; Sugden et al., 2009; Delmonte et al., 2010; Gasso et al., 2010; Weber et al., 2012). Dust has played an important role in Patagonia since the last glacial maximum (Delemonte et al., 2008; Sugden et al., 2009); where dust deposition was approximately 50 times greater than at present (Lambert et al., 2008).

Contemporary Patagonian dust is sourced predominately from alluvial fans, ephemeral lake beds and loess (Gaiero et al., 2013), and emissions have been increasing in magnitude due to changing land practices after European settlement (McConnell et al., 2007). Dust events occur all year round (Gasso and Stein, 2007; Gaiero et al., 2013) with the highest frequency of events occurring in spring and

summer. During these periods, low pressure systems move northwards, which generate extremely high wind speeds (e.g. 20 m s^{-1} , Lassig et al., 1999) causing large scale deflation. In winter and autumn events are likely to be suppressed by seasonal increases in precipitation (Gaiero et al., 2013).

Dust deposition in the Southern Ocean and on the Antarctic ice sheet has long been associated with Patagonian dust sources (Wolff et al., 2006; Gasso and Stein, 2007; Li et al., 2008). The deposition of material into the Southern Ocean is extremely important as it provides nutrients to a high nutrient low chlorophyll environment (Meskhidze et al., 2007). Li et al. (2008) showed that up to 85% of dust deposited in the Vostok Ice Core, Antarctica, was sourced from Patagonia.

Patagonia has benefited from the increased capabilities of satellite remote sensing (Figure 1.11). Gasso and Stein (2007) and Gasso et al. (2010) showed that contemporary dust plumes, sourced from Patagonia, can travel $>1500\text{km}$ from source over the Southern Ocean. This capability, teamed with modelling efforts, has allowed a clearer picture into dust transport pathways and dust source identification in the region (Li et al., 2008; Albani et al., 2012).

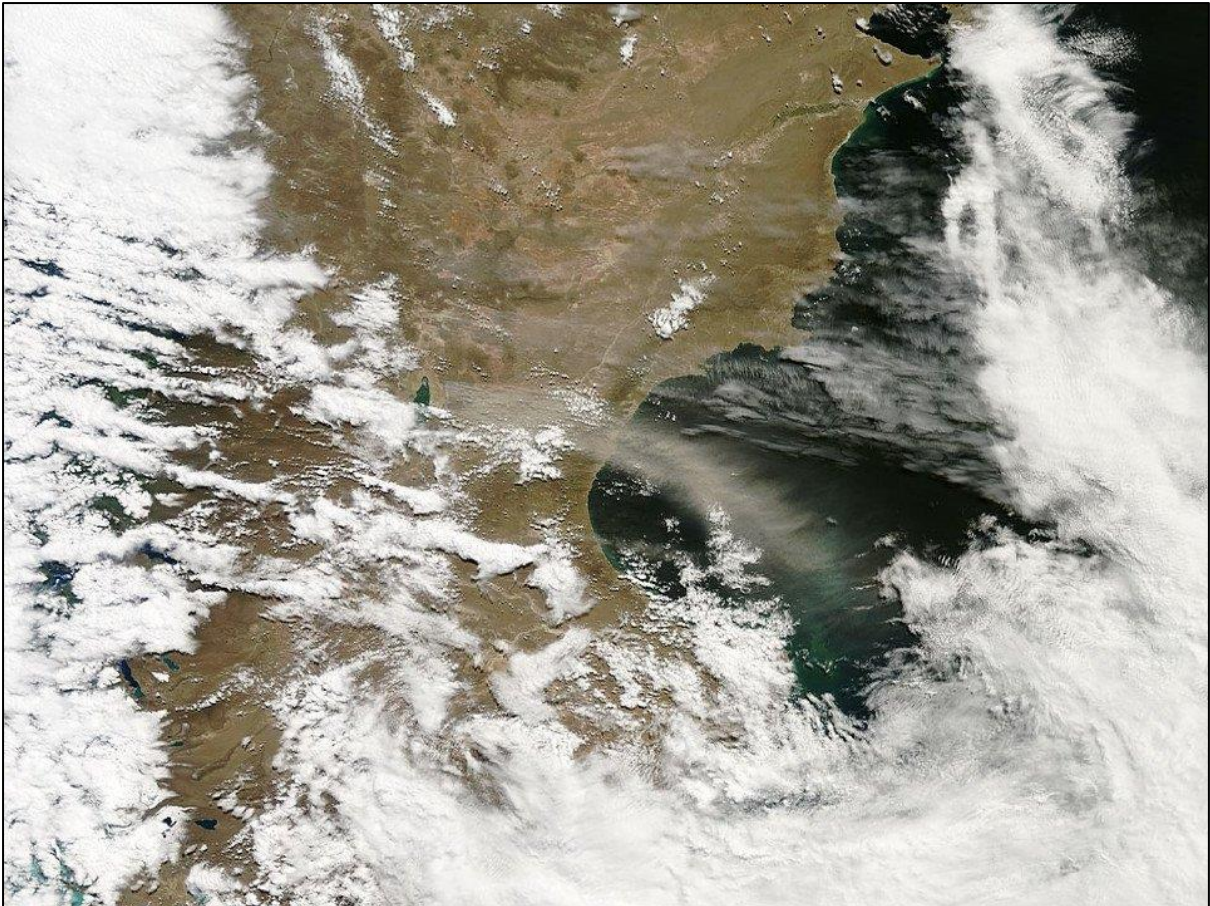


Figure 1.11: MODIS Terra Level 1b (19/11/16) image of a Patagonian dust storm

1.4.6 New Zealand

Dust sources in New Zealand are primarily located on South Island and have been shown to contribute to deposition in the Southern Ocean and in Antarctica (Marx et al., 2005; Li et al., 2008; Neff and Bertler, 2015). Emissions are associated with large braided river systems linked with local glacial systems, ephemeral lakes and exposed shorelines (McGowan and Sturman, 1996; McGowan, 1997; Marx et al., 2005; Marx and McGowan, 2005). As in Patagonia, changing land practices (e.g. vegetation removal) after European settlement led to extreme land degradation which has led to an increased availability of sediments for aeolian transport (McGowan and Ledgard, 2005).

McGowan and Sturman (1996) indicated the importance of katabatic winds in generating dust emissions. Field data showed that windstorms of 7.5 m s^{-1} at 2.65 m

above the surface were capable of entraining dust sized sediments from braided river channels. Most dust events occur during the daytime, however in environments where high winds are topographically promoted, dust can occur during any period of the day. Marx et al., (2005) showed that dust deposition from these sources ranged from 0.21 – 118.9 kg ha⁻¹ month⁻¹ which is comparable to mid latitude environments (e.g. Reheis and Kihl, 1995; McTainsh et al., 2005).

Dust has been shown to occur all year round in New Zealand and is fundamentally controlled by variations in surface wind speed. In winter months, dust is transported in anticyclonic conditions which lead to the dominance of strong south westerly winds (Marx et al., 2014). In spring/autumn, westerlies dominate as synoptic conditions are circumpolar in nature. Due to high humidity, seasonal rainfall peaks are unlikely to impact dust emissions with only the strongest wind events able to entrain material (Marx et al., 2005). As New Zealand is in a known dust transport pathway from Australia (O'Loingsigh et al., 2017), it is important to be able to differentiate between long transported dust from Australia and locally derived dust from New Zealand. This can be achieved by geochemical fingerprinting of material from known trace elements (Marx et al., 2014).

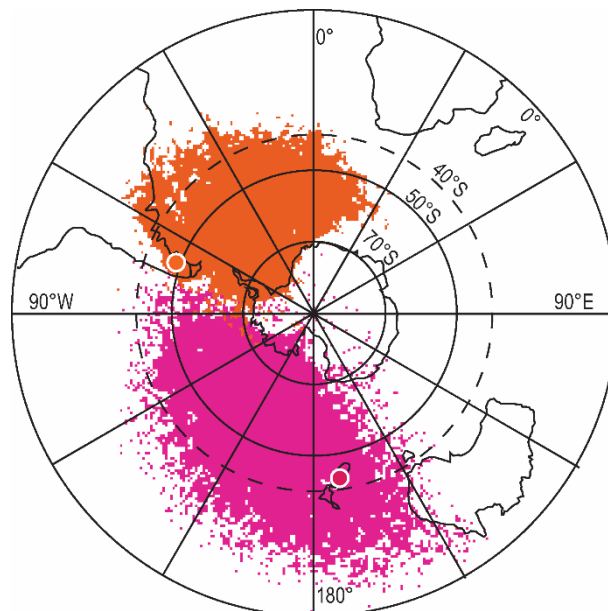


Figure 1.12: Potential dust deposition locations from New Zealand (pink) from 5-day HYSPLIT air parcel trajectory model outputs (Bullard et al., 2016; adapted from Neff and Bertler, 2015).

The downwind transport pathways of New Zealand source dust were assessed by Neff and Bertler (2015). Using 5-day forward HYSPLIT trajectories (Figure 1.12), it was shown that material potentially would be deposited in the Southern Ocean and Antarctica. They estimated that even though the total dust loads from New Zealand were relatively minor compared to Patagonia, Australia and Southern Africa, that potentially 8.5% total dust deposited in the Southern Ocean and Antarctica was sourced from New Zealand respectively.

1.4.7 Antarctica

Most of the research conducted on dust in Antarctica has focused on the deposition of material from Patagonia (e.g. Basile et al., 1997; Gasso and Stein, 2007; McConnell et al., 2007; Lambert et al., 2008; Li et al., 2008; Sugden et al., 2009), New Zealand (Marx et al., 2005; Neff and Bertler, 2015) and Australia (Gaudichel et al., 1992; Basile et al., 1997; Revel-Rolland et al., 2006; Li et al., 2008). The most dominant contemporary source is believed to be Patagonia (Li et al., 2008), however Alabani et al. (2012) showed that at the last glacial maximum, Australia was the largest net dust depositor in Antarctica.

Because only 2% of Antarctica is ice free (Doran et al., 2002), the spatial scale of dust emissions sourced from Antarctica is relatively small. However, studies from these areas have shown active aeolian systems do exist. Most aeolian research has focused on the McMurdo Dry Valleys. Gillies et al., (2013) showed over a 2-year field campaign the characteristics of the aeolian system. It was shown that saltation activity was controlled by thermally-driven wind regimes in the daytime (09:00 – 24:00) in spring and summer but are driven by katabatic winds in winter and autumn. The threshold wind speed for motion was calculated at approximately 4.2 m s^{-1} at the surface, with most events occurring in westerlies in autumn/winter and easterlies in spring/summer. Although this study did not explicitly deal with dust-sized sediments in transport, it could be assumed that there is a relationship between saltation activity of larger grains and the release of dust-sized sediments in this environment (Shao et al., 2011). Lancaster (2002, 2004) and Lancaster et al. (2010) showed that deflation of finer material was related to saltation activity, and that fine particles are transported and deposited in nearby local glacier and ice-covered lakes.

Although field studies have offered a unique insight into source processes in Antarctica, these studies are temporally limited (Lancaster, 2002; Gillies et al., 2013). Ayling and McGowan (2006) used a 35-year snow pit chronology to suggest that aeolian transport is greatest in winter, when westerly katabatic winds dominate. Atkins and Dunbar (2009) and Chewings et al., (2014) showed that wind-blown sediments from exposed moraine systems can accumulate on sea ice in McMurdo Sound at a rate of $0.2 - 55 \text{ g m}^{-2} \text{ y}^{-1}$. Sediment size varied from larger sand grains (<5 km from source) to finer material further downwind (>100 km from source). It was suggested that as sea ice melts, these sediments can become available in the marine environment. However, Chewings et al. (2014) concedes that aeolian inputs from the Dry Valleys may be limited as surface deflation lags often protect fine sediments from becoming entrained.

Bhattachan et al. (2015) argued that the McMurdo Dry Valleys may also be an important source of bioavailable iron for the Southern Ocean. Using a laboratory dust generator and HYSPLIT forward trajectory analysis, Bhattachan et al. (2015) showed the dust emission potential of sediments sourced from the Dry Valleys in releasing Fe is comparable to sediments sourced from subtropical dust sources. Forward trajectories indicated that a majority of air parcels from the Dry Valley source regions are transported towards the Southern Ocean. Although no link between direct dust entrainment and deposition of material in the Southern Ocean has been made, as the Antarctic warms and ice-free areas increase in size, the amount of suitable sediment for the aeolian system may increase (Bullard, 2013; Bhattachan et al., 2015).

1.4.8 Eurasia

Although it is certain that dust events occur in Eurasia, there has been little research conducted in this region. Dust storms are most likely to occur in areas of Asia and Siberia which have been affected by desertification or significant land disturbances (Bullard et al., 2016).

Bazhenova and Tyumentseva (2015) reported average erosion rates associated with dust storms in southern Siberia to be between $0.1 - 2.5 \text{ mm yr}^{-1}$. The resuspension of volcanic ash has also been reported at the Kamchatka peninsula (Flower and Kahn, 2017). However, there are significant gaps in our understanding of the aeolian system in Eurasia, regarding the timings, magnitudes and intensities of dust events.

However, Engelstaedter et al. (2003) indicates from his global map of dust observations (adapted by Bullard et al., (2016) in Figure 1.6) that there are numerous sources of dust within Eurasia. It is however difficult to disentangle whether the WMO stations are recording local dust entrainment or long-distance travelled material from the recognised Asian dust sources.

1.5 Summary

This chapter has introduced the important role that dust particles play in the global climate cycle. Dust emissions are predominately sourced from desert regions in the sub-tropics. However approximately 5% of the global dust budget is sourced from high latitude cold climate regions, where our understanding of processes which drive dust emission, transport and deposition is limited. Our understanding is fundamentally driven using secondary data sets and ad-hoc observations of dust events. This is because of a lack of field measurements of high latitude dust events informing our understanding of dust emission process and remote sensing techniques which are used within the sub tropics successfully to monitor the magnitude, frequency, intensity and transport pathways of dust events are often not applicable at high latitudes. Field measurements of dust concentrations and how they are governed by meteorological, sedimentological and geomorphological factors are key to deciphering the importance of dust emissions from the high in the Earth's contemporary climate system.

As shown in table 1.1 (Bullard et al., 2016) significant gaps exist in our understanding of these systems, which can be attributed to incomplete data sets, a lack of field monitoring (of which studies have been confined spatially and temporally) and the inability to consistently rely on satellite data. Certain factors, such as dust source geomorphology and threshold shear velocity seem to be well-confined (e.g. Bullard, 2013; Bullard et al., 2016), however, these estimates and classifications have been based on the limited datasets available and therefore should be taken with caution. Measurements are required which link dust source characteristics (sediment supply) and the factors which control dust emission at source (transport capacity and sediment availability).

Of the 9 identified high latitude cold climate dust source regions, Iceland is the most heavily researched. However, significant gaps in our understanding of dust events in Iceland exist. Chapter 2 will address the current understanding of Icelandic aeolian

research and where our current knowledge gaps lie. It will also address the purpose of using Iceland as a representative example for exploring concepts which relate to all high latitude cold climate dust environments.

1.6 Thesis justification

Although this work will focus on data from only one of the identified high latitude dust sources, it could be argued that Iceland is a good proxy for high latitude dust sources in general due to the range of geomorphologies which are associated with dust emissions (e.g. Arnalds, 2001; Arnalds et al., 2016).

In all source regions we lack field measurements of high latitude dust events and a detailed understanding of the relationship between source sedimentology and dust particle properties. These measurements are important for two reasons. Firstly, without sufficient field measurements, attempts to model the contribution of high latitude dust for the global atmospheric dust budget is problematic. Models require source measurements of dust concentrations and meteorological factors associated with driving dust events to verify and tune model parameters (Lu and Shao, 1999; Kok et al., 2012; Groot Zwaaftink et al., 2017). Secondly, contemporary dust emission processes in the high latitudes may provide a modern analogue for processes which occurred previously (e.g. at the last glacial maximum). Understanding these processes furthers our understanding of paleo landscape development such as the development of loess deposits (Ashwell, 1966; Jackson et al., 2005)

A detailed understanding of sedimentology, of both surface and airborne particles associated with the high latitude dust system, is needed to assess the relative importance particle deposition may have on numerous global biomes. As will be discussed later, efforts to link sedimentology, geomorphology and dust emissions has been successful in the sub-tropics due to data sourced from satellite sensors. In high latitudes, where these approaches are often not applicable, other methods are required (e.g. UAVs, ground based remote sensing). These will be explored in this thesis.

As stated at the beginning of the chapter, the main aim of this thesis is:

To assess the sources, drivers and sedimentology of Icelandic dust events

This will be achieved through outlining our current understanding of the Icelandic dust cycle (Chapter 2) and three empirical chapters. The empirical chapters include:

Chapter 3 – Sedimentological characteristics of Icelandic dust sources

Where the main aim is:

To compare the sedimentological characteristics of two Icelandic dust sources and assess the impact these sediments have on dust particle characteristics

This will be achieved through the following objectives:

1. For an active dust source area, what proportion of this area has high dust emission potential?
2. For the areas identified as having a high dust emission potential, what are the physical characteristics of these particles?
3. How do variations in surface sedimentology affect dust particle properties?

Chapter 4 - The Icelandic dust storm: magnitudes, characteristics and pathways at the event-scale

Where the main aim is:

To compare the sedimentological characteristics of two Icelandic dust sources and assess the impact these sediments have on dust particle characteristics

This will be achieved through the following objectives:

1. Determine the relationship between wind speed and PM10 concentrations from field data at the event scale
2. Using the conceptual model proposed in section 2, classify each dust event according to the primary control
3. Use time series analysis, field observations and secondary meteorological data to infer factors which may affect/promote sediment availability during dust events and to validate the model

4. Determine the spatial distribution of potential pathways for dust events using air parcel trajectory modelling
5. Use CALIOP satellite retrievals to assess potential boundary layer heights for Icelandic dust events

Chapter 5 – The role of aeolian abrasion in creating dust sized sediments for high latitude dust events

Where the main aim is:

To examine the susceptibility of three different Icelandic dust source sediments to aeolian abrasion

This will be achieved through the following objectives:

1. How much dust is already available in the surface samples?
2. During an active dust event, how much dust is generated by aeolian abrasion processes?
3. What is the effect of temperature and humidity on potential dust production rates and generated particle size?

Each section will be divided into a brief introduction, methods specific for the chapter, results and a stand-alone discussion. A summary including further research questions will be presented at the end of the thesis in Chapter 6

2. The Icelandic dust cycle

In Chapter 1, dust in the Earth's system was discussed before outlining the state of knowledge on dust emissions from high latitude environments. This thesis is focused on Iceland as an example of a high latitude dust source. Therefore, the aim of Chapter 2 is to set out the current state of knowledge about the Icelandic dust cycle and identify the research gaps which have driven the aims and objectives of this thesis.

2.1 Introduction

Iceland has long been identified as a major high latitude dust source and is the most researched high latitude dust source region in the world (Arnalds, 2001; Gísladóttir et al., 2005; Arnalds, 2010; Thorsteinsson et al., 2011; Prospero et al., 2012; Dagsson-Waldhauserova et al., 2013; 2014a, 2014b; 2015; Arnalds et al., 2013; 2016; Baddock et al., 2017; Groot Zwaafink et al., 2017; Wittman et al., 2017). The Icelandic dust cycle is driven by the relationship between local climate, active volcanism and significant glacial activity (Thorsteinsson et al., 2011). Iceland's landscape has undergone significant disturbance since approximately AD 874 where the removal of vegetation and changes in land use practices have exacerbated soil erosion rates (Arnalds et al., 2001; Dugmore et al., 2009).

2.2 Background

Iceland is an island located south of the Arctic Circle (63N – 66N°, 13W – 24W°). The total land mass is 103,000 km², of which approximately 22,000 km² is prone to wind erosion (Arnalds, 2001; Arnalds et al., 2016). The climate is predominately controlled by the Irminger current (south Iceland) and East Greenland current (west and north Iceland) (Einarsson, 1984). The mean annual temperature is between 0-4°C (Arnalds et al., 2016). Precipitation exceeds 1500 mm on the south coast, with a decreasing precipitation gradient towards the north (Einarsson, 1984; Mitchell et al., 2008). Humidity often exceeds 75% (Arnalds et al., 2016) but varies significantly dependent on the synoptic climatic conditions (Einarsson, 1984; Olafsson et al., 2007). For example, dust events have been related to the dominance of dry stable air masses which causes a decrease in humidity (Arnalds et al., 2016).

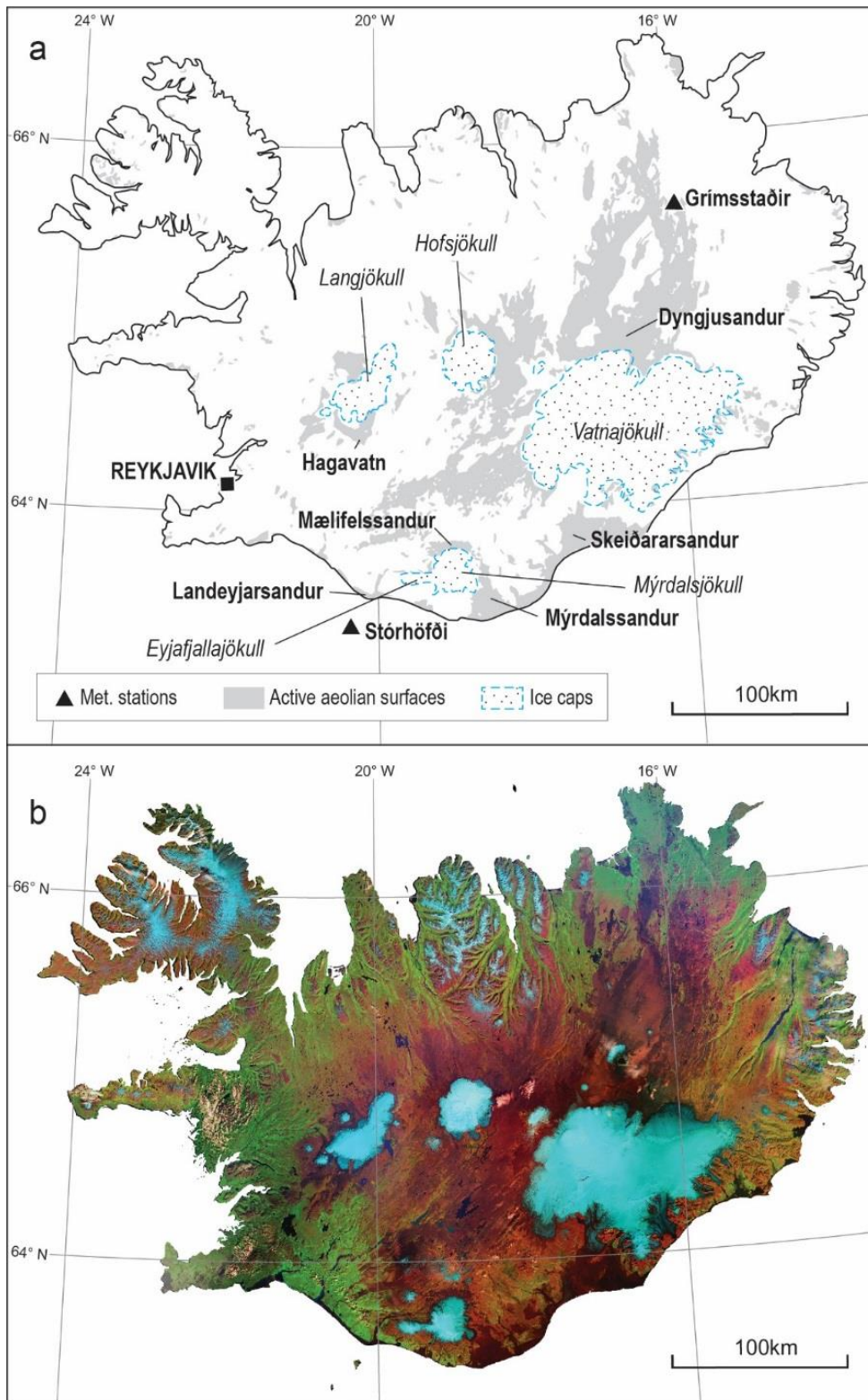


Figure 2.1: a) Icelandic dust source map based on Arnalds (2001) aeolian susceptibility index (Table 2.1). Major dust source units labelled in bold. Major glacial systems labelled in italics. Met stations used for Figure 2.5 labelled with triangles. b) Landsat 8 Thematic Mapper mosaic of Iceland showing dominant land cover types. Blue areas indicate ice/snow (Arnalds, 2001; Baddock et al., 2017)

High surface wind speeds ($> 10 \text{ m s}^{-1}$) are a common occurrence as cyclones track through the Arctic (Einarsson, 1984). These atmospheric low-pressure systems are often referred to as the Icelandic low (Serreze et al., 1997), and typically tracks from the south west of Iceland into the centre of the country. During summer months, the low splits into two separate air masses. One part of the low tracks south providing northerly and easterly flows on the south coast, with the other part of the low tracking north providing southerly flows in the northern part of the island (Einarsson, 1984; Baddock et al., 2017). Wind speed regularly can reach 20 m s^{-1} and exceed 50 m s^{-1} at the surface during severe winter storms.

2.3 Dust source geomorphology

Dust sources are closely coupled to the Icelandic volcanic-glacial systems (Arnalds et al, 2001; Arnalds et al, 2016; Baddock et al, 2017). Material supplied to these systems is predominately volcanic, transported through the glacial and fluvial systems and deposited on large glacial outwash plains (or sandurs). These sediments are often extremely fine in nature, and once they have been sufficiently desiccated, are available to be transported by the wind either in saltation or suspension (Arnalds, 2001). In Iceland, areas which are prone to wind erosion were mapped by Arnalds (2001). It was shown that over $20,000 \text{ km}^2$ of the surface was susceptible to 'considerable erosion', 'severe erosion' or 'extremely severe erosion' (Figure 2.1) (Arnalds et al, 2001; Arnalds et al. 2016). Within this $20,000\text{km}^2$, Arnalds (2001) showed that different dust emitting units could be classified based on their geomorphologies. The geomorphological characteristics of Icelandic dust sources was split into 3 separate units: 'sand fields'; 'sandy lag gravel' and 'sandy lava'. The percentage total land proportion of each unit is shown in Table 2.1 (Arnalds et al. 2016).



Figure 2.2: Dust event at a sandy field in Iceland (June 2015).

Of these units, sandy fields are the most active areas for aeolian activity (Figure 2.2), and have been attributed the term ‘dust hot spot’ (e.g. Arnalds et al., 2016). These areas vary sedimentologically, with some areas being dominated by sediments with high percentages of silt (e.g. areas closest to the ice margins), whereas areas located further from contemporary ice margins are dominated by soils with high % sand content (Arnalds et al., 2001; Gisladottir et al., 2005; Arnalds et al., 2016). Their formation can be attributed to the development of alluvial fans, or ‘hochsandur fans’ (Kruger, 1997; Russell et al., 2001; Kjaer, 2004; Mountney and Russell, 2004), where material is transported in glacio-fluvial meltwater channels and deposited in active channel systems or during high magnitude events across the entire floodplain.

Sandy lag gravel areas account for > 12,500 km² of the total aeolian active areas in Iceland (Table 2.1). Predominately, these environments are formed on glacial tills, raised shorelines and alluvial sediments and are now disconnected from the glacio-fluvial system (Arnalds, 2001; 2010). The gravels act as a sediment trap for particles which are transported via aeolian processes and are accumulating at a rate of 0.1 – 1 mm yr⁻¹ (Arnalds, 2001).

Table 2.1: Different Icelandic dust source units and their total area (km²) based on the severity index proposed by Arnalds (2001)

Geomorphology	Susceptibility to erosion index (Arnalds, 2001)			Total area (km ²)
	Considerable	Severe	Extremely severe	
Sand fields	318	1087	2828	4233
Sandy lag gravel	5407	6217	1286	12910
Sandy lava	1366	1757	1620	4743
Total area	7091	9061	5734	21886

The geomorphological unit of sandy lag gravel can also be used to describe the gravel braided river systems of Iceland, which have been demonstrated to be a major source of dust (Prospero et al., 2012). These areas are not disconnected from the glacio-fluvial system. When temperatures increase in the spring/summer, this leads to higher melt rates in the glacial system. In turn, this causes an increased river stage/discharge in the associated glacio-fluvial channels (Hodgkins, 1999). As river stage increases in the main channel, river flow extends across the floodplain (Figure 2.3). The river is then able to cut fresh meltwater channels into the gravel bars. Once the water retreats, areas of unarmoured, unvegetated silt deposits are left (Figure 2.4). Once these sediments have been desiccated and factors which make them unavailable for sediment transport have been removed (Kocurek and Lancaster, 1999; Bullard et al., 2008), these particles can be entrained in a dust event (Prospero et al., 2012).

Sandy lag gravel regions have been shown to be susceptible to wind erosion during high intensity wind events (Arnalds et al, 2001; Gisladottir et al., 2005). However, Arnalds et al (2001) showed that the potential surface threshold friction velocities for motion are considerably higher on sandy lag gravel surfaces (12 – 15 m s⁻¹ at 2 m) than on the sandy field surfaces (5-8 m s⁻¹ at 2 m). This can be attributed to the impact lag deposits have on disrupting air flow (e.g. Nickling and McKenna Neuman, 1995) and the ability of soil matrices with large proportions of fine material to retain moisture in surface sediments (McKenna Neuman and Nickling, 1989; Fécan et al., 1998), therefore restricting dust emission due to high surface soil moisture rates (Ravi et al., 2006).

Sandy lava areas cover approximately 4,750 km². These Holocene lavas have accumulated over significant proportions of Iceland (Licciardi et al., 2006). Initially,

landscape development is shaped by the deposition of volcanic tephra. As these surfaces expand, they become an aeolian deposition trap for sediment travelling from the ice margins. It is estimated that approximately 3,500 km² of the sandy lava areas are severely or extremely severely affected by aeolian activity (Arnalds et al, 2001; Arnalds et al, 2016). The frequency and magnitude of dust events from sandy lava areas has been shown to increase following large scale volcanic eruptions (Arnalds et al. 2010), as fresh tephra is re-distributed following deposition.

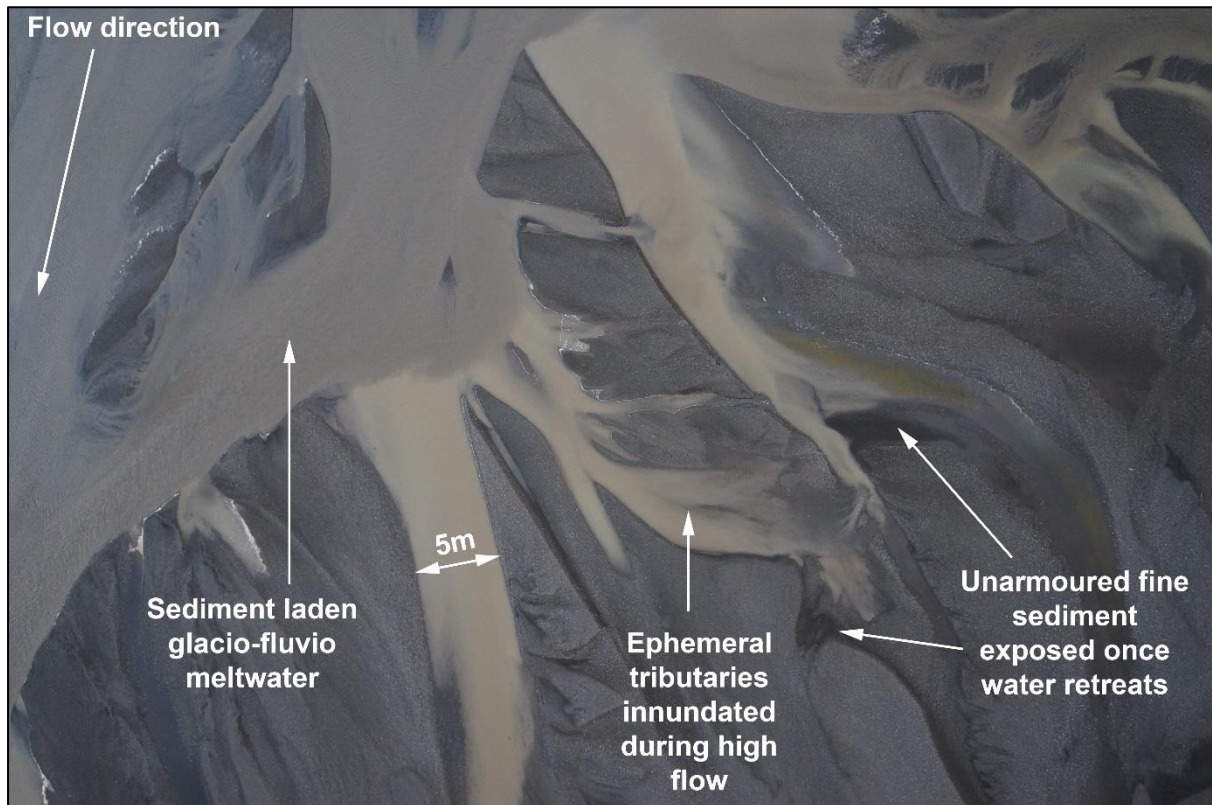


Figure 2.3: The Markarfljot ephemeral channel system, June 2014. Image acquired from a UAV survey flown at 100m altitude. As river stage in the main channel increases, floodwater enters the outer sections of the floodplain

Although studies have been carried out focusing on the geomorphology and sedimentology of outwash plains in Iceland (e.g. Krigstrom, 1962; Bluck, 1974; Hine and Boothroyd, 1978; Maizels, 1993; Kruger, 1997; Gomez et al., 2000; Kjaer et al., 2004; Russell et al., 2001; Baratoux et al., 2011), much of this work has focused primarily on the structure and development of the underlying stratigraphy. Little work has been conducted linking the geomorphology and sedimentology of outwash plains with aeolian processes. Mountney and Russell (2004) characterised glacial outwash regions adjacent to the Askja region in northeast Iceland (e.g. Dyngjusandur) and the

dominant aeolian processes occurring at the surface. It was concluded that spatial and temporal geomorphological and sedimentological differences within the outwash plain were associated with the dynamic seasonal relationship between the volcanic, glacial, fluvial and aeolian systems. However, this study's focus was to show how aeolian processes are important in shaping landscape development within the outwash plain. It does not address how the sedimentological and geomorphological characteristics of the outwash plain impact aeolian processes and the generation of aeolian sediments. Although the work of Arnalds (2001, 2010; 2016) does attempt to draw differences in aeolian activity between the geomorphological classifications of dust source, the relationship between dust source geomorphology, sedimentology and meteorology and how that influences rates of transport from the Icelandic aeolian system is poorly defined.

2.4 Dust emission at the field scale

Studies focusing on aeolian activity at the field/landscape scale have been sparse at high latitudes (Bullard et al., 2016). Although Iceland is the most well researched high latitude dust source region (Arnalds et al., 2016), very few direct field measurements of dust events have been conducted. Those that have are discussed below.

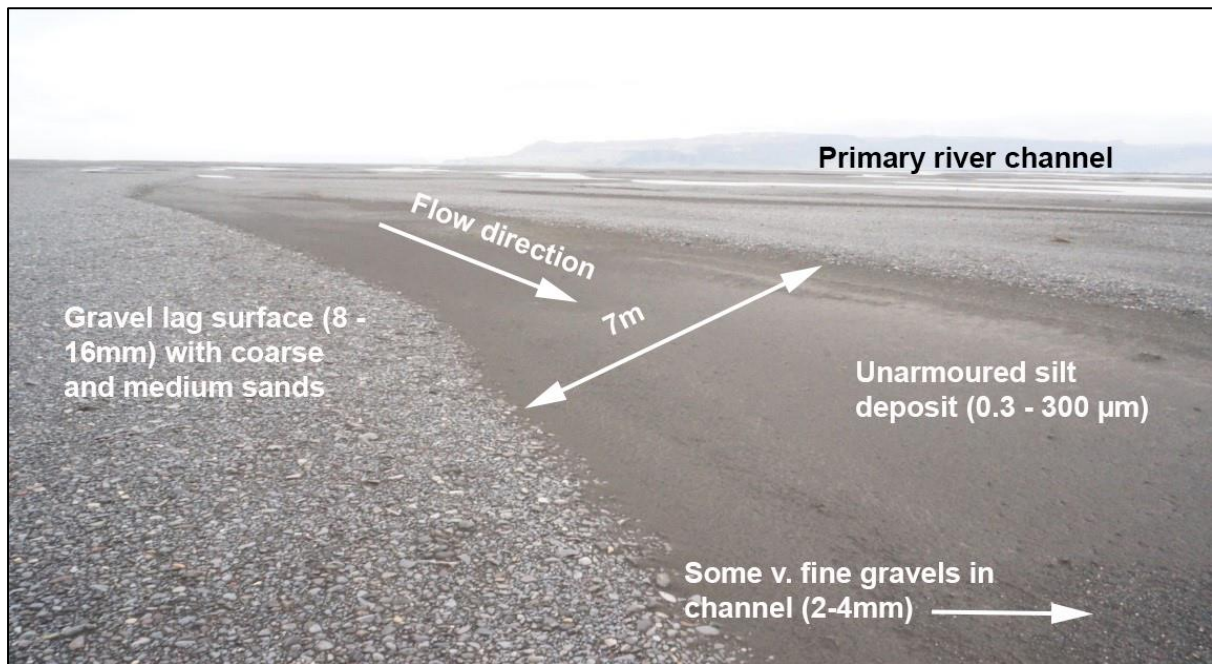


Figure 2.4: The Markarfljot ephemeral channel system, May 2014. Large areas of silt are left unarmoured and unvegetated after river water has retreated.

Early work focused on characterising aeolian transport rates of particles travelling in saltation. Big Spring Number Eight traps (BSNE) and SENSIT saltation counters were used to calculate total horizontal mass fluxes (kg m^{-1}) and threshold shear velocities for motion. Gisladdottir et al., (2005) found that under northerly dry winds at the Hagvatn region (south of Langjökull), the threshold shear velocity for motion for sand grains occurred at 6.2 m s^{-1} on a non-rough flat surface and 10.7 m s^{-1} on rougher surfaces. Total horizontal mass flux exceeded $1000 \text{ kg m}^{-1} \text{ hr}^{-1}$ at wind speeds $> 17 \text{ m s}^{-1}$.

Thorarinsdottir and Arnalds (2012), using a single wind vane sampler at the Mt Hekla basin, showed that aeolian transport rates varied considerably between 25 separate locations within the landscape unit. Maximum total flux varied on an event basis between $0 - 1788 \text{ kg m}^{-1}$, with an average total flux of $244 \text{ kg m}^{-1} \text{ hr}^{-1}$. Spatial differences in sediment transport were attributed to spatial differences in surface sedimentology and proximity to the volcanic system.

Arnalds et al. (2013) measured aeolian transport of freshly deposited ash from the Eyjafjallajökull eruption in 2010. 30 aeolian events were recorded at wind speeds $> 10 \text{ m s}^{-1}$. Horizontal transport fluxes reached $11,800 \text{ kg m}^{-1}$ at a rate of $1,440 \text{ kg m}^{-1}$ (over 6000 saltation counts per minute) in the most intense wind erosion event recorded at the high latitudes.

Although horizontal mass flux is related to total dust flux (Shao et al. 1993; Lu and Shao, 1999; Grini et al., 2002; Shao, 2004), active measurements of dust concentrations are sparse in Iceland. The use of BSNEs to calculate dust concentrations for particles which are $< 10 \mu\text{m}$ (e.g. PM₁₀) has been shown to be problematic. Goosens et al. (2012) showed that the absolute efficiency for BSNEs decreases significantly when wind speed is $> 5 \text{ m s}^{-1}$. Dust events in Iceland commonly occur in wind speeds between $6 - 10 \text{ m s}^{-1}$. (Gísladóttir et al., 2005; Arnalds et al., 2013; Dagsson-Waldhauserova et al., 2014b). Direct measurements of PM₁₀ have focused mainly on monitoring direct volcanic eruptions in Iceland (e.g. Leadbetter et al., 2012) rather than the resuspension of volcanic material as dust storms (Thorsteinsson et al., 2012).

An exception is the work of Dagsson-Waldhauserova et al., (2014b) who measured dust concentrations using a DustTrak Optical Sizer at Mælifellsandur during a dust event in May 2013. Maximum mass concentration per minute was recorded at $1757 \mu\text{g m}^{-3}$ at the peak of the event. Dagsson-Waldhauserova et al. (2015), using a GRIMM EDM 365 located at source, measured a winter dust event at Mýrdalssandur in March 2013. This event reached a maximum concentration per minute $>6500 \mu\text{g m}^{-3}$, with a 24-hour average of $1281 \mu\text{g m}^{-3}$. Although the measurements of Dagsson-Waldhauserova et al (2014b, 2015) are invaluable due to the lack of active dust concentration measurements in high latitude environments, only one dust event was measured. No study has been conducted measuring multiple events during a season at source in Iceland, or within the high latitudes.

2.5 Dust event seasonality

As stated above, there have been no studies conducted focusing on the potential seasonal changes in dust emissions from active field measurements at source in Iceland. Due to this, we lack a significant understanding about the intensity and magnitude of dust events in Iceland and how this potentially varies seasonally. Iceland does have a well-established high-density network of manned WMO weather stations

Table 2.2: World Meteorological Organisation (WMO) weather codes relating to dust events. Codes are assigned every 3 hours in manned WMO weather stations

Synop code	Weather description
06	Widespread dust in suspension in the air, not raised by wind at or near the station at the time of observation
07	Dust or sand raised by wind at or near the station at the time of observation, but no well-developed dust whirl(s) or sand whirl(s) and no dust storm or sandstorm seen
08	Well-developed dust whirl(s) or sand whirl(s) seen at or near the station during the preceding hour or at the time of observation, but no dust storm or sandstorm
09	Dust storm or sand storm within sight at the time of observation, or at the station during the preceding hour
30	Slight or moderate dust storm or sandstorm has decreased during the preceding hour
31	Slight or moderate dust storm or sandstorm no appreciable change during the preceding hour
32	Slight or moderate dust storm or sandstorm has begun or has increased during the preceding hour
33	Severe dust storm or sandstorm has decreased during the preceding hour
34	Severe dust storm or sandstorm no appreciable change during the preceding hour
35	Severe dust storm or sand storm has begun or has increased during the preceding hour
98	Thunderstorm combined with dust storm or sandstorm at time of observation, thunderstorm at time of observation

which record weather codes. These stations assign a code to the current weather type every 3 hours. Of these weather codes, 11 codes are used to indicate the presence of a dust event (O’Loingsigh et al., 2014; Dagsson-Waldhauserova et al., 2014a; Baddock et al., 2017; Bullard and Mockford, 2018). These codes are displayed in Table 2.2. It is therefore possible to create a seasonal dust pattern based on these codes. Figure 2.5 shows the seasonal pattern of dust days (code 06) from Stórhöfði (south Iceland) and Grímsstaðir (north Iceland) from 1992 – 2012 (Bullard et al., 2016). Other codes were emitted in this particularly study because in Stórhöfði it is evident that only code 06 is used to indicate the presence of a dust event (Bullard and Mockford, 2018).

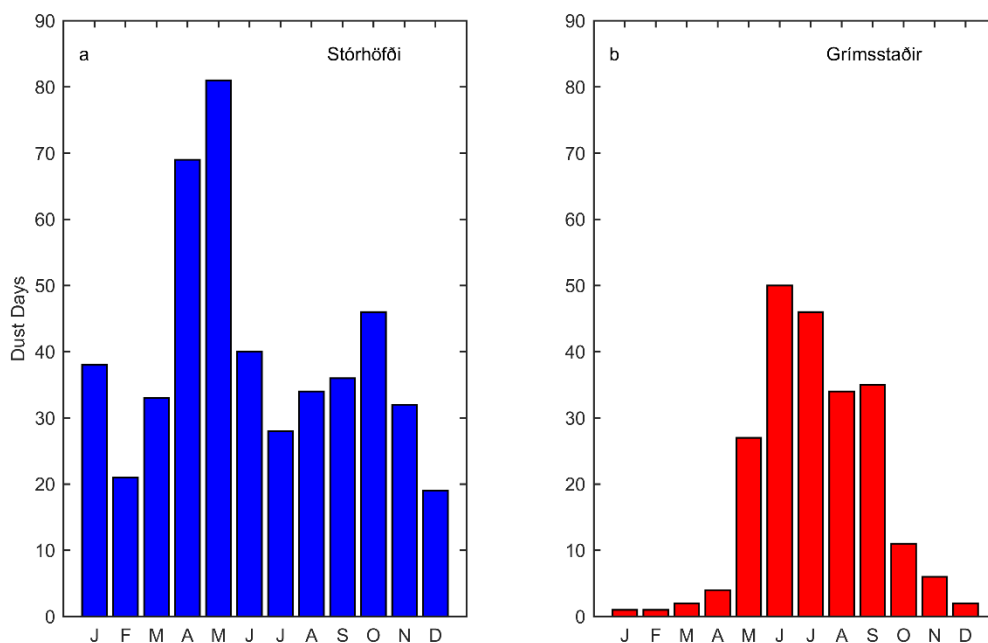


Figure 2.5: Seasonal dust day record for Stórhöfði (South Iceland) and Grímsstaðir (North Iceland) based on a 20-year WMO meteorological data set (Bullard et al. 2016).

In south Iceland, dust occurs all year round but two peaks can be identified during early spring (April/May) with a smaller peak in autumn (September/October). This is also confirmed by active dust measurements taken by Prospero et al. (2012) (Figure 2.6). Measurements were taken at Heimaey, which is approximately 30km offshore south of the Icelandic mainland. A clear peak in spring can be seen for the 6-year record.

In north Iceland, dust events peak in the summer (June/July) and are almost non-existent during winter. Dagsson-Waldhauserova et al (2014a) used a 70-year WMO weather code dataset and concluded the same seasonal pattern differences between north and south Iceland.

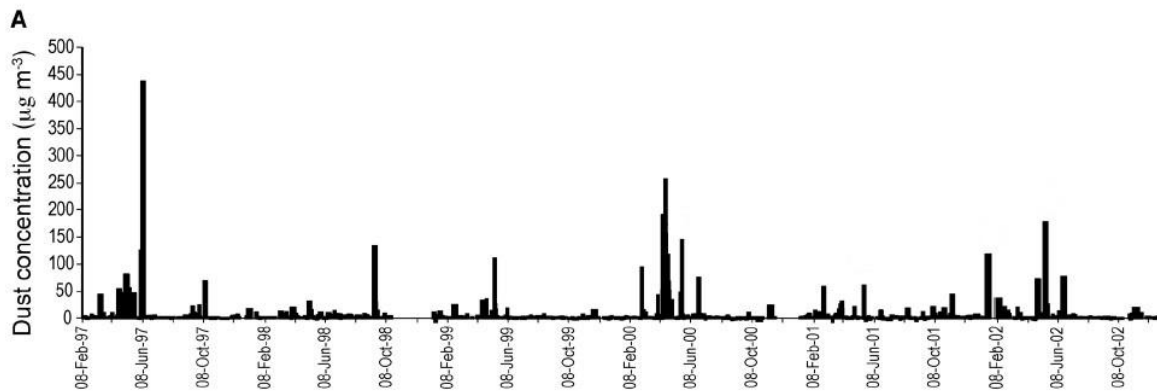


Figure 2.6: 6-year daily dust concentration ($\mu\text{g m}^3$) from Heimaey, Iceland (Prospero et al., 2012). The sensor was placed in a well-defined dust transport pathway (Arnalds, 2014; Baddock et al. 2017)

The temporal differences between north and south Iceland (Figure 2.5) can be attributed to the importance of differing surface drivers which are promoting/inhibiting dust emission. In the north, persistent snow cover during the winter inhibits transport as surface sediments are protected. In the south, snow cover is spatially and temporally sporadic and often does not persist throughout the winter allowing dust emissions to occur. The seasonal dust frequency peaks in early spring and autumn can be attributed to pulses of meltwater suspended sediment which occur as glacial activity increases during spring/summer melting (Hodgkins, 1993; Prospero et al., 2012).

Although the analysis of Dagsson-Waldhauserova et al. (2014a) and Bullard et al. (2016) found the same seasonal patterns with slightly different analytical methodologies, it is important to note that dust storms may be missed at WMO weather stations. This is because weather stations are often not located at dust source and may only be representative of a defined dust storm pathway (Baddock et al., 2017). For example, Storhöfði which has often been used to characterise dust storm activity in southern Iceland (Prospero et al., 2012; Groot Zwaaftink et al., 2017) is located 30 km offshore to the south of the Markarfljot river basin. For dust to be recorded at

Storhöfði, northerly winds must transport material from the Markarfljot river basin to the south. If dust were to be transported in a different direction other than southwards, these dust events will be missed in the record at Storhöfði.

2.6 Remote sensing observations

Remote sensing has shown to be an invaluable tool for identifying dust sources and dust storm frequencies, intensities and magnitudes in the sub tropics at a number of spatial scales (Prospero et al., 2002; Schepanski et al., 2007; Bullard et al., 2008; Ginoux et al., 2012). However, global remote sensing analysis of dust sources has often overlooked sources in Iceland and the high latitudes. For example, Prospero et al. (2002) identified major global dust source areas based on TOMS analysis of daily absorbing aerosol index values. This analysis was restricted to 45°N and S therefore not including Iceland. Ginoux et al. (2012), who used MODIS Deep Blue to analyse global dust sources, did not consider dust sources >50°N or >55°S therefore not including Iceland within the analysis. This is problematic as high latitude dust sources represent a sizable proportion of the global atmospheric dust budget (Bullard et al., 2016).

Although data from numerous satellites has been shown to provide invaluable information on high latitude cold climate dust events (Gasso and Stein, 2007; Crusius et al., 2011; Thorsteinsson et al., 2011; Gaiero et al., 2013), these are often single events. In Iceland, satellite images from MODIS and LANDSAT have been used to identify single dust events (e.g. Thorsteinsson et al., 2011; Dragoniscs et al., 2016; Wittman et al., 2017). These can be of particularly high quality (Figure 2.7) enabling point sources of dust activity to be identified.

However, a systematic continuous assessment of dust storm frequency in the high latitudes using satellites is not possible due to winter darkness, high densities of cloud cover, low zenith angles of satellite sensors (for geostationary equatorial orbited satellites) and a lack of thermal characterisation of dust particles at the surface (Baddock et al., 2009). Therefore, other remote sensing techniques are required to assess dust emissions in the high latitudes.

The use of active remote sensing technologies, such as Cloud-Aerosol Lidar with Orthogonal Polarization (CALIOP) (Winker et al., 2003) and Cloud and Aerosol

Transport System (CATS) have yet to be explored in detecting Icelandic dust events. These types of remote sensing product may be preferential as the issue of cloud cover and winter darkness are negligible. The use of active remote sensing technology has been shown to provide valuable information regarding aerosol type and the height of potential dust plumes in other high latitude regions (Bullard et al., 2016). The issues with these sensors are that satellite overpass time is relatively long and the likelihood of retrievals being obscured by cloud is highly likely. However, the information gathered from a single CALIOP or CATS retrieval of an Icelandic dust event may provide novel information regarding dust in transport in Iceland (e.g. plume height and density).

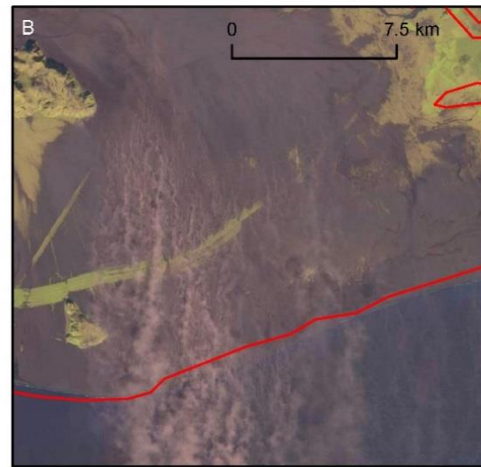
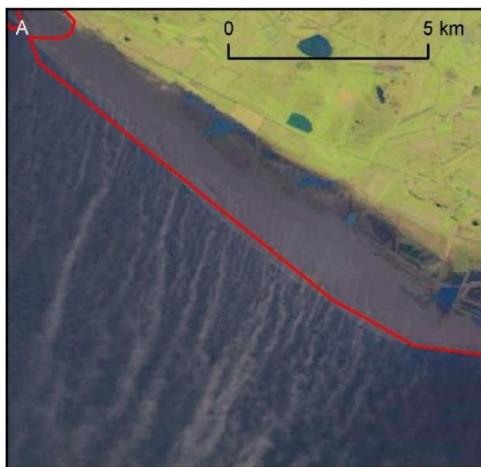
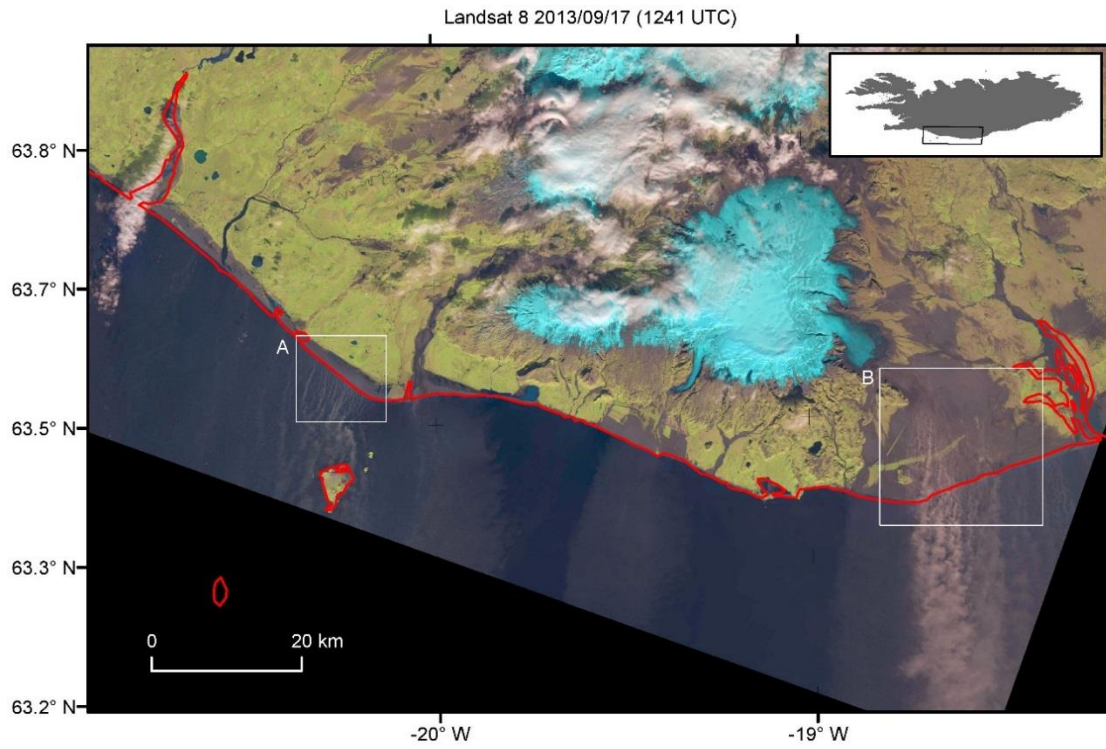


Figure 2.7: Top: Landsat 8 RGB image from South Iceland (17/09/2013). A) Dust storm at Landeyjsandur/Markarfljotsandur B) Dust storm at Mýrdalssandur. Figure courtesy of Matt Baddock

2.7 Modelling of Icelandic dust

With an increased interest in dust emissions in the high latitudes in the past decade, attempts are now being made to use regional and global dust models to predict vertical dust fluxes, dust transport pathways and dust deposition from the high latitudes. Prior to this, contemporary global modelling efforts have fundamentally ignored dust sourced from within the high latitudes. Modelling of dust emission and transport in Iceland has recently been conducted by Groot Zwaaftink et al. (2016; 2017), Wittman et al. (2017) and Baddock et al. (2017). Groot Zwaaftink et al. (2017) used FLEXDUST and FLEXPART simulations (e.g. Stohl et al., 1998) teamed with meteorological and reanalysis data, to estimate vertical dust emission and transport over 27 years. It was estimated that annual emissions from Iceland total $4.3 \pm 0.8 \text{ Tg y}^{-1}$ from 25 annual dust days. These estimates are an order of magnitude lower than those presented by Arnalds et al. (2014) and Dagsson-Waldhauserova et al. (2014). Deposition of material is observed in the high Arctic, but dust particles are not transported to the centre of the Greenland Ice sheet. A clear majority of dust deposition (58%) occurred in the marine environment. The transport pathways suggested by Groot Zwaaftink et al. (2016, 2017) agree with analysis by Baddock et al. (2017), who used HYSPLIT air parcel trajectory modelling to show that a high proportion of air parcels associated with dust transport travel towards the marine environment and not into cryospheric environments (Figure 2.8). Wittman et al. (2017) combined regional dust modelling (e.g. FLEXPART) with surface reflectance measurements from Vatnajökull to show the importance of dust deposition in altering surface ice albedo on the Icelandic glacier systems.

Although the modelling efforts have provided regional context for the relative importance of Icelandic dust emissions and transport pathways, these results need to be taken with care. Groot Zwaaftink et al. (2017) removed the soil moisture function of FLEXPART to promote dust emissions in model simulations. In a high latitude environment, where high humidity and persistent rainfall is normal, the relationship between dust emission and surface soil moisture may be very important.

The surface ice albedo modelling estimates by Wittman et al. (2017) at Vatnajökull significantly overestimate dust deposition in comparison to surface measurements. This again may have been due to the overestimating of dust emission due to the

removal of the soil moisture and precipitation parameters within the model. Baddock et al. (2017) used WMO weather code meteorological data to identify dust activity and only ran simulations on dust days. However, all simulations were run for 72 hours regardless of the magnitude of the dust event. It could be argued that many of the HYSPLIT trajectories are therefore overestimating the potential distance that dust particles may travel before being deposited.

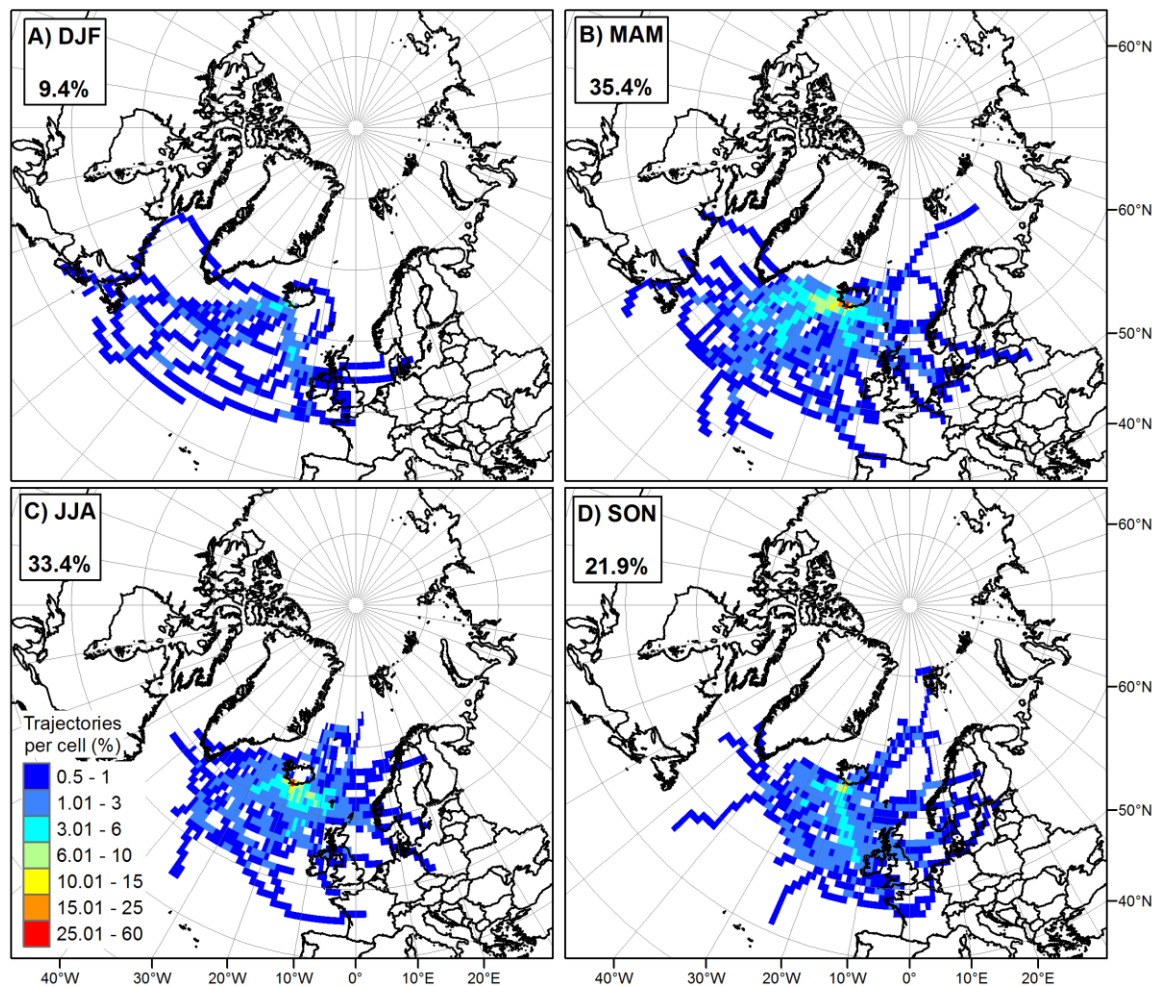


Figure 2.8: Seasonal variation in trajectory line density for 72-hour HYSPLIT air parcel trajectory model outputs started at 100 m height originating from Vatnsskarðshólar on days of observed dust 1992–2012. Input data is the 2.5 ° NCEP/NCAR Reanalysis data (Baddock et al., 2017)

Modelling work is the best tool for estimating the overall impact dust has on the Earth's system and how potentially dust emissions may evolve due to climate change. As is

the case in most high latitude regions, there is still a lack of field measurements of dust activity to fully verify the outputs of these models.

2.8 The impact of dust deposition

Dust deposition plays a significant role in many of the Earth's landscape units (Tsoar and Pye, 1987; Jickells et al., 2005; Griffin, 2007; Ravi et al., 2011; Thorsteinsson et al., 2011; Painter et al., 2012; McKenzie Skiles et al., 2012). In Iceland, research has focused heavily on the impact of dust deposition on glaciers (e.g. Reijmer et al., 1999; Meinander et al., 2016; Dragosics et al., 2016), on soil development (Arnalds, 1987; Dugmore et al., 2009; Gisladdottir et al., 2010) and the impact of deposition in urban areas and the role this plays in decreasing air quality (Thorsteinsson et al., 2011; 2012; Carlsen et al., 2015).

Dust deposition on glaciers has been shown to affect glacial albedo, which in turn alters surface meltwater dynamics and the hydrological regime of the glacio-fluvial system (Painter et al., 2012; McKenzie Skiles et al., 2012). This is problematic in Iceland as approximately 11% of the total area of Iceland is covered by glaciers (Björnsson and Pálsson, 2008). Wittmann et al. (2017) showed through a combination of field measurements and modelling at Vatnajökull glacier, that small amounts of dust can cause a positive radiative forcing, leading to increase supraglacial melt rates. It was suggested that dust deposition in 2013 caused a 1.2 m water equivalent increase in meltwater discharge ($\text{m}^3 \text{s}^{-1}$) during a single melt season. However, dust particles can also insulate glacial ice from incoming solar radiation, hence reducing melt rates (Dragosics et al., 2016).

The relationship between dust deposition and ice/snow melt is extremely complicated. For example, dust particles which are deposited during winter months are likely to be buried by subsequent snowfalls (Painter et al., 2012; Bullard and Mockford, 2018). This means that these particles will not have a positive/negative impact on radiative forcing until the snow has melted. It is possible that particles will be infiltrated through the snow pack and transported out of the glacial system (McKenzie Stiles et al., 2012). Arnalds et al., (2016) suggests that sand sized particles will have a greater impact on reflectance than finer particles, even though silt/clay sized particles have been shown to clump together after several hours following deposition, forming sand sized aggregates (Dagsson-Waldhauserova et al., 2015). Larger particles, however, are

more likely to be transported from the glacial surface, as smaller particles tend to stick to single ice/snow crystals (Painter et al., 2012).

It has also been hypothesised that Icelandic dust deposition may impact the Greenland Ice sheet. This is based on the work of Arnalds (2010), who showed that Icelandic dust plumes can travel for over 1000 km and, Drab et al. (2002), who identified small amounts of volcanic particles in East Greenland. However, stable atmospheric conditions often mean that Icelandic dust particles do not ascend, and travel within 500 m of the surface (Groot Zwaaftink et al., 2016; Baddock et al., 2017; Bullard and Mockford, 2018). This suggests that long distance transport of particles to the Greenland ice sheet from Iceland is improbable. Baddock et al., (2017) showed using dust day identified HYSPLIT trajectories that air parcels sourced from Icelandic dust sources could not ascend onto the centre of the Greenland Ice Sheet and would often skirt the edges of the continent thus making deposition most likely in the coastal regions (Figure 2.7). This has also been shown through the modelling work of Groot Zwaaftink et al. (2016), who showed that the vast majority of deposition from Icelandic dust events occurred in the North Atlantic.

Dust deposition is a critical component to soil development in Iceland (Gunnarsson et al. 2015; Arnalds et al., 2016). Continuous volcanic activity provides one of the highest sedimentation rates in the world, where redistribution of volcanic tephra by wind action causes soil depth to increase between approximately 0.01 – 0.5 mm yr⁻¹ (Gunnarsson et al., 2015; Arnalds et al., 2015; Arnalds et al., 2016). The redistribution of soil has been noted since the arrival of human inhabitants in AD 874, where the introduction of land practices for agriculture and animal grazing caused large scale vegetation reduction, and in turn wind erosion (Dugmore et al., 2009; Gísladóttir et al., 2011). Evidence for this can be found in farm surveys, sagas and annals which clearly document landscape change (Arnalds et al., 2001a). The large-scale removal of vegetation has caused substantial parts of the Icelandic landscape to become unstable. This instability is heightened considerably after volcanic events, where sediments are deposited on unprotected unvegetated landscapes. The redistribution of volcanic tephra by the wind during these periods has been linked to increases in dust events and aeolian activity (Arnalds et al., 2010; Arnalds et al., 2016).

Aerosols from dust storms in Iceland are often transported to Reykjavik, where approximately 80% of the total population of Iceland reside (Thorsteinsson et al., 2011; Baddock et al., 2017). The WMO health limit for PM₁₀ air pollution is 50 $\mu\text{g m}^{-3}$ averaged over a 24-hour period (WHO, 2005). Thorsteinsson et al. (2011) reported that this limit was breached 20 times in 2009, 19 times in 2008, 17 times in 2007 and 29 times in 2006. These exceedances in Reykjavik PM₁₀ air quality have mainly been associated with natural dust sources from the south coast (Thorsteinsson et al. 2011; Baddock et al., 2017). Thorsteinsson et al. (2011) used HYSPLIT back trajectories and calculated potential source concentrations from known dust events at Landeyjsandur. It was shown that for PM₁₀ in Reykjavik to reach 200 $\mu\text{g m}^{-3}$, Landeyjsandur must produce approximately 35 $\text{g m}^{-2} \text{h}^{-1}$ at source. Baddock et al. (2017) used a systematic forward HYSPLIT trajectory analysis over a 20-year period to show that air parcels associated with dust events from the south coast a travel through Reykjavik approximately 6.25% of the time.

This is important because dust particle ingestion has been shown to be a serious human health concern in regions which are affected by dust events. The ingestion of material <10 μm has been shown to increase the risk of lung cancer, heart attacks, strokes and heart arrhythmias (Mossman et al., 2007). Particles which are ultrafine (<1 μm) have been shown to deposit in brain tissues (Calderon-Garciduenas et al., 2004) and affect child fertility by infiltrating into the placenta of fetuses (Wick et al., 2010).

Dust deposition in oceanic environments has been shown to provide an important nutrient source for aquatic ecosystems (Jickells et al., 2005; Li et al., 2008; Schroth et al., 2009; Crusius et al., 2011, Prospero et al., 2012). This is because dust particles provide a source of iron for phytoplankton communities to flourish (Jickells et al., 2008). However, the input of iron, from dust transport, may only be important in oceans which are iron limited, such as the Southern Ocean (Li et al., 2008) and the Gulf of Alaska (Crusius et al., 2011). Arnalds et al., (2016) suggested that dust which is deposited into the North Atlantic may have an impact on marine biodiversity. Arnalds et al. (2014) used a GIS based mapping approach to estimate iron supply from natural dust emissions in the North Atlantic. It was estimated that deposition rates varied from 1-800 g m^{-2} per year. However, no empirical link has been made between Icelandic dust and the fertilisation of the North Atlantic. Achterberg et al. (2013) observed increased

iron levels in surface waters in the North Atlantic directly after the 2010 Eyjafjallajökull eruption; however, these increases were short lived. The timing of deposition of soluble iron through dust events is critical to whether the iron can be used for an increase in oceanic productivity. This is often related to sunlight; as many iron limited oceanic systems are subjected to winter darkness. During these periods, ocean productivity is very low (Schroth et al., 2009). Arnalds et al. (2014) and Prospero et al. (2012) both suggest that because most dust events in South Iceland occur between March and May that during these periods, Icelandic dust may have an impact on surface water iron contents. However, as conceded by Arnalds et al. (2014), the stable input of nutrients via fluvial transport (e.g. the terrestrial glacio-fluvial environments), is most likely to have a greater impact.

It has been suggested that Icelandic dust emissions may increase with rising global temperatures causing an increase in available sediment for aeolian entrainment (Björnsson and Pálsson, 2008). Quantifying the mineralogy, size characteristics and shape of Icelandic dust particles from a range of dust source units to help us fully understand the potential impact these sediments may have on human populations in the future is, therefore, critical. The research has been mainly focused on pure volcanic ash (Pieri et al., 2002; Dellino et al., 2012). The spatial variability of sediment characteristics of Icelandic dust sources means that further work is required to understand the differences in dust particle properties in relation to their dust source. This research would allow research quantifying the relative impact of Icelandic dust on various ecosystems to consider differences in particle shape, size and mineralogy.

2.9 Summary

This chapter has outlined our current understanding of the Icelandic dust cycle. It is clear further research is required in understanding the relationship between dust source and dust particle properties and how this varies spatially. There is also need for further field measurements monitoring dust events at source. These measurements are not only valuable for understanding the Icelandic dust cycle but will provide much needed field measurements of high latitude dust events which can be used to verify regional modelling attempts. This thesis will now present three empirical chapters, which were set out at the start of this thesis, to assess the sources, drivers and sedimentology of Icelandic dust events.

3. Sedimentological characteristics of Icelandic dust sources

In the first of three empirical chapters, the differences in sedimentological characteristics of the dust source units at Markarfljot will be examined. These differences will be important in driving dust storm characteristics and will be vital in interpreting dust event morphology in chapter 4 and chapter 5.

3.1 Introduction

The sedimentological and geomorphological properties of dust sources vary considerably globally (Bullard et al., 2011) and are highly spatially variable (Prospero et al., 2002; Washington et al., 2003). The importance of dust source geomorphology and sedimentology in controlling dust emissions has been well documented in subtropical deserts (Bullard et al., 2008; Lee et al., 2009; Parajuli and Zender, 2017). It is generally accepted that although dust particle size and density alter during transport (Desboeufs et al., 2005), the initial grain surface sedimentology and conditions control dust particle properties (Gills et al., 2006; Mockford et al., 2013). This is important as the impact of dust deposition on atmospheric, cryospheric, oceanic, lacustrine and soil environments will be dependent on the physical properties of the particles (Jickells et al., 2005).

The relative importance of specific dust sources for the magnitude, frequency and intensity of dust emissions has often been quantified for selected regions using satellite remote sensing techniques (Bullard et al., 2008; Lee et al., 2009; Lee et al., 2012; Baddock et al., 2016). Bullard et al. (2008) assessed dust source contributions to dust loadings in the Lake Eyre Basin, Australia using MODIS. In the period 2003-2006, 529 dust plumes were classified from 11 unique land use units, with the highest proportion of dust plumes originating from areas with aeolian deposits (e.g. dunes, sand fields). Lee et al., (2009) identified a major dust event in the Chihuahuan region of Texas and New Mexico and the Southern High Plains. Within this single event, 146-point source plumes were identified in MODIS data. Of these, the largest unique dust source unit was cropland (58%), which has been related to extensive agriculture activity in this region (Lee et al., 2012). Although both studies indicate the prevalence

of different dust source units in emitting dust, they do not address the variation in dust particle properties between units.

The relative importance of dust emitting geomorphologies was evaluated by Bullard et al. (2011) who proposed a conceptual model for dust emission frequency from preferential dust sources (PDS) (Table 3.1). PDS is a simple land-based classification system which is used to determine the temporal and spatial characteristics of dust emitting units, as well as their likely sedimentology, soil erodibility and dust emission potential. The scheme was tested against dust plume identification from MODIS data for the Chihuahuan desert, the Lake Eyre Basin and North Africa. The analysis showed the importance of ephemeral lakes as dust sources, even though their relative surface area is minor compared to other land use units (e.g. aeolian sand sheets). Preferential dust source does not consider dust storm intensities but does provide valuable information regarding dust storm frequencies from separate geomorphological units. Baddock et al. (2016) teamed analysis using preferential dust source from the Chihuahuan desert with MODIS Deep Blue Collection Level 6 data (Ginoux et al., 2012). The PDS aligns with dust emission values from the Deep Blue Collection, showing surfaces that had been identified as prominent dust sources (ephemeral lakes, high relief unincised, and certain dune formations). However, the study was based on a long-term aerosol loading and does not help explain annual and seasonal variations in dust emissions. This is because local interactions between dust source geomorphology, sedimentology and meteorology control annual rates of dust emission. Although the technique proposed by Baddock et al. (2016) has been shown to work in subtropical deserts, this technique may prove difficult in high latitude environments ($>50^{\circ}\text{N}$, $<40^{\circ}\text{S}$), where cloud free days are rare (Bullard, 2017). Dust retrievals from Deep Blue and/or AOD are discontinuous in the high latitudes and, therefore, may under-estimate dust loadings from specific source areas.

Table 3.1: Preferential Dust Source Classification from Bullard et al. (2011)

Emission Sources	Typical Soil Textures	Limitation on Emissions	Dominant Temporal Pattern	Importance for Dust Emissions ^a
<i>Lakes</i>				
1a Wet	Sand, Silt, Clay	Availability-limited	No variability	Low
1b Ephemeral	Silt, Clay	Supply-limited	Periodic emissions triggered sediment supply and reworking following high rainfall	High (if sandblasting) – Medium [<i>high</i>]
1c Dry, consolidated	Silt, Clay	Availability-limited	No systematic variability	Low
1d Dry, non consolidated	Silt, Clay	Transport capacity limited	Emission when wind velocity > entrainment threshold	High (if sandblasting) – medium [<i>high</i>]
<i>High Relief Alluvial Systems</i>				
2a Armored, incised	Mega-gravel, Gravel, Sand	Availability-limited	No systematic variability	Low
2b Armored, unincised	Mega-gravel, Gravel, Sand	Availability-limited	No systematic variability	Low
2c Unarmored, incised	Gravel, Sand, Silt, Clay	Supply-limited	Periodic emissions triggered by sediment supply and reworking following high rainfall	Medium
2d Unarmored, unincised	Sand, silt, clay	Supply-limited	Periodic emissions triggered by sediment supply and reworking following high rainfall	Medium-High [<i>medium</i>]
<i>Low Relief Alluvial Systems</i>				
3a Armored, incised	Gravel, Sand,	Availability-limited	No systematic variability	Low
3b Armored, unincised	Gravel, Sand, Silt, Clay	Supply-limited	Periodic emissions triggered by sediment supply and reworking following high rainfall	Medium
3c Unarmored, incised	Sand, Silt, Clay	Transport capacity limited	Emission when wind velocity > entrainment threshold	Low
3d Unarmored, unincised	Sand, Silt, Clay	Supply-limited	Periodic emissions triggered by sediment supply and reworking following high rainfall	Medium
<i>Stony Surfaces</i>				
4 Stony surfaces: low angle surfaces; not connected to fluvial source of fines	Gravel, Sand, Silt, Clay	Availability limited	No systematic variability	Low
<i>Aeolian Systems</i>				
5a Sand sheet	Sand	Supply- and/or availability-limited	Variability dependent on vegetation cover, water table etc.	Low to medium [<i>medium</i>]
5b Aeolian sand dunes	Sand	Supply- and/or availability-limited	Variability dependent on dune type, dynamics, sedimentology and palaeohistory	Low to high [<i>medium</i>]
6 Loess	Silt, Clay	Availability-limited	Variability dependent on vegetation cover	Low to medium [<i>low</i>]
<i>Low Emission Surfaces</i>				
7 Low emission surfaces: bedrock, rocky slopes, duricrust (snow/ice permanent cover)	Mega-gravel, Gravel, Sand, Silt, Clay	Supply-limited	No systematic variability	Low

The use of satellites to map geomorphology and/or sedimentology of dust sources in the high latitudes is therefore problematic. Other techniques such as the use of aerial photograph and/or photogrammetry techniques may provide useful as it removes the issue of cloud cover. Aerial photography has long been used in the mapping of sedimentological units in a variety of geoscientific disciplines (La Chapelle, 1962; Okin et al., 2001; Ries and Marzloff, 2003; De Rose and Basher, 2011). Aerial photography can provide high resolution data sets which provide sedimentological information at the sub-basin scale (Bullard et al., 2008; Lee et al., 2009). In landscapes where the spatial variation in sediments is high, such as in outwash channel networks in high latitude environments, this level of resolution would be required to map subtle changes in surface sedimentology. This level of detail would not be available using freely available satellite data.

Aerial photography, often in tandem with satellite and ground-based measurements, has been used for many decades to map sedimentological differences within landscapes (Salama et al., 1994; Winterbottom and Gilvear, 1997; Harvey and Hill, 2001). The issue with aerial photography is that it is expensive to conduct repeat surveys (Anderson and Gatson, 2013). This has led to the rising use of unmanned aerial vehicles (UAVs) across the geosciences (Ryan et al., 2014; Tonkin et al., 2014; Sieberth et al., 2014; Ely et al., 2017). The use of a UAV for surveying allows users to repeat surveys at low costs at a variety of spatial and temporal resolutions (Anderson and Gatson, 2011). For mapping sedimentology, at an appropriate spatial scale, changes in the relative proportion of sub-basin scale landscape units is possible (Westoby et al., 2015; Woodget et al., 2017).

UAVs, using structure from motion photogrammetry approaches, have been used successfully to estimate grain size for gravels (Carbonneau et al., 2004; Woodget et al., 2017). However, for particles < 2000 μm , the spatial resolution of images provided is unlikely to provide sufficient information for this to occur. For dust sources, which are dominated by particles < 2000 μm , the best approach for characterising variations in grain size between units is ground-based measurements. Ground-based approaches, such as particle sediment sizing and optical microscope techniques, allow us to understand the physical properties of ground-based sediments, and in turn, the relationship between ground based and airborne particles.

Studies in Iceland have focused on the sedimentological components of several dust source regions (e.g. Krigström, 1962; Buck, 1974; Maizels, 1989; 1991; 1993; Magilligan et al., 2002; Marren et al., 2003), no study has linked dust particle properties with source sedimentology. Dagsson Waldhauserova et al. (2014b) studied the physical properties of dust particles collected during dust events at Mælifellsandi, Iceland by measuring dust concentrations and dust particle number concentrations using an in situ DustTrak 8533 aerosol monitor. It was shown that dust particles, at 1m height, were extremely fine with the highest proportions of material being between 0.3-0.337 μm . The relative proportion (%) of the finest particles also increased with increasing dust concentration. Mineralogical and geochemical analyses indicated the dominance of volcanic glass-sphered particles and plagioclases. The geochemical signatures and size distributions of dust particles are consistent with the analysis of Arnalds (2001) who expects to find large proportions of silt close to the glacial system, with an increasing sand content away from the glacial system (Gisladdottir et al., 2005; Arnalds et al., 2016).

However, the use of a DustTrak 8533 aerosol monitor for estimating dust particle size distribution is problematic as it only measures material $<10 \mu\text{m}$ (Goosens et al., 2012). Although most would agree that particles $<10 \mu\text{m}$ are the most important due to their potential to travel long distances; at source, it is important that the total dust suspension size distribution is assessed (Klose et al., 2017). These problems could be resolved with the simultaneous collection of material using a passive dust sampler (e.g. BSNE, MWAC) (Zobeck et al., 2003; Mendez et al., 2011), although passive samplers have been shown to have varying levels of efficiency for catching silt and clay sized particles in suspension (e.g. Mendez et al., 2011; Goosens et al., 2012).

From a given surface, there are two possibilities for the emission of dust particles. Firstly, dust sized particles (e.g. silts and clays) which are already in the surface sedimentology can be entrained. This has been referred to as the dust emission potential of sediments (Bhattachan et al., 2012; 2015). For example, Mockford et al., (2013) showed that the dust emission potential decreased with an increasing fine sand content, whilst increasing with increasing proportions of silt and clay within the parent sediment matrix. Preferential dust source (Bullard et al., 2011; Table 3.1) uses typical sediment textures of varying geomorphological units to assess the potential of dust emissions for a given surface. In reality, the proportion of silts and clays within the

parent sediment matrix, may not lead to an increase in dust emissions because of the rising importance other meteorological factors have on controlling the availability of sediments (Cornelis and Gabriels, 2003; Ravi et al., 2006). Secondly, dust sized particles can be actively created during transport through active aeolian abrasion (Whalley et al., 1987, Wright et al., 1998; Bullard et al., 2004; Bullard and White, 2005; Bristow and Moller, 2017). The importance of the process of aeolian abrasion for creating dust sized particles will be discussed at length during Chapter 5. The importance of these two factors will be governed by the sedimentological characteristics of the surface particles and the processes which drive dust emission at a given surface (Shao et al., 2011; Kok, 2011).

The impact of surface sedimentology on the dust emission potential of different sediment groups has been assessed in the subtropics. Gills et al. (2006) used a laboratory dust generator to assess how different soil textures affect dust emission. It was concluded that soils with high proportions of fine sand produced the smallest quantities of dust but emitted the highest proportions of particles $< 2\mu\text{m}$. This was attributed to sand particles being inherently difficult to abrade, but when abrasion did occur, very fine fragments would chip off from singular sand grains. This was also observed by Mockford et al. (2013) who found, from 45 different soil texture combinations, that the finest particles were created by the coarsest sands, whereas soil matrices with high proportions of silt and clay preferentially emitted particles within the ranges 2-10 μm . In this case, sands seem to have a low dust emission potential but have the potential to create dust sized sediments via aeolian abrasion.

Although laboratory experiments in generating dust are valuable, their validity in terms of representing the natural state of a dust emitting system is open to debate. For example, samples used in a dust generator must be air-dry, as otherwise it is likely that the original sample would stick to the inner transport tubes of the equipment. The impact of surface soil moisture on dust emission will vary dependent on surface sedimentology and regional meteorological controls. A soil matrix which is made up entirely of particles of silt and clay sized particles ($<63\mu\text{m}$), when dry, may be a significant source of dust because of the available sized sediments and a lower threshold friction velocity for motion (Gills et al., 2006). However, it could be argued, that without the impact of saltating sand sized sediments dislodging sediments (Shao et al., 2001; Grini et al., 2002), emissions from these surfaces will be low. Others have

argued that aerodynamic entrainment, particles being directly lifted from the surface without being impacted by other sediments (Macpherson et al., 2008; Klose et al., 2014; Parajuli et al., 2016), is a significant dust transport process. Regardless, surface water retention rates in soils in high clay/silt soils will be drastically greater than in soils with higher sand contents, due to different soil drainage properties (Nielsen et al., 1973; Rawls et al., 1982; McKenna Neuman and Nickling, 1989).

It is important to further understand the relationship between surface sedimentology and airborne particle size distribution because it will help improve regional and global climate models predict the impact dust has on the atmosphere, as the size distribution and shape of dust aerosols influences the radiation budget (Tegen and Lacis, 1996).

3.2 Aims and Objectives

Therefore, the main aim of this chapter is:

To compare the sedimentological characteristics of two Icelandic dust sources and assess the impact these sediments have on dust particle characteristics

This will be achieved by answering the following objectives:

- 1) For an active dust source area, what proportion of this area has high dust emission potential?
- 2) For the areas identified as having a high dust emission potential, what are the physical characteristics of these particles?
- 3) How do variations in surface sedimentology affect dust particle properties?

3.3 Methods

3.3.1 Study Site

The study region is displayed in Figure 3.1. Markarfljot is a large glacial river which is fed by the volcanic systems of Eyjafjallajökull and Mýrdalsjökull. The downstream outwash plains have been identified as contemporary dust sources from field observations and satellite imagery (Figure 3.1). Within this river basin, there are two separate dust source units. The first is an ephemeral channel system (Figure 2.3) which incorporates large areas of glacio-fluvial gravels with unarmoured silt drapes. Discharge from the main river channel often inundates large areas of this channel

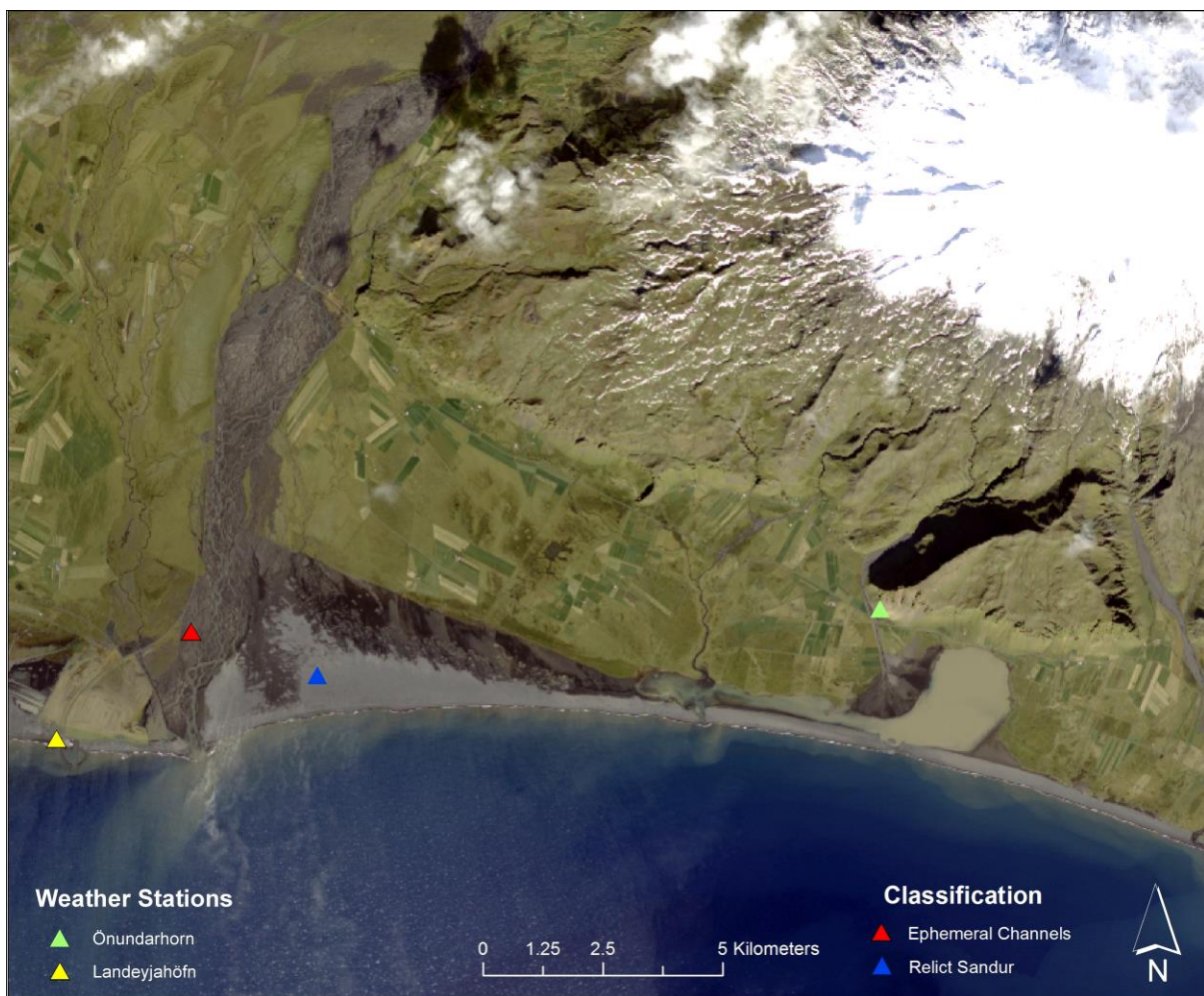


Figure 3.1: Landsat 8 image (19/09/2013) from Markarfljot, South Iceland. The two identified dust source regions are marked with triangles. Dust can be seen being entrained from both source regions. The ice cap is Eyjafjallajökull

system during periods of high flow (see Figure 2.3) and is assumed to be the main sediment supply to the area. The second is a relict sandur system (Figure 3.3), which has been identified to be Holocene jökulhlaup deposits (Maizels, 1991). Surface sediments are unarmoured and free of vegetation.

Markarfljot is an excellent location for this study, and in a wider context for this thesis, for several reasons. Firstly, it has been shown to emit dust regularly (Prospero et al., 2012). Secondly, there is two separate landscape units associated with the emission of dust particles. These units differ geomorphologically and sedimentologically. These units are also broadly representative of the main dust source units in Iceland (Arnalds et al., 2016). Thirdly, the site is easily accessible and is reasonably spatially confined.

3.3.2 Aerial mapping

For dust sources which have distinct geomorphological/sedimentological units, it may be possible to distinguish between them by aerial photography from an unmanned aerial vehicle (UAV). UAVs have become increasingly popular within geophysical research as they allow users to access previously inaccessible and dangerous areas (Obanawa et al., 2015) and cover large areas in relatively short periods of time. The spatial resolution of the output that the user requires will govern the choice of platform, type of camera and flying heights for any given UAV survey. For example, if the user were to require a very high-resolution DEM of a small area, the flying height could be reduced and the use of a rotary wing (e.g. helicopter) platform would be preferential to a fixed wing system.

The UAV used is a self-built delta wing platform (Figure 3.2). It has a wingspan of 1.2m and weighs approximately 1.4kg at full payload. It is fitted with an ArduPilot autopilot which makes the plane fully autonomous apart from in landing where an assisted manual mode is used. Aerial photographs are taken on a systematic basis from an attached down facing camera. A Sony Nex5R high quality compact camera is used in this study. The swath of the image is a function of the flying height which in this study is set to 100m (330ft). This camera provides 16.1-megapixel images covering an approximate area of 100m² when flown at a height of 100m. The choice of camera is solely based on UAV payload. It would be preferential to use a higher resolution camera (e.g. a standard DSLR), however the total payload of the UAV cannot exceed 2kg. Nevertheless, after optimising focus and shutter speed settings based on the

environmental characteristics of the surface, it provides extremely high-resolution photographs. The pixel size achieved with this set up is 2.92cm per pixel. For this study, the main purpose is geomorphological mapping and therefore the quality of the camera and photographs are more than sufficient. The camera is triggered using an integrated infra-red function controlled by the autopilot and takes photos approximately every 10m of horizontal flight (which is calculated by an on-board accelerometer). To achieve the highest quality results in UAV surveys, image overlap is imperative as it allows features to be identified in multiple images and allows the easy manipulation in photogrammetry analysis.



Figure 3.2: Loughborough University Delta Fixed Wing Unmanned Aerial Vehicle

One important part of a UAV survey is the ground control points (GCPs) which are used during the analysis to identify known points within the reconstruction. These geo-referenced points can be identified within individual photographs. GCPs were constructed by using pink spray paint to spray large crosses onto various points within

the ephemeral channel system. The points were surveyed using a Trimble differential GPS.

Orthophoto and DEMs were created using Agisoft Photoscan. Photoscan is photogrammetry software which uses the concept of structure from motion (SfM). SfM uses overlapping images to create 3D point clouds based on the identification of recognising objects within more than one image. The images are stitched together using camera locations from the UAVs autopilot and improved using the GCPs. Outputs from Photoscan were exported to ArcMap for visualisation purposes.

A survey, consisting of 4 separate flights, was conducted at the ephemeral channel network in May 2014 (Figure 3.3). Due to strong winds and persistent rainfall events during this field season, repeat surveys of the ephemeral channel network were not possible. In May 2015, surveys were scheduled for both the ephemeral channel system and the relict sandur system. However, due to mechanical and technical difficulties, these surveys were not conducted.

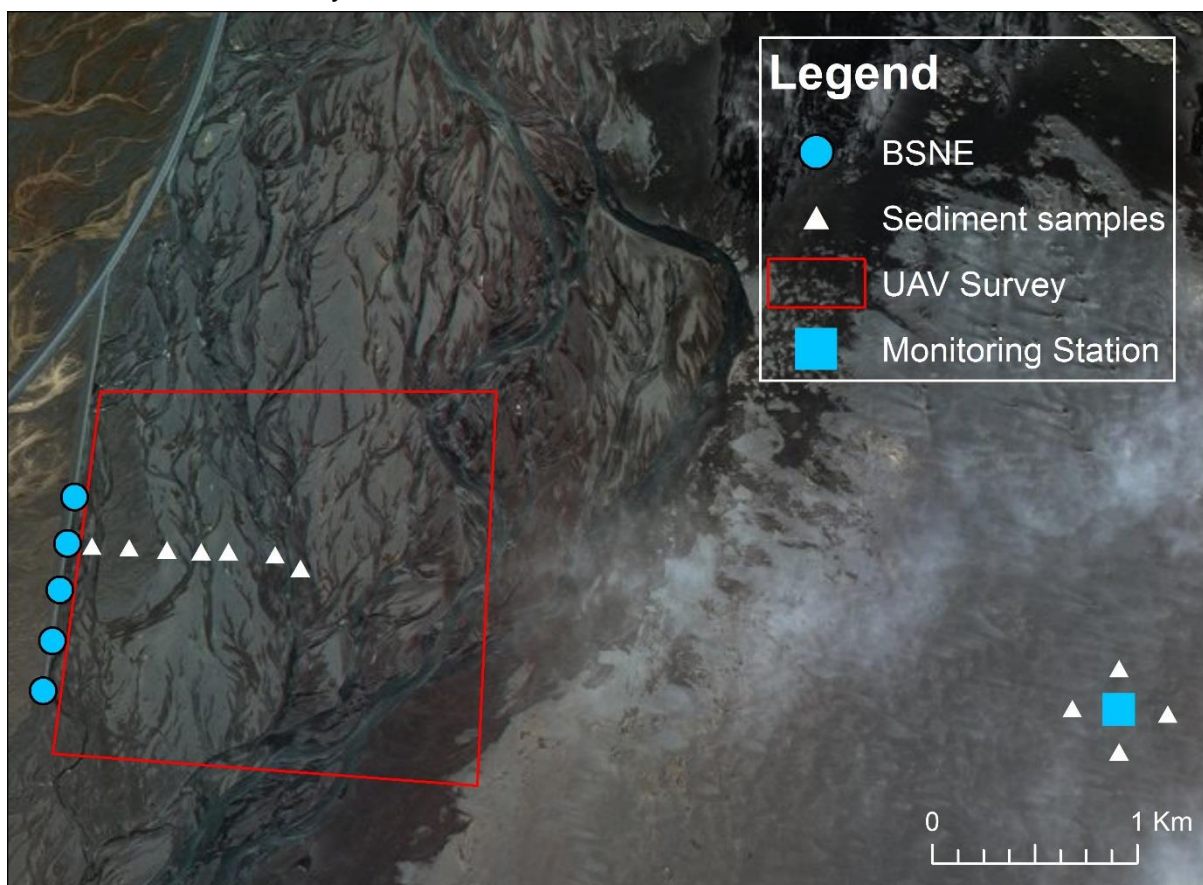


Figure 3.3: Sampling strategy for UAV, sediment sampling and aeolian monitoring at the Ephemeral Channel system and the Relict Sandur system

3.3.3 Sediment sampling

Surface sediments were collected to a depth of <5mm from both field sites. This was to ensure that only sediments which were likely to be prone to wind erosion were analysed. For the ephemeral channel system, 5 samples of each identified facies group were collected from the ephemeral channel system. These included unarmoured sediments within the exposed channel network and sediments which are blanketed by a gravel lag (see section 3.3.4 for details on the sizing of these sediments). At the relict sandur, 5 surface samples were taken; one at the site of the monitoring equipment and 4 others approximately 200m from the monitoring equipment in north, south and east and westerly directions (Figure 3.3).

Wind-blown sediments were captured using modified 'Big Spring Number Eight' (BSNE) traps (Fryrear, 1986) over a 6-week period at the ephemeral channel system in May/June 2014. An 8-week monitoring period in May 2015 was conducted at both the ephemeral channel system and relict sandur system. Goosens and Offer (2000) suggest that, for dust sized particles, BSNE traps are only 40% efficient. However, they have been widely used in aeolian field studies (Gillette et al., 1997; Bullard and Austin, 2011; Gillies et al., 2013).

All traps were emptied every 24 hours. Trap locations and placing differed between the two field sites. At the active ephemeral channel site, BSNE traps were not placed at the surface because of the possibility of flooding which would potentially destroy the samplers. Therefore, 5 traps were mounted at 0.5m on a 2m flood defense directly west of the channel system. At this height, material collected in the traps would be in suspension. Traps at the relict sandur site were placed in a vertical array and were mounted at 0.3 m, 0.6 m, 1.4 m and 2.4 m (Figure 3.4).

3.3.4 Particle size distribution analysis

Various techniques to determine particle size were undertaken in this project for sediments in distinct size classes.

For surface particles >1400 μm (e.g. gravels at the ephemeral channel system), the automated photographic approach SEDIMETRICS (Graham et al., 2005a, 2005b), was used. This approach was used to allow on site characterisation of surface gravels

without having to transport them back to the United Kingdom for analysis. Seven 10x10m sites were marked using a DGPS with 50-80 images being taken at each site (Triangles on Figure 3.3). The area was split into 10 transect lines, with a 1m gap between each line (Figure 3.5). This was done to allow the whole area to be represented in the particle size distribution analysis. These sites follow the sediment sample 1, which would show channel variation of gravel size as a function of distance from the main river channel (Figure 3.3). Images are taken vertically using an RGB camera over an oversized wooden frame with 4 bolts (Figure 3.6). Because the distance between each bolt is known, the relative size distribution of the particles within the area of the 4 bolts can be calculated (Graham et al., 2005a). Greyscale images are then transferred into the SEDIMETRICS package, where the distance between the four bolts are selected. An optimal image processing based on 416 permutations of model parameters allows for the relative sizing of grains (Graham et al., 2005b).



Figure 3.4: Monitoring wind erosion using BSNE Traps on the relict sandur system at Markarfjot (June 2015)

For all sediments $<1400\mu\text{m}$, sediment size was analysed using a Beckman-Coulter LS280 laser sizer, which assesses particle size in a range from 0.37 to 2000 μm in 93 size bins. This included surface sediments from the ephemeral channel network and the relict sandur system as well as all airborne sediments. Sediments were desiccated for 72 hours and shaken in DI water in a water bath for 30 minutes prior to analysis. This was to allow the break-up of aggregates allowing full particle dispersion. Particles were passed through a 1.4 mm sieve to exclude fine gravels. Runs were 60 seconds, and each sample was run 6 times.

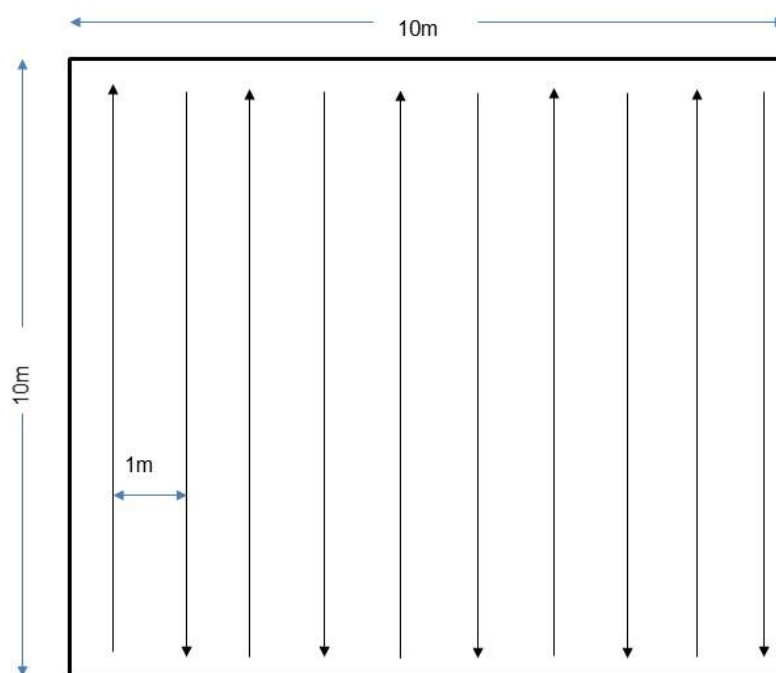


Figure 3.5: Conceptual diagram for SEDIMETRICAL surveys at the ephemeral channel system

The Beckman-Coulter LS280 has two modes to measure particle size distributions; one is to use a circulation chamber and other is to use a micro-volume unit. The use of the circulation chamber is preferred, however is inappropriate for when sample volume is small. As many of the dust events were low in magnitude, the micro-volume unit was used to assess these sediments after they had been combined into one sample. This was to allow a reliable dust particle distribution from both the ephemeral channel network and the relict sandur system. All other sediments were analysed

using the circulation chamber, however to allow an easy comparison, all other particle size distributions from the laser sizer are also combined samples.

3.3.5 Scanning Electron Microscope

A Field Emission Gun Scanning Electron Microscope (FEG-SEM) was used to assess particle morphology and geochemistry. The FEG-SEM is a high-resolution SEM ideal for assessing particles at the sub-micron scale. A sample is placed on an aluminium hub. If the sample is non-conductive, it will become electrically charged within the SEM. Therefore, particles are coated with a 5-10 nm gold palladium coat. This allows the SEM to produce high resolution sample images by beaming high energy electrons over the surface which interacts with the underlying atoms within the sample. A vacuum is used prior to analysis to eliminate any atmospheric composition which may have formed within the sample. The benefit of using a FEG-SEM instead of a standard



Figure 3.6: Automated sediment sizing using technique described in Graham et al., (2005a, 2005b)

SEM is that energy dispersive X-ray analysis (EDX) can be achieved simultaneously. All SEM micrographs are at the same resolution; the scale is image dependent.

Interpretation of the micrographs was achieved by using the sand grain atlas guides presented by Krinsley and Doornkamp (1973) and Mahaney et al (2003). Due to relatively small sample sizes (15 images per sample), features were not quantitatively measured, but qualitative interpretations are made from the presence of common features found on multiple grains from multiple images.

3.4 Results

3.4.1 Aerial mapping

Figure 3.7 is the UAV orthophoto generated for the ephemeral channel system from 4 survey flights (total 390 images). The XY error is 0.39 m, the Z error 1.35 m and the total RMS error 1.41m for the orthophoto. Three landscape units can be identified from the orthophoto. These include unarmoured ephemeral channel system networks, armoured gravel lag surfaces and channels inundated by meltwater. To calculate percentage area for each unit, a classification scheme based on texture analysis can be undertaken. Figure 3.8 shows a supervised classification of the ephemeral channel system. This has been post-processed to enhance morphological accuracy by shrinking and expanding pixel allocation based on location. The total unarmoured ephemeral channel system area is 28% in this part of the channel system, with the armoured gravel lag areas covering 61% and areas inundated with water making up 11%.

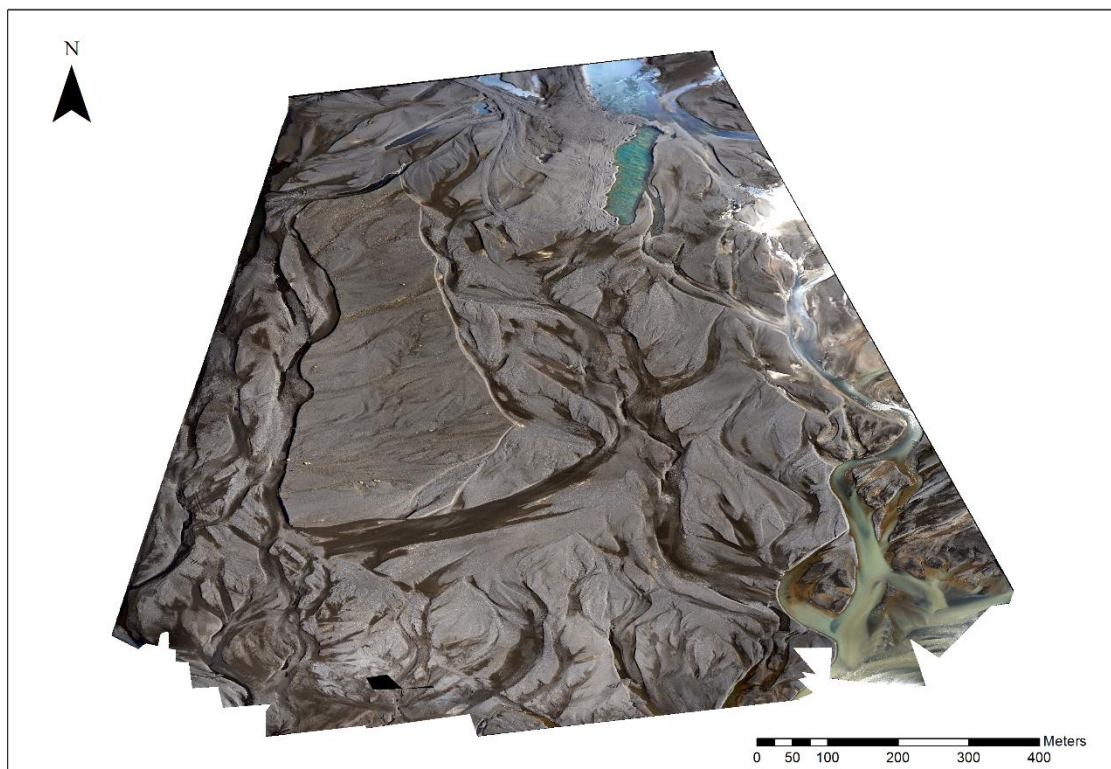


Figure 3.7: UAV Orthophoto of the ephemeral channel system in May 2014. The orthophoto was generated using Agisoft Photoscan.

Although the total percentage of channels which are inundated will vary by season, the total percentage water on the floodplain has been slightly overestimated. Figure 3.9 shows a zoomed in section of ephemeral channel network and its corresponding classification where all three landscape units have been classified. Although the classification generally achieves a high accuracy (Table 3.2) in distinguishing between the unarmoured channel sediments from the armoured gravel lag, it misidentifies lighter-coloured sediments which are often located on the edges of the unarmoured channels and within paleo meltwater channels (Figure 3.9). These sediments are sand sized and are being identified in some cases as water.

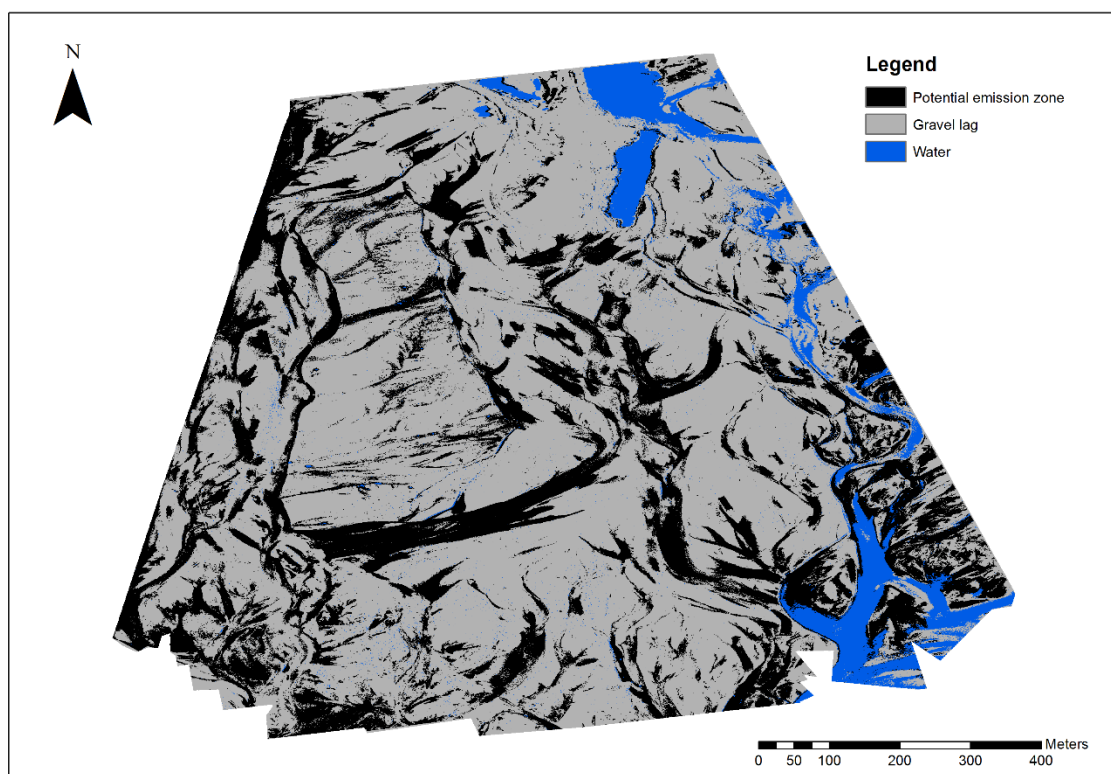


Figure 3.8: Supervised Classification of orthophoto from Figure 3.7 using texture analysis in ArcGIS

One benefit of using unmanned aerial systems for environmental mapping is the speed and efficiency with which photogrammetry can be used to produce digital elevation models (DEM). In this case, a DEM would be useful to monitor potential seasonal changes in channel morphology. However due to weather conditions in 2014 and technical difficulties in 2015, a DEM comparison cannot be achieved. From personal observations, minor change to ephemeral channel structure, sizing and spacing had

occurred between May 2015 and May 2017. Figure 3.10 shows the DEM created from the UAV survey in 2014. The DEM has taken on a dome effect, with many of the largest errors being concentrated in the centre of the DEM.

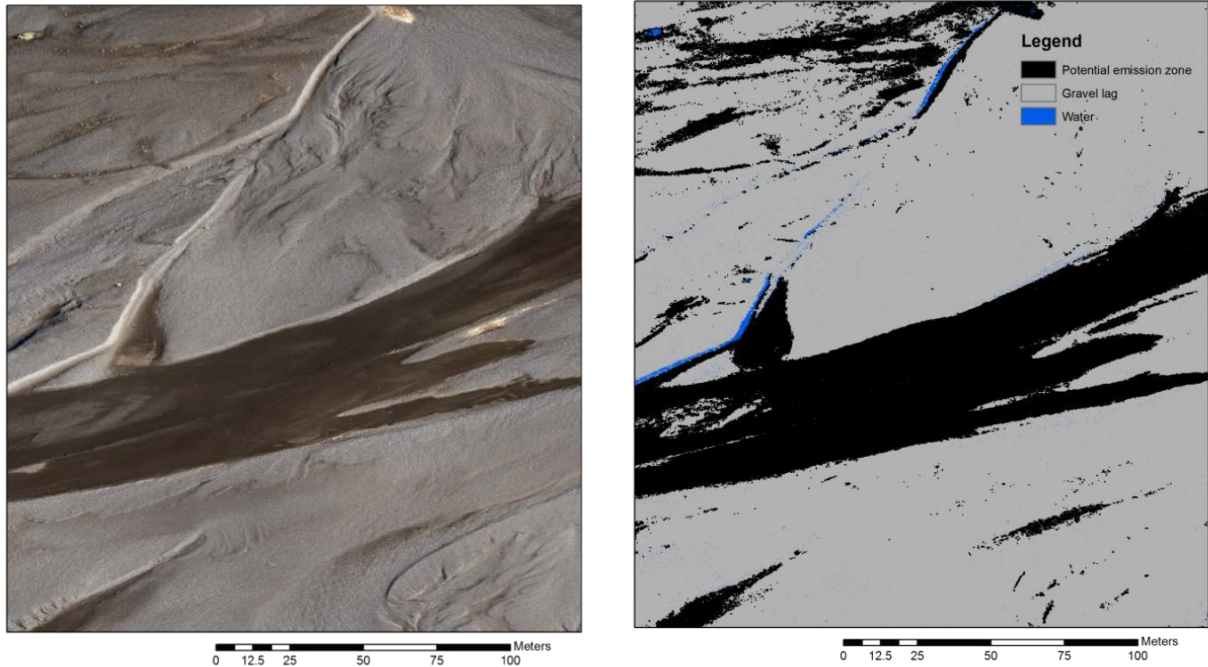


Figure 3.9: Segment of a) orthophoto and b) supervised classification indicating areas of misclassification in Figure 3.8

Table 3.2: Classification accuracy (Figure 3.8) produced from a confusion Matrix (using 100 random points)

Classification	Points	Points identified correctly	% identified correctly
Potential Emission	20	18	90.00
Gravel Lag	73	69	94.52
Water	7	6	85.71

The relict sandur site was not surveyed using the UAV as this site was not accessed until the May 2015 field season. During this time, the UAV could not be flown due to technical difficulties. The use of mapping spatial variations in sedimentology at the relict sandur system might not be particularly useful due to the homogenous nature of the sedimentology at this surface. However, the technique may be useful in mapping

changes in bedform topography before and after high magnitude dust events (Chapter 4)

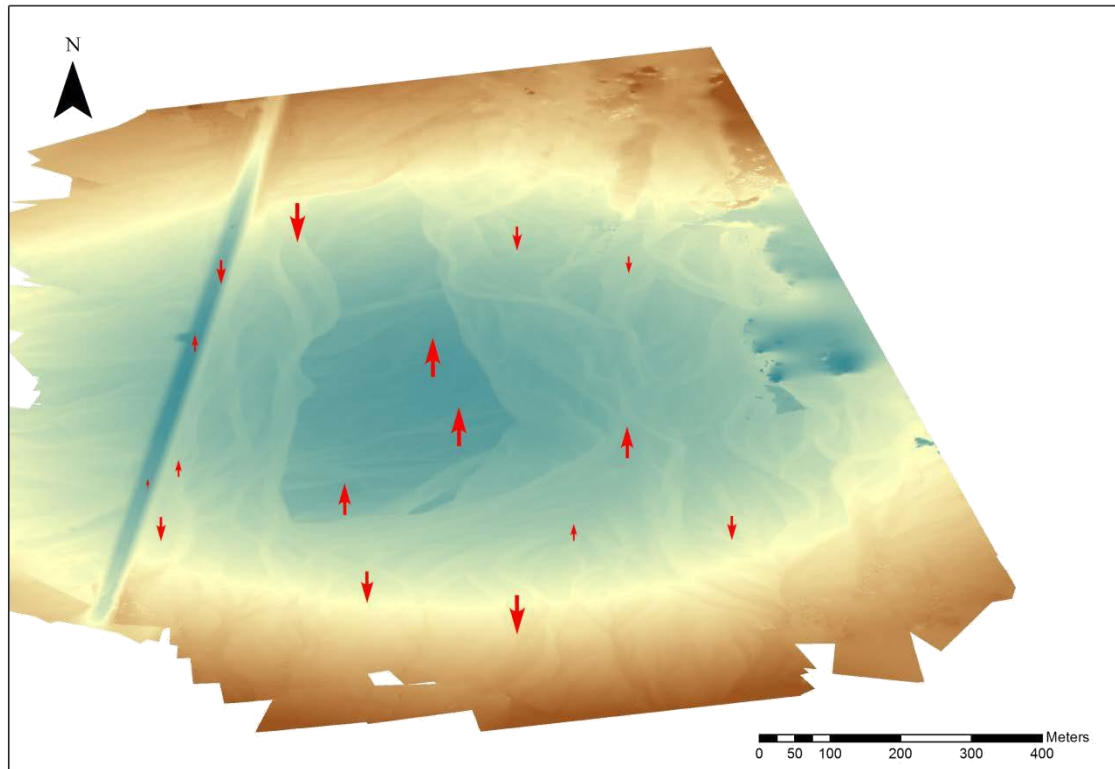


Figure 3.10: Digital Elevation Model of the ephemeral channel system created using UAV images in Agisoft Photoscan. Arrows represent the location of the ground control points and the proportional errors of height measurements in comparison to known heights at the surface. Blue represents low elevations

3.4.2 Site 1 – Ephemeral Channel System

3.4.2.1 Particle sediment size

The ephemeral channel system has been identified as a dust source from satellite remote sensing and other scientific studies (Arnalds, 2001; Prospero et al., 2012). However, no full characterisation of surface sedimentology in relation to the aeolian system has been carried out on this type of surface.

During the 2014 field campaign, small quantities (<0.1g) of material were collected during 3 low magnitude dust events. Figure 3.11 is a comparison of dust particle size

and varying facies particle size distributions from within the ephemeral channel network. The dust size ranges from 0.95 μm to 43.67 μm with the modal dust peak at 30 μm . This modal peak matches a peak in the unarmoured ephemeral channel with particles in these facies ranging from 0.375 μm to 716.9 μm with a modal peak at 36.2 μm . Particles analysed from the armoured gravel lag surface can be separated into two layers with a finer layer of particles located underneath fluvial gravels (Figure 8). The underneath layer consists mainly of coarse sands with some finer silts and clays, with a modal peak of 450 μm .

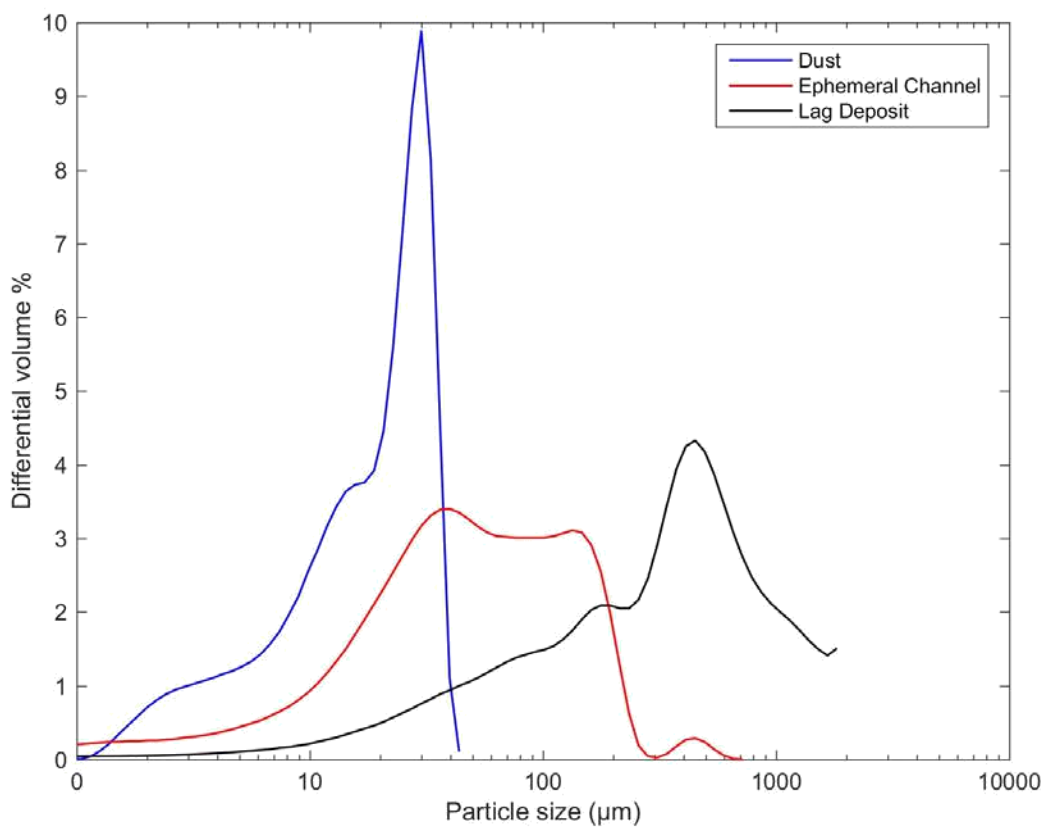


Figure 3.11: Particle Size Distribution of 3 dust events from the ephemeral channel system (2014). The size distributions of surface sediments from the lag deposit (i.e. gravel bars) and Ephemeral channel (i.e. unarmoured silt drapes) are drawn for comparison

The gravels at the ephemeral channel system were examined using SEDIMETRICS. Figure 3.12 shows the combined and separated particle size distributions from all sites (with g being the closest to the main river channel in Figure 3.5, a being the furthest from the main channel). The gravels are relatively fine with the largest class of material

between 24-32 mm. Over 50% of the total sediments are <32 mm. Variation in gravel size is minor across the ephemeral channel system. The mean between sites does not vary significantly, ranging between 14.18 – 17.87 mm (Table 3.2) and all sites display a moderate negative skewness (-0.46 – -1.12).

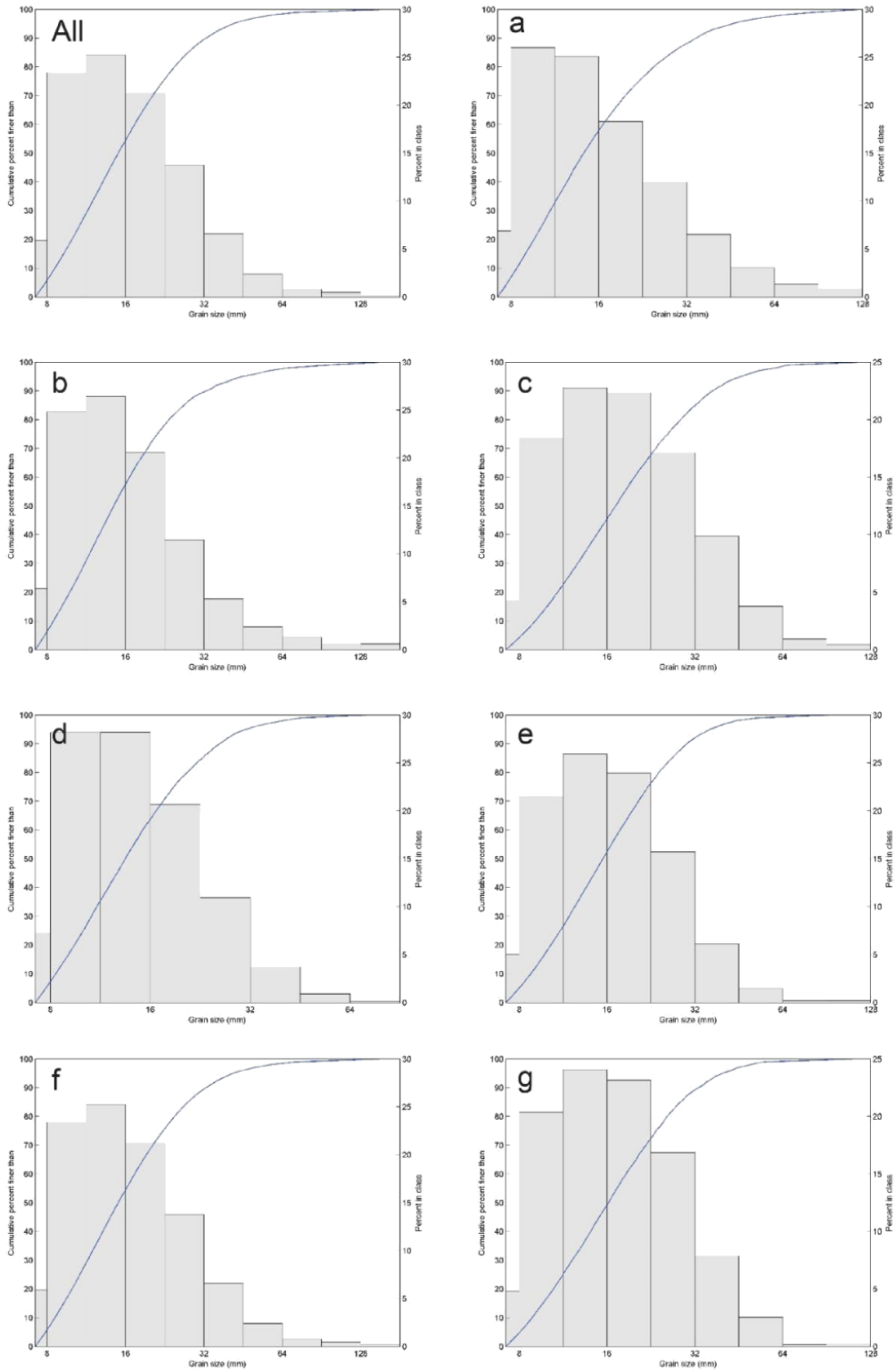


Figure 3.12: SEDIMETRICS particle size distributions for all sites at the ephemeral channel system (all) and singular sites with decreasing distance to the main river channel (a-g)

Table 3.3: Mean and skewness statistics of SEDIMETRICS surveys from Figure 3.12

Site	Mean (mm)	Skewness
A	15.80	-0.93
B	15.79	-1.12
C	17.87	-0.47
D	14.18	-0.61
E	16.01	-0.44
F	16.08	-0.82
G	16.73	-0.46



Figure 3.13: Markarfljot ephemeral channel system in June 2015. Channel inundation across the floodplain inhibited potential dust emission during this period

During the 2015 field campaign, dust emissions from the ephemeral channel system occurred infrequently. Dust collected in the wind vane sampler traps during this period was predominately material being transported from the relict sandur system. A potential explanation for low rates of dust transport during this period is because a

substantial proportion of the channel system was inundated by meltwater during the field campaign (Figure 3.13). Transport would therefore be improbable until the meltwater had retreated, and surface sediments had been sufficiently desiccated.

3.4.2.2 Particle characteristics

Figure 3.14 are SEM micrographs of the surface material collected in the unarmoured ephemeral channel system. Particle shape varies significantly, however most particles are angular to sub-angular. Particles often have sharp edges and are of high relief (Figure 3.14b). Micro textures include multiple craters (Figure 3.14b), chatter marks (Figure 3.14d), v-shaped percussion marks (Figure 3.14d) and precipitation defects (Figure 3.14c). The geochemical signature shows large proportions of silica (18.6%), iron (9.6%), aluminium (6.2%), calcium (4.3%), and magnesium (1.9%).

Dust particles collected in the wind vane traps during the 2014 field campaign are displayed in Figure 3.15 (a-d). Particle morphologies are like those found in the surface samples; they are angular and sub-angular (Figure 3.15). V-shaped percussion cracks (Figure 3.15c) and chatter marks (Figure 3.15a) are also present on high relief particles. Figure 3.15d shows that some of the smaller particles (<10 µm) have outgrowths where particles have most likely aggregated within the soil matrix. The geo-chemical signature is almost identical to that of the surface material, with silicon (17.4%), Iron (9.1) and aluminium (6.2%) being the dominant chemical elements.

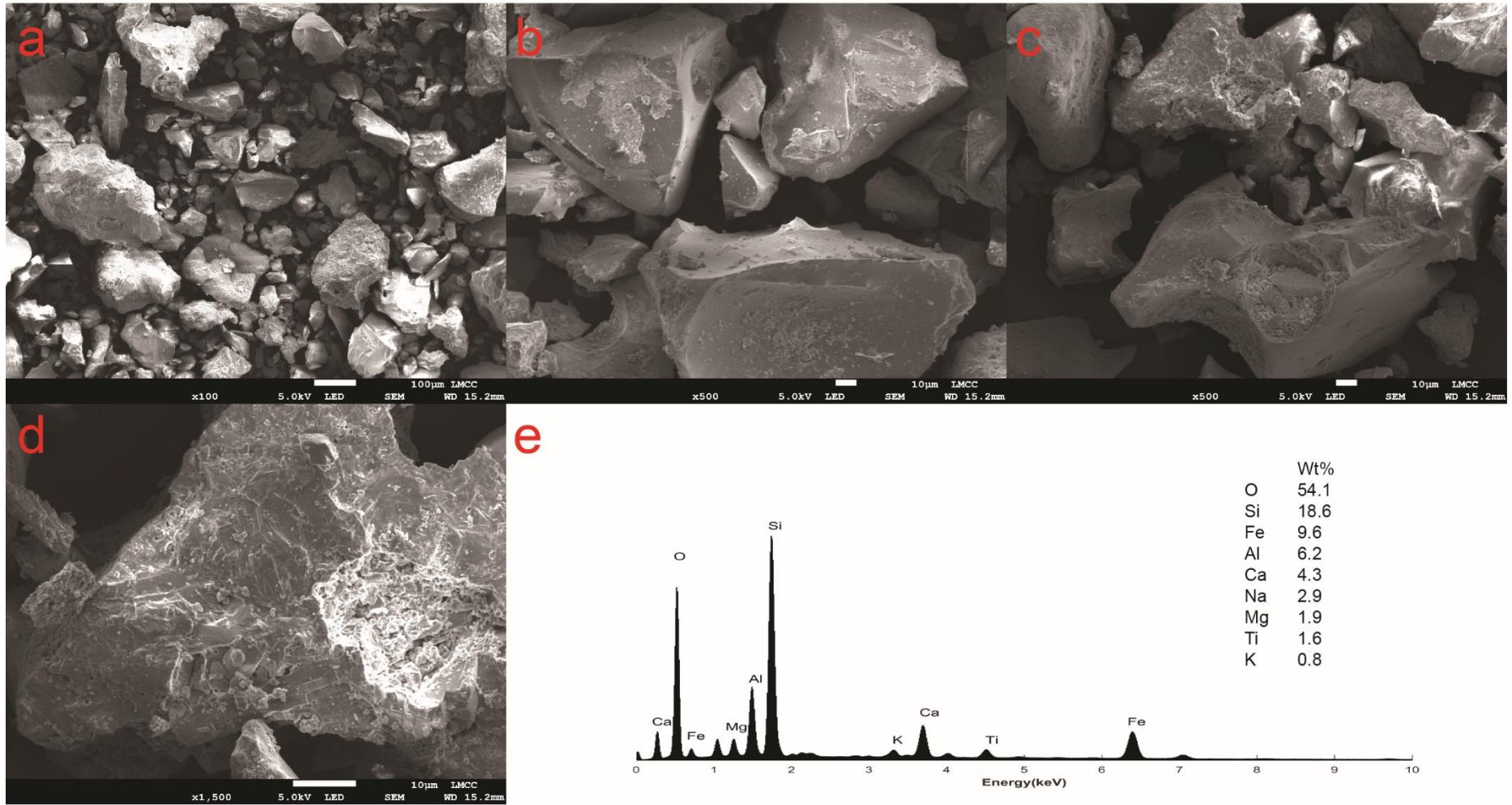


Figure 3.14: SEM Micrographs showing source sediments from the ephemeral channel system at Markarfliot (a-d). e is the geochemical fingerprint

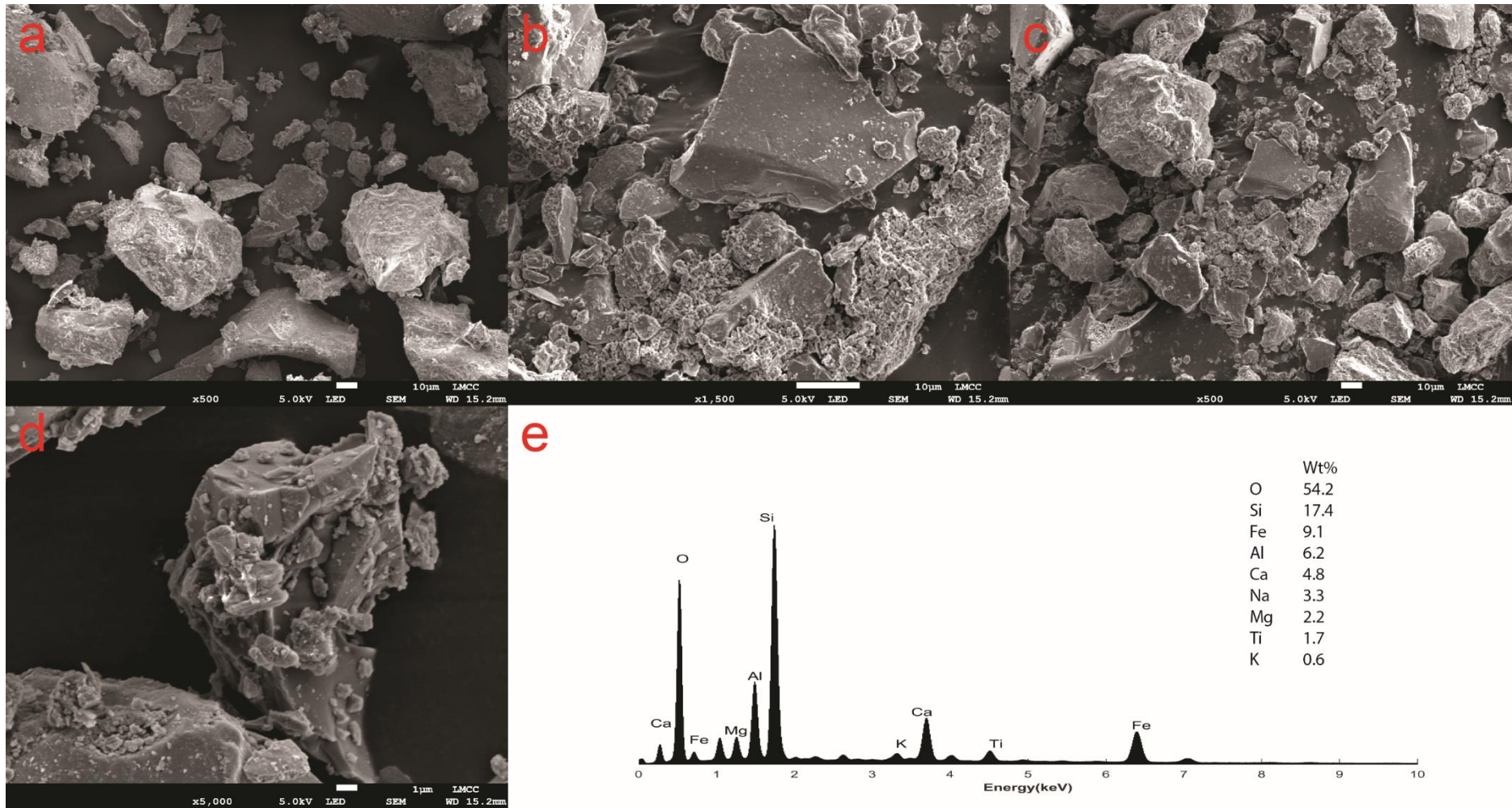


Figure 3.15: SEM Micrographs showing airborne dust sediments caught in suspension from the ephemeral channel system at Markarfljot (a-d). e is the geochemical fingerprint

3.4.3 Site 2 - Relict Sandur system

3.4.3.1 Particle sediment size

Figure 3.16 shows the differential volume (%) of particle sizes between 0.3 μm and 2000 μm for all combined surface samples and 5 combined dust events captured using wind vane samplers at 0.3 m, 0.6 m, 1.4 m and 2.4 m. Surface sediments are well sorted medium/coarse sand grains with a mode of 653 μm . There are no particles below 100 μm visible within the surface sediments. Material which is trapped in the 0.3 m and 0.6 m BSNE trap are similar in size. They are both relatively well sorted and have modal sizes of 373 μm and 409 μm respectively. In both traps, a finer portion (<100 μm) is present within the samples but it still makes up a very limited proportion of the overall size distribution (5.4 and 13.8% of total volume respectively). Particle sizes captured in the 1.4m and 2.4m BSNE traps are significantly different in comparison to the surface sediments and the 0.3 m and 0.6 m traps. The modal size for the 1.4m and 2.4m traps are 0.95 μm and 1.15 μm respectively. The largest particles within the samples are 15 μm . 35% of the 1.4 m and 31.3% of the 2.4m sample can be classified as PM₁, where 99.8% and 99.65 can be classified as PM₁₀ respectively. It is clear from the particle size distribution (Figure 3.16) that there are three dominant size categories: surface particles, particles travelling by saltation (0.3 m and 0.6 m) and particles travelling in suspension (1.4 m and 2.4 m). For the particle characteristics analysis (section 4.4.3.3), these are the groups which will be analysed.

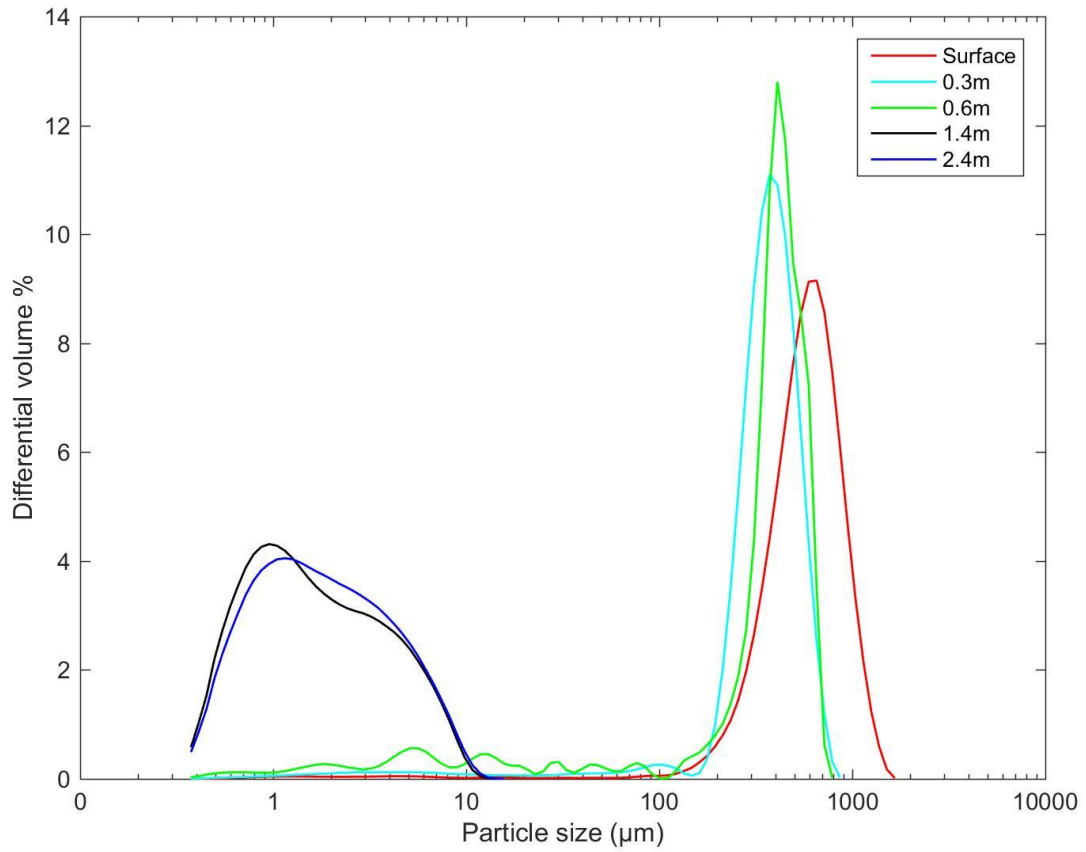


Figure 3.16: Particle size distribution of 5 dust events from relict sandur system (2015) at 0.3, 0.6, 1.4 and 2.4m. Surface sediments are overlaid for comparison.

3.4.3.2 Particle characteristics

Figure 3.18 are SEM micrographs of the surface sediments the relict sandur. The particles are generally rounded to sub rounded (Figure 3.17a) but can take sub angular forms. Within these grains, large V-shaped percussion cracks and elongated depressions can be identified (Figure 3.17a). Most of the grains also have signs of large indents and holes (Figure 3.17c), which are defined as bulbous edges. These edges vary in size and often displayed other features within the edges themselves. On the surface of the grain (Figure 3.17b), and particularly within other features (e.g. Figure 3.17c), a clay coating/lattice crystal structure has formed on the sand grains. These structures are clearly displayed in Figure 3.17d. These micro textures were identified on all surface grains from the relict sandur system examined in this study. The micro-textures are approximately $<3\ \mu\text{m}$ in size, with many of them being $<1\ \mu\text{m}$. Geochemically, particles analysed are made up of large proportions of Silicon (18.2%), Iron (6.7%), Aluminium (6.6 %) and Calcium (3.9%).

SEM images from wind-blown sediments from 0.3m and 0.6m trap are shown in Figure 3.18. Particle shape for larger sand grains can be seen to be rounded to sub angular (Figure 3.18a, b, d). The crystal lattice structure identified in Figure 3.18d is also visible on grains (Figure 3.18c). The most interesting part of this matrix is the development of finer material located between the sand grains (Figure 3.18b, 3.18d). These fine grains are not present in the surface sediments. The chemical composition of the particles is generally unaltered.

Dust particles in traps at 1.4m and 2.4m are displayed in Figure 3.19. As indicated from the particle size distribution analysis, particles are very fine. A variety of shapes and sizes of particles exist in the suspension layer, but the majority are extremely angular in nature. (Figure 3.19a, 3.19c). As is common with the sand size particles at the surface and within the saltation layer, the larger dust sized particles ($>3\ \mu\text{m}$) contain small micro textures on the surface of the particles (Figure 3.19d) with the finest particles resembling the micro textures associated with sand grains in figures 3.17 and 3.18. The chemical composition of the particles is like that of the surface particles and saltating particles, however a slight increase in Fe (7.8%) is observed. Micrograph scans of particles showed no evidence of preferential chemical elements presenting themselves as finer particles.

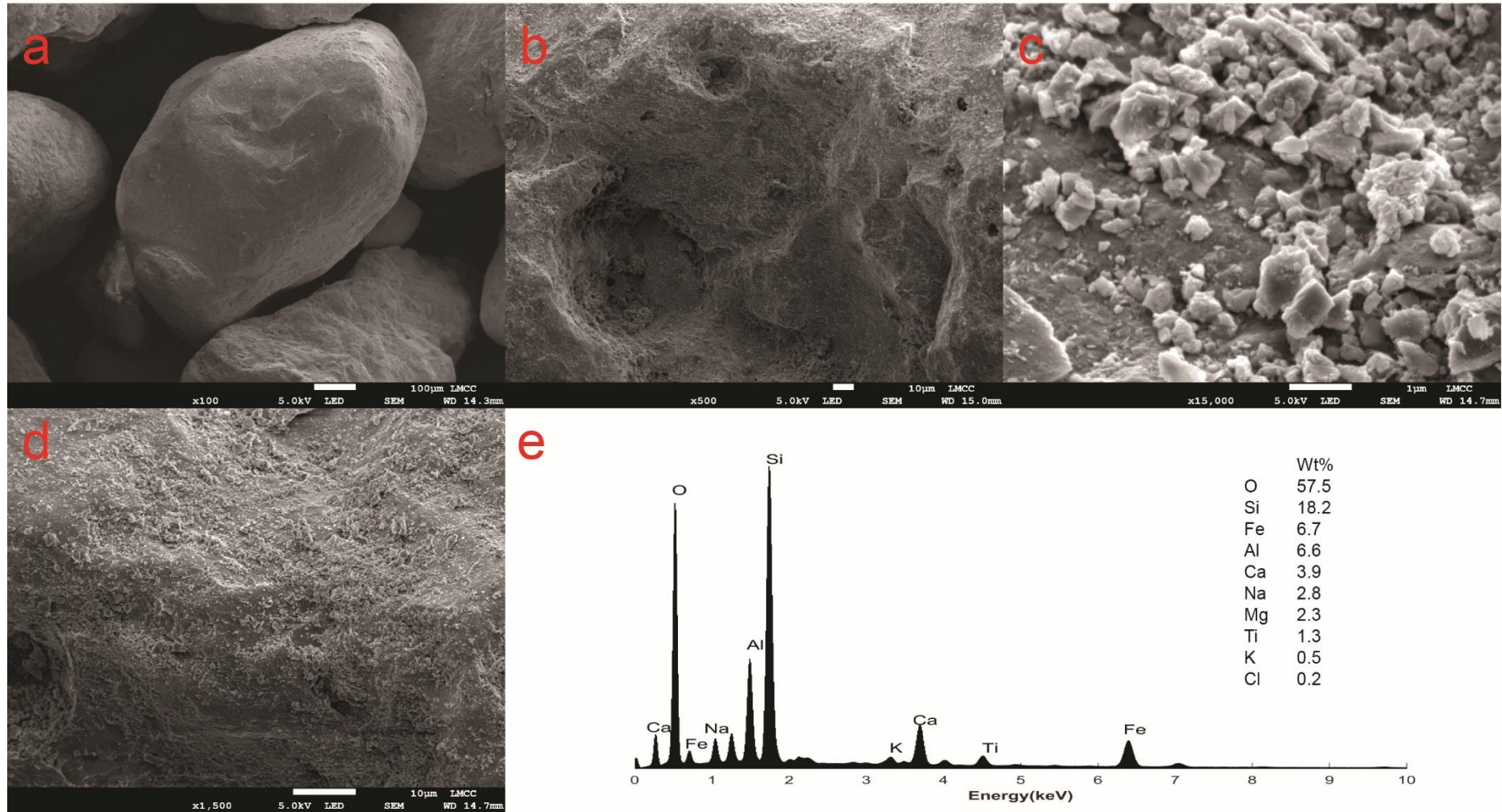


Figure 3.17: SEM Micrographs showing surface sediments from the relict sandur system at Markarfljot (a-d). e is the geochemical fingerprint

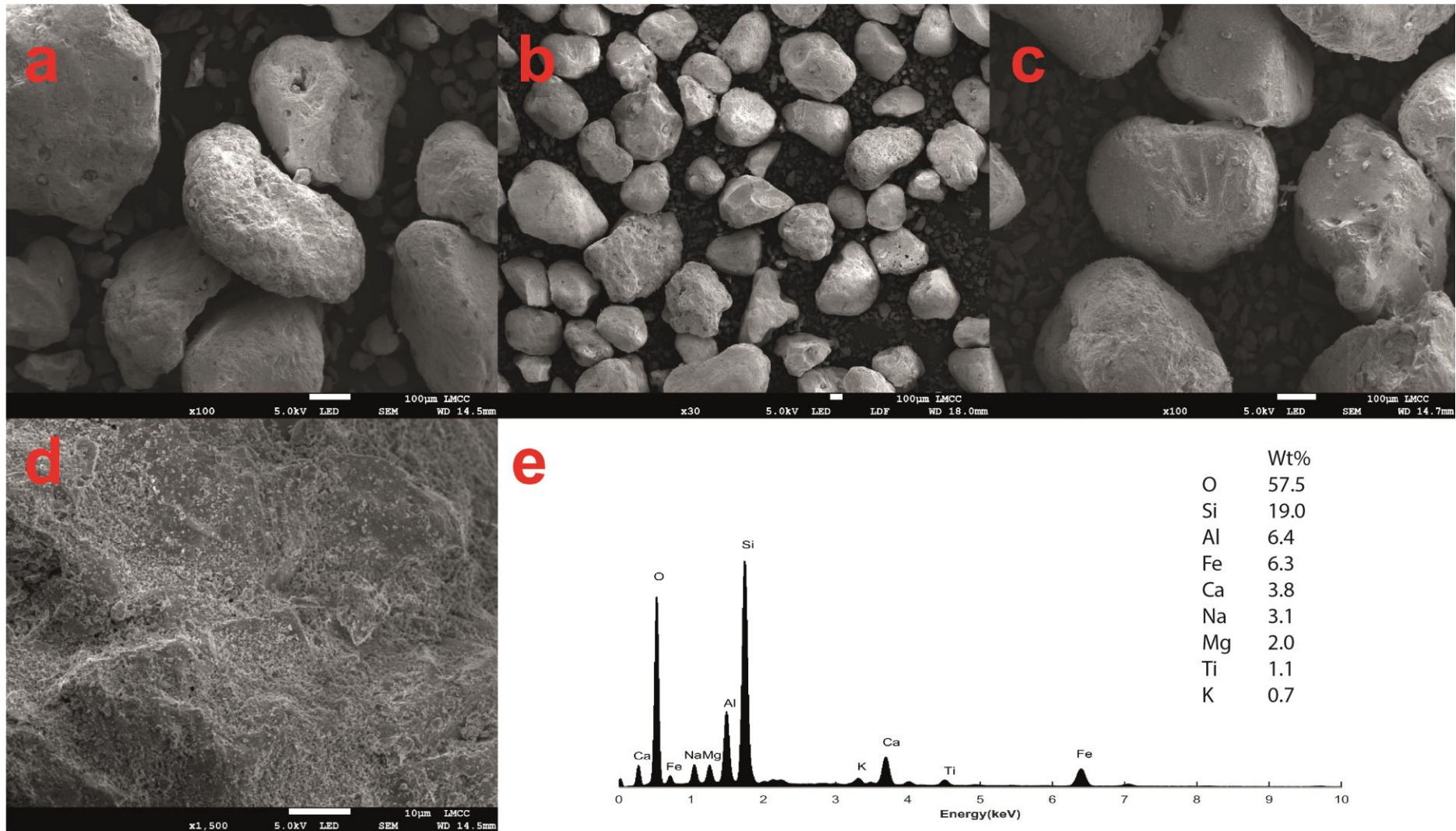


Figure 3.18: SEM Micrographs showing airborne sediments in saltation (0.3m and 0.6m BSNE traps) from the relict sandur system at Markarfljot (a-d). e is the geochemical fingerprint

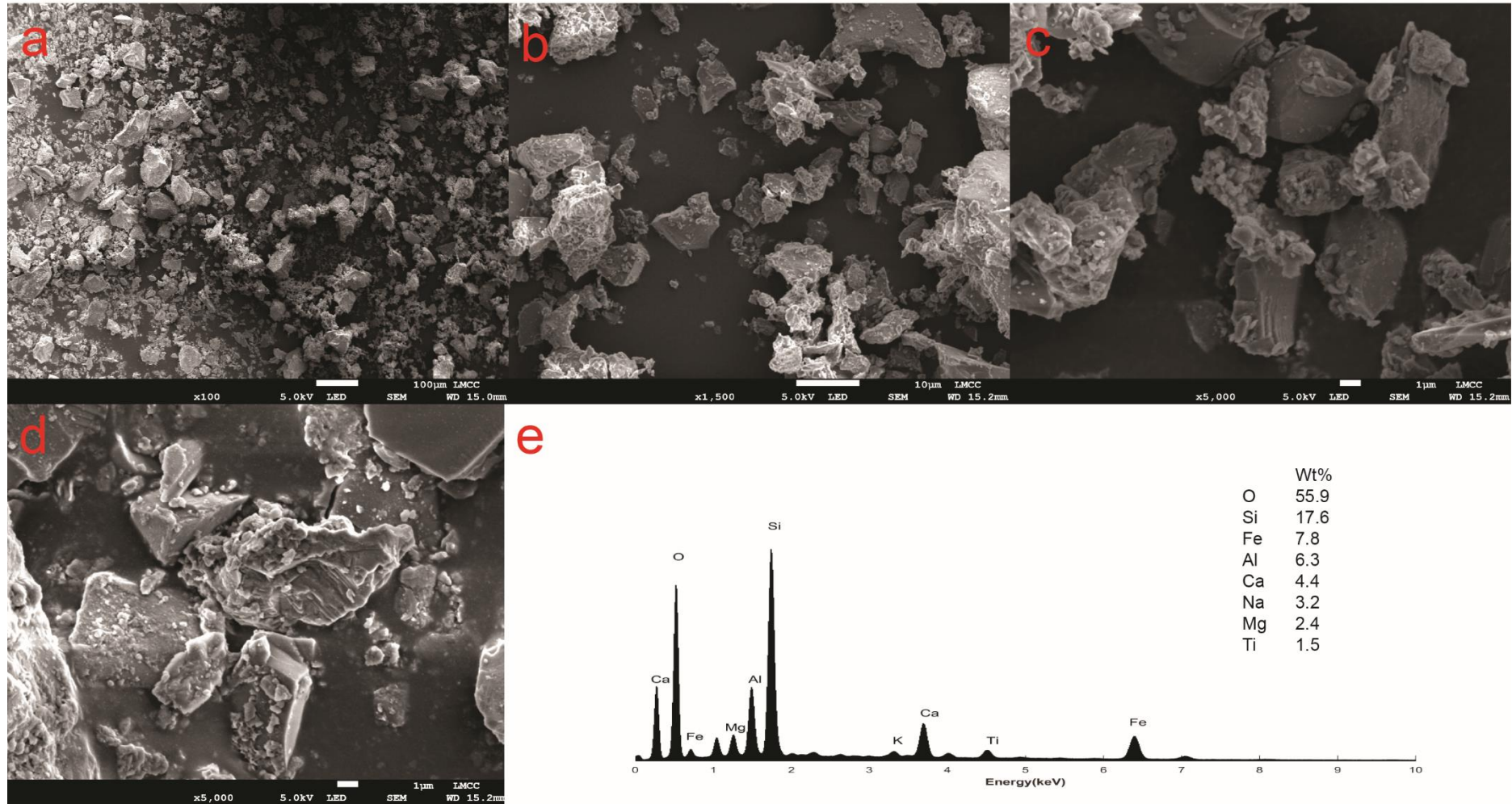


Figure 3.19: SEM Micrographs showing airborne dust sediments caught in suspension (1.4 and 2.4 m BSNE traps) from the relict sandur system at Markarfljot (a-d). e is the geochemical fingerprint

3.5 Discussion

3.5.1. Aerial mapping of high latitude dust sources

A method for monitoring proglacial landscape (and in turn, high latitude dust source) evolution is by periodically conducting sedimentological mapping. Many surveying techniques have been used to monitor proglacial channel development. Dunning et al. (2013) showed the role of glacial outburst floods at Gígjökull and the Markarfljot ephemeral channel system using terrestrial laser scanning (TLS) and time-lapse imagery. Dunning et al. (2013) successfully quantified the relative importance of rapid sediment deposition during jökulhlaups at Gígjökull following the Eyjafjallajökull eruption in 2010. Although the use of TLS and time-lapse photos was successful for this study, it should be noted that the study site was spatially limited. TLS has been shown to be a successful surveying technique in a range of geophysical fields (e.g. Montreuil et al., 2013; Dunning et al., 2013; Nield et al., 2013; 2014), however due to a low spatial swath and the length of the time which these surveys take, the technique does not lend itself to mapping larger geomorphological units.

UAVs have been used to infer the importance of aeolian processes in a variety of geophysical environments. Using digital photographs, Mauro et al. (2015) mapped the impact of dust particles on snow radiative properties in the European Alps to verify modelling outputs. Ramanathan (2006) used a UAV to assess aerosol-dust-cloud interactions in the western pacific using multi-spectral sensors. However, there are no studies which utilise multi-spectral approaches during dust storms to potentially assess variability in dust plume heights and concentrations. This is due to the technical difficulties in deploying UAVs in low visibility and high wind conditions (Akhlaq et al., 2012).

In this thesis, a UAV was successfully used to map 2-dimensional spatial variations in sedimentology at the ephemeral channel system at Markarfljot (Figure 3.9). Although this is not the first example of using a UAV to map spatial variations in sedimentology (Niethammer et al., 2012; Woodget et al., 2017), this is the first attempt to quantify the relative area of wind-erodible material using a UAV. For calculating total area, a 2D orthophoto provides enough detail for the purposes of texture analysis and therefore the calculation of the total area. Because images are georeferenced, via the use of an

on-board GPS and post processing of the flight path, it would be possible to survey this area systematically to determine seasonal change. This would be particularly useful if it was determined that the area of unarmoured silt deposits was continuously altering in response to changes in the volcanic-glacial system due to climate change (Oerlemans et al., 1998; Oerlemans, 2001; Björnsson and Pálsson, 2008).

However, the use of a UAV to map the ephemeral channel system to a sufficient vertical resolution was unsuccessful in this project. This is because the DEM which was created encountered a common issue called 'doming' (James and Robson, 2014). James and Robson (2014) indicate that doming is common in topographic reconstructions when the camera angle from a platform is near parallel. Wackrow and Chandler (2008, 2011) show that this systematic distortion can be lessened when camera angle direction is not parallel, and that image acquisition should focus on identified areas of interest (using a systematic convergent strategy). In our case, the camera is fixed securely to the UAV facing downwards. Although some images will not be perfectly parallel to the surface, for example when the UAV is banking or adjusting its altitude, many of the images taken will be near parallel which is likely increasing the vertical error within the DEM.

James and Robson (2014) suggest that sufficient quantities and the spacing of ground control points are critical in the reconstruction of a 3-dimensional surface. Although the technology is developing for the use of direct georeferencing for UAV photogrammetry retrievals without the use of GCPs (Chiang et al., 2012; Turner et al., 2014; Carbonneau and Dietrich, 2017), the current accepted methodology is the use of manual ground control points to constrain and verify model construction. The precise spacing and quantity of GCPs will depend on the size of the area of the survey site and flying altitude of the platform. However, it is suggested that GCPs should be in all corners of the survey site, with additional points placed in the centre of the survey zone. This is because SfM photogrammetry uses point clouds based on the quantity of images displaying features in overlapping images. At the outside of a survey area, the number of overlapping images will be lower than in the centre, meaning that less dense point clouds can be generated (James and Robson, 2014). Therefore, it is pivotal that external topographic data is available to enhance image analysis at the outskirts of a survey site. This could help explain the failure to create an accurate DEM for the ephemeral channel system. It was impossible to place GCPs in the corners

closest to the river channel as it could not be accessed safely. It could be suggested that the use of a direct georeferencing tool within environments which are inaccessible are key to the development of UAVs use in geomorphological mapping (Chiang et al., 2012; Turner et al., 2014; Carbonneau and Dietrich, 2017).

The UAV was not used to map the relict sandur system during this project. This was due to technical difficulties during the 2015 field campaign. Hypothetically, one potential issue with mapping surface sedimentology at the relict sandur is that there is little spatial variation in sediments across the landscape unit. However, the use of a UAV at the relict sandur system may be of more use to monitor changes in geomorphology. As will be shown in Chapter 4, alterations in bed form occur pre-and post-dust event, meaning that the use of a UAV may be applicable for monitoring vertical changes.

3.5.2 Variations in particle characteristics

There are major differences between surface sediments at the ephemeral channel and relict sandur systems. These differences are documented in Table 3.3. At the relict sandur, particles are mainly angular to sub angular. This angularity suggests that these particles have travelled short distances in the fluvial environment (Mahaney, 2002). After particles are transported out of the glacial system, they are transported in the glacial-fluvial system until they are deposited downstream. The distance from source to sink in this example is < 40 km, and grains, particularly smaller grains where collisions are low energy (Mahaney, 2002) are likely to keep their sub angular to angular nature (Figure 3.14b, c). It has been suggested that grains with high degrees of relief form when grain to grain contacts occur under high shear stresses in basal ice (Helland and Holmes, 1997; Pye, 2015). This indicates that these particles are most likely to be sourced from the subglacial environment. This is reinforced by

Table 3.4: Dominant sediment size (from particle laser sizer) and characteristics (from SEM micrographs) for the ephemeral channel system and the relict sandur system

	Site 1 – Ephemeral Channel		Site 2 – Relict Sandur	
Site 1 - EC	Surface	Dust	Surface	Dust
Shape	angular, rounded	sub-angular, irregular	rounded to rounded	sub-angular, irregular
Size (µm)	0.3 - 300	up to 40	160-800	<10
Dominant minerals	Si, Fe, Al, Ca	Si, Fe, Al, Ca	Si, Fe, Al, Ca	Si, Fe, Al, Ca
Dominant microtextures	multiple craters, chattermarks, v-shaped percussions		bulbous edges, lattice clay coatings, v-shaped percussions	
Environmental context	glacial and fluvial processes		aeolian processes. Some fluvial and glacial markings	

the presence of V-shaped percussion marks (Figure 3.14d), which are often formed in grain to grain collisions within high stress fluvial environments (Mahaney et al., 2001; Mahaney, 2002). This would indicate collisions during the transportation of particles through the glacio-fluvial environment in suspension (Krinsley and Doornkamp, 1973). A more prominent feature, the multiple craters (Figure 3.14c), could be interpreted as a sign of abrasion in water transport. However, Mahaney et al. (2001) indicates that if these craters are $> 50\mu\text{m}$ in diameter, they are more often a sign of fracturing and abrasion during glacial transport.

Surface grains at the ephemeral channel system have been interpreted to be of predominately glacial origin and that their dominant characteristics are formed within sub-glacial and to lesser extents glacio-fluvial environments. When assessing sediments from known dust sources, it would be expected that particles would display evidence of aeolian transport (Smalley and Glendinning, 1991; Mahaney et al., 2001). For these sediments, grains do not show any traditional textures which would be expected in a high energy aeolian environment. A reason for this could be due to seasonal recharging of sediments within the basin. Each spring, as glacial melt rates increase with summer air temperatures (Oerlemans et al., 1998; Björnsson and Pálsson, 2008), the glacio-fluvial environment sees an increase in water and sediment transport (Hodgkins, 1996; Hodgkins et al., 1999). River stage increases lead to the ephemeral channel system being inundated by increased flows. These flows, which are often of very low discharges, can transport fine sediments into the outreaches of the ephemeral channel system. Particles are then deposited on the surface in the unarmoured channels. These freshly created glacial sediments are now the surface sediments which are available for the aeolian environment. As they are fresh glacial sediments, no aeolian markings can be found on the sediments.

In contrast, surface sediments sourced on the relict sandur system are considerably rounder than surface sediments at the ephemeral channel site, although angular and sub angular particles are still present indicating an initially glacial origin to the sediments (Smalley, 1966; Mahaney et al., 2001; Mahaney, 2002). Rounding of sands in these environments is likely to occur in a fluvial or an aeolian environment governed by saltating sand (Mahaney, 2002; Pye and Tsoar, 2008), and the level of roundness has been shown to be linked to time active within these environments. Larger grains have also been shown to round faster based on higher energy collisions with other

particles (Marshall et al., 2012; Costa et al., 2013). Although some glacio-fluvial sediment characteristics can be identified on surface sediments from the relict sandur, these grains have been shaped and defined within a high intensity aeolian environment without interaction with other environments.

Bulbous edges (3.17c) are very common in aeolian sediments $>150\ \mu\text{m}$ (Vos et al., 2014). They form when particles are rotating during the process of saltation (Haff and Anderson, 1993; Mahaney, 2002; Cheng et al., 2006). This rotation aids the rounding process but also helps form surface depressions. The edges of these depressions are further rounded to form a smooth edge during particle rotation (Mahaney, 2002). The lattice crystal structure (Figure 3.17d) has been shown to intensify in bulbous edges (Mahaney et al., 2001), however further grain analysis would need to be undertaken for an empirical quantification. The lattice crystal structure is a common feature in aeolian sands and is likely to be a sign of high magnitude aeolian transport (Pascoe, 1961; Mahaney, 2002; Krinsley and Doornkamp, 2011). Mahaney (2002) suggests that as grains saltate in aeolian transport, they are subjected to numerous high energy collisions with other particles in the saltation cloud. These collisions cause a particle to become electrostatically charged, with the vibration and energy waves within a single particle shifting within a grain during saltation. Pascoe (1961) developed the theory of abrasion fatigue, which suggests that the surface of any given grain is physically and chemically reactive and when electrostatic charging during the process of transport, this surface attracts smaller particles to adhere to the side of larger grains. The removal of the lattice crystal structure (e.g. clays) on larger sand grains has previously been identified as a potential method for dust particle production, called aeolian abrasion (Bullard and White, 2005). Further testing on these sediments in a laboratory confined experiment is required to try and quantify the relative role of aeolian abrasion for producing dust sized particles for the relict sandur sediments. This will be quantified in Chapter 5.

3.5.3 Variations in particle size

Surface particles at both dust sources have been shown to be significantly different due to the environments which control their composition and shape. The particle size distribution of airborne particles is controlled by surface source particle characteristics.

The relationship between surface and airborne particle size distributions may also help us draw insights into potential mechanisms for uplift and entrainment for dust emission.

At the ephemeral channel system, airborne particles have a similar mode compared to that of the unarmoured ephemeral channel network sediments. Although the size distribution of particles can also be seen in the underlying armoured gravel sediments, it is unlikely that dust is being entrained from these surfaces. This is because larger gravel sediments will form a protective lag from finer sediments being entrained (McKenna Neuman, 1993; Nickling and McKenna Neuman, 1995). Nickling and McKenna Neuman (1995) indicated that sediment transport may be initially enhanced due to non-erodible roughness elements because of kinetic energy retention in elastic collisions. However, increasing densities of these roughness elements leads to a decreased likelihood that grains can be ejected into aeolian transport as declining shear stress partitioning occurs at the surface (Raupach, 1992). The role of secondary airflows may become significant by decreasing aerodynamic roughness and shear stress at the bed (Raupach, 1992; McKenna Neuman and Nickling, 1995). Saltation drag and grain supply in the airstream is then significantly reduced (McKenna Neuman and Nickling, 1995). Because of the high percentage coverage of armoured gravel surfaces in the ephemeral channel system, it would be appropriate to suggest that this is the mechanism for why material is unlikely to be ejected from this facies group. However, if gravels were to be redistributed within the environment e.g. if there was a large flood event and gravels were removed or sediment reworking allowing an increase in fine sediment at the surface; these areas could hypothetically be prone to wind erosion.

On the relict sandur, particles caught in suspension are much finer than at the ephemeral channel system. These particles, none of which are larger than 10 μm , are absent in the surface sediment particle size distribution (160-800 μm). This would indicate dust particle generation during transport, with a possible mechanism being the removal of the micro-textures which are adhered to the sand grains (Figure 3.18). SEM micrographs indicate the presence of adhering clay and silt sized particles to larger sand grains. This would suggest that as sand sized particles are entrained in transport, adhering silt and clay sized particles are removed from the sand grains and then being ejected into the suspension as dust particles. This also provides an explanation for why dust sized particles collected at source are extremely fine.

However, other forms of abrasion may also be occurring during aeolian entrainment at this dust source. Gills et al. (2006) and Mockford et al. (2013) found that sand sized particles $>250\mu\text{m}$ would chip under laboratory generated abrasion using a dust generator. Fine sands produced the finest particles (Mockford et al., 2013). Sand particles are inherently resistant to being abraded (Gills et al., 2006), however will preferentially break on sharp edges whilst particles rotate during saltation (Mahaney, 2002). From this dataset, it will be difficult to identify the relative roles of the removal of clay coatings and particle chipping in total dust particle production. However, it may be possible to assess the role of both forms of production on sediments from Markarfljot using a laboratory abrasion chamber and optical microscopy.

The concept of aeolian abrasion for fine particle creation has been shown to be an important process in desert environments in creating particles for dust storms (Bullard et al., 2004; 2005) and in the development of loess (Smith et al., 1991; Wright et al., 1998; Wright, 2001). Bullard et al. (2004), using a laboratory dust generator, found that the main source of fine particles from red dune sands in Australia were from the clay surface grain coatings of sand particles. The percentage of particles $<10\mu\text{m}$ generated increased when the sample was sieved to remove all particles below $<250\mu\text{m}$. This would indicate that in samples with existing fine material in the surface soil matrix, these particles are more likely to be entrained initially than particles which are being generated by abrasion. On the relict sandur, where there is no fine component in the surface soil, particles must be generated by abrasion to be available for entrainment as dust in suspension. Therefore, the process of aeolian abrasion at the relict sandur seems to be the driving mechanism for dust particle creation.

3.5.4 Can particle size indicate the mode of aeolian transport?

The differences in size distribution between source and airborne particles may indicate the mode of aeolian transport which is present during dust events at both sites. Most aeolian systems have been shown to be associated with dynamic entrainment/saltation bombardment systems (Shao et al., 1993; Shao, 2001). Essentially, sand sized particles in saltation drive the total rate of dust particles in suspension by releasing these particles into the airstream as impacts between particles increase in the saltation layer in increasing shear velocities (Alfaro et al., 1997; Shao, 2001). Dust particles will be either be released from the surface (Shao et al.,

2001) or created through processes such as aeolian abrasion of sand sized particles (Bullard et al., 2004; Bullard and White, 2005). Although saltation was not actively measured during field experiments (e.g. using a SENSIT), dynamic entrainment seems to be the dominant process on the relict sandur system, as during all dust events, saltation occurred (Chapter 4).

Aerodynamic entrainment has also been shown to be a significant dust transport mechanism in certain environments (Macpherson et al., 2008; Klose et al., 2014; Parajuli et al., 2016). Aerodynamic entrainment occurs when dust particles are mobilised without the influence of saltating particles near to the bed and are lifted directly into suspension. Macpherson et al. (2008) showed the importance of aerodynamically entrained particles for several supply limited systems in the USA. Many of the field sites examined by Macpherson et al. (2008) were dry, ephemeral lakes, with high concentrations of silt/clay within the surface sediments. Most of the sites experienced very low horizontal mass fluxes (which can be used as a proxy for saltation) but high magnitude total dust emissions. Although horizontal mass fluxes were not recorded at the ephemeral channel system, no personal observations of saltation were recorded at the ephemeral channel system. The dominance of silt and clay and the lack of larger sand sized particles in the source sedimentology, shown by the particle size distribution, could indicate that this type of environment is susceptible to dust emissions by aerodynamic entrainment. This is further strengthened by observations of small dust whirls within the channels; a process which has often been linked to the aerodynamic entrainment of dust sized material (Klose et al., 2014). However, further empirical measurements understanding the relationship between saltation and dust storm activity within the ephemeral channel systems are required.

Although a discussion on dust storm magnitude and frequency is outside the scope of this section (see Chapter 4), the relative importance of both sources as contributors to aerosol loading in Iceland is required. From observations during May/June 2015, the relict sandur source emitted dust on a much more regular basis than the ephemeral outwash network. Firstly, river stage levels at Markarfljot steadily increased just prior to the start of the 2015 monitoring system. This led to the complete inundation of the ephemeral outwash plain network during this period. Although the water retreated quickly, sediments were then unavailable due to elevated levels of surface soil moisture. Second, dry northerly winds have been identified as the main dust raising

winds in south Iceland (Arnalds et al., 2016). This would promote entrainment from the ephemeral channel system at Markarfljot due to the orientation of the river and associated outwash channels. This pathway was also identified by Prospero et al. (2012) and Baddock et al. (2017). However, during the field monitoring period in June 2015, the dominant wind direction associated with dust events was south-easterly (see Section 4). This wind direction is associated with the dominant tracking of the Icelandic low (Arnalds et al., 2016; Baddock et al., 2017), with initially south-westerly wind directions switching to south-easterly before the air mass is split. With a south-easterly wind direction, air flow is disturbed by large areas of gravel lag deposits. Although this was not fundamentally tested, the hypothesis that the aerodynamic roughness properties of the gravel lag surface will be significantly higher than the unarmoured silt deposits (McKenna Neuman and Nickling, 1995). This disruption in flow may cause turbulent eddies within the airflow, which would promote small scale blowouts (Klose et al., 2014) and could help strengthen the argument for the importance of aerodynamic entrainment as a dust lifting mechanism on this surface.

3.6 Conclusion

Dust source sedimentology can vary significantly in south Iceland within a single glacio-fluvial basin. These variations lead to specific dust source units producing fundamentally different dust particles in terms of their particle size distribution and particle properties. Entrained particles from the ephemeral channel system seem to be considerably larger than particles created at the relict sandur system and this will have an influence on the potential impacts those sediments have on other ecosystems and the ability of those particles to be transported long distances. This is particularly relevant to the ultra-fine particles ($< 2 \mu\text{m}$) which were captured at the relict sandur system which have potential for global dust transport (this will be quantified in Chapter 4). The type of emission mechanism is potentially different between the two source units and this is controlled by source surface sedimentology. The relationship between source surface sediment composition, dust emission mechanism and factors that affect sediment availability needs to be established for a range of different surfaces in the high latitudes to aid the verification of regional dust models.

Where dust source units have unique facies groups which can be distinguished by texture composition, the use of surveying techniques such as a UAV may provide

useful insights into the behaviour and development of areas within the system which are prone to wind erosion. Although it was not specifically tested in this project, a technique has been described which could be used to monitor the activity of ephemeral outwash channel development to calculate seasonal/decadal changes in potential dust source areas within a channel system. If these areas were to dramatically increase under increasing global temperatures, due to an increased sediment load from the glacio-fluvial system, the change could be quantified. However, due to the temporal limitations of this study, this was not empirically tested. Further work is required to implement the creation of 3D SfM models in these regions due to the inaccessibility of parts of the floodplain.

4. Icelandic dust event magnitudes, characteristics and pathways at the event-scale

Chapter 3 has shown that dust sources in Iceland have large spatial sedimentological variations within a single basin. The sedimentology of the dust source controls the sedimentological characteristics of the emitted dust particles and therefore in turn, the transport and depositional impacts of these particles is governed by the source sediments from which the particles were derived.

During two field seasons at the Markarfljot river basin, the highest magnitude dust events occurred at the relict sandur system (Figure 3.1). Due to equipment constraints, this was the only source to be instrumented during the 2015 season. Although it would have been possible to collect data from both systems downwind of both sources, it was decided that one of the largest gaps in our understanding of high latitude dust emissions has come through a lack of reliable measurements conducted at source. This chapter draws upon field observations, remote sensing and modelling outputs to determine the drivers and transport pathways of southern Icelandic dust events.

4.1 Introduction

The broad-scale global distribution of dust sources is well-understood (Prospero et al., 2002) and there is an increasing body of knowledge about regional (basin) to local (sub-basin) scale dust sources (Bullard et al., 2008; Lee et al., 2009; Parajuli and Zender, 2017). Research on dust emissions, transport and deposition takes place at a range of temporal scales from the long-term Quaternary record (Zhang et al., 1999), through decadal variations driven by changes in climate indices (e.g. Southern Oscillation Index) and drought (Middleton, 1985), to seasonal patterns (Littman, 1991; Meloni et al., 2008; Reheis and Urban, 2011). There has also been a focus on very short-term, turbulence-driven dust emission processes (Stout, 2010). The global and longer-term spatial and temporal patterns of dust emissions reflect the cumulative impacts of multiple individual dust events. Although dust events in the subtropics have been well-studied with respect to identifying dust sources, they have received comparatively little attention with regards to their event-scale evolution; i.e. following dust emission processes from the start to the end of an individual dust storm (typically <2 days duration). This is despite where emphasis has been put on similar scale

(diurnal) patterns of aeolian activity, useful insights into the drivers of aeolian transport has been gained (Stout, 2001; 2010).

When dust events have been considered at the event scale, analysis has often focused on dust transport pathways (Perez et al., 2006; Baddock et al., 2017) and the vertical distribution of dust particles within the boundary layer (Huang et al., 2007; Liu et al., 2008a). This is probably due to the ability to track single dust events using a range of satellite remote sensing techniques (Ackerman, 1997; Liu et al., 2008b; Prospero et al., 2012).

The systematic analysis of dust transport pathways has been achieved through several different approaches. The easiest way to assess transport pathways are from true colour, visible spectrum satellite images (Ackerman, 1997; Baddock et al., 2009). This has proved particularly popular in the sub-tropics due to a lack of cloud cover (Baddock et al., 2009), daily retrievals (MODIS) and the ability to spectrally enhance images to identify dust plumes (Ackerman, 1997; Miller, 2003; Roskovensky and Liou, 2003; Baddock et al., 2009). Although, these approaches work well for pin-pointing the upwind locations of dust sources (Bullard et al., 2008; Lee et al., 2009), dust plumes disperse downwind as they move away from source (Baddock et al., 2014). To assess the potential regional scale transport pathways, other approaches must be taken.

One particularly popular approach is the use of the HYSPLIT model (Hybrid Single-Particle Lagrangian Integrated Trajectory model (Draxler et al., 2003). The use of this model in assessing dust transport pathways varies considerably within the literature. Initially, pathways were assessed using a 'climatological approach' (McGowan and Clark, 2008; Neff and Bertler, 2015), where trajectories are run every day regardless of whether dust is known to be entrained. Baddock et al., (2017) refined this technique by running trajectories only on days when dust is observed, identifying these days using observations (e.g. dust codes). It was shown that the climatological approach vastly overestimated the spatial extent of dust transport pathways, and that the dust day approach identified preferential corridors of dust transport. However, Baddock et al. (2017) did not consider the magnitude of dust events due to the inconsistent use of dust codes (Bullard and Mockford, 2018). McTainsh et al. (1988) created the dust storm index (DSI) to try and assign intensity values of dust storms based on certain dust code frequencies in Australia. Although dust code attribution should be uniformly

applied using the WMO definitions globally, in practice, evidence suggests that the manual identification of dust events using dust codes is inconsistent (O’Loingsigh et al., 2014; Bullard and Mockford, 2018).

It is also difficult to pin point sources when taking the approach of Baddock et al. (2017) as many of the stations which record dust observations are often in pathways associated with a range of known dust sources (Arnalds et al., 2016). Although this could potentially be solved by using secondary meteorological data to assess local wind variability, the use of surface wind observations may not be the most useful in assessing potential long-range transport patterns (Baddock et al., 2017). This problem is reduced if the recording stations for both wind speed and dust observations are located directly at dust source.

Understanding how a dust event develops within the boundary layer is important as it indicates the impact the material might have on the Earth system. If material is transported into the upper atmosphere, such as in the Saharan Air Layer (Carlsen and Prospero, 1972; Prospero and Carlsen, 1972), it may have major impacts on ultraviolet radiation backscatter (Torres et al., 1998), large-scale synoptic weather patterns (Dunion and Velden, 2004; Evan et al., 2006) and allow particles to travel long distances (Muhs et al., 1990; Marticorena et al., 1997; Barkan and Alpert, 2010). If material is transported in the lower boundary layer, closer to the surface, the impact of the dust deposition will likely be more local/regional (Groot Zwaafink et al., 2016; Dragosics et al., 2016).

Monitoring the boundary layer development of dust storms can be achieved in a variety of ways. Ground based LIDAR systems are often teamed with satellite remote sensing platforms (Murayama et al., 2001) and other ground-based instruments such as sun photometers (e.g. Aeronet, Omar et al., 2005) and optical particle counters (Takamura et al., 1994; Moulin et al., 1997) to assess the optical and transport properties of dust storms. However, ground-based LIDAR systems are very expensive, require continuous maintenance for reliable data output and are constrained spatially to a selected location.

To combat spatial limitations, the use of the Cloud-Aerosol Lidar and Infrared Pathfinder Satellite Observation satellite (CALIPSO, Winker et al., 2009) has been used to assess the global height of dust aerosols using information gathered from the

Cloud-Aerosol Lidar with Orthogonal Polarization (CALIOP, Liu et al., 2008). Liu et al. (2008) argues that the use of CALIOP for assessing the potential radiative forcing effects of dust aerosols is far superior to other passive remote sensing methods. Passive products, such as the Total Ozone Mapping Spectrometer (TOMS; Prospero et al., 2002), MODIS (Kaufman et al., 2005) and the Advanced Very High-Resolution Radiometer (AVHRR; Carlsen, 1979), often are limited to oceans (for AVHRR and MODIS) because they are unable to distinguish between different types of aerosol (for TOMS). Liu et al. (2008) provided a global estimation for dust aerosol height for a variety of global dust sources (North Africa, Asia, Australia), however the analysis was restricted to below 60°N and S.

To fully understand dust storm dynamics in the high latitudes, we require surface measurements at source. In this chapter, a model has been developed to understand event scale variations in dust emissions based on a conceptual model proposed by Kocurek (1998). At the Quaternary timescale, Kocurek (1998) suggested that the interactions between variables that control dune field development could be encapsulated within a conceptual aeolian system sediment response framework. This framework formalised the notion that aeolian systems respond to the cumulative impacts of sediment production, availability and transport capacity and can be differentiated as transport-capacity limited, sediment availability limited, and sediment supply limited systems. At stratigraphic timescales, the key controls on the system state are humidity and aridity which control rates of weathering (sediment production), vegetation cover (sediment availability) and surface wind speeds (transport capacity). Bullard and McTainsh (2003) suggested that this conceptual framework could be applied at much shorter timescales, for example seasons, and to contemporary processes. Bullard et al. (2011) further suggested that the framework could not only be applied to sand transport systems but also dust emission processes. Therefore, in this study, dust event measurements will be applied to a modified version of the Kocurek (1998) sediment system framework to determine the temporal drivers of dust emissions at the event scale. This will be the first attempt to classify dust emissions at an event scale using a conceptual dust emission framework in either the sub-tropics or high latitudes.

4.2 Dust storm classification

At the event-scale, drivers of dust emission include surface wind speed (Gillette, 1967); surface soil moisture (Chepil, 1956); humidity (McKenna Neuman, 2003); water table fluctuations (Reynolds et al. 2007); formation of lag deposits (Bullard and Austin, 2011) and sediment supply (Bullard et al. 2011). The drivers do not operate in isolation and changes in, for example, humidity can in turn alter the threshold wind speed required to entrain particles (McKenna Neuman, 2003).

It is proposed here that any individual dust event can be characterised based on the primary temporal control; the transport-capacity of the wind, the availability of sediment for aeolian transport, or the supply of sediment to the aeolian system. Some of these controls are less persistent than others; for example, wind speed varies at the hertz scale, some controls on sediment availability change very rapidly (e.g. soil moisture) whereas others, such as vegetation or lag cover are of longer duration; sediment supply is typically seasonally-driven. It is important to note, that these states are rarely mutually exclusive (Bullard and McTainsh, 2003).

4.2.1 Transport-Capacity Limited

Transport-capacity limited dust events are controlled by fluctuations in surface wind speeds (Figure 4.1a). Once the surface threshold shear velocity is exceeded, dust emissions will increase and decrease in parallel with fluctuations in wind speed. This may occur as aerodynamic entrainment (Macpherson et al., 2008) where dust emissions occur through direct suspension of fine particulates or through saltation bombardment where material is released by sandblasting (Shao and Raupach, 1992). In sources where saltation bombardment must occur to allow emissions, a saltation impact interval (T_0 - T_1) may exist. The length of this interval will be controlled by surface soil characteristics (Cahill et al., 1996), wind turbulence (Klose and Shao, 2012) and surface wind velocities (Shao and Raupach, 1992). The saltation impact interval can occur in all states but will not be discussed further.

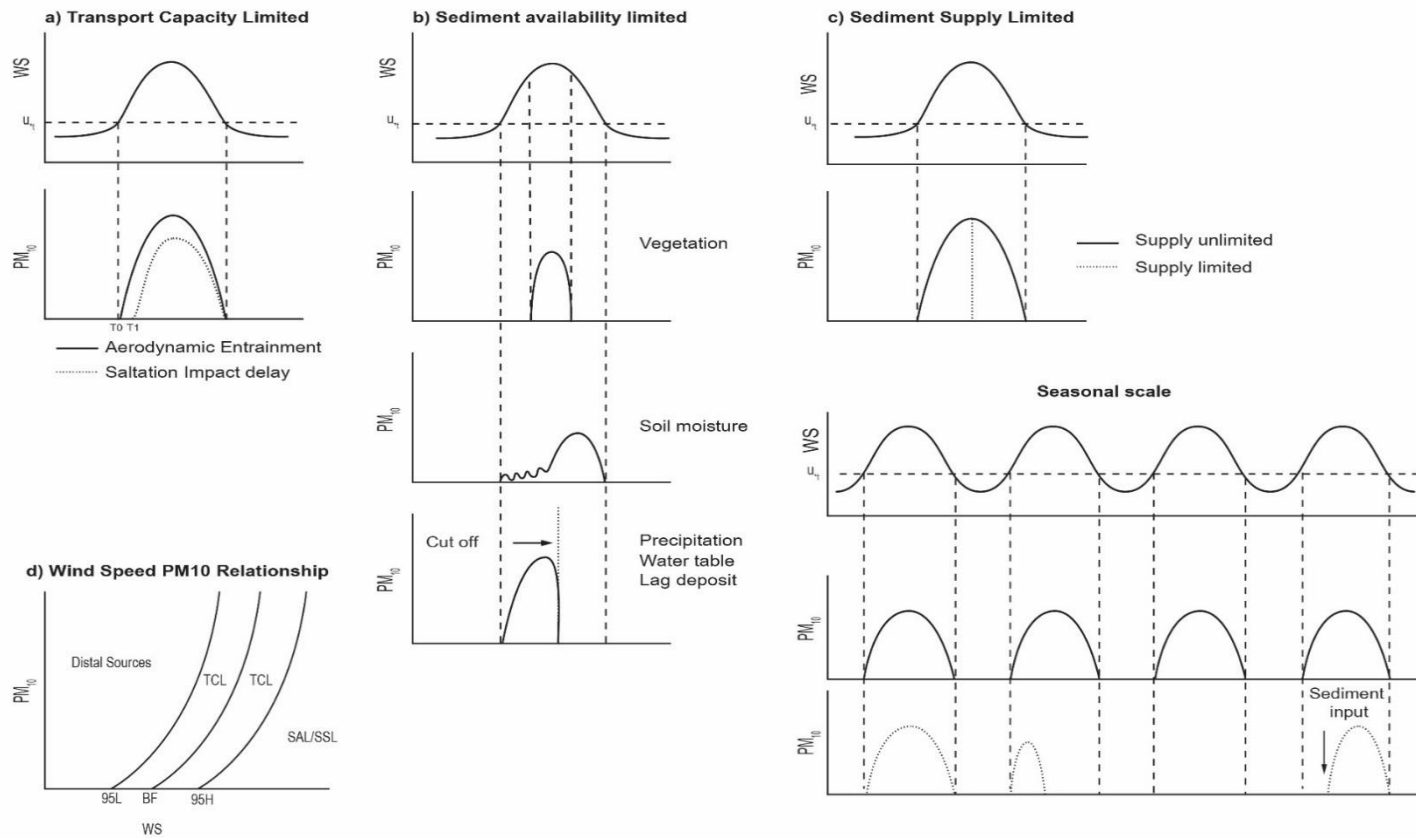


Figure 4.1: Conceptual model for event-scale dust emissions: a) Transport-Capacity Limited (TCL), b) Sediment-Availability Limited (SAL), c) Sediment-Supply Limited (SSL), d) Wind speed-PM10 relationship. T0-T1 is the potential saltation lag impact for aeolian activity. BF is the best-fit mathematical function for the wind speed-PM10 relationship. 95L and 95H are the 95% confidence bounds of BF

4.2.2 Sediment-Availability Limited

Sediment-availability limited events are those in which fine particulates (<100 µm) are present but factors other than wind speed and sediment supply prevent them from being entrained (Figure 4.1b). The factors include vegetation, surface moisture or the development of a coarse particle lag.

Vegetation reduces sediment availability directly by protecting surface sediments from entrainment and indirectly by decreasing air flow momentum (Lancaster and Baas, 1998) and absorbing shear stresses (Stockton and Gillette, 1990). Therefore, because vegetation increases the threshold shear velocity, entrainment will only occur during the highest wind speeds. This modified threshold will vary according to vegetation density, spacing and height (Lancaster and Baas, 1998). In some instances, low vegetation densities can cause localised decreases in threshold velocities due to the pattern of wind flow around individual plants (Logie, 1982) or where plant spacing is regular (e.g. soil streets, Okin and Gillette, 2001). Where vegetation is present, any dust entrainment is often of limited duration because particles travelling near the surface can be trapped within the canopy (Okin et al., 2006).

Surface soil moisture can restrict aeolian transport by increasing the threshold wind velocity (Wiggs et al., 2004). Where moisture is restricted to the surface sediment, its impact can be short-lived as the uppermost layer of particles may dry rapidly due to solar radiation or wind desiccation. The rate at which the surface dries is also controlled by soil texture. These controls on drying rate are typically spatially and temporally variable and the consequence is intermittent and patchy dust emissions. Where sub-surface moisture reaches the surface, for example due to relative changes in water table, emissions can be shut off. This may also occur under intense precipitation. Sediment availability can also be limited where a surface lag is present. In some locations, lag deposits have been shown to develop very rapidly, potentially cutting off emissions at the event-scale (Bullard and Austin, 2011).

4.2.3 Sediment-Supply (un)Limited

For dust events to occur a sufficient quantity of appropriately-sized sediment needs to be present at the surface. Where there is unlimited sediment available for aeolian

entrainment the system is controlled by transport capacity or sediment availability. In many areas, dust emissions are limited by a lack of suitable sediment (Bullard et al 2011). Sediment may be input to the source area periodically, for example where flood events transport fine sediments to ephemeral lakes (Mahowald et al. 2003) or to glacial outwash plains (Prospero et al. 2012). This influx of sediment becomes a source for dust emissions, assuming transport-capacity is reached, but when the material is exhausted, aeolian activity shuts off and will not recommence until source replenishment occurs (Figure 4.1c). On a seasonal scale, emissions may occur on several occasions before the source is fully exhausted (Macpherson et al. 2008).

4.2.4 Wind speed PM₁₀ relationship

Based on the argument above, for transport capacity limited events, there should be a strong relationship between wind speed and dust concentration for measurements taken at source (Figure 4.1d). All events within a sample with a correlation >0.8 (Spearman's Rank Correlation Coefficient) can be used to create a site-specific model to represent the relationship between wind speed and dust emission concentration. This relationship may be non-linear in certain environments as grain interactions/collisions increase with increasing wind shear velocities (Nickling, 1988). Points which fall within the 95% confidence intervals of this relationship would be classified as transport capacity limited.

For sediment-availability and supply-limited events, a weak or no relationship would be expected at the source and points would lie outside the boundaries of this relationship. Dust storms originate at a source, but then travel along pathways dictated by wind direction. Where dust has originated at a different source to that being monitored, the likelihood is that there may be high dust concentrations at low wind speeds. These points are classified as dust from distal sources.

This is a novel approach developed for this thesis in determining the relative importance of wind speed and the factors that affect sediment availability in controlling dust emissions at source.

4.3 Aims and Objectives

The main aim of this chapter is to:

To determine the dominant drivers and characteristics of Icelandic dust events through field and secondary data sources

This will be achieved by the following objectives:

- 1) Determine the relationship between wind speed and PM10 concentrations from field data at the event scale
- 2) Using the conceptual model proposed in section 4.2, classify each dust event according to the primary control
- 3) Use time series analysis, field observations and secondary meteorological data to infer factors which may affect/promote sediment availability during dust events and to validate the model
- 4) Determine the spatial distribution of potential pathways for dust events using air parcel trajectory modelling
- 5) Use CALIOP satellite retrievals to assess potential boundary layer heights for Icelandic dust events

The methods are in section 4.4. Results are presented in three separate sections in section 4.5:

Section 4.5.1: Measured dust events at source using primary field data and assigning events to the conceptual model

Section 4.5.2: Measured dust events using secondary data sources (WMO meteorological codes, AOD, CALIOP) and modelled transport pathways

Section 4.5.3: Expanded dust event record (from meteorological weather codes) and modelled transport pathways from 2010 - 2015

4.4 Methods

4.4.1 Field measurements

Field measurements were conducted at the Markarfljot relict sandur from the 29th May 2015 – 30th June 2015. The monitoring period was chosen to coincide with the spring dust peak identified in chapter 2 (Prospero et al., 2012; Dagsson Waldhauserova et al., 2014a; Baddock et al., 2017). Instrumentation included vertical arrays of Vector A-100R cup anemometers and BSNE sediment traps with rain hoods (Figure 4.2) (Shao et al., 1993). These were set at heights of 0.3 m, 0.6 m, 1.4 m, and 2.4 m. A Vector W-200P wind vane was placed at 1.4m. The anemometers logged to a Campbell Scientific CR800 Data logger and recorded 10 second averages. Due to issues with anemometers malfunctioning during the field observation period, wind data from 1.4m will be used in this chapter to compare to dust concentration measurements from the

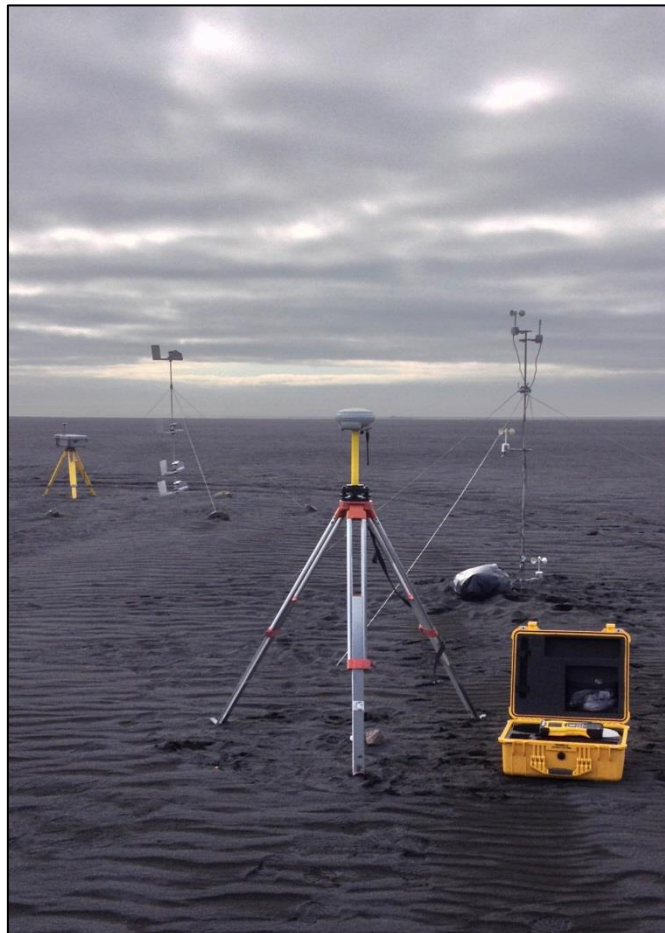


Figure 4.2: Field equipment set-up, Markarfljot, May/June 2015. DustTrak DRX, BSNE traps, cup anemometers

same height. BSNE traps were emptied daily. Samples were emptied into pre-weighed bags, transported back to the laboratory, desiccated and weighed before further analysis.

A TSI DustTrak DRX Aerosol Monitor 8533 was mounted on a tripod at 1.4m. At this height, only material in suspension is likely to be recorded. The DRX is an active dust sensor which measures in-situ dust concentrations in real time. It is a laser photometer. The DRX has five size bins: PM1 μ m, PM2.5 μ m, PM10 μ m, respirable and total emissions. Although the module is not designed to record any material > 15 μ m, no upper limit is defined by the manufacturer (Goosens and Buck, 2012) and therefore in this study, only PM10 values are used for analysis. The unit is powered by two 6600mAH Lithium Ion batteries. An external pump was used to allow continuous operation during sudden temperature fluctuations. It was only possible to run the DustTrak for 14-hour periods due to power constraints, therefore it was deployed in the morning (7-9am) and retrieved in the evening (8-11pm). Between each run, all exposed sensors were cleaned, and the module was zeroed using a zero filter. Data were recorded at 10 second intervals.

4.4.2 Meteorological data

Meteorological data were retrieved from several Icelandic meteorological office permanent weather stations (<http://en.vedur.is/weather/stations/>). These weather stations run all year round and have an excellent distribution across Iceland (Dagsson-Waldhauserova et al., 2014a, Baddock et al., 2017).

Landeyjahöfn weather station, which is located 4.5km from the field site, is used for all meteorological variables excluding precipitation and weather code observations. Variables used within this chapter include wind speed (mph), wind direction and humidity (%). All variables are measured as 15-minute averages. In this work, wind speed and direction from the meteorological stations were used to verify wind speed and direction measurements at source. Relative humidity was used in time series analysis for certain events where fluctuations in wind speed could not fully explain PM10 concentrations. Total hourly precipitation (in mm) is recorded at Önundarhorn; 25km east of the field site. All weather stations used record at a height of 5 m.

4.4.3 WMO meteorological weather codes

Manual weather observations are made at Stórhöfði and Eyrarbakki weather stations. Current weather type is assigned a SYNOP code for the dominant weather type every 3 hours (O’Loingsigh et al., 2014). These include 11 codes for the identification of dust events (Table 2.2) (O’Loingsigh et al., 2014, Baddock et al., 2017, Bullard and Mockford, 2018). Although weather codes are useful for indicating dust storm frequency, due to issues with the manual recording of weather observations (O’Loingsigh et al., 2014, Baddock et al., 2017), they do not provide a reliable representation on the magnitude and/or intensity of dust events. Therefore, they are used within this thesis only as an observation that dust was present at/near the weather station at the time of recording. This is particularly the case at Stórhöfði, where 80% of the codes recorded from 2010 – 2015 were Code 06. It could be assumed that the observer is labelling many events with this code, not because they are all the same magnitude, but because this is the preferred weather code for dust observation at this particular location.

4.4.4 HYSPLIT air parcel trajectory modelling

The Hybrid Single-Particle Lagrangian Intergrated Trajectory model (HYSPLIT) is an air parcel trajectory model developed by the Air Resources Laboratory of the National Oceanic and Atmospheric Administration (Draxler and Hess, 1997; 1998; Draxler, 1999; 2003). HYSPLIT has been used to investigate dust transport pathways. For a specified place and height; an air parcel driven by three-dimensional winds is computed from a user selected start location. It can be used to project forward or back trajectories.

SYNOP weather code data (all dust code days) from 2010 – 2015 were acquired for Stórhöfði. This period was used to represent contemporary dust emission patterns from the Markarfljot river basin. 125 unique dust days were identified during this period. However, to assure that events are likely to have come from the Markarfljot sandur region, only days with a dust SYNOP code and a northerly wind direction (305° - 45°N) at both Stórhöfði and Landeyjahöfn were used. These wind directions, along with a dust observation, allows us to assume that the material must be from the Markarfljot basin as it is the only upwind dust source (Prospero et al., 2012). This left 82 dust days

for this period. Forward trajectories were also calculated for the 9 dust events recorded in the field at Markarfljot in May/June (2015) (Table 4.1).

All trajectories were started at the time of the dust observation and at a height of 100m above sea level. Start heights vary significantly amongst users trying to determine dust transport pathways. McGowan and Clark (2008) used a 500m ASL start height, whereas Neff and Bertler (2015) used a 100m ASL start height. Baddock et al. (2017) indicates the importance of start height by showing the different trajectory pathways and air parcel vertical distributions for both 100m and 500m. 100m was used in this study as it has been indicated that particles from Icelandic dust events may sit predominately low within the atmosphere (Blechsmidt et al. 2012). The model used the monthly NCEP/NCAR global reanalysis data set (Kalney et al., 1996; Stein et al., 2015) and 3-D kinematic trajectories which use vertical wind fields to calculate parcel trajectory. Harris et al. (2005) explored the use of multiple datasets with varying trajectory analysis techniques under different environmental conditions, and concluded that 3-D kinematic trajectories in a high Arctic environment were 600m higher than an isentropic trajectory. Little difference was found between the NCEP/NCAR reanalysis and ERA-40 input datasets (Harris et al., 2005; Baddock et al., 2017).

Trajectories were run for 72 hours, outputting points hourly, from the initial observation of a dust event. Others have used much longer time periods to assess dust transport pathways; McGowan and Clark (2008) ran 8-day trajectories, whereas Neff and Bertler used 10-day trajectories. It has been suggested that the horizontal and vertical accuracy of HYSPLIT air parcels decreases with time (Stohl, 1998). Therefore, a shorter time period is used within this study to allow a more accurate representation of dust transport pathways for this region, even if it then fails to address the maximum possible extent of Icelandic dust emissions (Baddock et al., 2017). HYSPLIT control files were automatically created using MATLAB and ran through HYSPLIT Version 4; analysis of the resulting trajectories was performed in ArcMap.

4.4.5 CALIPSO

Satellite data has been used to identify dust events at a variety of spatial scales (Prospero et al., 2002; Kaufman et al., 2005; Baddock et al., 2009; Bullard et al., 2011; Ginoux et al., 2012). However, as previously discussed, there are challenges in high latitude environments because of long periods of winter darkness and persistent cloud cover (NASA, 2014)

In this study, three satellite products are used to try and identify dust events visually and to assess the potential distribution of particles within the atmosphere. This was achieved by identifying dust event timings from Moderate Resolution Imaging Spectroradiometer (MODIS, Remmer et al., 2005) Level 1b 1km data (acquired from LAADS, <https://ladsweb.nascom.nasa.gov/>) and Landsat 7 and 8 (acquired from LandsatLook Viewer, <http://landsatlook.usgs.gov/>) RGB images.

One way to address the difficulties in using RGB remote sensing images (e.g. passive products) in high latitude regions is to use active remote sensing approaches such the Cloud-Aerosol Lidar and Infrared Pathfinder Satellite Observation (CALIPSO) (Liu et al., 2008). CALIPSO data are used to determine the altitude of aerosol layers within the atmosphere, and has been used to identify the vertical distribution of dust particles globally (Huang et al., 2007; Liu et al., 2008; Guatum et al., 2009).

1064 nm attenuated backscatter coefficients and vertical feature masks were acquired for days which were identified as dust event days from MODIS/LANDSAT between 2010 - 2015 and all dust days observed during the monitoring period. Where possible, these data were also paired with MODIS Aerosol Optical Depth (AOD) retrievals.

4.5 Results

4.5.1 Section 1 – Field measurements of dust events

4.5.1.1 Frequency and Magnitude

In this part of Iceland, background dust emissions from DustTrak concentration measurements are in the range 10 to 70 $\mu\text{g m}^{-3}$. For this thesis, the onset of a dust event is defined as where PM_{10} concentrations exceed 250 $\mu\text{g m}^{-3}$. These definitions are based on data collected during field monitoring using measurements which were conducted directly at source. Using these criteria, during a 6-week monitoring period, 9 dust events were recorded. These events varied significantly in magnitude, duration and intensity

Event characteristics are listed in Table 4.1. Average PM_{10} concentrations (based on the time the source was active) ranged from 269 $\mu\text{g m}^{-3}$ - 2654 $\mu\text{g m}^{-3}$. The maximum 10-second PM_{10} concentration recorded was 8860 $\mu\text{g m}^{-3}$. Durations of events differed considerably, with high magnitude events often lasting >14 hours.

The relationship between horizontal mass flux (e.g. Shao et al., 1993) and average event DustTrak concentration is displayed in Figure 4.3

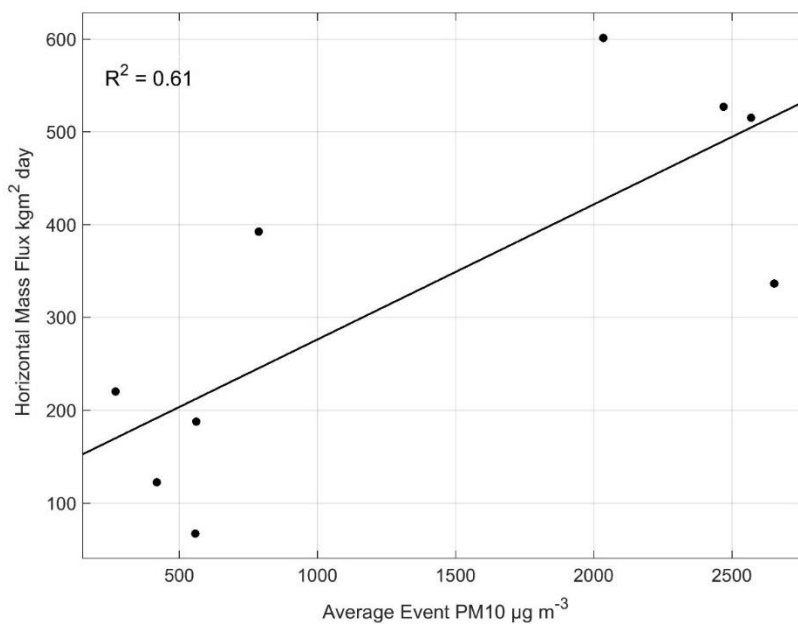


Figure 4.3: Relationship between dust event average PM_{10} ($\mu\text{g m}^{-3}$) and horizontal mass flux for 9 dust events at Markarfljot

Horizontal mass flux during dust events varied from 67.2 to 601.6 kg m⁻²/day. The relationship indicates that horizontal mass flux increases with average dust concentration in a strong linear relationship ($R^2 = 0.61$).

4.5.1.2 Event classification

To apply and test dust concentration data against the conceptual framework (Figure 4.1), measurements are required to populate the wind speed PM10 relationship displayed in Figure 4.1d. To formulate the mathematical relationship from figure 4.1d, the data set needs to be located at source and must include a number of events which can be classified as transport capacity limited.

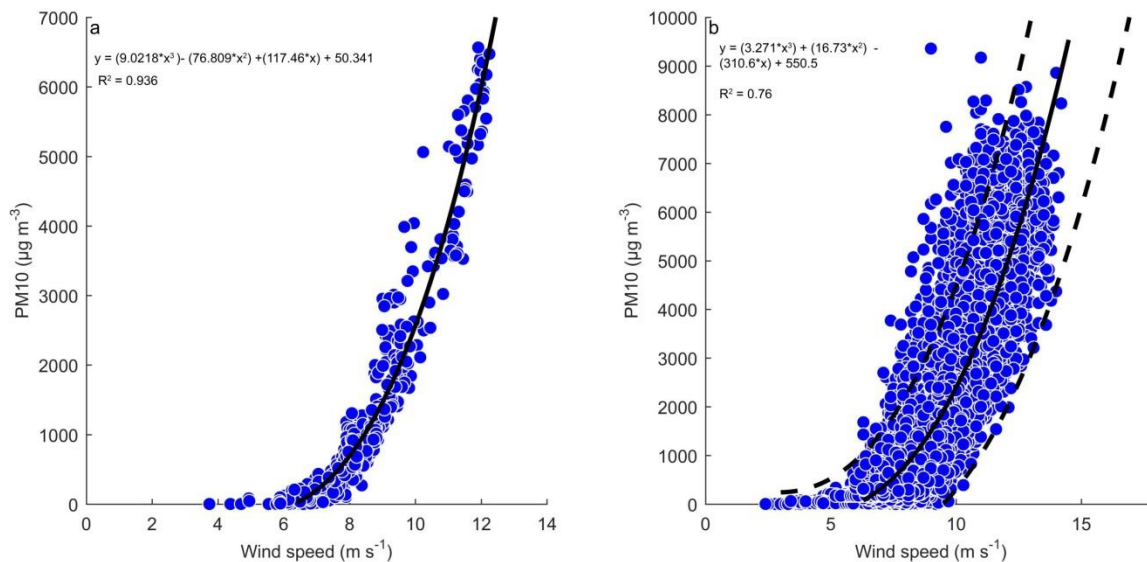


Figure 4.4: a) 5-minute averaged wind speed and PM10 relationship for 3 TCL events b) 10 second average wind speed and PM10 relationships for same events (including 95% confidence intervals)

Table 4.1: Dust storm characteristics for 9 dust events at the Markarfljot relict sandur. Bold represents values used for population of Figure 4

Event	Date	Duration (hr)	Average event wind speed (m s ⁻¹)	Average Event PM10 (µg m ³)	Maximum second (µg m ³)	10- PM10	Horizontal Mass Flux (kg m ² day)	Temporal Control	Wind speed PM10 correlation
1	30/05/2015	>14	11.96	2570	7330		515.4	SAL/SSL	0.294
2	31/05/2015	3	9.43	2654	8040		336.7	TCL	0.894
3	02/06/2015	8	7.42	787	3670		392.6	TCL	0.832
4	06/06/2015	2	6.94	269	869		220.3	TCL	0.678
5	15/06/2015	>14	12.6	2470	7350		527.4	SAL/SSL	0.262
6	19/06/2015	8.5	6.42	418	1780		122.7	TCL/SAL	0.787
7	24/06/2015	7	7.77	561	2020		188.0	TCL	0.665
8	27/06/2015	>14	12.01	2035	8860		601.6	TCL	0.842
9	28/06/2015	10	6.64	558	1870		67.2	SAL/SSL	0.104

Dust storms were therefore initially classified based on the relationship between wind speed and PM₁₀ (Table 4.1). To test/apply the proposed framework, data is required to populate Figure 4.4. These events must be transport capacity limited to create an equation which reflects only the relationship between dust emission and wind speed. Where there is a high non-linear correlation coefficient (Spearman's Rank Correlation Coefficient > 0.8) between dust emissions and wind speeds above the threshold velocity, events are classified as transport-capacity limited. Of the 9 Iceland events, 3 are clearly in this category (Table 4.1). The nature of the mathematical relationship between the two variables is very clear when 5-minute averages of wind speed and dust concentration are plotted (Figure 4.4a). However, to determine appropriate confidence bounds, a high number of observations are required; in this instance, the frequency of observations is increased, but in some instances a longer record may provide sufficient observations. Ten-second averages from the three-transport capacity limited events were used to create a cubic model (Figure 4.4b), including the upper and lower 95% confidence bounds. It is generally agreed that the relationship between wind speed and dust concentration is either cubic or polynomial (Shao et al., 1993; Kok et al., 2011). This study uses a cubic relationship.

The assumption is that dust concentrations which fall within this envelope are controlled by wind speed. Points outside of this envelope do not follow the relationship between wind speed and PM₁₀ concentrations, therefore other factors are potentially controlling emissions. It is also possible to calculate the threshold velocity for motion from the three-transport capacity limited events as there is a strong relationship between wind speed and PM₁₀ concentrations at these points. From Figure 4.4a, it can be estimated that the threshold velocity for motion for dust emissions on this surface is approximately 6.5 m s⁻¹ (at 1.4m).

The relationship between wind speed and PM₁₀ concentration for all events is shown in Figure 4.5 where observations within the envelope are in black and outside in red/blue. Red points (above the upper 95% confidence boundary) will indicate sediment availability/sediment supply limited events because high wind speeds are unable to produce the PM₁₀ concentration seen in transport capacity limited events under the same wind velocities. Examination of the evolution of the dust event through time makes it possible to discern what is driving the sediment availability/sediment supply limited events.

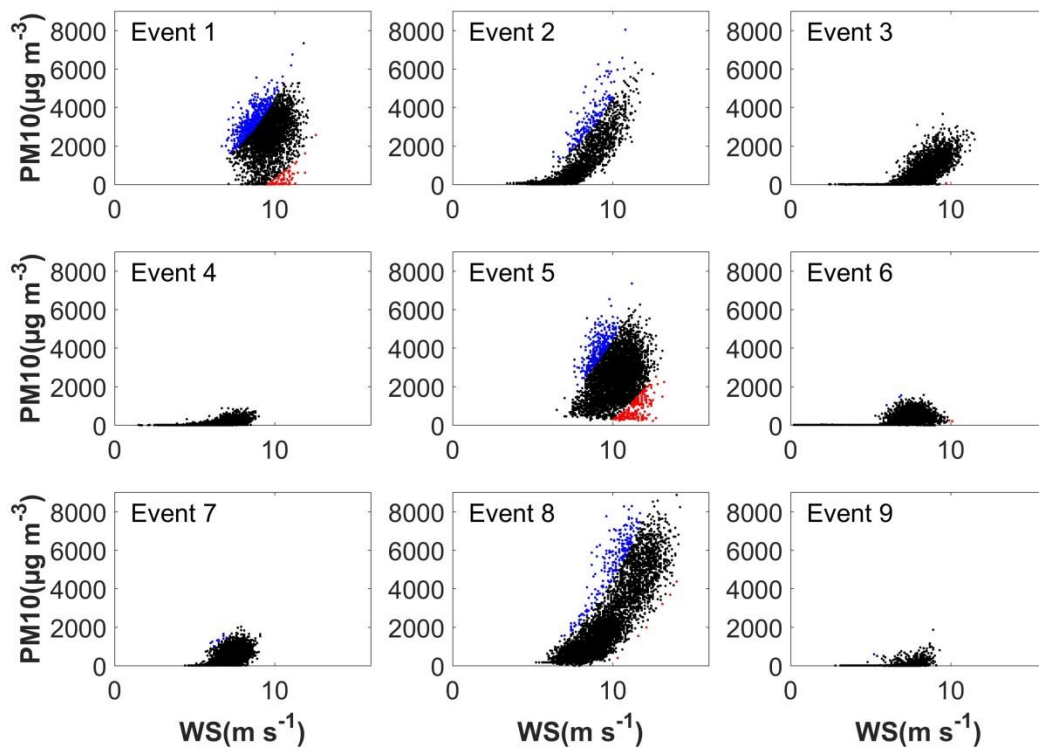


Figure 4.5: Wind speed PM10 relationships for events listed in Table 1. Black dots represent points inside the mathematical relationship from Fig.2b, whereas red and blue dots represent points outside

4.5.1.3 Selected examples of each event type

4.5.1.3.1 Transport capacity limited events

A high magnitude event occurred on 27th June 2015 (Event 8 Table 4.1). A time series of wind speed, wind direction and PM₁₀ can be seen in Figure 4.6. Over a 14-hour period, average wind speed was 12.01 m s⁻¹ and average PM₁₀ was 2035 µg/m³ (with a maximum of 8860 µg/m³). A SSE wind was dominant throughout the event. During the event, wind speed and PM₁₀ concentration increase and decrease in parallel (with no obvious saltation lag) reaching a sustained maximum for 3 hours approximately 6 hours after the start of the event. During the final third of the event dust emissions decrease to c. 800 µg m⁻³ and this concentration is sustained for a further 6 hours at wind speeds of approximately 8 m s⁻¹.

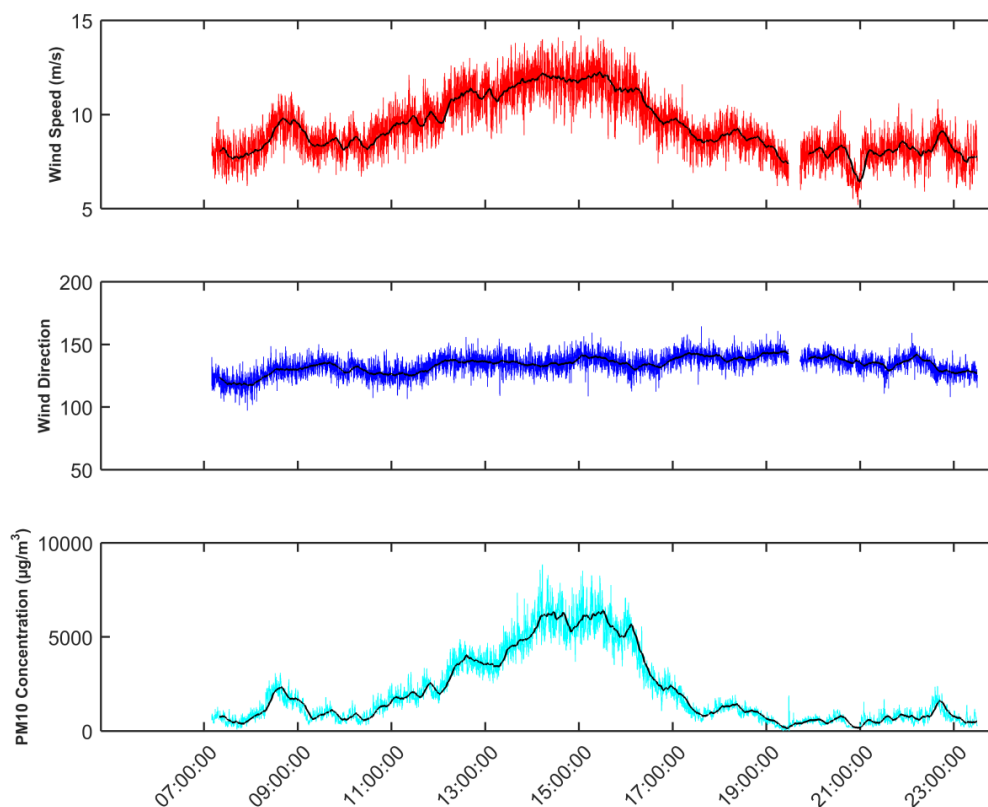


Figure 4.6: Event 8, 27th June 2015, a) Surface wind speed b) wind direction c) PM₁₀ concentration

Event 3: 2nd June 2015

8 of the 9 dust events occurred during SSE winds. A high magnitude event did occur with a non-SSE wind on 2nd June 2015 (Figure 4.7). The event duration was 8 hours, with an average wind speed of 7.42 m s^{-1} , an average PM10 concentration of $787 \mu\text{g m}^{-3}$ and a dominant N wind direction (Figure 4.8). Like in Event 8, wind speed and PM10 decrease in tandem throughout the period, with notable periods of dust emission stopping as wind speed falls below the threshold shear velocity.

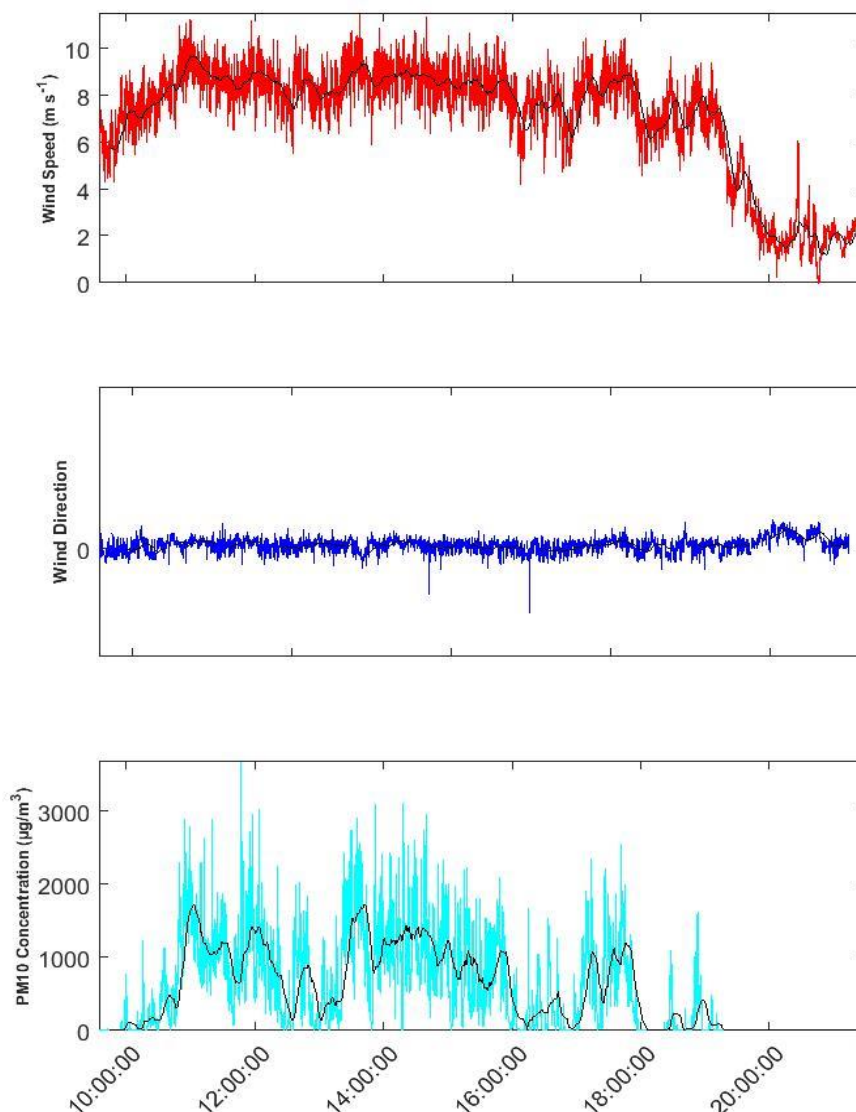


Figure 4.7: Event 3, 02nd June 2015, a) Surface wind speed b) PM10 concentration

4.5.1.3.2 Sediment availability limited events

Event 5: 15th June 2015

A high magnitude event occurred on 15th June 2015 (Event 5 Table 4.1). A time series of wind speed, wind direction and PM₁₀ can be seen in Figure 4.8. Like event 8, the duration was >14 hours. The event magnitude was slightly greater than event 5, as average wind speed was 12.6 m s⁻¹ and average PM₁₀ was 2470 µg m⁻³. The event was also controlled by a dominant SSE wind. However, there are noteworthy differences between event 5 and event 8. Wind speed and PM₁₀ increase and decrease in tandem for approximately 6 hours with emissions reaching 7500 µg m⁻³. During the second half of the event, wind speed stays constant at approximately 10.5 m s⁻¹ but emissions slowly decline, with periods of recovery, until they fall below 500 µg m⁻³ at the end of monitoring. Even above the expected threshold velocity, no relationship exists between wind speed and PM₁₀.

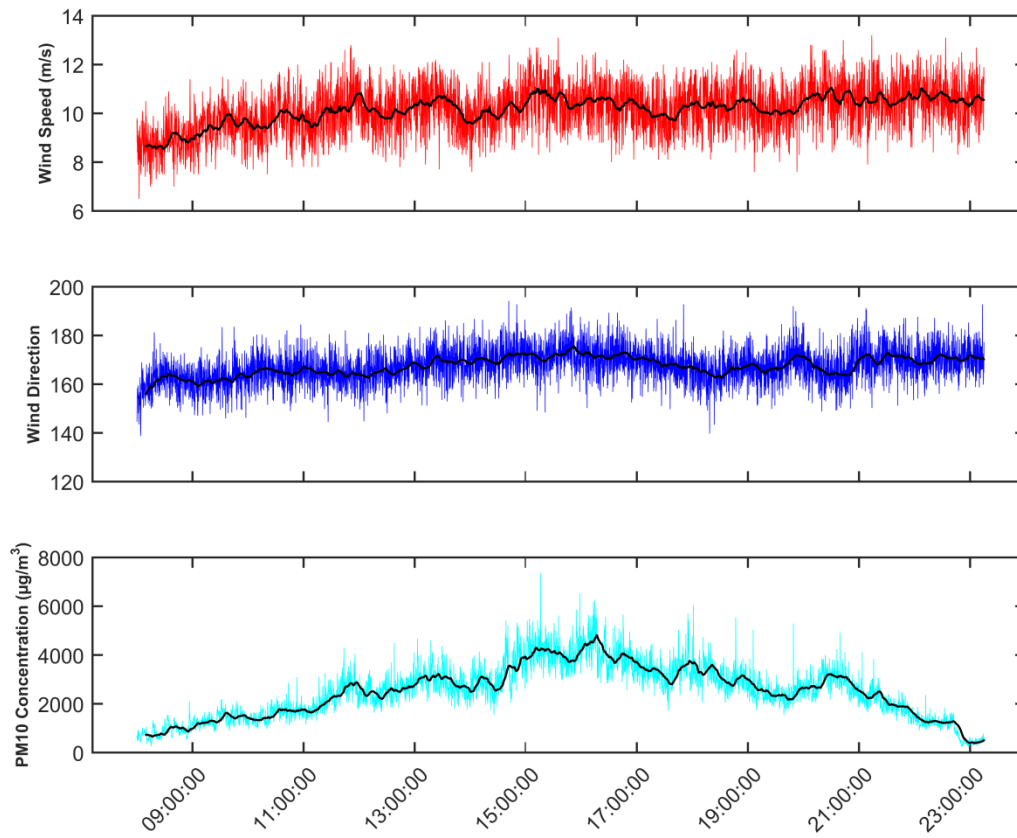


Figure 4.8: Event 5, 15th June 2015, a) Surface wind speed b) wind direction c) PM10 concentration

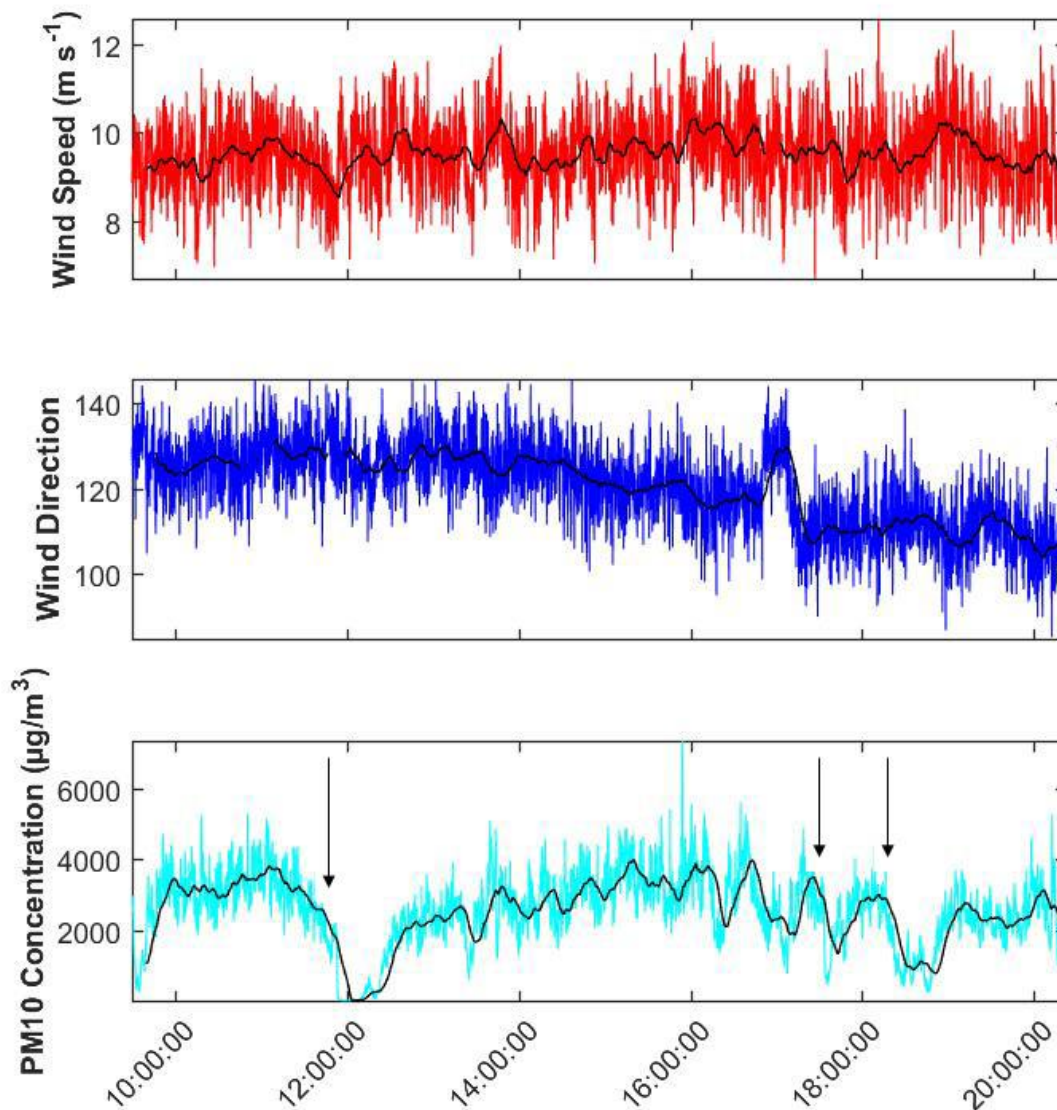


Figure 4.9: Event 1, 30th May 2015, a) Surface wind speed b) wind direction c) PM10 concentration. Black arrows indicate periods of low intensity rainfall (<0.2mm)

Event 1: 30th May 2015

The relationship between wind speed and PM10 is also weak during an event on 30th May 2015 (Figure 4.9). Event metrics are like those seen in events 5 and 8; average wind speed was 11.96 m s⁻¹, average PM10 concentration was 2570 µg m⁻³. (Maximum: 7330 µg m⁻³) and an SSE wind direction dominated. Wind speed and PM10 increase and decrease in tandem during much of the record, however sharp declines in PM10 occur regularly whilst wind speed remains above the threshold velocity. The time the system requires to recover varies; near the beginning of the record PM10 is

reduced to $0 \mu\text{g m}^{-3}$ for approximately 20 minutes before intermittent emissions recur prior to a full recovery of the system. In the second half of the event, dust concentration falls substantially (e.g. from $3000 \mu\text{g m}^{-3}$ to $<500 \mu\text{g m}^{-3}$) for periods of 20-40 minutes before rapidly (<20 minutes) returning to previous levels.

4.5.2 Section 2 – Secondary data sources for measured dust events

4.5.2.1 Dust Transport Pathways

Figure 4.10 shows NOAA HYSPLIT air parcel trajectories associated with all dust events recorded during the field monitoring campaign (Table 4.1, Section 5.1).

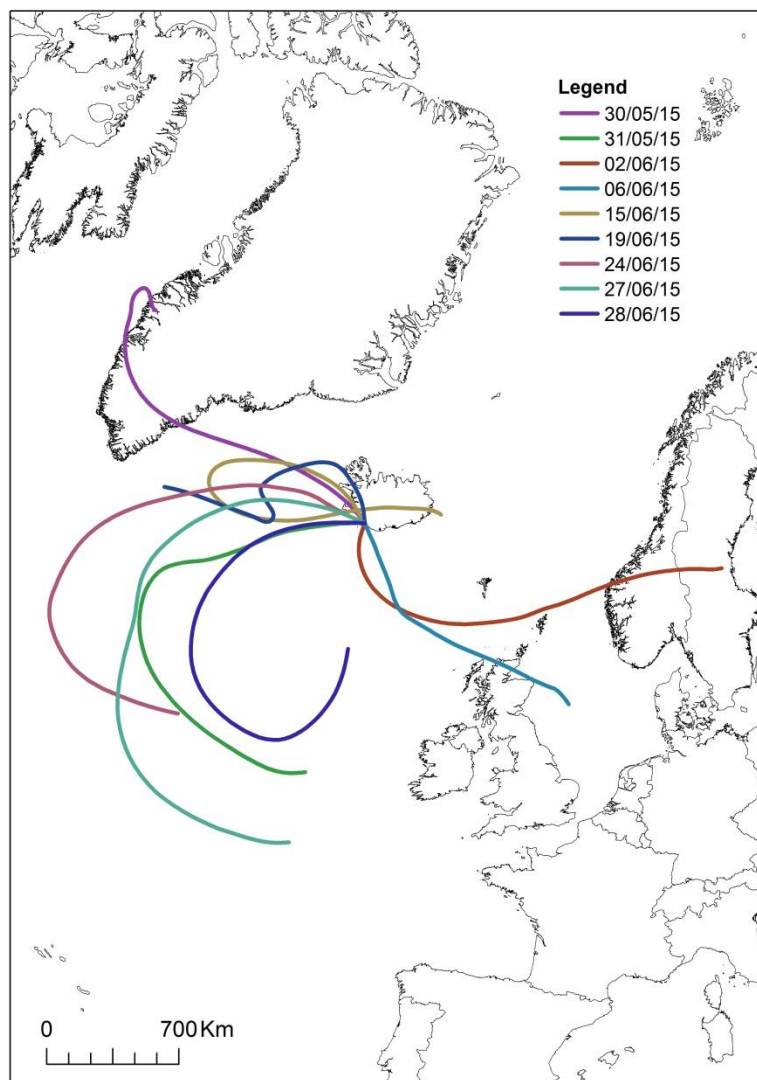


Figure 4.10: 72hr HYSPLIT forward trajectories for 9 dust events recorded at Markarfljot

Most trajectories are routed SSE towards the North Atlantic Ocean. One event (event 1) routes across the Greenland Ice Sheet towards the Denmark Strait. Two events (Event 3 and 4) are routed south towards the United Kingdom and Baltic Sea respectively.

4.5.2.2 Dust transport to Reykjavik

One of the highest magnitude events, event 5, occurred during a consistent SSE wind direction (Figure 4.10). Due to the longevity of this event, dust emissions increased the PM10 concentrations in the city of Reykjavik (Figure 4.11). Background concentrations of PM10 ($<10 \mu\text{g m}^{-3}$) were recorded until 10:00. Large increases in PM10 concentration occurred from 12:00 to a maximum of $318 \mu\text{g m}^{-3}$ at 16:00. PM10 concentration then decreases to $126 \mu\text{g m}^{-3}$ by 19:00. A sharp increase, over a 2-hour

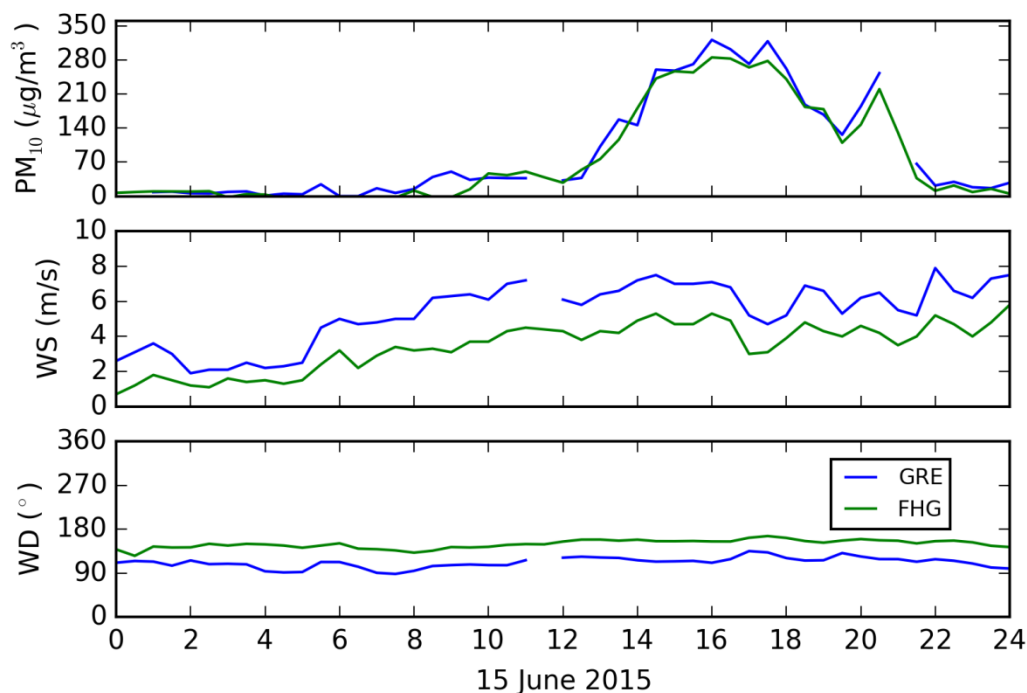


Figure 4.11: Reykjavik aerosol monitoring stations (GRE, FHG) on 15th June 2015. a) PM10 concentration b) 15-min average wind speed c) 15-min averaged wind direction. Figure courtesy of Throstur Thorsteinsson

period, sees another increase in PM10 concentration to $252 \mu\text{g m}^{-3}$. PM10 then decreases below $<50 \mu\text{g m}^{-3}$ by 22:00. Wind direction in Reykjavik during the period stayed relatively constant, with a range between 88° and 132° .

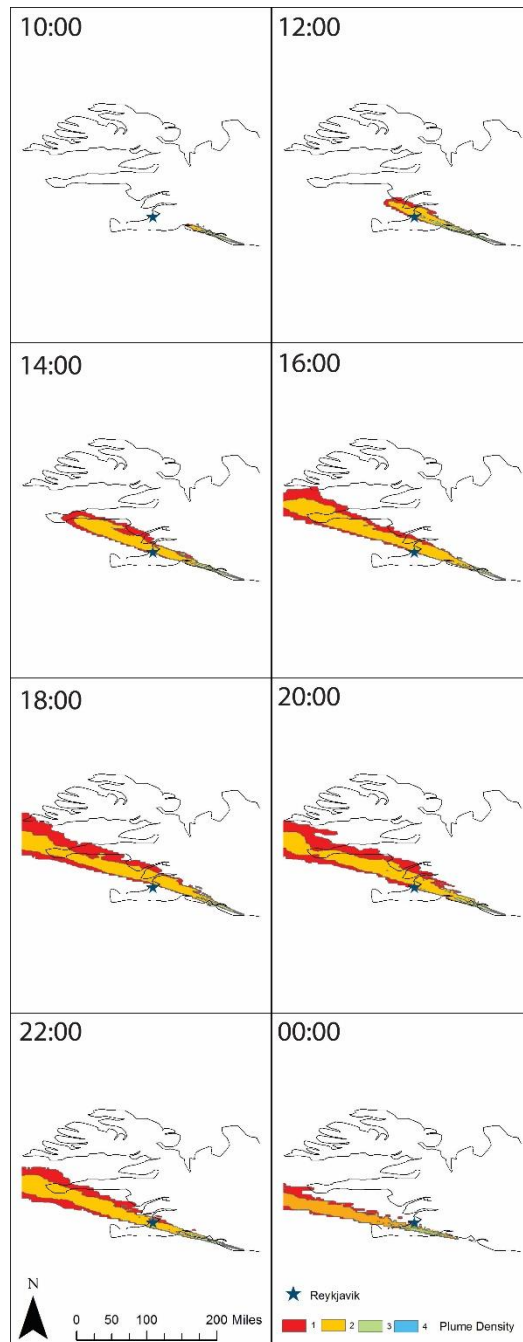


Figure 4.12: NOAA HYSPLIT Dispersion model 2 hourly plume model for Markarfljot on 15/06/15 (Event 5). Reykjavik is located with star

This dust event was modelled using the HYSPLIT Dispersion model (Figure 4.12). The plume is shown to arrive in Reykjavik between 10:00 – 12:00. The plume shifts

northwards between 16:00 – 18:00, with the densest part of the plume moving away from the city, before shifting back south between 20:00 – 22:00. The plume continues to shift south until 00:00, where the plume is no longer affecting Reykjavik.

4.5.2.3 Meteorological dust codes

Dust codes are recorded at Storhöfði (south) and Eyrarbakki (east). Dust codes give an indication on the timing and frequency of dust events. For the 9 events recorded during the field campaign, only event 1 (30/05/15) and event 9 (27/06/15) were recorded at Eyrarbakki in the SSE dust transport pathway (Figure 4.10). None of the events were recorded at Storhöfði.

4.5.2.4 MODIS/AOD/CALIPSO

MODIS Aqua/Terra Level 1b km data and their associated AOD retrievals were assessed for all events. Due to extensive cloud cover over ocean and land during all dust events, no visual identification of dust plumes could be made. CALIPSO retrievals during this time period were also unsuccessful due to the satellite tracking significantly to the south of Iceland in the direction of the Denmark Strait.

4.5.3: Section 3 – Expanded secondary dust measurements

As only 9 events were recorded during the field monitoring (Table 4.1), dust days from Storhöfði were identified from 2010 – 2015 from northerly wind directions. With these wind directions, it can be assumed that dust observations at Storhöfði are associated with blowing dust from the Markarfljót river basin. Figure 4.13 shows the seasonal plot of 82 identified dust days associated with blowing dust at Markarfljót from Storhöfði. The season plot is comparable to that shown in Chapter 2 (Bullard et al., 2016) with dust observations recorded all year round with a notable peak of observations during spring.

4.5.3.1 Transport pathways

Between 2010 and 2015, 125 dust observation codes were recorded at Storhöfði. Of these events, 82 of them occurred during NW-NE wind directions. Because of these wind directions, it is probable that the material observed was from the Markarfljót river basin. Figure 4.14 is the total percentage of all trajectories which travelled through a

1 x 1° grid. A substantial proportion of the trajectories route south in the North Atlantic, with some trajectories extending south beyond 40°N. Fewer trajectories route towards the Denmark Strait, with no trajectories reaching above 80°N. Only 1 trajectory skirts the south-westerly coastline of the Greenland Ice Sheet. No trajectories reach the central part of the Greenland Ice sheet. A large corridor of trajectories route towards the British Isles; areas of Scotland and Ireland receiving 5-7% of all air parcel trajectories originating from the Markarfljot river basin.

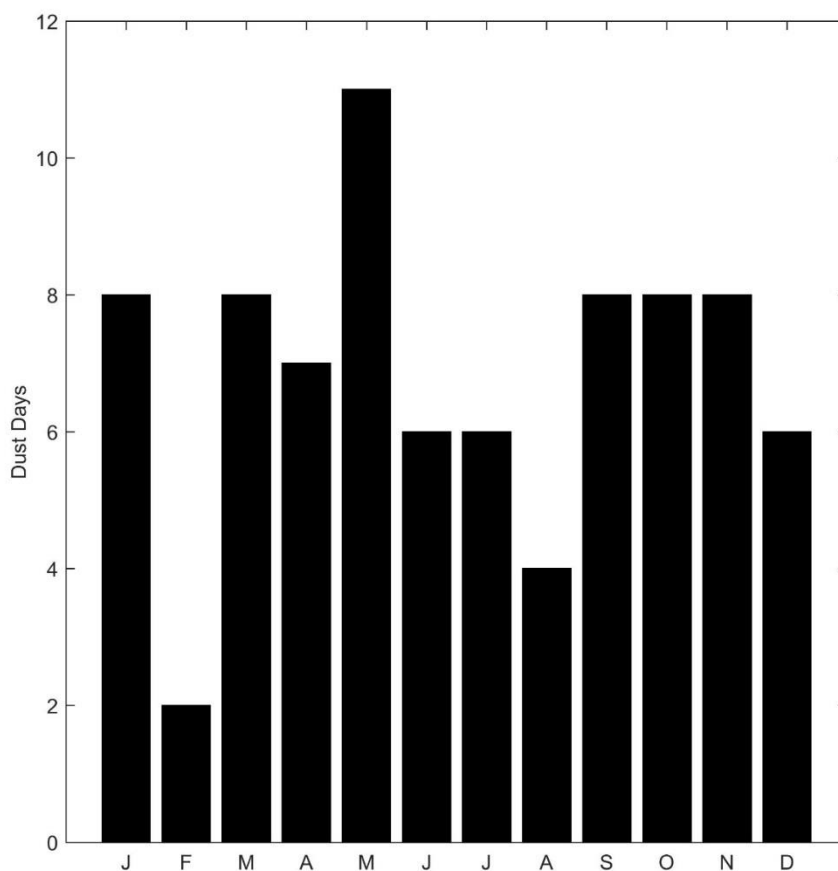


Figure 4.13: Seasonal dust day record for Storhöfði (South Iceland) from northerly wind directions from 2010 - 2015

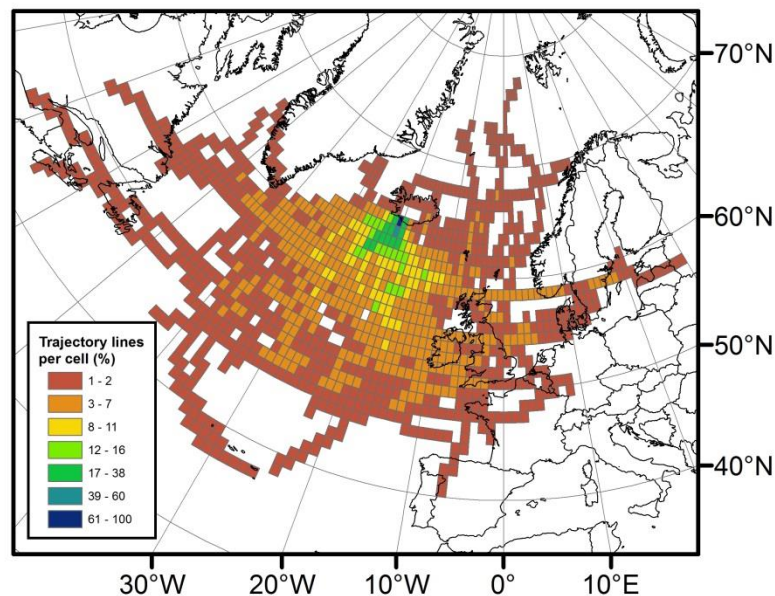


Figure 4.14: Trajectory line density (% of trajectories per 1°x1° cell) for 72h forward HYSPLIT simulations at a 100m start height for all northerly wind direction days from Markarfljot where a dust observation was recorded at Storhöfði (1995-2015)

Modelled air parcels are split by season in Figure 4.15. The highest proportion of trajectories occurred during March, April and May (MAM) (31.7%) and September, October and November (SON) (29.3%). Both December, January and February (DJF) and June, July and August (JJA) had relatively smaller proportions (19.5%). The pathway direction also shifts between seasons. During DJF, one clear preferential pathway can be seen heading SW with relatively few trajectories heading towards the SE. During MAM, the SE pathway has developed, and both the SE and SW pathways are easily identifiable. During JJA, the SW pathway seems to be disintegrating, with an S/SE pathway being the dominant route. When reaching SON, the SE pathway is the only preferential route, with the highest proportion of trajectories moving towards the British Isles.

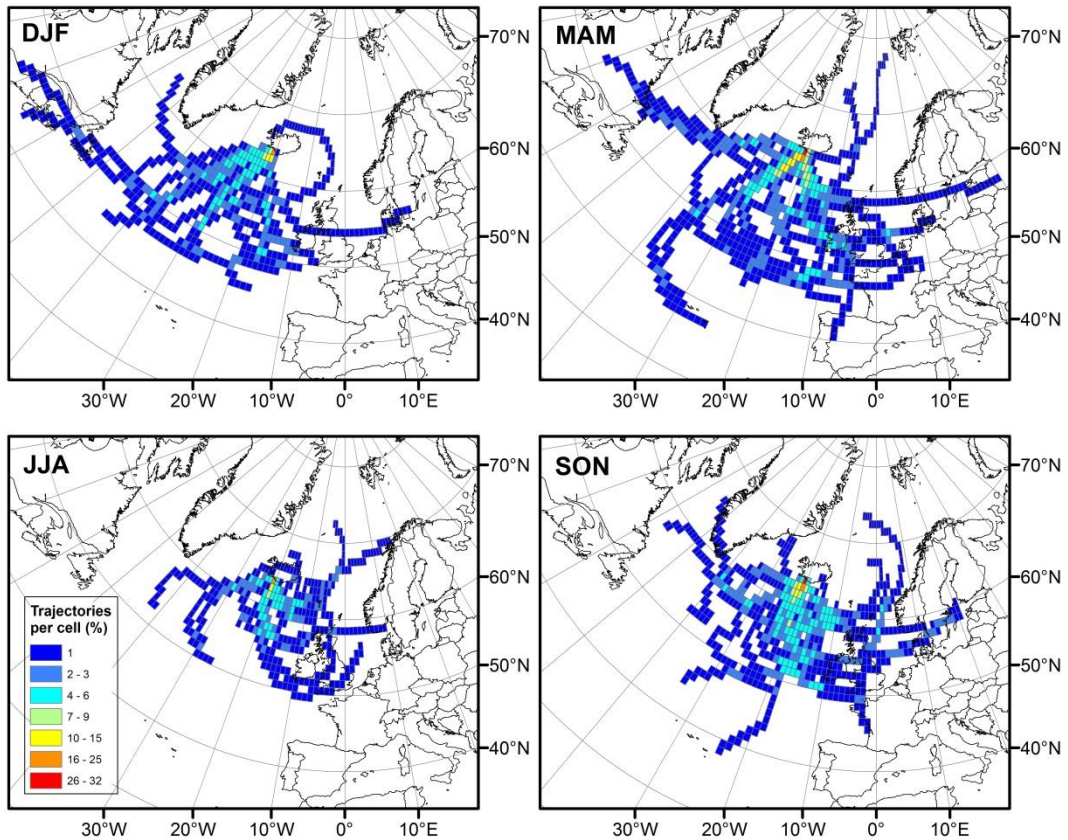


Figure 4.15: Trajectory line density (% of trajectories per 1°x1° cell) for 72h forward HYSPLIT simulations at a 100m start height for all northerly wind direction days from Markarfljot where a dust observation was recorded at Storhöfði (2010-2015) split by season

Heights of all air parcels are displayed in Figure 4.16. The vast majority of air parcels are located below 100m in the atmosphere (62.5%). These air parcels travel in S/SE/SW directions and are most highly concentrated close to source. 17.6% of the trajectories travel to between 100-200m within the atmosphere. There is a slight dominant pathway towards the south-west of Iceland. 11.25% and 6.9% of trajectories are located between 200-500m and 500m-1000m respectively. At both of these heights, trajectory points are further from source than at the previous two heights and are located predominately in the North Atlantic. At 200-500m, a higher proportion of trajectory points are located in the North Atlantic closer to the Greenland Ice sheet. Only 1.6% of all air parcel trajectories reach 1000m, with the highest proportion of

them located over the highlands of Iceland. Very few trajectory points above >1000m reach Greenland, Europe or North America.

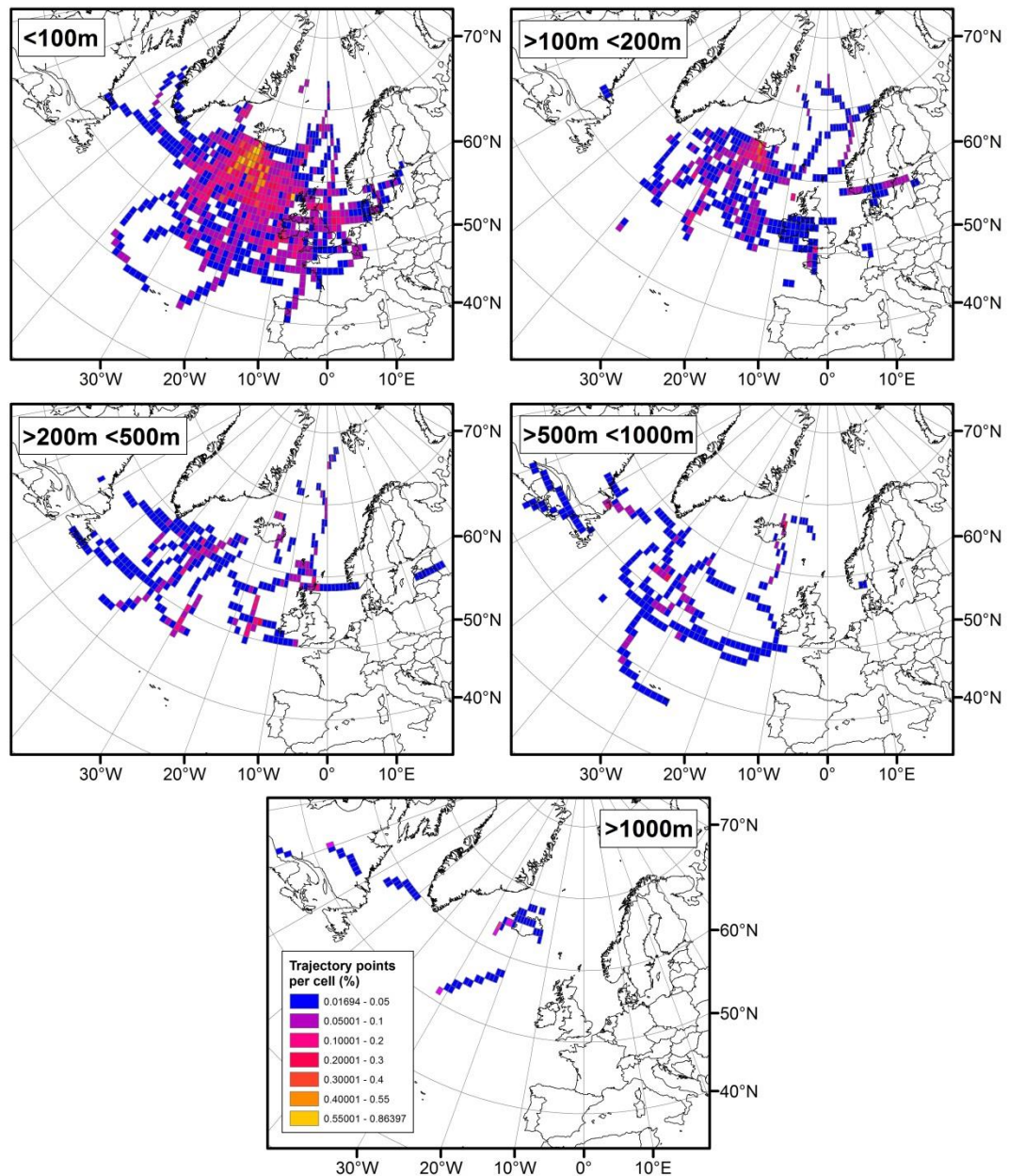


Figure 4.16: Trajectory point density (% of trajectories per 1°x1° cell) for 72h forward HYSPLIT simulations at a 100m start height for all northerly wind direction days from Markarfljot where a dust observation was recorded at Storchöfði (2010-2015) split by altitude

4.5.3.2 MODIS/AOD/CALIPSO

From 125 dust events identified at Storhöfði between 2010 - 2015, 14 dust events were identified in the MODIS Aqua/Terra Level 1b km data from South Iceland. Of these events, 12 events were located at the Markarfljot river basin. Due to the resolution of MODIS data, it is difficult to distinguish in which part of the river basin the dust is sourced from. Of the 14 identified events, only one event can be identified in a CALIOP track (17/09/2013). Figure 4.17a shows the dust storm identified in the MODIS 250km level terra 1b data; the Terra level 1b aerosol optical depth (Figure 4.17b), the CALIOP 532nm total attenuated backscatter (Figure 4.17c) and the corresponding CALIOP vertical feature mask (Figure 4.17d). The dust storm can be seen to have come from numerous sources on the southern Icelandic coast, with the largest plumes being sourced from Mýrdalssandur and Skeiðarársandur. Plumes are also sourced from the Markarfljot river basin, and these plumes extend into the CALIOP track as seen in the AOD retrievals (0.4 – 0.6). Where the plumes have been identified in the AOD, these are clearly reflected in an increase in backscatter from the CALIOP sensor (Figure 4.17c), which is identified to be aerosol. The identified aerosol is all located below 1km within the atmosphere.

4.6 Discussion

4.6.1 Dust storm characteristics

Table 4.2 shows the maximum DustTrak concentration ($\mu\text{g m}^{-3}$) and horizontal mass flux ($\text{kg m}^{-1} \text{day}^{-1}$) values from this study in comparison from other field studies conducted in Iceland (Arnalds et al., 2012; Dagsson Waldhauserova et al., 2014b;), Antarctica (Gillies et al. 2013) and sites within subtropical deserts (Kimura and Shinoda, 2010; Alghamdi et al., 2015; Stout, 2015) using the same types of active and passive sediment samplers.

The highest horizontal mass flux recorded in this study is in the same order of magnitude with the study of Arnalds et al. (2012) in Iceland and with Victoria Valley West (Gillies et al. 2013). The extremely high horizontal mass flux recorded at Victoria Valley East can be attributed to a very high magnitude wind event in which saltation (e.g. dust) only occurred for c.2-3 hours.

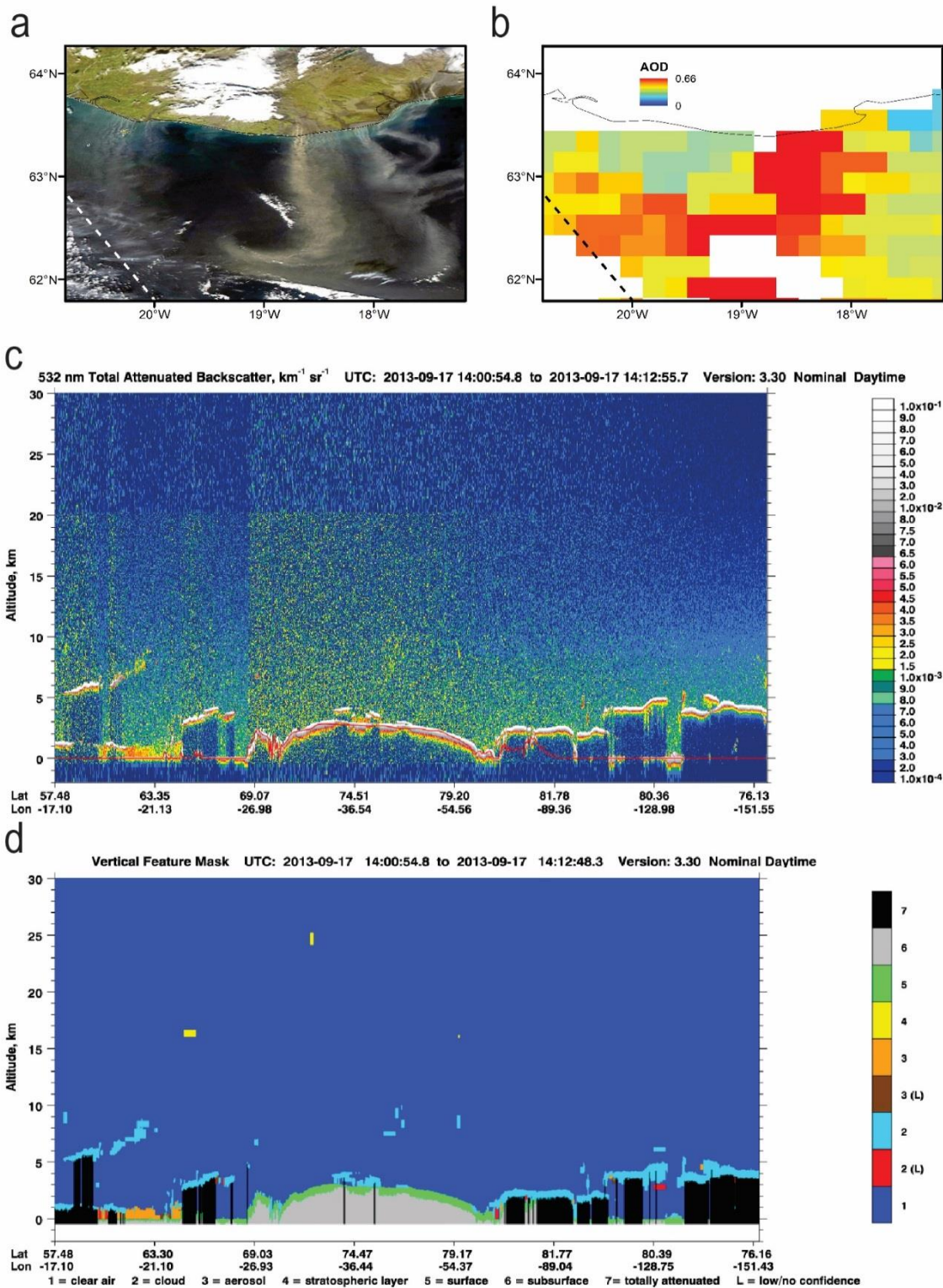


Figure 4.177: Dust event from South Iceland on 17/09/13 identified by a) MODIS 250km level terra 1b data (at 12:50) b) terra level 1b aerosol optical depth c) CALIOP 532nm total attenuated backscatter (at 14:12) d) corresponding CALIOP vertical feature mask. Dotted line in a and b is CALIOP transect

Table 4.2: Horizontal mass flux ($\text{kg m}^{-1} \text{day}^{-1}$) and maximum dust concentration ($\mu\text{g m}^{-3}$) comparison with other field calculated aeolian transport rates from subtropical and high latitude dust sources

Study	Location	Maximum event horizontal mass flux ($\text{kg m}^{-1} \text{day}^{-1}$)
This study	Markarfljot, Iceland	601.06
Gillies et al. (2013)	Victoria Valley East, Antarctica	15827.8
Gillies et al. (2013)	Victoria Valley West, Antarctica	1068.9
Arnalds et al. (2012)	Geitasandur, Iceland	395
		DustTrak Maximum PM10 Concentration ($\mu\text{g m}^{-3}$)
This study	Markarfljot, Iceland	8860
Dagsson-Waldhauserova et al. (2014b)	Maelifsandur, Iceland	1757
Stout et al. (2015)	South Plains, USA	c. 13000
Kimura and Shinoda (2010)	Bayan Unjuul, Mongolia	c. 5000

Very few studies have been used to measure source dust concentrations using DustTraks; most studies have used DustTraks in a controlled wind tunnel setting (e.g. Kim et al., 2000; Loosemore and Hunt, 2000; Sweeney et al., 2008; McKenna Neuman et al., 2009). Maximum DustTrak concentrations are comparable to studies from other high latitude regions (Dagsson-Waldhauserova et al. 2014b) and the sub-tropics (Kimura and Shinoda, 2010; Stout et al. 2015). The maximum DustTrak concentration recorded by Dagsson-Waldhauserova et al. (2014) is comparable to other events recorded during this study (Table 4.2). These events, of lower magnitude, were often classified by figure 4.1 as sediment-availability limited events. This coincides with Dagsson-Waldhauserova et al. (2014) indicating prominent levels of soil moisture present following precipitation events. Both examples from the sub-tropics occurred

during dry conditions, and these values are representative of the high magnitude transport capacity limited events which are recorded at Markarfljot.

Horizontal mass fluxes associated with dust events at Markarfljot (Table 4.1, Figure 4.3) indicate that dust events coincide with the saltation of sand sized particles at the surface (Table 4.1). Horizontal mass flux increases with dust concentration (Figure 4.3), however this relationship is relatively noisy in nature. This is probably for two reasons. Firstly, the relationship between saltation and shear stress is often modelled as a non-linear process (Iversen and White, 1982; Shao et al., 1993; Marticorena and Bergametti, 1995; Shao and Lu, 2000; Shao, 2001). This is due to the shift to steady state saltation, an increase in saltator impact speed and the modification of the wind profile during sand transport (Kok et al., 2012). Dust events which rely on saltators to disrupt finer particles at the surface, either by soil aggregate disintegration or saltation aggregate disintegration (e.g. dynamic entrainment, Shao, 2008; Kok et al., 2012) will therefore be a function of horizontal mass flux rates and are likely to follow the same mathematical relationship (Shao et al., 1993). This non-linear flux of dust concentration is present at Markarfljot during dust events (Figure 4.5) and confirms the use of a non-linear model for classification purposes in the theoretical framework (Figure 4.4).

Second, the efficiency rates of both the DustTrak and BSNE traps vary significantly dependent on meteorological conditions during dust events. Goosens et al., (2000) shows that the absolute efficiency of a BSNE trap above 11 m s^{-1} drops below 100%. Many of the events monitored during this study recorded wind speeds at 0.3 m above 15 m s^{-1} . The efficiency of the trap seems to decrease further with decreasing grain size. The efficiency of a DustTrak DRX varies with wind speed (TSI Instruments, 2000), and it is suggested that a DustTrak should not be deployed when wind speed is $>10 \text{ m s}^{-1}$. Of the measured events, 4 were associated with wind speed above 10 m s^{-1} at the height of recording (1.4m). The use of DustTraks for monitoring dust emissions at source has obvious benefits, however total flux magnitudes must be interpreted carefully. The use of these instruments in cold climates is also more problematic than in hot, arid desert regions because of generally higher surface wind speeds (Mitchell et al., 2005).

The threshold shear velocity for motion in transport capacity limited events was calculated at 6.5 m s^{-1} at 1.4m above the surface. This value is similar to calculated by Gisladottir et al., (2005), who calculated a threshold shear velocity for sand transport on a number of different surface types in Iceland between 6.2 m s^{-1} and 10.7 m s^{-1} at 2 m height.

4.6.2 Temporal controls of dust events

The relationship between wind speed and dust concentration has been well documented in field studies from a variety of different dust emitting environments (Shao et al., 1993; Macpherson et al., 2008). However, it has been shown here that factors other than wind speed may be exceptionally important when examining dust concentrations from high latitude environments.

Event 8 is shown clearly to be controlled by fluctuations in surface wind speed (Figure 4.6). The non-linear relationship between dust concentration and wind speed during this event (and the other dust events with a strong positive correlation between dust concentration and wind speed) would indicate that there is a slight time lag between increases in wind speed and increases in dust concentration (Figure 4.5) (e.g. hysteresis, Whitfield, 1981; House, 1998; Kok, 2010). This hysteresis effect was also documented for dust events by Li and Zhang (2011), who showed for dust events in the Gobi Desert, that dust concentrations lag behind fluctuations in surface wind speed. In dust emitted systems which are controlled by saltation bombardment, increases in surface shear velocity will lead to an increased horizontal mass flux (e.g. saltation flux), which in turn will increase dust concentrations outside of the saltation zone (as shown by the relationship between dust concentration and horizontal mass flux in Figure 4.3) However, an increase in dust concentration is unlikely to occur instantaneously as fine particles need to be released and/or generated from larger sediments before being entrained in suspension. This lag is unlikely to exist where dust is primarily emitted via aerodynamic entrainment of fine sediments directly from the surface (Macpherson et al., 2008).

Field observations indicate that surface moisture affected sediment availability during events 5 and 1. During event 5 conditions were dry, but continued deflation of the surface removed the uppermost dry sediments exposing damp sediments (Figure 4.18). These damp sediments are cohesive and require higher threshold velocities to

be entrained (Chepil, 1956; McKenna Neuman and Nickling, 1989; Fécan et al., 1998); where wind speeds remain constant, surface soil moisture limits sediment availability (Wiggs et al., 2004). Exposure of damp sediments at the surface to wind will start to dry them out making them available for transport (Cornelius and Gabriels, 2003). This does not occur uniformly across a surface as micro-topography and sediment texture can affect moisture retention and rates of desiccation (Ravi et al., 2006). As patches of sediment dry, this can cause localised resumption of dust emissions which would explain the sporadic increases in dust concentration during the second half of the dust event.

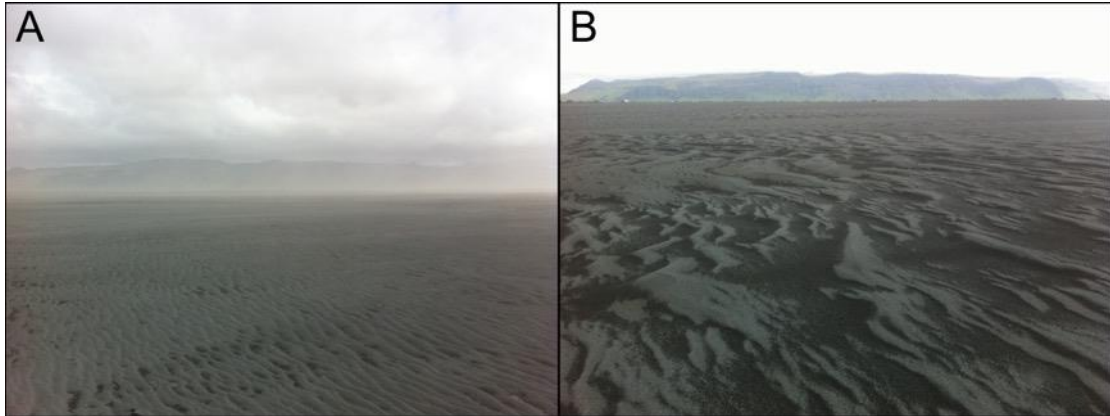


Figure 4.18: Markarfljot sandur after a) 1 hour of dust emissions and b) 14+ hour of dust emissions during event 5 (15/06/15). Spacing between ripples is approximately a) 10-20cm b) 50cm-1m

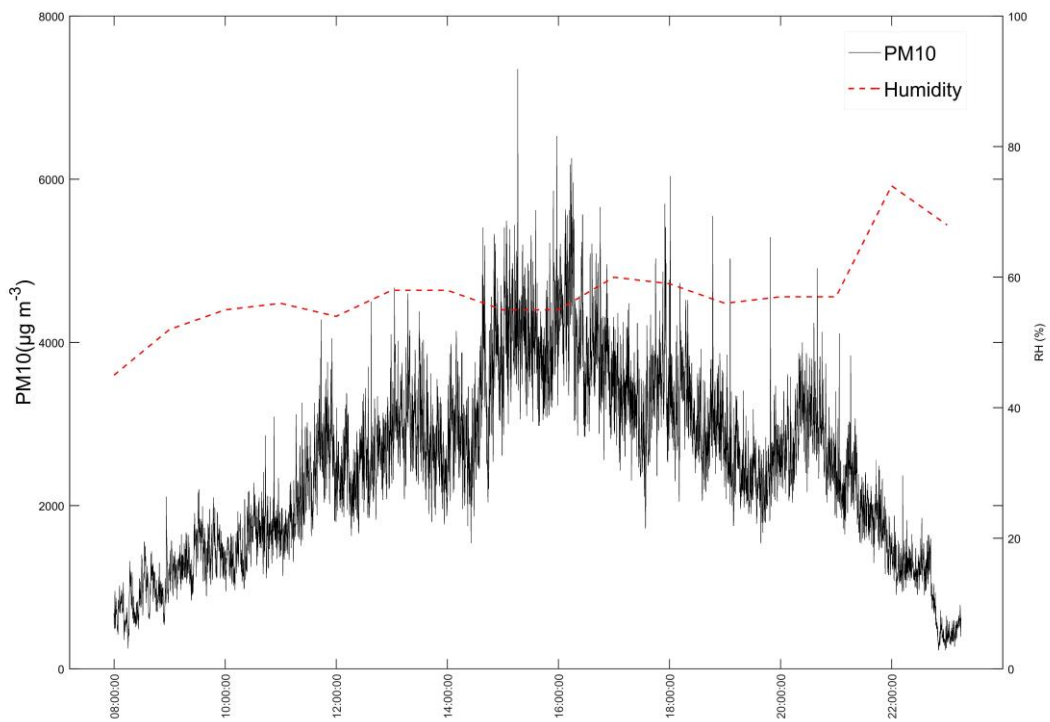


Figure 4.19: PM10 concentration ($\mu\text{g m}^{-3}$) and hourly relative humidity (%) at Markarfljot during event 5 (15/06/15)

At the end of event 5 there is a much sharper decrease in dust concentration which is related to a rapid increase in relative humidity (Figure 4.19). Ravi et al. (2006) found that for loamy mixed sand, which is of a similar textural composition to the material at this site, surface soil moisture retention rates increase with relative humidity. Cornelius and Gabriels (2003) show a sharp increase in threshold shear velocity for sand particle motion for increasing relative humidity. As this increase in relative humidity occurred at a time when large proportions of exposed surface sediment were already unavailable, this led to a further decrease in dust concentration.

Although the studies by Cornelius and Gabriels (2003) and Ravi et al. (2006) focus on sand-sized material, it should be noted that dust emissions at this surface are linked to saltation. As saltation mass flux increases so do total dust emissions; when saltation ceases, so do dust emissions.

During event 1, sudden drops in dust concentration (Figure 4.9) can be explained by low magnitude pulses of rainfall (typically <0.3 mm) despite the wind remaining above threshold. Dust emissions are not reduced to zero during all rainfall events; for example, Ashwell and Hannell (1960) observed dust storms occurring during light rain with winds of 6 m s^{-1} in Iceland. When emissions do decrease sharply or halt altogether, concentrations within the record recover quickly, and in some cases instantly following short periods of precipitation. In high latitude regions, where wind speed is generally higher than in the sub-tropics (Mitchell et al., 2005), surface soil desiccation by high wind speeds may compensate for the lack of evaporation desiccation. This differs from sub-tropical regions, where surface sediments will dry due to high temperatures and low relative humidity (McTainsh et al., 2005).

Bergametti et al. (2016) showed the importance of rainfall in inhibiting wind erosion in the Sahel and suggests that dust emission would be halted immediately during rain events as rain droplets wash out dust particles. These data, which are also for a saltation-driven dust system but with different soil and climate conditions agree with this. However, Bergametti et al. (2016) also suggests that global dust models should consider a 12h soil moisture factor, which would inhibit dust emissions from a surface where rainfall had occurred (6h for <2 mm total rainfall). Our data indicate that dust emissions can occur almost instantly following rainfall events. Although it is imperative to include information regarding soil moisture and other factors which affect sediment

availability in dust models, the relationship between surface sedimentology, wind speed and soil moisture retention and its influence on dust emissions must be better understood as it will vary on a source by source basis.

The influence of humidity on dust emissions is extremely important in high latitude environments. Much of the work that has focused on this relationship has not focused on dust-sized material, rather on sand-sized material (McKenna Neuman, 2003; Cornelius and Gabriels; 2003; Ravi et al., 2006). Where process work has focused on the impact of relative humidity on silt and clay sized material, it has been conducted in laboratory-controlled experiments and has not focused on natural variations seen within a field environment (McKenna Neuman and Sanderson, 2008). Further work is required to understand how spatial and temporal changes in humidity, surface soil moisture, soil texture and threshold velocity interact and control sediment availability for dust emissions in high latitude environments.

For dust events driven by saltation bombardment, the relationship between humidity and saltation, which has been defined in the subtropics is probably useful for high latitude environments (McKenna Neuman, 2003). However, when emissions are detached from saltation activity (e.g. aerodynamic entrainment, Macpherson et al., 2008), it is likely that the impact of humidity will be greater due to an increased moisture holding capacity of finer sediments (Ravi et al., 2004).

4.6.3 Conceptual framework for event scale variations in dust emissions

Both events which were controlled by sediment availability were successfully identified by the conceptual model. Initially, the relationship was defined by the relationship between wind speed and dust concentration, however to identify the specific controls on what is causing the sediment availability limiting factors, time series analysis is required. The results indicate that it is possible to gain some insight into the primary controls on dust emissions at the event-based scale using the conceptual model proposed. However, certain conditions are required for this to be achieved successfully.

First, high resolution measurements of wind speed and dust concentration are required at source. Measurements from dust transport pathways, rather than the source itself, are likely to be affected by variables other than emission intensity (such

as plume dynamics and dispersion). For example, if there is slight change in wind direction during an event, dust concentrations measured away from the source might decrease as the monitoring station may no longer be in the centre of the dust plume (Thorsteinsson et al., 2011). This change in wind direction may not actually decrease dust concentration at source and would therefore render the conceptual model invalid. This is demonstrated in this thesis in Reykjavik during Event 5, as confirmed by the meteorological station and HYSPLIT plume dispersion analysis.

Second, there needs to be a statistically-significant relationship between wind speed and PM10 for transport-capacity limited events at the dust source. This was defined as a cubic relationship for the sites in Iceland; however, it will be very dependent on the source. For example, we would expect differences in the mathematical relationship between regions with a significant saltation component (e.g. dynamic entrainment) and regions where aerodynamic entrainment dominates (Macpherson et al., 2008).

The mathematical relationship can be used to estimate, at the event-scale, what proportion of dust concentration can be attributed primarily to wind entrainment, sediment supply or distal sources. However, to understand why an event is transport capacity limited or sediment availability limited it is important to examine the evolution of the event to identify when and how the relationship between wind speed and dust concentration breaks down. Once the primary temporal control has been identified, event-scale time series and additional data (e.g. rainfall, soil moisture) can be used to identify the potential factors which are controlling dust emissions.

Originally, this type of sediment system framework was applied at a stratigraphic timescale (Kocurek, 1998) but it has been shown here to have value at the event-scale. The series of events examined here was not sufficiently long to test the impact of sediment supply on dust emissions but has demonstrated how the model can be applied under transport-capacity limited and sediment-availability limited conditions. This research was conducted at a high latitude dust source and the processes which control aeolian activity in high latitude environments are fundamentally the same as those in subtropical regions (Bullard, 2013); this means the conceptual model can be further tested using dust events from other regions. At the field sites used here, all the dust events were associated with saltation-driven emissions which opens the

opportunity to explore whether such a conceptual framework could be used to elucidate controls on saltation in dune environments (Baas and Sherman, 2006).

4.6.4 Transport pathways and heights

Trajectory analysis indicates preferential pathways from the Markarfljot river basin route towards the south, with few trajectories heading north. This agrees with Arnalds et al. (2014) who suggested that dry north easterly winds are the primary driver of dust transport in south Iceland. The analysis also agrees with Baddock et al. (2017) who indicated a clear southerly transport route during all periods of the year. The result here may be influenced by the relationship between the location of the meteorological station and the downwind dust source. Storhöfði weather station is located 30km south of the Markarfljot river basin. Therefore, if material from Markarfljot was to blow in any other direction, other than to the south, the weather station is unlikely to record the dust observation. This is clearly the case as the days which dust was observed at source during the field campaign were not recorded at Storhöfði. This is because the dominant wind direction during these events was south-easterly. Therefore, it is important when conducting dust transport analysis which is informed by meteorological observations that the relationship between the meteorological station and dust source is considered (e.g. Baddock et al. 2017).

Dust events (Table 4.1) recorded during field experiments display a different pathway than that presented by the systematic HYSPLIT analysis. This is because during this period a south-easterly wind direction was dominant (Figure 4.20). This type of flow is attributed to the dominant track of the Icelandic low (Einarsson, 1984; Arnalds et al., 2016), a cyclonic low-pressure system from the northeast and south. As this system interacts with the polar front, individual low-pressure systems move from west to east across Iceland creating the generation of strong surface winds (Seerezze et al. 1997; Nawri, 2015). During the summer months, the pressure systems often split reversing flows from westerly to easterly in the south. This route is also documented by Baddock et al. (2017) from the Vatnsskarðshólar meteorological station, located 60km east of Markarfljot. However, Arnalds et al. (2014) in their trajectory analysis did not consider this route for potential inputs of dust into adjacent marine environments.

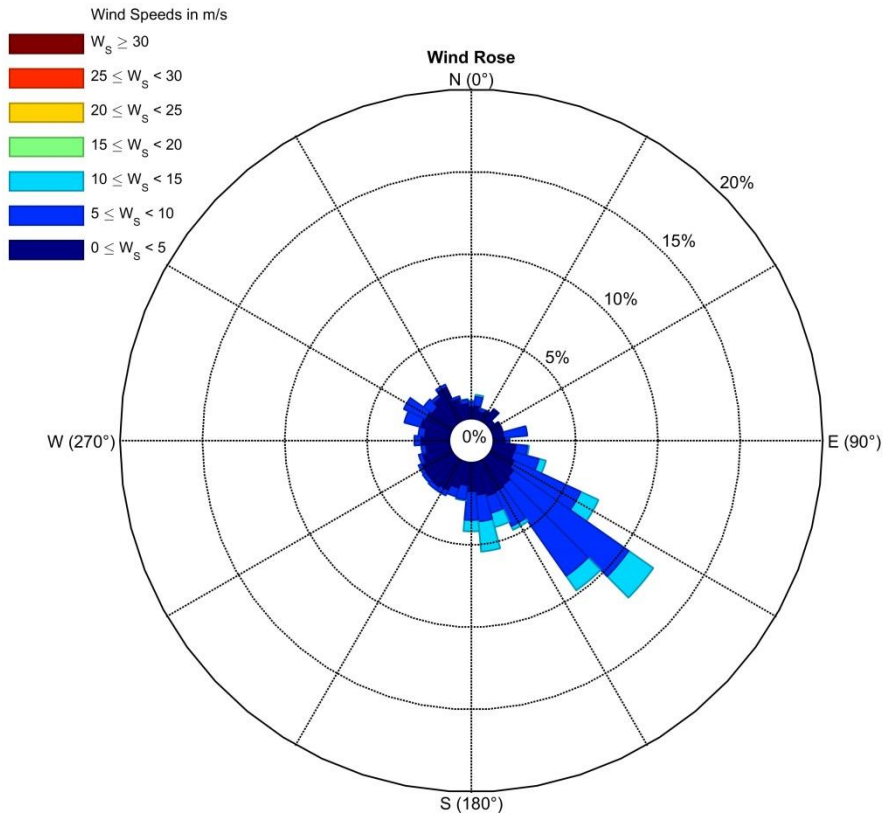


Figure 4.20: Wind direction ($^{\circ}$) and wind speed (m s^{-1}) at Markarfljot Automated weather station between 01/05/15 – 30/06/15

Of the 9 dust events recorded over the 6-week period, all exceeded the Icelandic air quality health limit at source ($50 \mu\text{g m}^{-3}$ for a 24-hour average; Thorsteinsson et al., 2011). Of the larger magnitude events, 4 of these occurred during south-easterly winds and dust was transported towards the city of Reykjavík. These events increased PM10 concentrations in Reykjavík to $>100 \mu\text{g m}^{-3}$. This transport pathway is well-recognised and particularly important during spring and summer months (Baddock et al., 2017).

Of the dust events monitored, the 15th June was modelled using the HYSPLIT dispersion model, which has been used to monitor dust storm dispersion in other dust source regions (Draxler et al., 2001; Wang et al., 2011). The benefit of using the dispersion model over the single-particle lagrangian integrated trajectory is that it considers dust storm dispersion during transport. In the specific case of the 15th June, Maximum PM10 concentrations in Reykjavik (Figure 4.11) coincide with when the dust

plume is centred over the city (Figure 4.12). As the plume shifts northwards at approximately 18:00, this is reflected with a significant decrease in PM10 concentration recorded in Reykjavik. An increase in concentration is then recorded as the plume shifts back through the city at 20:00 before heading further south. This indicates firstly, that dust storms from the Markarfljot can cause significant levels of PM10 in the city of Reykjavik, where approximately 80% of the total population of Iceland live (Thorsteinsson et al., 2011). Secondly, air pollution levels, which has been shown to be heavily influenced by natural dust events, will have a severe impact on public health if these events were to increase in frequency and/or becoming larger in magnitude. Thirdly, the sensitivity of aerosol concentrations from specific dust sources on cities is highly dependent on subtle changes in wind direction and atmospheric characteristics.

One issue with the dispersion model is that it is difficult to produce reliable potential dust concentrations. Although it is possible to include a dust concentration at source for a single model run (Draxler et al., 2001; Stein et al., 2015), the model assumes that dust is only emitted from a single point source. This means that it will underestimate the total concentration of a given event if numerous point sources are contributing to a single dust event.

The seasonal pattern of the systematic trajectory analysis indicates the dominance of the southerly pathway during all seasons. This can once again be attributed to dry north-easterly winds which are dominant in south Iceland (Arnalds et al., 2014). In MAM; two separate preferential pathways are identified with the dominant southerly tract accompanied by a south-westerly trajectory. This trajectory is most likely a product of cyclonic easterly flows (Einarsson, 1984). Trajectories to the southwest are most common in JJA and SON. Although westerly flows, and therefore westerly surface winds at source are uncommon in South Iceland (Einarsson, 1984). It should be noted that surface wind speeds at source are unlikely to control long distance transport routes. These are more likely to be controlled by changes in upper atmospheric circulation (e.g. Baddock et al., 2017). The highest % of trajectories were recorded in MAM (32.1%) and SON (29.3%) respectively. This agrees with Prospero et al. (2012), Dagsson Waldhauserova et al. (2013) and Bullard et al., (2016) who all indicate, through field and meteorological data analysis, that these time periods are the most active dust periods in South Iceland. Dust events can also occur in the winter

months, but are less frequent (Prospero et al., 2012), most likely because sediments are unavailable for large periods of time due to increased winter precipitation rates (Arnalds, 2001).

The heights of air parcels for the HYSPLIT trajectories (Figure 4.16) indicate that air parcels which are associated with dust storms in Iceland stay low within the atmosphere (>75% below 200m). This is most likely due to the stable atmospheric conditions found over the Icelandic mainland preventing trajectories (and in turn dust particles) from reaching high altitudes (Baddock et al., 2017). Arnalds et al. (2014) suggested that dust storms in Iceland are linked to stratified stable flow and that air masses travel short distances over land before reaching the coast, thus receiving very limited opportunity for advection, and in turn, lifting.

It should be noted that the results of the vertical motion of air parcels may be a function of the input data set required to compute the HYSPLIT trajectories. Although there is no empirical method for assessing the accuracy of the input data, most research testing the validity of reanalysis data for trajectory modelling has compared different trajectory analyses with different input data sets in a variety of environments. Harris et al. (2005) assessed the relative accuracy of 3D (e.g. pressure field driven heights) and isentropic (e.g. DEM generated heights) generated trajectories with ERA-40 and NCEP/NCAR reanalysis data sets. They concluded that, in a high latitude environment with similar atmospheric conditions to that of south Iceland, a vertical difference in 50m after 96h was found between the two input data sets. The difference in vertical motions for 3D trajectories and isentropic trajectories after 96h was vastly different, with the 3D trajectory calculating trajectory heights 600m greater than for the same isentropic trajectories. The use of 3D trajectories in this study is therefore justified on the basis that it is less likely to under-estimate the height of air parcels relatively to the isentropic trajectories.

4.6.5 Use of satellite remote sensing in the high latitudes

The use of passive remote sensing techniques to understand dust storm dynamics and dust plume extents in the high latitudes is problematic (Gassó and Stein, 2005; Crusius et al., 2011; Bullard et al., 2016). None of the events recorded during the field measurement campaign were captured by MODIS and therefore no insights could be gained from the use of this technique. The main issue, particularly in Iceland, is

sustained periods of dense cloud cover (Bullard et al., 2016) in summer and no satellite retrievals during winter (NASA, 2014). The use of passive remote sensing techniques has proved invaluable in the subtropics (Prospero et al., 2002; Baddock et al., 2009; Ginoux et al., 2012), where events are rarely missed in the satellite record.

In the high latitudes, where retrieval levels are exceptionally low, insights into dust storm frequency, magnitude and transport properties cannot be easily quantified. This is shown further by only 14 of 125 events during the period 2010 – 2015 at Storhöfði being picked up by MODIS. The best use of these data sets seems the verification that an event has occurred and to use the data to potentially verify the magnitude of events on an event by event basis in tandem with other sources of data (e.g. WMO weather codes) (Gassó, personal communication).

The fundamental issue with the use of CALIOP at high latitudes is cloud cover often obstructing retrievals (Bullard et al., 2016). The narrow instrument swath means that repeat revisits over the same location are uncommon, therefore making the capturing of high latitude dust events using CALIOP extremely rare. Although only one CALIOP retrieval is presented here (Figure 4.17), the dataset complements the HYSPLIT analysis indicating low trajectory dust events in south Iceland. Dust storms sitting low within the atmosphere might not just be confined to Iceland as CALIOP has been used in other high latitude environments. Bullard et al. (2016) used CALIOP, teamed with AOD retrieval, to show a dust event from the Copper River basin, Alaska. The CALIOP data shows clearly that the dust is limited to below 1.2km in the atmosphere (within the marine boundary layer).

4.6.6 Use of meteorological weather codes for defining dust events

Of the 9 dust events which were recorded in the field monitoring period (Section 5.1, Table 4.1), two of these events were identified at Eyrarbakki and none at Storhöfði. This result clearly shows the issues surrounding the use of weather codes as the primary tool for estimating the frequency of dust events. Dust codes have been identified as a useful tool for indicating the frequency and seasonality of dust activity (Dagsson Waldhauserova et al., 2014a; Bullard and Mockford, 2018). However, as stated by Baddock et al. (2017) who used dust codes to initiate HYSPLIT trajectories in Iceland, weather stations which record dust codes are normally in defined dust transport pathways and not directly at source. This means that a dust code will only

be recorded if the exact meteorological conditions allow a dust event to travel along the appropriate pathway for a weather station to record the event. This means that, in areas where there are high densities of manual weather stations that record WMO weather codes (e.g. Australia,), the problem is unlikely to affect the creation of a realistic dust storm frequency record. Although Iceland does have a high density of weather stations, particularly on the south coast (Dagsson Waldhauserova et al., 2014; Arnalds et al., 2016; Baddock et al., 2017), it is evident that dust events are being missed.

This study did not explicitly test the relationship between magnitude at source and the related dust code which was recorded at the WMO weather stations. This is because only two of the events were recorded and both of these events were labelled as the same code (06 code). 9 dust codes are used to distinguish between different magnitudes of dust event (O’Loingsigh et al., 2014), ranging from dust whirls (07) to a sustained increasing magnitude dust storm (32-35). Although recorders at the station are meant to use the entire range of codes to allow users to distinguish between different magnitudes of event, this often does not occur. Bullard and Mockford (2017) showed that dust code assignment in West Greenland varied significantly in a 70-year period, with the first 30 years of data only consisting of the use of one code (07). In Iceland, and particularly at the two sites which have been used in this thesis to constrain potential dust activity from Markarfljot, the majority of dust events are designated as 06 dust codes. This either means that all events are low in magnitude or that the full set of codes is not being utilised. It is clear from the DustTrak data that events from Markarfljot are not low magnitude, therefore concluding that the full range of weather codes to define dust events is not being utilised in south Iceland.

4.7 Conclusions

Dust events at Markarfljot are of similar magnitude to those found in other parts of Iceland, other high latitude environments and identified subtropical deserts. The primary controls on dust emission, from a saltation-driven (dynamic entrainment) environment, are wind speed and soil moisture. The relationship between wind speed, surface soil moisture and surface sedimentology may be of significant importance in high latitude environments in controlling the magnitude, frequency and characteristics of dust events. Dust from south Iceland is transported predominantly south towards

the North Atlantic Ocean, where its deposition may have an impact on marine ecosystems. Particles also travel west, which have an impact on air quality in the city of Reykjavik and potentially may be deposited in other terrestrial ecosystems (e.g. lakes, glaciers). Trajectories were mostly confined to the lower atmosphere (<100m) because of the inability for particles to be thermally lifted in stable arctic air parcels. This was confirmed by CALIOP lidar retrievals which indicated all material was confined to <1km in the atmosphere. Because of the low altitudes achieved by dust particles in transport, it is likely that material which is transported westerly from Iceland will have little impact on the Greenland Ice Sheet. This is because particles would not be transported to the higher altitudes found in the centre of the ice sheet.

The study has indicated the importance of long term source measurements of dust events in the high latitudes, as our understanding of high latitude aeolian processes is very limited. These data have demonstrated the importance of the factors which affect sediment availability as being key drivers in the Icelandic dust system. For Iceland, research understanding the linkages between wind speed and surface drying would allow for a more thorough understanding of how long it takes sediment to dry and become available for the aeolian system. For other high latitude dust source regions, the dominant factors will differ. It should also be noted that much of the field experimental work on high latitude aeolian processes has occurred during summer months, and that factors which drive/inhibit winter dust storms might differ significantly.

To justify the creation of a conceptual model on dust storms at the event scale, further source measurements are required in both high latitude and subtropical deserts on a variety of surfaces (e.g. crusted, non-crusted), with varying surface sediment types to confirm the impact of other sediment-availability and sediment supply limiting factors on dust entrainment. This study has shown how a dust event can be characterised under transport-capacity limited conditions and some sediment-availability limited situations (e.g. moisture, humidity, changes in bed morphology).

5. The role of aeolian abrasion in creating dust sized sediments for high latitude dust events

In chapter 4, it was shown that the relict sandur system at the Markarfljot river basin is a significant dust source in south Iceland. This is a surprising result after it was indicated that this particularly source has no fine particles ($<100\mu\text{m}$) in the surface parent material. It could therefore be hypothesised that for dust sized particles to be emitted from this surface, processes during aeolian transport such as aeolian abrasion are leading to the creation of silt and clay sized particles. This chapter will test the susceptibility of Icelandic sediments to aeolian abrasion during transport using an abrasion chamber. For this chapter, three separate Icelandic dust source sediments with varying sedimentological make-ups are compared to understand differences in total dust production rates and created particle size distribution. These three sediment groups are representative of the major dust source sedimentologies in Iceland, as well as in other high latitude dust source regions. The impact of temperature on the abrasion process is tested to determine whether the process of aeolian abrasion is a key additional control on the generations of dust particles beyond parent sediment properties.

5.1 Introduction

The shape and size of dust particles vary between environments (Pye, 2015). This is important because dust particles have different impacts on the radiation budget (Mischchencko et al., 1995; Tegen et al., 1996) and on terrestrial ecosystems (Jickells et al., 2005; Ravi et al., 2011) depending on their physical and optical properties (Dubovik et al., 2002).

The creation of fine particles has been related to processes from several geomorphological settings (Pye, 2015). For particles of silt size (2 - $63\mu\text{m}$), dominant processes include: glacial grinding (Smalley, 1990; Wright, 1995; Smalley, 1995; Wright et al., 1998); physical and chemical weathering (Johnsson and Meade, 1990; Wright, 2001), fluvial abrasion/comminution (Smith et al., 1991; Wright, 1993; 1998; Wright, 2001; Smith et al., 2002) and aeolian abrasion (Whalley et al., 1987; Wright et

al., 1998; Bullard et al., 2004; Bullard and White, 2005; Bullard et al., 2007; Baddock et al., 2013). For clay sized particles ($< 2 \mu\text{m}$), this has been mainly linked to chemical weathering (Bullard et al., 2004; Pye, 2015) and the removal of surface coatings during abrasion (e.g. Bullard and White, 2002; Baddock et al., 2013).

This chapter will focus on the importance of aeolian abrasion as a mechanism for creating silt and clay sized particles for the aeolian system. The abrasion and breaking of sand grains in transport has long been studied in the context of the formation of silt sized particles for the formation of loess (Whalley et al., 1987; Wright et al., 1998). This is because sand grains are susceptible to rounding, chipping and spalling when being transported in saltation (Knight, 1924; Mahaney et al., 2002; Pye, 2015). This work which was started in the 1920s by Knight (1924) and Anderson (1926), and later continued by Kuenen (1960), Whalley et al., (1987), Smith et al., (1991) and Wright et al., (1998). This work primarily linked the abrasion of poorly sorted coarse quartz sand to the creation of loess sized particles in the range of $20 - 60 \mu\text{m}$ to help explain the generation of loess at low latitudes where glacial processes were unlikely (Smalley, 1966; Smalley and Vita-Finzi, 1968; Smalley et al., 2001). These studies also indicate that abrasion of coarse sand particles is unlikely to generate substantial quantities of dust sized particles during aeolian transport (Kuenen, 1960).

These conclusions are not supported by the fact that dust events are common from large sand seas globally (Prospero et al., 2002; Crouvi et al., 2010; Ginoux et al., 2012). There are numerous sources of sandy soils which are potentially susceptible to aeolian abrasion and are therefore potential dust sources (Breed et al., 1979; Shao et al., 1993; Baddock et al., 2016; Parajuli and Zender, 2017). However, even though sand seas have been shown to emit large quantities of dust (Prospero et al., 2012), there is limited evidence to suggest that dust from these regions can be related to the creation of newly generated dust particles.

Much of the research which has focused on mechanisms for the creation of silt and clay sized particles for the aeolian system from sands has occurred in subtropical desert regions (e.g. Bullard et al., 2004; Bullard and White, 2005; Bullard et al., 2007; Crouvi et al., 2010; 2012; Baddock et al., 2013). Although aeolian abrasion has been shown to be an important process in these environments for the creation of dust sized particles, the impact of this process in the high latitudes is not well understood.

This study will quantify the susceptibility of three sediment samples to aeolian abrasion from different high latitude dust sources. The aim of this chapter is to quantify the relative role of particle creation and the removal of fine particles already present in the parent soil material. As these sediments are sourced from high latitude dust sources, the impact of temperature and humidity will also be considered, as this may impact total dust production created from a given sediment type (McKenna Neuman, 1993; 2003; 2004; 2008).

5.2 The process of aeolian abrasion

The process of aeolian abrasion has been shown to be a mechanism for creating silt and clay sized particles in dust emitting regions. This is supported by the spatial relationship between dust source areas and sand seas globally (Prospero et al., 2002; Ginoux et al., 2012). Bullard et al., (2011) showed that 32.63% of all dust sourced from the Lake Eyre Basin, Australia was from aeolian sands (e.g. dunes). Lee et al., (2012), for the Southern High Plains region, USA, showed that approximately 84% of dust source points were from aeolian sand sheets and sand dunes. Although sand seas and sand dunes often have the largest amount of point sources of dust in each environment (e.g. Lee et al., 2012; Baddock et al., 2016), the relative importance of these sources when their total land area is considered is often much smaller than other known dust source geomorphologies. For example, Lee et al. (2012) and Baddock et al. (2016) showed that ephemeral lakes have a much higher relative dust emission in terms of their emission frequency in terms of the relative area. Regardless of this, sand seas are without doubt one of the most important dust source geomorphological units globally.

At dust sources where the surface parent soil sedimentology is dominated by sand, aeolian abrasion, alongside weathering (Goudie and Viles, 1997), is likely to be an important process in the creation of silt and clay sized particles. For example, Crouvi et al. (2008) showed the link between an advancing sand sea and the creation of coarse dust particles in the Negev and Sinai deserts, Israel. It was suggested that aeolian abrasion of larger sand grains in saltation led to the creation of the coarse dust particles.

There are several mechanisms for how sand particles can be abraded during aeolian transport. Wright (1993) (Figure 5.1) indicated four processes which lead to the creation of silt and clay sized particles during aeolian transport. First, that corners and protuberance can be removed. Second, that fatigue effects from saltation activity cause grain surface weaknesses which lead to increased fracturing. Third, that particles can be completely fractured and broken into multiple grains. Fourth, that fine chips, fragments or surface coatings can be removed from the surface of grains. The relative importance of each of these processes will be dependent on the initial grain characteristics of the parent sediments (e.g. particle size and shape) and most likely, the characteristics of aeolian transport (Rice et al., 1995).

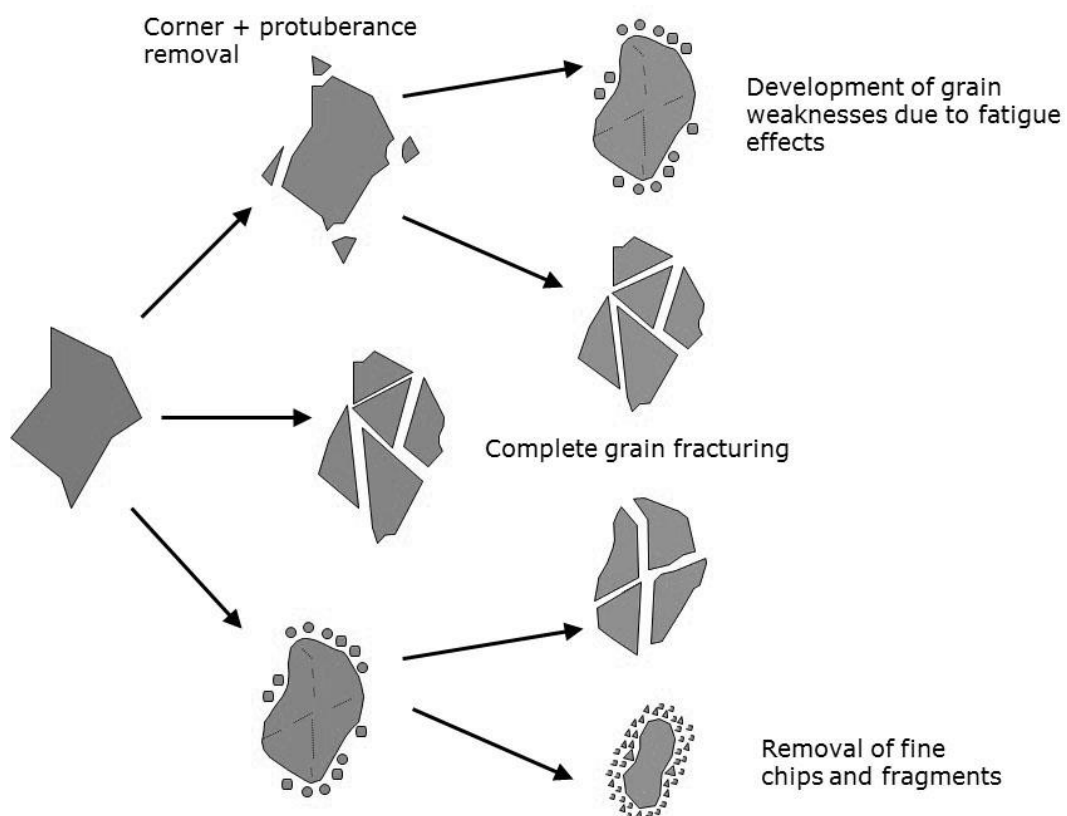


Figure 5.1: Conceptual diagram indicating mechanisms which lead to the creation of silt and clay sized particles from sands travelling in aeolian transport (Wright, 1988)

The initial size and shape of surface parent sediments will impact the rate at which a particle can be effectively abraded (Kuenen, 1960, Wright et al., 1998, Mahaney, 2002). Particles which are highly angular in nature (e.g. glacial, volcanic sediments) are likely to experience higher rates of abrasion than rounder grains (e.g. fluvial,

aeolian grains; Mahaney, 2002). This is because angular grains have higher densities of corners/perturbations which can be preferentially removed (Kuenen, 1960; Wright et al., 1998; Wright, 2001, Mahaney, 2002). Whalley et al. (1987) and Wright et al. (1998) both showed that whilst angular particles often show prominent levels of abrasion, the rate at which the particle is abraded decreases with time as particles are rounded.

The shape and size of grains are governed by the source environment and processes to which particles have been subjected (Mahaney, 2002). The origin of the grain is a key factor in determining the potential impact that aeolian abrasion may have in specific environments. For example, in sub-tropical desert environments where sand grains have a long history of aeolian activity or have been further rounded by fluvial action, grains may not be hugely susceptible to contemporary aeolian abrasion processes. However, in high latitude environments such as Iceland, where sediments associated with the aeolian environment are often highly angular from a volcanic-glaciogenic setting (see Chapter 3), these particles may be inherently more susceptible to abrasion during aeolian transport.

Particle surface characteristics will influence the relative importance of the different forms of aeolian abrasion by which a grain can be abraded. As shown in chapter 3, surface grains of particles are exceptionally complicated with particles often forming clay coatings and/or surface adhesions from either abrasion fatigue (Kuenen, 1960; Mahaney, 2002), chemical precipitation modification or electrostatic charge changes after deposition (Wopfner and Twidale, 1988; Pell and Chavis, 1995). The removal of these surface coatings has been linked to aeolian abrasion, however the relative importance of the process for providing silt/clay sized sediments is debated (Evans and Tokar, 2000; Wopfner and Twidale, 2001; Pye, 2015).

Research undertaken by Walker (1979) shows that clay coatings are preferentially removed from larger grains. This is because larger grains exert higher levels of kinetic energy when they are transported (Anderson and Haff, 1988; Zou et al., 2001; Kok, 2012) and therefore collisions with other particles and/or with the surface are of higher intensity (Lu and Shao, 1999; Shao, 2001).

Research from subtropical deserts has shown the potential importance of the removal of fine chips and fragments from sand sized particles to create silt and clay sized

particles for dust events. Baddock et al., (2013) found that iron-rich nano particles were released from Australian dune sand during abrasion experiments. Bullard et al., (2004, 2005) suggested that there should be a notable difference in the particle size distribution of dust particles depending on whether particles are generated from clay coating removal or by chipping/spalling as clay coating removal will produce the finest sediments. However, Gill et al. (2005) showed using a laboratory dust generator, that sand particles without surface clay coatings are inherently resistant to abrasion. It was found that these sands produced the finest particle sizes due to corner removal during abrasion.

5.3 Dust particle creation in high latitude environments

Our understanding of processes which lead to the creation of silt and clay sized particles for the aeolian system in high latitude environments is somewhat limited (Nahon and Tompette, 1982; Assallay et al., 1998). It has been shown that particles created in the glacial system, often during high stress grain to bed interactions in glacial systems provide a vast source of silt and clay sized particles (Tuck, 1938; Pewe, 1951; Dowdeswell, 1982; Crusius et al., 2011; Bullard, 2013).

As shown in Chapter 3, large spatial differences in dust source sedimentology can occur within a single landscape unit. The relative impact of different aeolian abrasion processes will likely vary between dust sources based on their respective sedimentology (Wright, 1998, Bullard et al., 2014).

This is further the case because the meteorological and climatological drivers of dust events is different in high latitudes than in the subtropics (Bullard et al., 2016; Arnalds et al., 2016). For example, the role of temperature and humidity has been shown to impact aeolian transport rates. McKenna Neuman (2003), showed that temperature and humidity impact aeolian sediment transport in three ways. Firstly, by affecting air viscosity and, in turn, fluid drag forces which are responsible for dislodging particles from the surface. Secondly, lower temperatures increase the viscosity in the turbulent wake from these particles and thirdly, and debatably the most important, increases in temperature and humidity increase particle cohesion in the surface soil matrix by absorbing water. Chapter 4 showed the role of relative humidity in influencing dust production at the event-scale from field measurements, indicating that sudden peaks in relative humidity will decrease dust production.

It is difficult in a natural field setting to constrain temperature and humidity (Cornelius and Gabriels, 2003; Ravi et al., 2004), therefore empirical research which has attempted to link aeolian activity with temperature and humidity has been somewhat limited to laboratory experiments (McKenna Neuman, 1990; 1993; 2003; 2004; 2006; 2008). Much of this body of work has dealt with the entrainment of sand sized particles and has not addressed the impact temperature and humidity have on the entrainment of dust sized particles. However, most dust events are driven by the saltation of sand particles (Shao et al., 1993; Lu and Shao, 1999; Grini and Zender, 2004), and therefore the work is likely to be comparable. It could, therefore, be hypothesised that decreasing temperatures will increase total dust production (McKenna Neuman, 2003).

Changes in temperature may impact the process of aeolian abrasion in two ways. First, decreases in fluid drag and air viscosity during colder temperatures allow particles to travel at greater velocities for a given shear velocity (McKenna Neuman, 2003). If particles are travelling at greater velocity, it is likely that particle collision velocity and the number of collisions will increase. It could, therefore, be hypothesised that particles are likely to have a higher potential to completely fracture during transport (Figure 5.1). Second, the elasticity properties of grains are altered in colder temperatures (Dvorkin and Nur, 1996; Jacoby et al., 1996). In high latitude regions, seasonal thawing and freezing of cold sediments may provide a mechanism for changes in elasticity due to temperature (e.g. permafrost). Changes in elasticity may result in a change of shape in particles, causing further corners and proturbences to be available for abrasion during transport.

A change in the dominant abrasion process caused by changes in temperature may have significant outcomes for the generated particle size distribution of a dust event for a given source. This outcome would have important implications for global dust models, as currently a fixed particle size distribution of dust based on surface sedimentology is used (Kok, 2011).

5.4 Aim and Objectives

Therefore, the main aim of this chapter is:

To examine the susceptibility of three different Icelandic dust source sediments to aeolian abrasion

The specific research questions which this chapter will attempt to answer include:

- 1) How much dust is already available in the surface samples?
- 2) During an active dust event, how much dust is generated by aeolian abrasion processes?
- 3) What is the effect of temperature and humidity on potential dust production rates and generated particle size?

5.5 Methods

5.5.1 Parent sediments

To fully understand the impact of aeolian abrasion on dust emissions from Iceland, a range of sediments are required which represent the different sedimentological units associated with dust events in Iceland. Therefore, for this experiment, 3 different sediment groups were used (Figure 5.2). Surface sediments were obtained from the top 1cm from the following locations (Table 5.1):

- 1) Markarfljotsandur (e.g. relict sandur) – The sedimentological characteristics of these sediments are examined in Chapter 3 and the properties of dust events from this surface are discussed in Chapter 4. As seen in Figure 5.2, sediments from Markarfljotsandur are well sorted sand grains between 200 μm – 1000 μm . No fine component (e.g. <63 μm) is present within these sediments
- 2) Markarfljot ephemeral channel system – The surface sedimentological characteristics of these sediments are examined in Chapter 3. They are associated with the seasonal recharging of sediments from the glacio-fluvial system during peak spring flows. A considerable proportion of the sediments are below 63 μm (Figure 5.2), with particle size varying between 0.3 μm – 300 μm .

3) Mýrdalssandur – This surface has yet to be discussed but has been described by others (Arnalds, 2001; Arnalds et al., 2016). Mýrdalssandur is one of the largest dust source regions in Iceland (Arnalds et al., 2016; Baddock et al., 2017). Particle size distribution analysis (Figure 5.2) shows that the particles are not well sorted, and size varies from 0.3 μm – 1400 μm . Sediments are sourced from the Mýrdalsjökull ice sheet and are deposited during glacio-fluvial flood events (Arnalds, 2001; Arnalds et al., 2016).

Table 5.1: Experiment sediment source locations and PDS classification (Bullard et al., 2011)

Site ID	Latitude	Longitude	PDS Classification (Bullard et al., 2011)
Markarfljotsandur	63.546°	-20.029°	Sand sheet (5a)
Markarfljot Ephem	63.549°	-20.067°	Armoured, unincised (3b) and Unarmoured, unincised (3d)
Mýrdalssandur	63.486°	-18.732°	Unarmoured, unincised (3d)

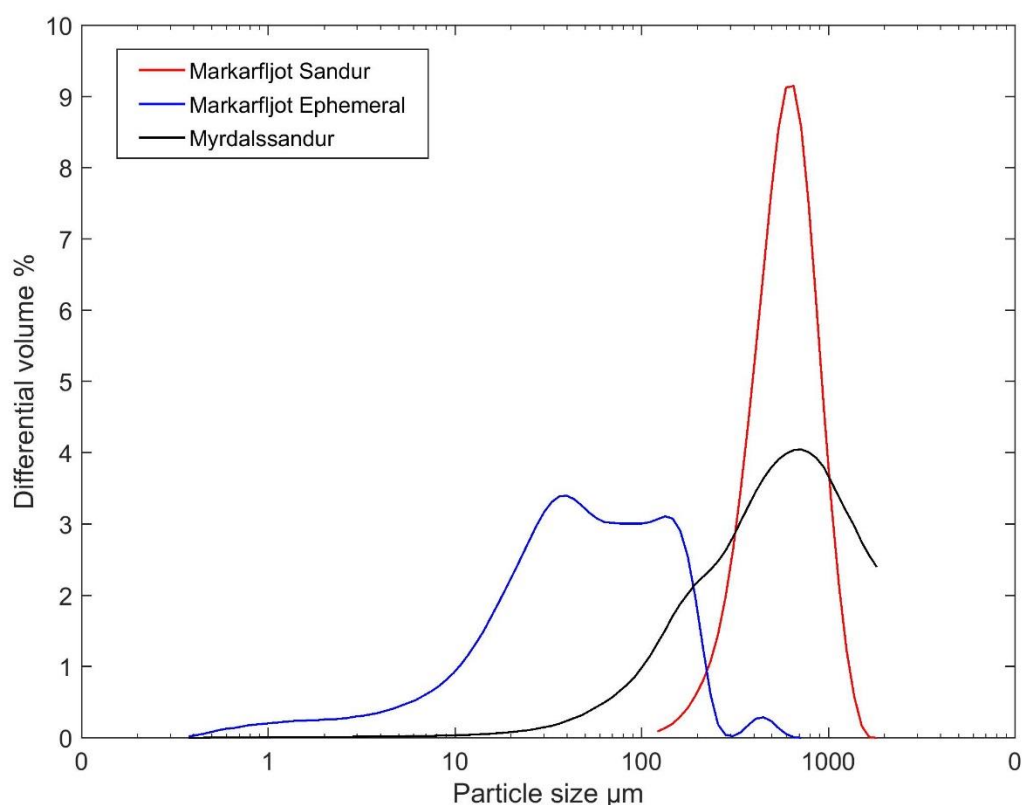


Figure 5.2: Parent soil material particle size distribution for the three sediment groups used in the abrasion chamber experiments

The different sediment compositions within these three sites are representative of the main dust source geomorphologies in Iceland (Arnalds, 2001). Therefore, this experiment will not only explore the role the relative susceptibility to aeolian abrasion of from particles from the three sources, but also the relative potential total dust production rates generated under the same laboratory conditions.

5.5.2 Abrasion Chamber

This experiment utilises a laboratory abrasion chamber which has been used previously to quantify rates of fine particle production (Wright et al., 1998; Bullard et al., 2004; 2007). This is the first attempt to quantify the creation of fine particles for the high latitude dust system, where our understanding of dust emission processes is limited (McKenna Neuman, 2003; Bullard et al., 2016).

Sediments are dried for 72 hours in a drying oven at 40°C. 10g of sediment is then weighed to 4 decimal places. It is almost impossible to weigh exactly 10g of sediment, therefore all analyses in this chapter dealing with total dust productions will present the total percentage of sediment lost compared to the initial starting weight of the sediments within the abrasion chamber. Sediments are then placed in a large cylindrical test tube (Figure 5.3). The test tube is held into place using clamps and a metal stand, and is sealed using a rubber plug (Figure 5.3).

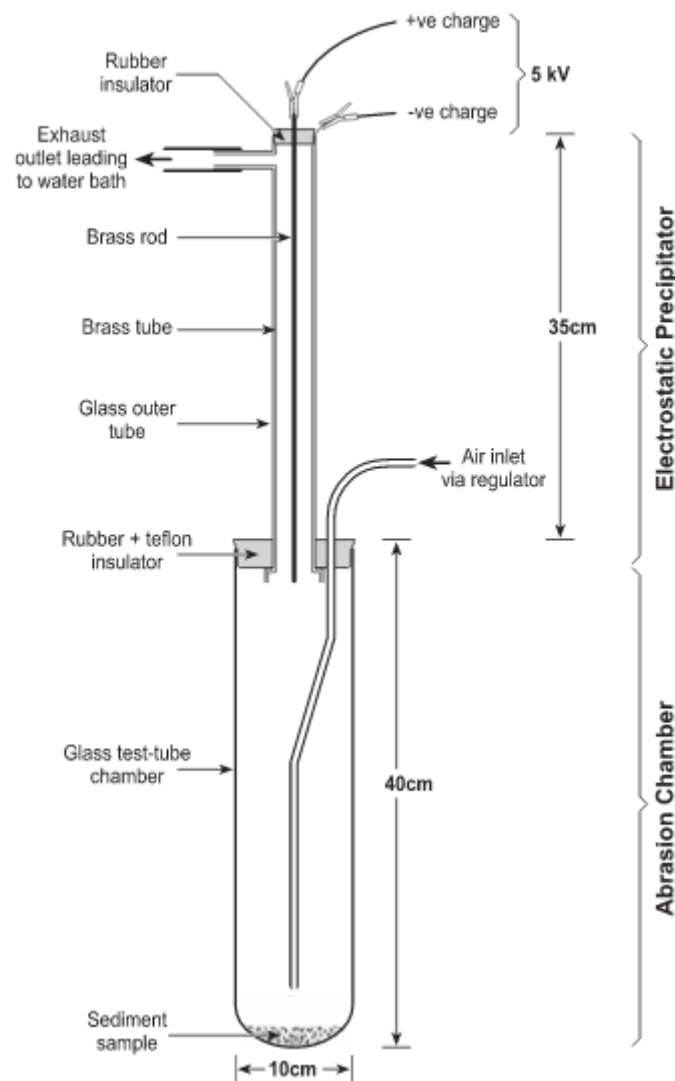


Figure 5.3: Laboratory set up of aeolian abrasion chamber (Bullard et al., 2004)

A given airflow is then applied to the sediments to allow them to saltate (e.g. bounce) within the cylindrical test tube. For this experiment, sufficient air flow was provided so that the sediments located in the test tube would rise approximately 10cm. This means that the airflow between experiments would be altered dependent on the amount of air flow required to lift different sediments to this height. This means that this experiment is not examining the difference in the amount of dust which is generated from differing surface sediments under the same flow conditions, but the differences in total dust production and dust particle size of sediments produced by saltating sediments being lifted to the same height.

The reason for this distinction is because it is understood that saltation is the key driver of dust emissions globally (Shao et al., 2001; Klose and Shao, 2012). In this experiment, it is assumed that saltation is a key driver of dust emissions on all surfaces in Iceland (Arnalds, 2001). As particles bounce within the abrasion chamber, they are being lifted to approximately 10 cm, which initiates collisions comparable to those which occur during saltation (e.g. Shao et al., 1993). As the main aim of this chapter is to assess the importance of aeolian abrasion on fine particle production, it is important to try and represent the main dust emitting process within the laboratory experiment to the best of our ability. If the same flow was applied to the Markarfljot ephemeral channel system and Mýrdalssandur sediments that was applied to the larger Markarfljotsandur sediments, sediments would be entrained above what is considered an acceptable height for the saltation layer (Bagnold, 1941).

When the appropriate flow has been set, sediments start saltating and collisions can occur between particles. Due to the relative low mass of finer particles in comparison to coarser sand particles, these particles are either released from the parent material and/or created by collisions with other particles/with the test tube. These fine particles will rise to the top of the cylindrical test tube, where a brass outer tube and an inner brass rod are located to collect particles during experimental runs. The inner rod is charged with a 5000w power supply, whereas the outer rod is earthed. The charging of the inner brass rod makes both surfaces electrically charged and when particles travel through the outer brass tube, particles are attracted to both the tube and inner rod. This means that particles will stick to the sides of both pieces of apparatus until the charge has been fully removed. The relative efficiency of the apparatus (e.g. the amount of dust sized material which was not effectively trapped by the apparatus) was

not measured during this experiment, however the accuracy of this particularly abrasion chamber was measured at approximately 90% by Bullard et al., (2004) and Bullard and White (2005).

An aim of this chapter is to assess how total dust production and particle size distribution of the generated sediments vary through time. Therefore, dust sediments were retrieved from the outer brass tube and inner rod at 1, 2, 4 and 8 hours. Once particles had been retrieved from the outer brass tube and inner rod, these components were thoroughly washed using DI water and dried for a minimum of 1 hour in a drying oven. Once a full 8-hour run had been concluded, the remaining sediments located in the cylindrical test tube are removed and weighed.

Three runs of each sediment type in both temperatures were run to allow the statistical testing of differences in potential total dust production rates and generated dust particle size between samples. The total dust production curves in this chapter are therefore an average of all three runs. However, due to equipment malfunction, only two runs are used to calculate the relative particle size distributions.

The use of a laboratory abrasion chamber to assess the process of aeolian abrasion has some limitations. The biggest issue is representing the natural state of sediments within the chamber. Sediments are often aggregated in nature which causes significant disruptions to aeolian activity (Gillette, 1967). Clay minerals often bond under chemical precipitation to form sand sized particles (Pell and Chivas, 1995). These fine sediments are then released under the process of saltation/sandblasting (Gillette and Walker, 1977; Gomes et al., 1990; Shao et al., 1993, Shao, 2001). When preparing samples for the abrasion chamber, samples are desiccated, dried and disaggregated (Wright, 1998; Bullard et al., 2004; 2007; Bullard and White, 2005). This means that the finest particles (e.g. particles $<2\mu\text{m}$) within the experimental samples will not be aggregated (Bullard et al., 2004; Bullard and White, 2005) thus not representing actual field conditions and potentially overestimating dust production rates.

5.5.3 Particle Size Distribution

All particles generated from the abrasion experiment were analysed using a Beckman Coulter particle counter 2, as documented in Chapter 3. The only difference for this

analysis than that documented in Chapter 3 is the removal of sediments from the filter papers described in section 3.2. Filter papers were sub sampled because too much material for particle size analysis was created. This was done by cutting $\frac{1}{4}$ of the filter paper using a sterile scalpel. The sub-sample was placed in a 100ml test tube, wet with 10ml of DI water and was sonicated in a water bath for 30 minutes to remove the particles from the filter paper. This process means that the laser sizer analysis will show the fully dispersed particle size characteristics (Haberlah and McTainsh, 2011).

5.5.4 Temperature/Humidity

All other experiments using abrasion chambers have conducted experiments at laboratory temperature, as the role of temperature was not being tested. The relationship between temperature, humidity and surface sedimentology has been shown to be important in influencing dust emission rates in a variety of environments (e.g. McKenna Neuman, 1993; Fécan et al., 1998; McKenna Neuman, 2005). Because this study has used sediments from Iceland, where spring/summer temperatures are on average 5°C (Einarsson, 1984), the role of temperature and/or humidity could be a key factor in the aeolian system. Identical experiments using the laboratory abrasion chamber were conducted at room temperature (26-29°C) and in a walk-in laboratory fridge (3-6°C). Temperature and humidity were both measured using an I-Button which was located directly inside the abrasion chamber at the top of the glass test tube. The I-Button recorded temperature and humidity at 1-minute intervals for the entirety of the experiment.

5.6 Results

5.6.1 Total dust production as a function of soil texture

Dust produced during abrasion experiments varied considerably between samples with differing sedimentologies (Table 5.2). Total dust production rates over 8 hours from the Markarfljot ephemeral channel system and Mýrdalssandur were of the same order of magnitude, producing on average 0.236g and 0.329g respectively. This represented a total dust % from the initial sample weight of 2.354% for Markarfljot ephemeral channel system and 3.275% for Mýrdalssandur. Total dust production from the Markarfljot sandur sediments was notably lower, only producing 0.030g which represents only 0.31% of the initial parent sample weight.

Table 5.2: Summary of average total dust produced in 8 hours (g), total dust as a % of the initial sample weight, % of dust produced in first 1 hour and % of dust produced in first 2 hours for all samples at 26 - 29°C (W) and 8 - 12°C (C)

Sample	Dust produced in 8h (g)		Total dust as % of initial sample		% of dust produced in 1h		% of dust produced in 2h	
	W	C	W	C	W	C	W	C
Markarfljotsandur	0.030	0.069	0.310	0.697	23.521	6.272	41.871	43.251
Markarfljot Ephem	0.236	0.153	2.354	1.526	39.892	32.403	60.354	41.010
Mýrdalssandur	0.329	0.176	3.275	1.753	34.772	25.134	49.136	38.484

Figure 5.4 shows dust production through time during 8-hour abrasion experiments for all three sediment groups. Error bars are generated from 3 separate experimental runs. Dust production at Markarfljotsandur is reasonably constant throughout the 8-hour abrasion experiments. This is reaffirmed by Table 5.2, where after 1 hour of abrasion, 23.5% of the total dust during the 8-hour experiment was collected; by the end of hour 2, 41.87% of the total dust was collected.

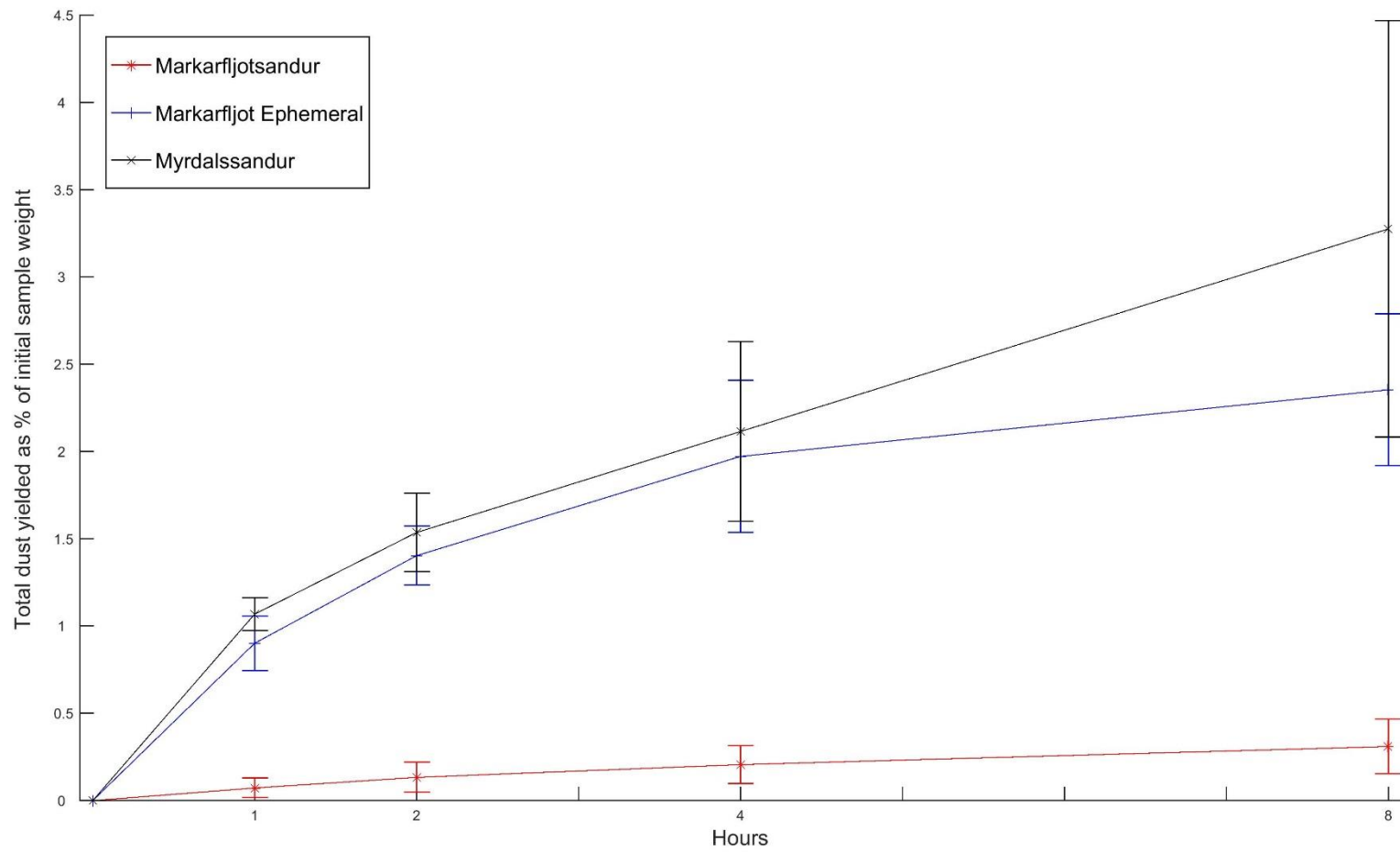


Figure 5.4: Total dust % produced as a function of initial sample weight during 8-hour abrasion experiments at 26 - 29°C with error bar

For the Markarfljot ephemeral channel sediments, dust production is highest in the initial 2-hour period, before slightly decreasing between 2-4 hours, with a further decrease in rate between hours 4-8 (Figure 5.3). Within the first 2 hours, 39.89% of the total % of dust yielded is collected. A comparable rate of dust production is found at Mýrdalssandur, with the initial hour yielding 34.77% of the total dust (Table 5.2), before slightly decreasing in hours 2-4, and further decreasing from hours 4-8.

Error bar differences between samples and time periods indicate that as total dust productions increase so does the spread and uncertainty of the values. The lowest errors are associated with the lowest dust productions from the Markarfljotsandur sediments. When the error is considered, there is no difference in total dust productions between the Markarfljot ephemeral channel system and Mýrdalssandur at any of the time intervals.

5.6.2 Total dust production as a function of temperature and humidity

Temperature and humidity differences between warm (W) and cold (C) experiments can be seen in Table 5.3. Table 5.3 shows that dust production at different temperatures varied dependent on the characteristics of the parent material. Figure 5.5 shows the total dust generated through time for all samples for both the warm and cold abrasion experiments.

Table 5.3: Summary of combined average temperature (°C) and average relative humidity (%) during abrasion experiments in warm (W) and cold (C) conditions

Sample	Temperature		Humidity	
	W	C	W	C
Markarfljotsandur	29.13 ± 2.3	11.91 ± 2.89	38.78 ± 12.77	49.62 ± 10.09
Markarfljot Ephem	26.97 ± 3.25	8.24 ± 0.48	34.99 ± 12.35	53.04 ± 6.78
Mýrdalssandur	26.53 ± 2.21	9.96 ± 1.03	32.04 ± 10.01	55.07 ± 4.79

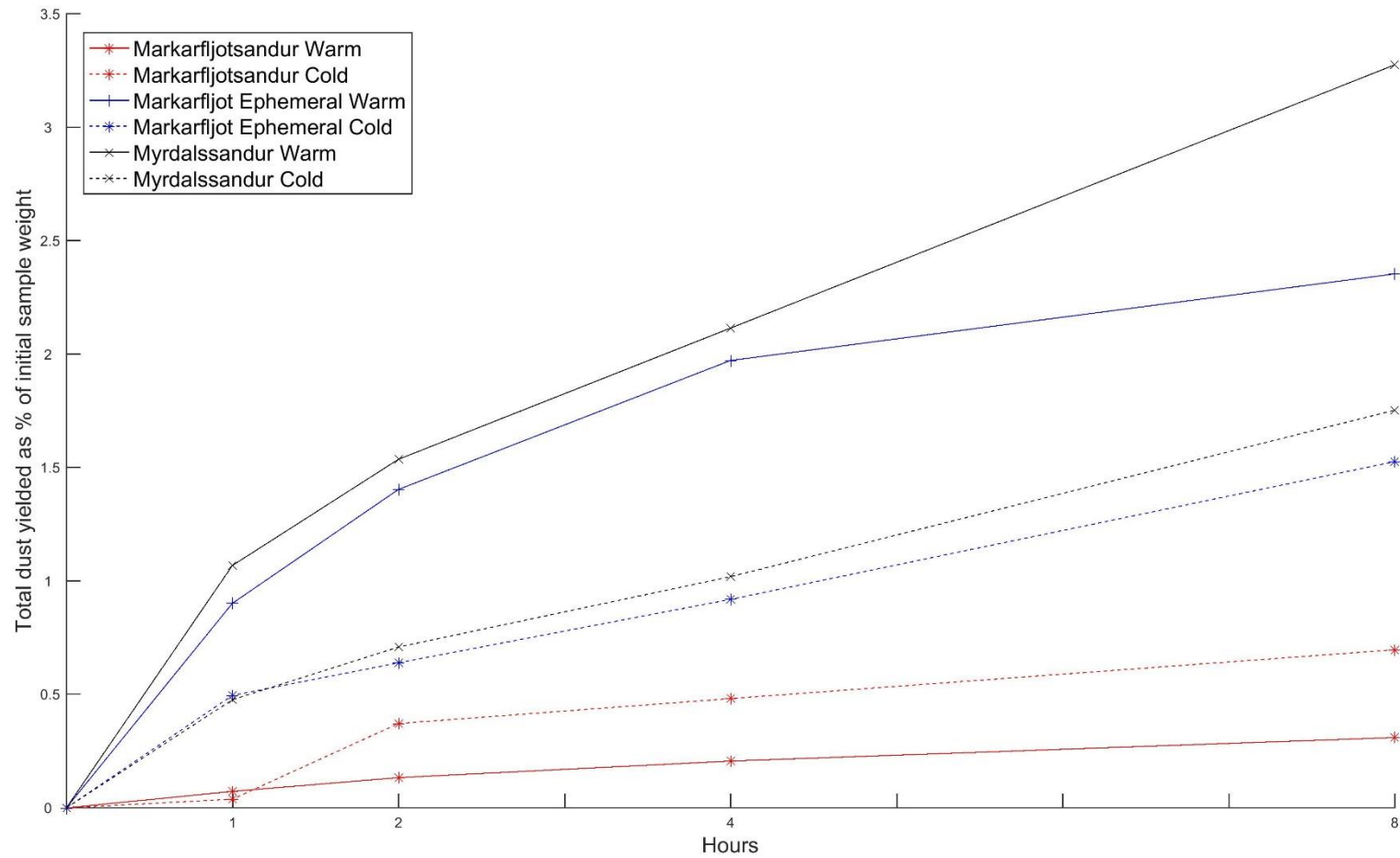


Figure 5.5: Total dust % produced as a function of initial sample weight during 8-hour abrasion experiments at 26 - 29°C (solid line) and 8-12 °C for all sediments (dashed lines)

At Markarfljotsandur, the smallest amount of dust was generated during the warm experiments with a 2x increase in total dust production in the cold experiments. Total dust yield as a function of initial starting weight percentage, in hours 1 and 2 of the experiment. Figure 5.7 shows that the nature of the production is similar between the warm and cold experiments. Table 5.4 provides t-test p values for the relationship for all time periods of average total dust productions in warm and cold conditions for all sediments. No point in the Markarfljotsandur total dust production curve shows a statistically significant difference between the warm and cold abrasion experiments.

This increase in total dust production during the experiments at cold temperatures was only seen in the sediments at Markarfljotsandur. At Markarfljot ephemeral channel system, under colder conditions, total dust production decreased from 0.236g (2.35% of initial sample weight) to 0.153g (1.52% of initial sample weight). Less material, as a % of the initial sample weight, was also emitted in the first 2 hours of the experiment. In hour 1, only 11.4% of the sample was collected, rising to only 24.9% by the end of hour 2. By the end of hour 2 in the Markarfljot ephemeral channel system sample in the warmer conditions, almost 50% of the total dust produced had been collected. The rate of production between hours 2 and 8 are comparable between the warm and cold experiments.

A similar magnitude of decrease during cold experiments can be seen from particles at Mýrdalssandur. Total dust production decreased from 0.329 (3.275% of the initial sample weight) in warm conditions to 0.176 (1.753% of the initial sample weight) during the cold experiments. This is partly due to the differences in production seen in the first two hours of the experiment; only 18.05% of the total sediments were generated by hour 2 in the cold experiments whereas over 55% were created in warmer conditions. As is seen at Markarfljot ephemeral channel system, the rate of production between hours 2 and 8 for the Mýrdalssandur sediments is in the same order of magnitude between warm and cold conditions.

Table 5.4 suggests statistically significant differences between total dust production at 3 of the 4-time intervals for both the Markarfljot ephemeral channel system and Mýrdalssandur under warm and cold conditions.

Table 5.4: Differences in total dust production from warm and cold abrasion runs from all sediment types. Statistically significant P-values are displayed in red (P < 0.05)

Hours	Markarfljotsandur			Markarfljot Ephem			Mýrdalssandur		
	W	C	P	W	C	P	W	C	P
1	0.073	0.038	0.184	0.902	0.496	0.074	1.068	0.477	0.021
	± 0.056	± 0.018		± 0.156	± 0.362		± 0.093	± 0.337	
2	0.133	0.372	0.206	1.404	0.639	0.017	1.537	0.709	0.020
	± 0.086	± 0.443		± 0.168	± 0.380		± 0.224	± 0.423	
4	0.206	0.482	0.163	1.972	0.919	0.010	2.115	1.019	0.030
	± 0.109	± 0.412		± 0.435	± 0.232		± 0.516	± 0.522	
8	0.310	0.697	0.094	2.354	1.526	0.030	3.275	1.753	0.056
	± 0.157	± 0.393		± 0.435	± 0.341		± 1.194	± 0.506	

5.6.3 Impact on parent sediments

5.6.3.1 *Markarfljotsandur*

Figure 5.6 is the particle size distribution of the parent sediments and 8-hour abraded sediments for warm and cold conditions at Markarfljotsandur. Whilst there is not a noticeable difference of size characteristics following abrasion runs in the warm and cold experiments, two notable differences between the abraded sediments and the non-abraded sediments can be seen. Firstly, in both the abraded sediments, a significant loss in sand sized particles between 150 μm and 400 μm has occurred (Table 5.5). There has been a significant decrease in sediments $< 400 \mu\text{m}$ during abrasion in warm and cold conditions. This coincides with a coarsening of sediments, as the percentage of sediments $>400 \mu\text{m}$ increases from approximately 80% in the non-abraded surface sediments to over 90% when particles have been abraded. Secondly, in the non-abraded surface sediments, there are no particles $<100 \mu\text{m}$. After abrasion, the creation of fine particles ($<100 \mu\text{m}$) can be seen in both the warm and cold abraded sediments. The amount of this size fraction in the abrasion sediments varies between the warm and cold sediments, with 2.5% and 0.36% accounting for the $<100 \mu\text{m}$ particle size respectively.

Table 5.5: Particle size fraction breakdown of surface sediments from Markarfljotsandur before and after abrasion experiments

Sample	%<100 μm	%<400 μm	%>400 μm
Original	0	17.6	80.4
Warm abraded	2.5	4.5	92.1
Cold Abraded	0.36	5.1	94.2

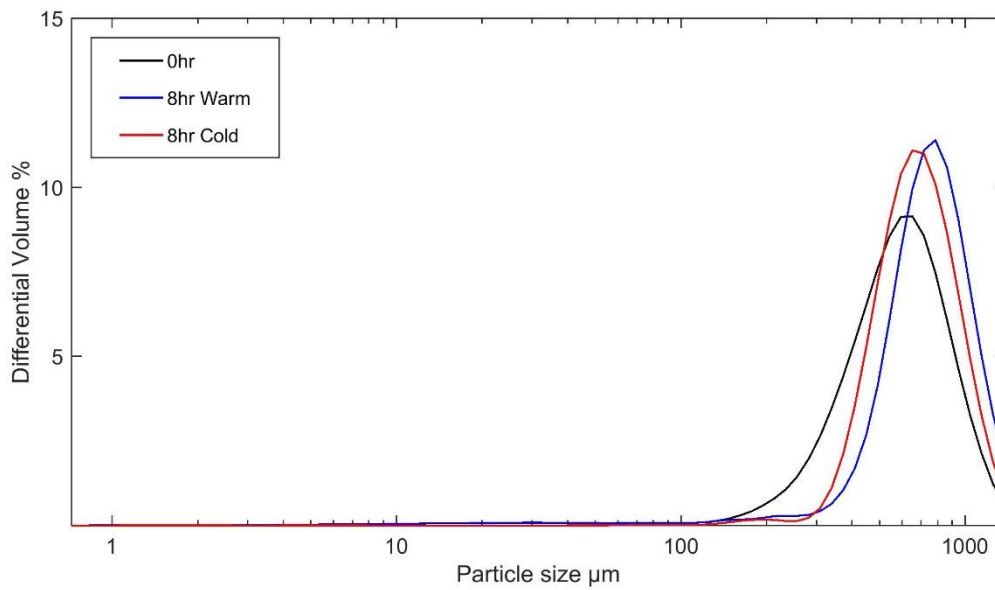


Figure 5.6: Particle size distribution of surface sediments from Markarfljotsandur: Surface sediments (0hr) (black), 8-hour abraded sediments in warm conditions (26 – 29 °C) and 8-hour abraded sediments in cold conditions (8 - 12°C).

5.6.3.2 *Markarfljot ephemeral channel system*

Figure 5.7 is the particle size distribution of the parent sediments and 8-hour abraded sediments for warm and cold conditions at the Markarfljot ephemeral channel system. The major particle size difference between the non-abraded sediments and the abraded sediments is the removal of fine grains under $<100\ \mu\text{m}$ in the abraded sediments, leading to a coarsening of the sediments.

Before the experiment, the sample contained 11.3% of particles $<10\ \mu\text{m}$ and 62.5% of particles between 10 and $100\ \mu\text{m}$. After abrasion in both of these size bins, the percentage of total sediments has decreased significantly (Table 5.6). This has led to a dominance in larger particles, increasing the % of particles over $100\ \mu\text{m}$ in the warm and cold sediments to 89.5% and 87.3% respectively. This is a significant increase from the original parent material which comprised of 26.2% of sediments $>100\ \mu\text{m}$.

5.6.3.3 *Mýrdalssandur*

Figure 5.8 is the particle size distribution of the parent sediments and 8-hour abraded sediments for warm and cold conditions at Mýrdalssandur. There is very little difference in the size distribution of the non-abraded sediments and the warm abraded material. Slight differences are seen for the cold abraded material. An increase in particles $<100\ \mu\text{m}$ to 9.6% from 6.9%, with a decrease in particles $>500\ \mu\text{m}$ (38.2% from 48.6%) (Table 5.7). All distributions take a similar shape, with the notable peak of material between 100 and $500\ \mu\text{m}$ being almost unaltered during the abrasion experiments.

Table 5.6: Particle size fraction breakdown of surface sediments from Markarfljot Ephemeral Channel System before and after abrasion experiments

Sample	%<10 μm	%>10 μm < 100 μm	%>100 μm
Original	11.3	62.5	26.2
Warm abraded	0.6	9.9	89.5
Cold abraded	0.4	11.3	87.3

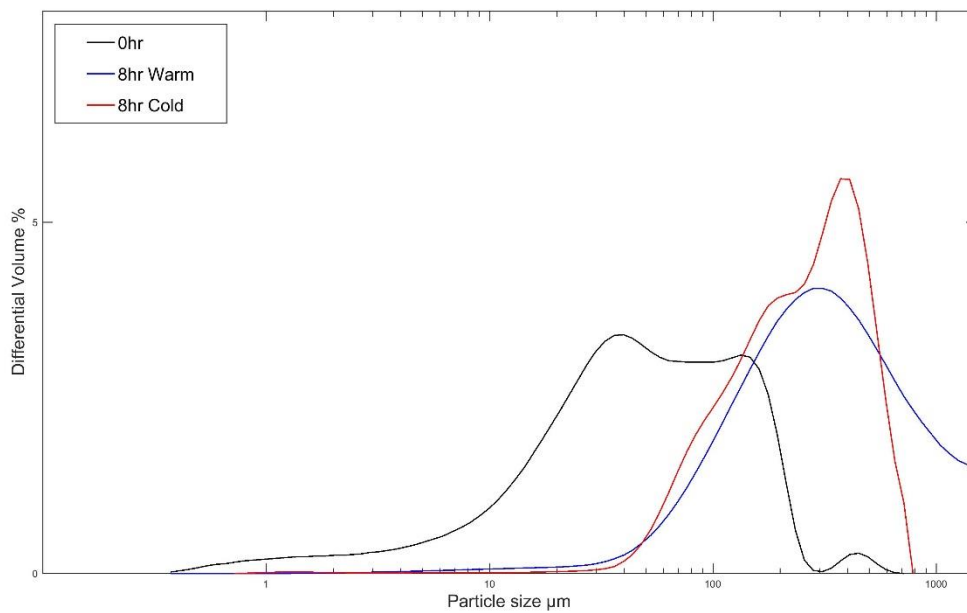


Figure 5.7: Particle size distribution of surface sediments from Markarfljot ephemeral channel system: Surface sediments (0hr) (black), 8-hour abraded sediments in warm conditions (26 – 29 °C) and 8-hour abraded sediments in cold conditions (8 - 12°C).

Table 5.7: Particle size fraction breakdown of surface sediments from M Mýrdalssandur before and after abrasion experiments

Sample	%<100 μm	%>100 μm <500 μm	%>500 μm
Original	6.9	42.5	48.6
Warm abraded	4.5	43.4	45.8
Cold Abraded	9.6	42.0	38.2

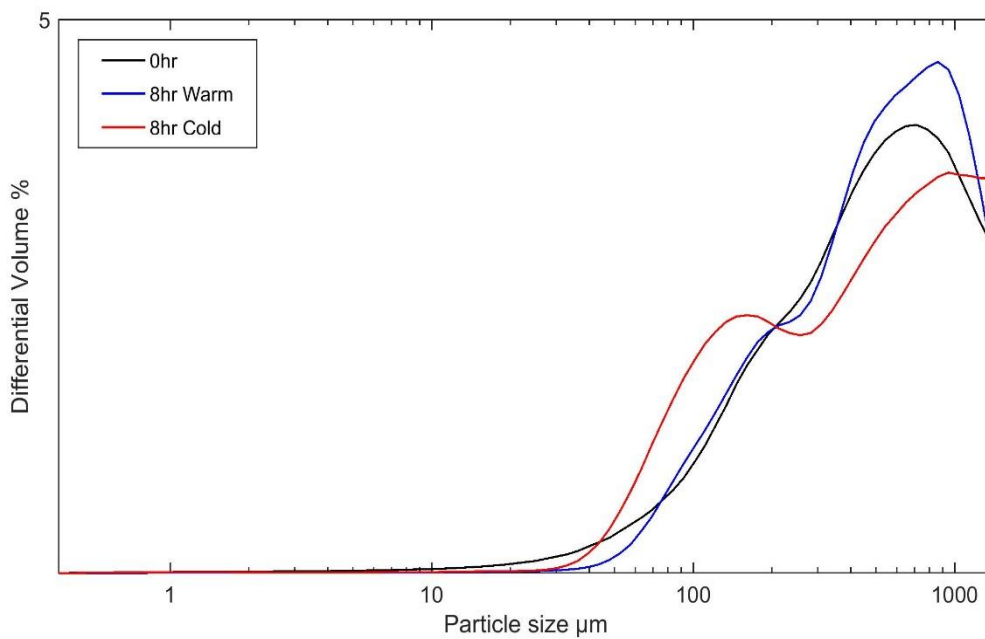


Figure 5.8: Particle size distribution of surface sediments from Mýrdalssandur: Surface sediments (0hr) (black), 8-hour abraded sediments in warm conditions (26 – 29 °C) and 8-hour abraded sediments in cold conditions (8 - 12°C)

5.6.4 Dust particle size distributions

5.6.4.1 Markarfljotsandur

The size distribution of the created dust particles from Markarfljotsandur varies through time. Figure 5.9 displays the particle size distributions of dust sediments collected at 1, 2, 4 and 8-hour intervals during the abrasion process. Table 5.8 is the size fraction % of particles <10 µm, between 10 µm and 63 µm and above 63 µm. These data are exclusively from these time intervals and are not cumulative totals.

Dust particle size from Markarfljotsandur in the first 4 hours is dominated by particles between 10 µm - 63 µm, with a mode ranging between 29 – 33 µm for the time intervals of 1,2 and 4 hours. The proportion of material <10 µm did increase by approximately 10% from hour one (29.4%) to hours 2 (41.4%) and 4 respectively (38.1%). After 8 hours, the size distribution of the dust sized particles fined significantly, with a decrease in the modal peak at 30 µm, with particle sizes <10 µm increasing to 68.5% of the total particles generated. The modal size was approximately 4 µm. A very small proportion of particles above >63 µm were present during the entirety of the abrasion experiments; the largest proportion being recorded at the 4-hour time interval (1.8%).

The main difference between the particle size distributions generated under warm and cold conditions is the % of particles generated <10 µm. For all time intervals, the % of particles < 10 µm is higher during cold conditions. For both warm and cold conditions, there is a lack of material collected which is > 63 µm.

Table 5.8: Particle size fraction breakdown (%) of created dust particles from the Markarfljotsandur sediments for all time periods

Hour	% < 10 μm		% >10 < 63 μm		% >63 μm	
	W	C	W	C	W	C
1	29.4	46.3	69.3	53.7	1.3	0
2	41.1	54.9	58.9	45.1	0	0
4	38.1	62.5	60.0	37.5	1.8	0
8	68.5	79.7	31.5	20.3	0	0

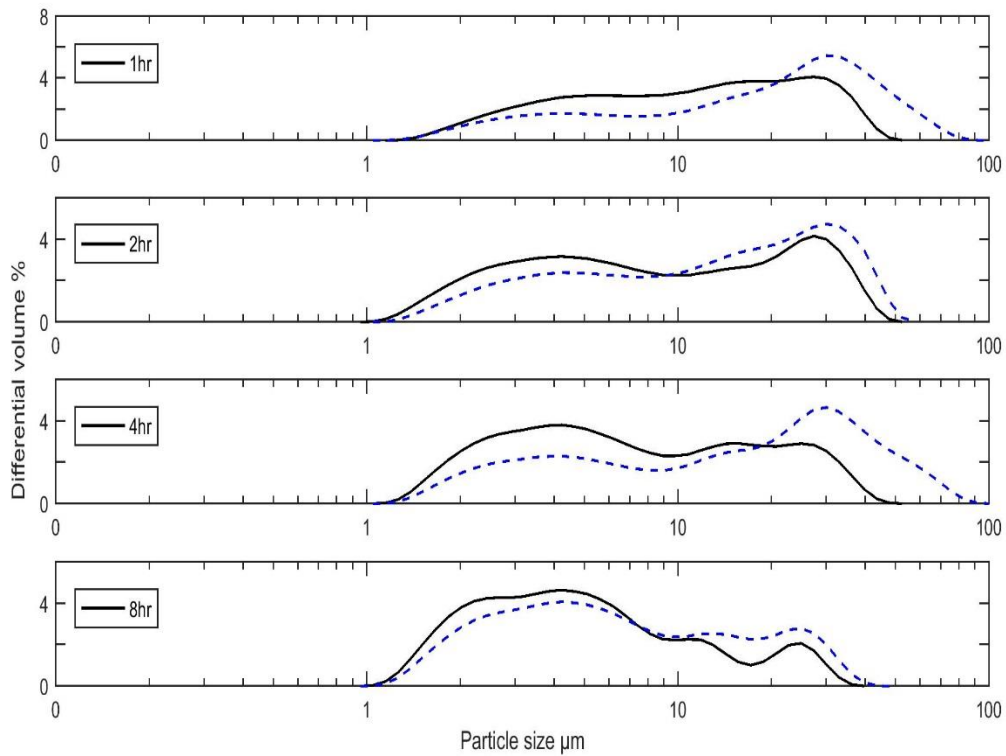


Figure 5.9: Particle size distribution of created dust particles from Markarfljotsandur sediments for 1,2,4 and 8hrs of abrasion at warm (dashed) and cold temperatures

5.6.3.2 Markarfljot ephemeral channel system

The size distribution of dust particles created from sediments from the Markarfljot ephemeral channel system are less variable than those created at Markarfljotsandur (Figure 5.10).

In the first hour of abrasion, a clear unimodal distribution is observed, with the dust particle size presenting a mode of approximately 28-30 μm . This coincides with 63.3% of all created particles being between 10 and 63 μm (Table 5.9). In time intervals 2 and 4 hours, a bimodal distribution is formed with modes at 2 hours of 5 μm and 22 μm , and 4 hours of 5 μm and 24 μm . This is expressed with extremely similar total % for particles below 10 μm (53.3% at 2 hours, 49.6% at 4 hours) and particles between 10 μm and 63 μm (49.6% at 2 hours, 50.4% at 4 hours). A slight difference in size distribution is apparent at 8 hours, with finer particulates becoming more dominant; 59.8% of all particles created are <10 μm . The distribution is still bimodal with peaks at 4 μm and 24 μm . There are almost no sand sized particles created at the Markarfljot ephemeral channel system (>63 μm).

Differences in particle size between warm and cold experiments on the Markarfljot ephemeral channel system sediments are shown in Figure 5.10. Unlike at Markarfljotsandur, fewer particles <10 μm are collected throughout all time intervals during cold experiments than during warm experiments. This is more pronounced during the 1 and 2-hour time intervals, where a clear modal peak of sediments is collected between 27-30 μm ; this coincides with 79% and 51.4% of all sediments collected during these time intervals respectively being between 10 and 63 μm . The distribution becomes distinctively bi-modal after hour 1, and by the end of hour 8, two modal peaks are evident in the sample at 4 μm and 25 μm . By the end of the experiment, distribution curves for both the warm and cold experiments are almost identical. The biggest difference in particles generated which are <10 μm is during hour 1; 20.1% of particles during the cold experiment are in this size fraction which is considerably lower than the 36.6% collected during the warm experiments.

Table 5.9: Particle size fraction breakdown of created dust particles from the Markarfljot ephemeral channel system sediments for all time periods

Hour	% < 10 μm		% > 10 < 63 μm		% > 63 μm	
	W	C	W	C	W	C
1	36.6	20.1	63.3	79	0.9	0
2	53.3	48.6	46.7	51.4	0	0.01
4	49.6	49.5	50.4	50.5	0	0
8	59.8	53.3	40.2	46.7	0	0

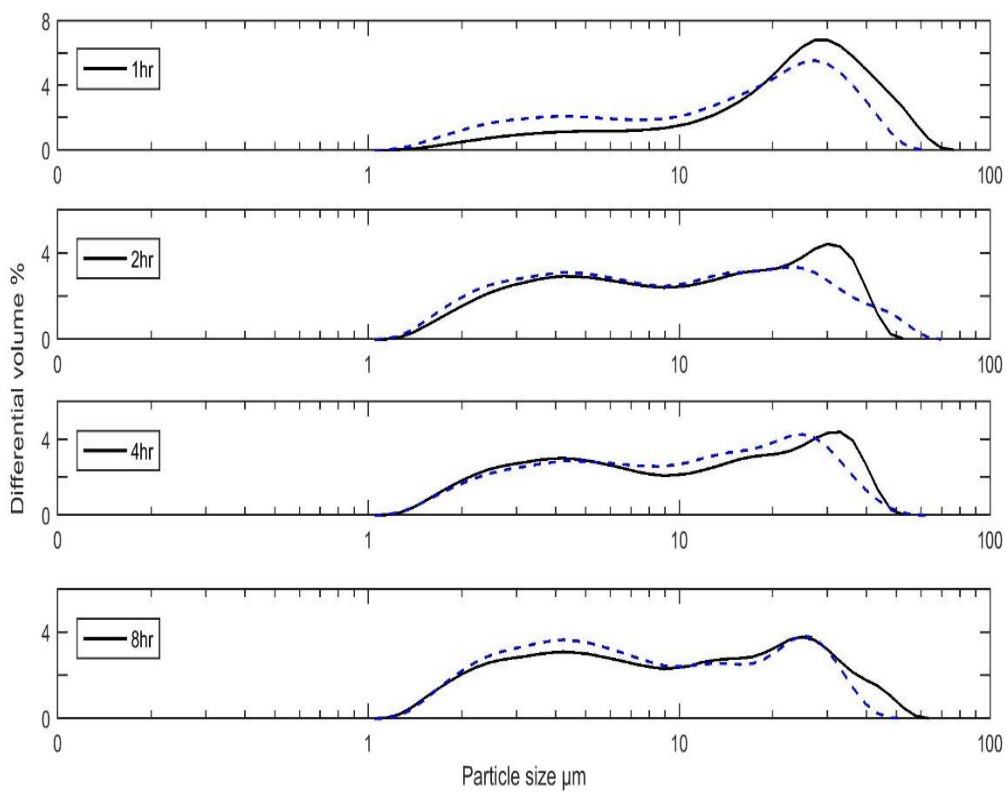


Figure 5.10: Particle size distribution of created dust particles from the Markarfljot ephemeral channel system sediments for 1,2,4 and 8hrs of abrasion at warm (dashed) and cold temperatures (solid)

5.6.3.3 *Mýrdalssandur*

There is very little variation in the created dust particles between time intervals from *Mýrdalssandur* sediments (Figure 5.11). All time intervals display a clear bimodal distribution.

Differences in particle size between warm and cold experiments on the *Mýrdalssandur* sediments can be seen visually in Figure 5.11. Major differences in particle size between warm and cold experiments are seen in hours 1 and 8. In hour 1, a very limited proportion of material <10 μm is collected during the cold experiments (19.9%) in comparison to the corresponding runs in the warm experiments (49.7%). As such, there is a clear modal peak at 30 μm , with 78.5% of all particles being sized between 10 and 63 μm . At time intervals 2 and 4, the distribution becomes more bi-modal (4 μm and 25 μm), with increases in material <10 μm (46.0% and 50.9% of the total sample). In these periods, there is very little difference between the particle size distributions generated in the warm and cold experiments. After 8 hours of abrasion, particles < 10 μm dominate the size distribution in the cold experiment (61.8%), which is far greater than that observed during the warm experiments at the same time interval (51.3%). Very little material is above 63 μm , with the largest proportion seen in hour 1 at 1.6%.

Table 5.10: Particle size fraction breakdown of created dust particles from the Mýrdalssandur sediments for all time periods

Hour	% < 10 μm		% > 10 < 63 μm		% > 63 μm	
	W	C	W	C	W	C
1	49.7	19.9	50.3	78.5	0.01	1.6
2	51.2	46.0	48.8	54.0	0	0
4	51.5	50.9	48.5	49.0	0	0.1
8	51.3	61.8	48.7	38.2	0	0

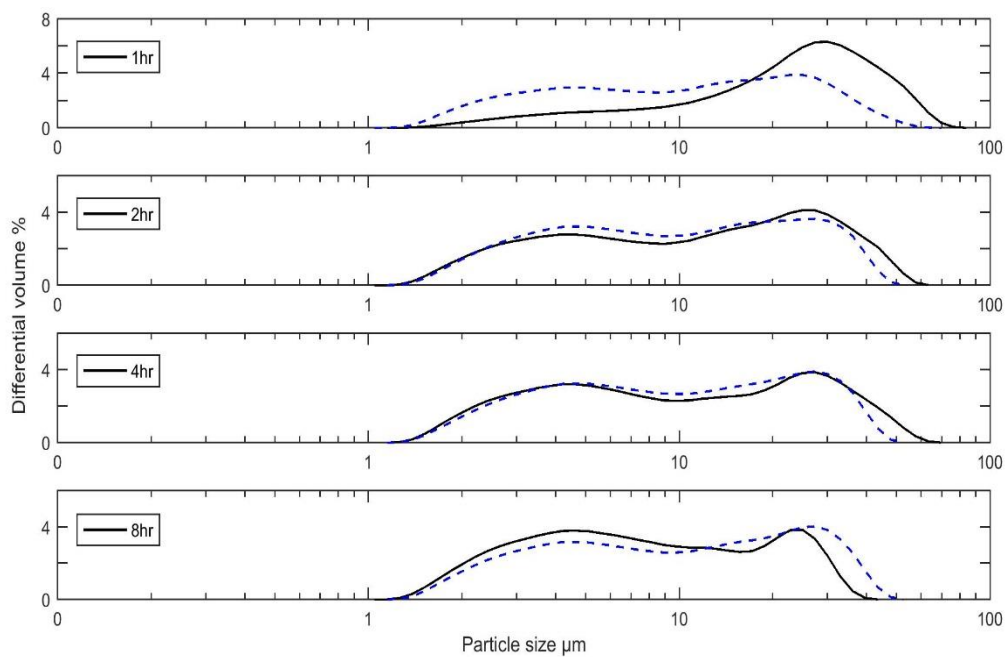


Figure 5.11: Particle size distribution of created dust particles from the Mýrdalssandur sediments for 1, 2, 4 and 8hrs of abrasion at warm (dashed) and cold temperatures (solid)

5.7 Discussion

5.7.1 The impact of sediment texture on total dust production and aeolian abrasion

The effect of surface soil sedimentology in controlling total dust production has been well documented in subtropical environments (Gillette, 1976; Gill et al., 2006; Alfaro, 2008; Mockford et al., 2013; Gherboudj et al., 2015; Parajuli et al., 2016). Sediment texture controls the physical and binding properties of surface particles (Alfaro, 2008; Gill et al., 2006), and is therefore a key control on the dust emission potential of a given surface (Bhattachan et al., 2012; 2013; 2015).

The results from this study indicate that as soil texture coarsens, the relative dust production potential decreases (Figure 5.4). The lowest total dust produced was by the Markarfljotsandur sediments, which are comprised purely of sand sized particles (Table 5.5). Total dust production was several orders of magnitude higher in the poorly sorted sediments from the Markarfljot ephemeral channel system and Mýrdalssandur.

The results indicate that dust sources in which sand particles dominate surface sediment texture (e.g. sand sheets and sand dunes) are unlikely to be efficient sources of dust. This has been shown for sand seas as their relative contribution to dust emissions in comparison to the total surface area is often small (Bullard et al., 2011; Baddock et al., 2016).

However, sand dunes have been shown to be efficient dust emitters in certain regions of the world. The ability for sand dunes to be efficient dust producers will vary dependent on dune type and dune surface sediment particle size (Bullard et al., 2008; Crouvi et al., 2012). Bullard et al. (2011) found that 57% of all dust plumes at Lake Eyre Basin are sourced from sand dunes accounting for 0.0010 per 1km⁻² of plumes per km²; the second most efficient emitter. In the Chihuahuan desert, 13.8% of all plumes were sourced from sand dunes accounting for 0.0032 per 1km⁻² of plumes per km².

Dune fields also vary sedimentologically, and the results presented by Bullard et al. (2011) may be a function of preferential landscape units within dune fields producing the majority of dust plumes. Bhattachan et al. (2012) showed that vegetated dunes and inter dune zones had higher percentages of surface silt and clay than non-

vegetated dunes. From the results of this work, it could therefore be hypothesised that sedimentological units with higher proportions of silt and clay have a higher dust emission potential leading to the preferential of dust emission from this units within dune landscapes. However, Strong et al. (2010) showed that vegetation restricts dust emission in dune fields by increasing roughness. This increase in surface roughness leads to a reduction in surface wind velocities and, in turn, sediment deposition (Wiggs et al., 1994). These sediments, if clay or silt sized in nature, would only be available for transport once vegetation cover levels decreased. This may occur following post wildfire or after anthropogenic landscape disturbance (Strong et al., 2010). Regardless, the ability for the geomorphological unit of sand dunes to emit dust may be related to content of silt and clay within the surface parent sediments, instead of the ability for sand to abrade during transport (Bhattachan et al., 2012).

Sand particles have been shown to be difficult to abrade (Gill et al., 1999; Zobeck et al., 1999; Madden et al., 2010, Mockford, 2013). Gill et al. (1999), using a laboratory dust generator, found that particles with high % of sand content were the lowest dust emitters because particles are unlikely to be prone to large scale break ups during impacts. Mockford (2013) showed a significant relationship between increasing sand content and decreasing total dust productions from 45 varying soil types in the Southern High Plains. Dust emission when the percentage of very fine sand exceeded the percentage of coarser sand grains.

Although sand grains may be inherently difficult to abrade, other grain factors may help promote aeolian abrasion. As shown in Chapter 3, the sediments from Markarfljotsandur have a high percentage of ultra-fine surface adhesions which are attached to the surfaces of individual sand particles. The removal of these adhesions during aeolian transport may be important in creating dust sized particles.

Wright (1993) indicated that there are four ways for sand to be abraded in the aeolian system. Bullard et al (2004, 2007), focusing on the generation of material for dust events, showed that particles are likely to be released in three ways. Firstly, by the removal of initial fines within the parent material (Assallay et al., 1998; Pye, 2015). Secondly, by the chipping and spalling of particles during impact (Wright et al., 1998) and thirdly, the removal of clay coatings/surface adhesions from the surfaces of larger grains (Gillette and Walker, 1977). The release of initial fines from the

Markarfljotsandur sediments cannot occur, therefore indicating that abrasion must occur during aeolian transport for dust sized sediments to be created.

The relative importance of aeolian abrasion processes may change through time and this can be disentangled from changes in dust particle size (Figure 5.5). Bullard et al. (2004) indicated that particles $<10\mu\text{m}$ are likely to be sourced from the removal of surface coatings from sand-sized particles, particles in the range of $10\text{-}63\ \mu\text{m}$ are created through the process of chipping and spalling of sand sized grains, and particles above $63\ \mu\text{m}$ are the release of resident fines within the surface sample.

Following this definition, it would suggest that the sediments at Markarfljotsandur during the abrasion experiments are being subjected to both the removal of coatings and chipping/spalling in tandem throughout the abrasion experiment. This is shown by a bi-modal particle size distribution during all time periods within the experiment (Figure 5.9). The importance of chipping/spalling seems to dominate in the first 4 hours of experiments, with a shift towards the removal of surface coatings in hours 4-8. This result is surprising as the kinetic energy required to chip and spall sand grains is higher than to remove surface grain coatings (Kuenen, 1960). However, as particles are abraded they are likely to become rounded (Goudie and Watson, 1981; Thomas, 1987). As particles round, the ability of particles to chip and spall may decrease because of the removal of sharp corners and proturbences (Wright, 1993; Wright et al., 1998).

The role of aeolian abrasion processes in producing silt and clay sized particles is most likely different for the Markarfljot ephemeral channel and Mýrdalssandur sediments. For the sediments at Markarfljot ephemeral channel system and Mýrdalssandur, the total rates of dust production are in the same order of magnitude as each other and follow a similar rate of dust production through time (Figure 5.4). The largest rate of dust production occurs within the first 2 hours for both sediments, before the slope flattens, indicating a decrease in total production in the latter part of the experiment.

The higher total dust production rates of both these sediment groups in comparison to the sediments from Markarfljotsandur are most likely governed by initial sediment texture characteristics. Both sediment groups have considerable amounts of clay and

silt which have been shown to have significant dust emission potential (Chandler et al., 2002; Singer et al., 2003; Mockford et al., 2013).

However, sedimentological units which are dominated by high clay content are likely to be poor dust emitters. Gill et al. (1999) suggested that soils with clay contents above 60% may become clumped into larger aggregates or become protected via the formation of physical or biological soil crusts (Belnap and Gillette, 1997). This was also concluded by Zobeck et al., (1999) who found that a 10x increase in dust production occurred when clays were mixed more evenly with sand sized particles within the surface soil matrix. This is most likely due to the ability for larger sand grains to detach smaller clay particles during saltation (Shao et al., 1993; Cahill et al., 1996). For sediments at Markarfljot ephemeral channel system and Mýrdalssandur, this problem does not exist as the sediments still have relatively high proportion of total sand (>50 %) and particles were fully disaggregated prior to the experimental run.

The initial high rate of total dust production from the Markarfljot ephemeral channel system sediments (Figure 5.4) in hour 1 indicates the release of resident fines within the sample (Whalley et al., 1987; Wright et al., 1998; Bullard et al., 2004). This conclusion is based on a higher quantity of larger particles (>10 μm) being emitted during this period, and the fact that these sediments are already present within the surface sample (Figure 5.2). However, it has been suggested that resident fines would normally be above >63 μm (Assallay et al., 1998, Bullard et al., 2004; Pye, 2015) and that particles in the range 10 – 63 μm are often associated with chipping and spalling of single particles during impact (Wright et al., 1998, Bullard et al., 2004). This removal of sediments from the original parent sediments is clear from the particle size analysis of the abraded sediments against the non-abraded parent material (Figure 5.7, Table 5.6).

The analysis technique employed makes it difficult to disentangle the relative role of aeolian abrasion against the capturing of fine sediments already located within the surface sediments (Bullard et al., 2004). However, changes in particle size distribution of the generated dust through time from the Markarfljot ephemeral channel system and Mýrdalssandur sediments might indicate a shift in the process responsible for dust sized particle collection. In both samples, during the first hour the distribution is bimodal with a clear unimodal peak (at approximately 30 μm). During hours 2 – 8, this

bi-modal relationship becomes more pronounced with an increased proportion of particles < 10 µm collected in both samples (Table 5.9 and 5.10). This shift coincides with a decrease in total dust production after 4 hours. This decrease in total dust production with an increasing fine content (< 10 µm) shows that particles are most likely being abraded during this time period following the initial release of parent fines in the first hour (Figure 5.4)

5.7.2 The impact of temperature and humidity on total dust production and aeolian abrasion

Air temperature has been seen to have a significant impact on the rate of aeolian entrainment in previous research (McKenna Neuman, 1993; 2003; 2004). McKenna Neuman (1993, 2003) suggested that a decrease in temperature increases the density of airflow whilst decreasing air viscosity and the saturation evaporation pressure. This would lead to an altering of the turbulent properties of a grain in transport and increase the magnitude of inter-particle force (McKenna Neuman, 1993). Because aerodynamic drag is fundamentally controlled by air density (Shao and Lu, 2000), particles will express higher aerodynamic drag coefficients with decreasing temperatures as water vapor in the airflow and the potential for water to be absorbed onto the particles decreases (McKenna Neuman, 2004). It is therefore suggested that lower temperatures could lead to increases rates of aeolian entrainment for a given shear velocity.

Total dust productions for sediments at Markarfljotsandur increased 2x when temperature was decreased (Figure 5.5). This would agree with results generated from McKenna Neuman (2003) who found with a variety of sand-sized soil matrices (210 µm, 270 µm and 610 µm), that it was easier to entrain particles by the wind at low temperatures (-40°C) than at high temperatures (33°C). McKenna Neuman (2003) indicated that for a given wind speed, particle entrainment would occur at particle sizes approximately 40-50% greater in the lowest temperatures in comparison to the warmest temperature.

However, total dust production rates from Markarfljot ephemeral channel system and Mýrdalssandur sediments decreased by an order of magnitude when temperature decreased (Figure 5.5). The possible explanation for this comes from the relationship that may exist between surface sediments and increased relative humidity (%). As

there is no direct control on humidity within our laboratory fridge, an increase in humidity from 32-38% in the warm abrasion experiments to 49-55% in the cold abrasion experiments occurred. This is because warmer air can hold more moisture than cold air (Lawrence, 2005). If the water content of the air is constant, a temperature decrease will lead to an increase in relative humidity (McKenna Neuman, 2004).

These changes in relative humidity might help explain the decreased total production rates recorded for the Markarfljot ephemeral channel system and Mýrdalssandur sediments during these experiments. It has been shown that relative humidity can have a significant effect on aeolian entrainment by affecting the moisture content of surface sediments (Cornelius and Gabriels, 2003; Ravi et al., 2006; Chapter 4). Ravi et al., (2004) showed, for a loamy mixed sand, that soil moisture retention rates increased with relative humidity, whereas Cornelius and Gabriels (2003) found an increased threshold shear velocity with increasing relative humidity during wind tunnel experiments. As displayed in Chapter 4, dust productions at the event scale can be altered significantly by sudden increases in relative humidity.

Although the relationship between relative humidity and aeolian transport has shown this relationship, most of the work has focused on the transport of sand sized particles in saltation (McKenna Neuman, 2003; 2004; Cornelius and Gabriels, Mockford et al., 2017). As noted by Gill et al., (1999) and Zobeck et al., (1999), soil matrices with high percentages of clay/silt may be more susceptible to clumping as surface moisture levels increase; therefore, decreasing the potential possibility of aeolian entrainment due to an increased shear velocity required for motion (Fécan et al., 1998). Moisture has been shown to have a greater impact on surface sediments which have high proportions of fine material (Fécan et al., 1998; Cornelius and Gabriels, 2003). This increase in relative humidity within our abrasion experiments would likely have this impact on the sediments from Markarfljot ephemeral channel system and Mýrdalssandur (Figure 5.7).

The biggest difference in the dust production rates from these sediments occurs during the first 4 hours of the experiment (Figure 5.7), where an increased relative humidity has promoted interparticle bonding, suppressing total dust production (McKenna Neuman, 2003; Ravi et al., 2004). In nature, the wind is an efficient mechanism for desiccating surface sediments with high surface moisture. This might be particularly

important in high latitude environments, where temperatures are lower and cloud cover restricts desiccation from direct solar radiation. In the final 4 hours of the experiments, the total dust production rate for both the Markarfljot ephemeral channel system and Mýrdalssandur sediments is comparable to that seen in the warm experiments (Figure 5.5). This would indicate that the air flow is desiccating the sediments during the experiments. After 4 hours, sediments have fully desiccated and reached an equilibrium where the factors affecting the sediment availability (e.g. increased moisture from the high relative humidity) have been removed and normal rates of total dust production are achieved.

This assertion is supported by the generated dust particle size distributions for both sediments (Figure 5.10, Figure 5.11). After the first hour, particles collected which are $<10\ \mu\text{m}$ decrease from 36.6% to 20.1% from the Markarfljot ephemeral channel system sediments and from 49.7 to 19.9% from the Mýrdalssandur sediments. As has been noted above, the finest particles will be the most affected by an increased moisture content due to high particle moisture retention rates for fine particles (McKenna Neuman, 2003).

Increased humidity seems to have a negligible effect on the Markarfljotsandur sediments (Figure 5.5). As noted by Namikas and Sherman (1995) and Wiggs et al. (2004), surface sands can quickly remove moisture due to increased pore spacing between particles. The ability for surface sands to quickly remove surface moisture, due to increased pore space between particles, allows these types of sediments to be relatively unaffected by changes in surface soil moisture. Increases in relative humidity have been shown to increase surface moisture rates of sand-based soils (e.g. Ravi et al., 2004), however there is likely a higher critical threshold for moisture in determining whether aeolian entrainment can occur (Bergametti et al., 2016). This threshold was unlikely reached during these experiments (see Chapter 4), therefore allowing sediments from Markarfljotsandur to benefit from decreased temperatures, which promoted increased total dust production (McKenna Neuman, 2003; 2004; 2008).

5.7.3 A comparison of total dust production

Figure 5.12 is a time series comparison of the dust concentrations from samples from this study in comparison with two linear dune deposits from the Simpson Desert, Australia (Bullard et al., 2004) and a sample from Pannonian Sands, Hungary (Smith et al., 1991). These samples are directly comparable as the same apparatus and research methodology is used.

Linear dune sands from Bullard et al., (2004) produce overall higher concentrations of dust sized particles than the sediments from Markarfljotsandur but are an order of magnitude lower than concentrations recorded from the Markarfljot ephemeral channel system and Mýrdalssandur sediments. A probable reason for this is due to the differences in initial surface sedimentology. The samples from Bullard et al. (2004) have mean particle sizes of 249 μm (R7) and 160 μm (R66) and contain small fractions of silt and clay in the parent sample, whereas the Markarfljotsandur sediments mean particle size is 653 μm and have no particles in the parent sample $<100 \mu\text{m}$. As was discussed at length in section 5.2, sand particles are inherently difficult to abrade (Gill et al., 1999) and the potential for abrasion processes to produce fine particles decreases with increasing particle size (Mahaney et al., 2002). The initial release of parent silt and clay sized particles from the linear dune sands will also increase total dust concentrations.

The Markarfljot ephemeral channel system and Mýrdalssandur total dust concentrations match extremely well with the Pannonian sands (Smith et al., 1991) with the trend of the concentration curve being almost identical. This is a surprising result due to the vastly different sedimentological characteristics of surface samples between the Iceland sediments, which have a high proportion of silt and clays in the initial sample and the Pannonian sands, which are sieved to form a particle size distribution of 350 – 500 μm . It could be expected that the Pannonian sands would behave like the Australian linear dune sands from Bullard et al. (2004).

However, after the first 4 hours, where the initial high rates of dust concentration occur in two of the Icelandic sediments and the Pannonian sands, all rates of dust concentration between all samples are comparable. After 4 hours, it is likely that the resident fines from within the samples have been removed (e.g. Bullard et al., 2004). The Markarfljotsandur sediments are the only sample not to have this initial peak in

dust concentration with the relationship being consistent over the 8-hour experiment time. This indicates that resident fines are unlikely to be contributing to the total dust concentration and that the process which is responsible for producing dust sized sediments may not change through time within these sediments.

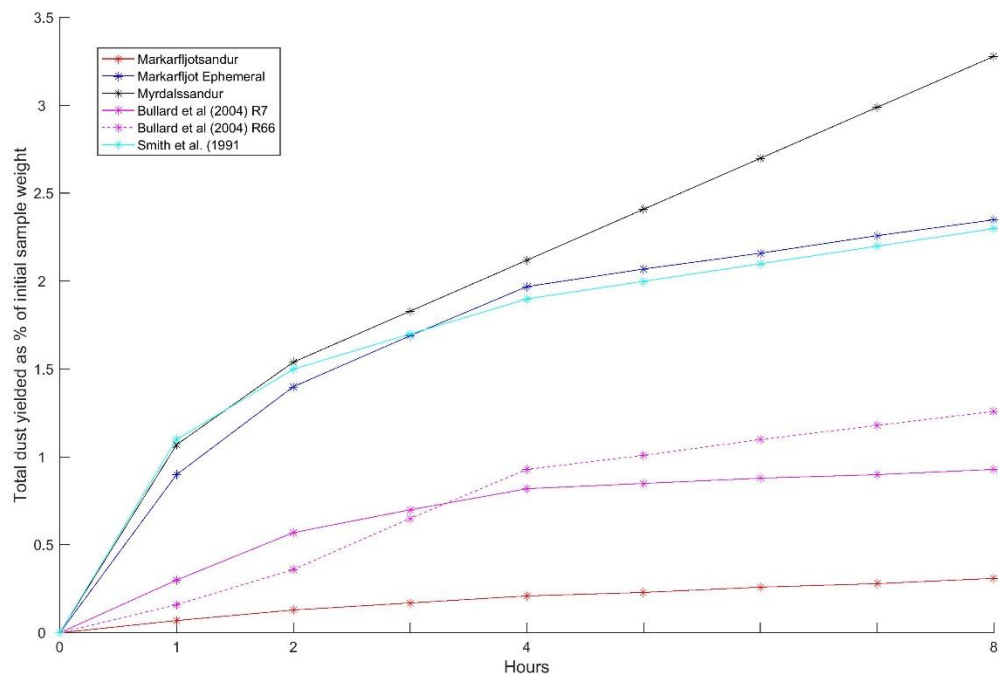


Figure 5.12: Total dust concentration from an aeolian abrasion chamber comparison between three Icelandic sediment types (this thesis) and other sediment types from the literature (Smith et al., 1991; Bullard et al., 2004)

5.8 Conclusion

The concept of aeolian abrasion as a dust particle generator has been shown to be an important concept in driving dust emissions at mid latitude dust sources. This is the first attempt to quantify this process for dust sources in the high latitudes. From the three main source sedimentologies associated with Icelandic dust emissions, rates of production and the generated size distribution of dust particles, varied as a function of soil texture, temperature and humidity.

For well-sorted sand sized sediments, the process of aeolian abrasion seems to be a key in the development of dust sized particles by the removal of surface adhesions and the chipping and spalling of sand particles. The rate of abrasion seems to increase with decreasing temperature as the magnitude of particle collisions is increased due a decrease in air density. This leads to an increased total dust production and an increase in the proportion of particles created below 10 μm . Relative humidity seems to be negligible, however further experimental work exploring a wide range of humidity is required.

For poorly-sorted sediments with varying soil texture contents (e.g. sand, silt and clays), the process of abrasion seems to be initially negligible as the release of resident fines within the parent soil are preferentially released. The impact of abrasion is likely to occur following the release of the resident fines, however discriminating between sediments which are created via aeolian abrasion and particles which are released from the parent sediments is challenging. Research focused on analysing the abrasion properties of only the sand sized component of these sediments is required to fully understand the impact abrasion may have on dust particle generation for these sediment groups. Decreasing temperatures decreased the total dust productions generated from these sediments. This was attributed to an increased relative humidity leading to an increased moisture retention rate within the parent material. The effect of an increased moisture retention rate seemed to diminish through time as air flow provided a mechanism for sediments to desiccate sufficiently during the experiments.

Results from this chapter may have implications for global dust models which are critical in providing information to global climate models to ensure an accurate representation of dust in the global climate system (e.g. Shao et al., 1993; Marticorena and Bergametti, 1995; Kok et al., 2015). Temperature and humidity has never been

exclusively considered in a global dust model to attempt to define vertical dust fluxes. This is because the major global dust sources are in the subtropics and dust events are not associated with low temperatures and high humidities. The results from this chapter indicate that the relationship between temperature, humidity and surface sedimentology may have a significant impact on total dust production and the associated particle size characteristics of dust particles sourced from the high latitudes.

6. Summary, future research and concluding remarks

This thesis has focused on quantifying the sources, drivers and processes which lead to high latitude dust events in south Iceland. The aim of this chapter is to highlight the major contributions and findings that this thesis has presented to further our understanding of Icelandic/high latitude dust events. As these are discussed, research questions and avenues will be proposed that would build upon the findings of this thesis.

6.1 Field measurements of dust events in the high latitudes

This research presented in this thesis is not the first attempt at quantifying dust concentrations from field measurements in the high latitudes (Nickling, 1978; Bullard and Austin, 2011; Arnalds et al., 2013; Dagsson-Waldhauserova et al., 2014; 2015). However, as stated in Chapter 4, the majority of field monitoring efforts to measure high latitude dust events have either focused on the calculation of horizontal mass flux rates within the saltation layer (e.g. Bullard et al., 2011; Gillies et al., 2013) or used data from single dust events (Arnalds et al., 2013; Dagsson-Waldhauserova et al., 2014b; 2015). Although both approaches provide valuable measurements in regions where field data is temporally and spatially sparse, it is difficult to understand the complexity of dust storm dynamics in the high latitudes from these limited data sets.

This thesis presents a record of 9 dust events from a source in south Iceland and provides the first active concentration measurements of multiple, successive dust events in the high latitudes. The only other study to provide multiple dust event measurements in the high latitudes is Nickling (1978) who measured 15 dust events at Slims Valley, Yukon, Canada. However, material in suspension (e.g. the dust component) were trapped in passive dust samplers over a 24 hour period meaning the evolution of the dust events through time could not be determined. The high temporal resolution of the data set presented in this thesis has shown the importance of the ability of different factors which promote/inhibit dust emissions at an event-scale in high latitude environments (section 6.4).

The results from the field monitoring show that dust events in southern Iceland are comparable in magnitude to those in sub-tropical regions. Although it was suggested by Arnalds et al., (2013, 2016) that dust events in Iceland can be some of the most

intense globally, these measurements did not directly measure dust concentration but rather horizontal mass flux of sediments travelling in saltation. These measurements cannot be explicitly linked to dust concentration measurements, and therefore the conclusion that these events are the most intense dust events in the world is problematic. The dust concentration measurements from this thesis are directly comparable to measurements taken during subtropical dust events and clearly show that dust events from Iceland are in the same order of magnitude.

Although the recording of 9 dust events from a single dust source has increased our understanding of the event-scale dynamics of dust emission in a high latitude environment, the data set is still temporally and spatially limited. As stated by Bullard et al., (2016), most field studies monitoring dust emissions from high latitude regions are restricted to spring and summer. Although the frequency of dust events may increase during this period, dust events have been shown to occur all year round in Iceland and several other high latitude dust source regions (Bullard et al., 2016; Bullard and Mockford, 2018). Gaps can be filled in by using secondary data sets, such as WMO weather codes, but this thesis has shown that these data sets are likely to miss a substantial proportion of dust events as weather stations are often not located at source. From the 9 high latitude dust sources, Iceland has the highest density of weather stations. It could therefore be argued that if dust events in Iceland are regularly missed by these weather stations, this issue is likely to be worsened in other high latitude dust source environments.

6.1.1 Further measurements

The spatial and temporal limitations of spring/summer measurement periods and the possibility that a considerable portion of dust events are missed by secondary data sources suggests the need for continuous field monitoring of source dust concentrations to fully verify the magnitude, frequency and relative intensity of dust events in high latitude environments.

Although there are very few continuous field measurements of dust emissions in subtropical environments (e.g. Webb et al., 2016), it could be argued that the difference between seasons is enhanced at the high latitudes because of the seasonal timings of frost, snow and a lack of vegetation in winter and high evapotranspiration and rapid seasonal vegetation growth in summer. These vast seasonal changes in

local meteorological factors will control seasonal variations in dust event frequency and magnitude. It could, therefore, be argued that continuous, or multi-season, monitoring of high latitude dust emissions is more important than the equivalent monitoring within the sub-tropics.

The measurements required can be seen in Figure 6.1. Measurements would also be required on a range of dust source geomorphologies with a variety of sedimentological profiles. This is supported by the results of chapter 3 and 5 which indicate the relative importance of surface sedimentology in driving differences in dust particle properties.

Source measurements provide critical values for modellers (e.g. Groot Zwaaftink et al., 2015; 2017; Wittman et al., 2017) who require information on vertical dust fluxes and the variability of meteorological variables to justify model parameters. Without continuous measurements at source (Figure 6.2), it will be impossible to refine regional dust model parameters. Regional models are often upscaled and nested into global dust models (Liu et al., 2011), where the relative contribution of high latitude dust emissions was not included until recently (Bullard et al., 2016). Regional models provide better spatial resolution than global dust models, which is especially important in the high latitudes, as dust sources are often spatially confined.

Remote sensing methods for enhancing dust retrievals have typically focused on using differences in temperature between the land surface (relatively warm) and atmospheric dust (relatively cool) (Baddock et al. 2009). This temperature-difference approach is less effective over cold land surfaces; however, continuing work on retrieval algorithms may lead to improvements in aerosol detection and enhancement at high latitudes. For example, it may be possible to develop radiative transfer look-up tables to overcome problems of low viewing and solar zenith angles (Lipponen, 2017). If new remote sensing techniques were developed which provided an uninterrupted dataset for monitoring high latitude dust events, continuous source measurements would provide a verification for these systems.

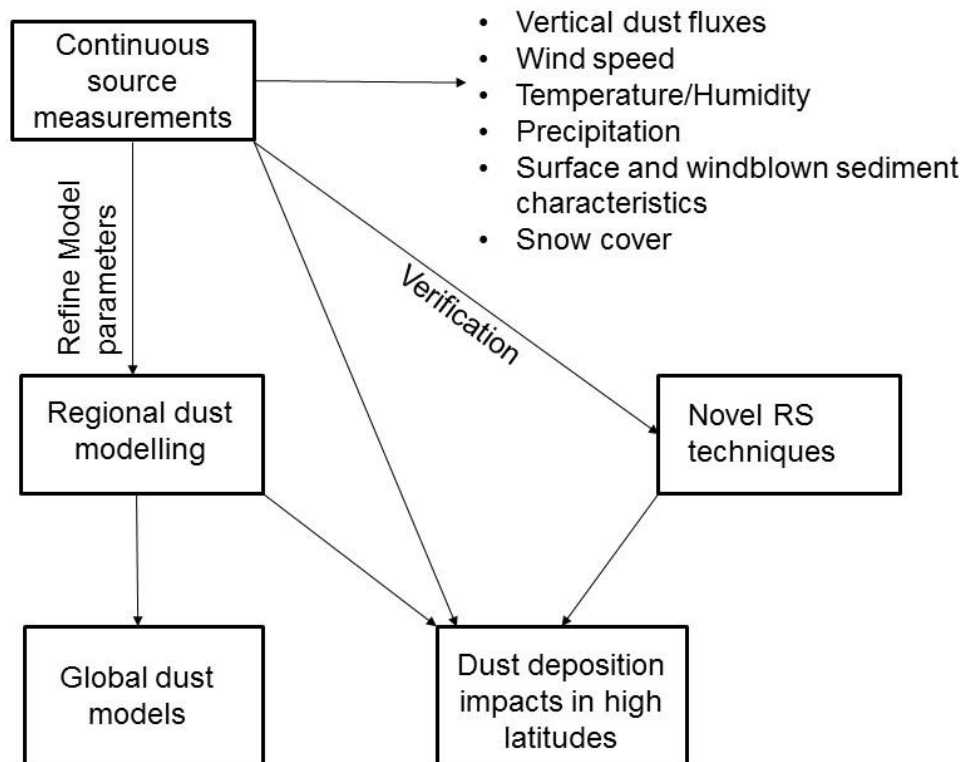


Figure 6.1: The underlying importance of continuous source measurements for high latitude dust research

6.2 The creation of ultra-fine sediments at source

If dust particles are caught using passive dust samplers at source during a dust event, it is likely that you will record the entire range of particle sizes in transport (Klose et al., 2017). As particles travel downwind away from source, it is assumed that larger particles are preferentially deposited leading to a downwind fining of the dust storm particle size distribution (Van der Does et al., 2016). This means that the finest particles in a dust storm are likely to have their greatest impact away from source.

In Chapter 3, it was shown that dust particle size varied considerably between dust sources at Markarfljot. Particles from the Markarfljot ephemeral channel system, which ranged between 0.5 – 40 μm , may have important implications for local soil erosion and deposition in oceanic environments but are unlikely to have regional implications for deposition. Whereas, the ultra-fine particles (<2 μm) recorded at source during dust

events from Markarfljotsandur may have significant implications on a variety of regional ecosystems due to their ability to be transported long distances.

Data from chapter 5 indicates that the process of aeolian abrasion drives the creation of dust particles from the Markarfljotsandur sediments. This is shown as well by the relationship between horizontal mass flux (e.g. saltation) and dust event concentration. As sand particles are transported in saltation, collisions between particles promote aeolian abrasion. Sand grains at Markarfljotsandur have developed micro-adhesions through time (Chapter 3), these adhesions are dislodged during collisions in saltation, and ultra-fine dust particles are then available for transport in suspension.

One major impact of this material, which was shown in Chapter 4, is the transport of these fine particles 150km causing significant rises in PM10 concentration in the city of Reykjavik. This result was clearly displayed by time series of dust source and city PM10 concentrations as well as plume dispersion modelling. This source may be of greatest importance in terms of a human health hazard in Iceland as it has been shown that the ingestion of particles $<10\ \mu\text{m}$ will have substantial impacts on human health (Griffin and Kellogg, 2004; Griffin, 2007). Particles can travel through the oesophagus into the lungs, stick onto the surface and cause fibrosis (Cooke, 1924). Particles are also unlikely to be exhaled. Ruckley et al. (1984) found that a constant exposure to high levels of PM10 would cause the lungs to retain large quantities of particles increasing the chances of severe emphysema and lung disease.

The deposition of ultra-fine particles in Iceland may also have an impact on a range of ecosystems. Results from HYSPLIT transport modelling in Chapter 4 indicate that most pathways would lead to deposition within the North Atlantic. SEM data from Chapter 3 also indicated that dust particles from both Markarfljotsandur and the Markarfljot ephemeral channel has substantial proportions of Fe within their geochemical compositions. These sediments therefore may provide a suitable source of bio-available iron for oceanic environments (Jickells et al., 2005; Schroth et al., 2009; 2017).

There has long been a debate about the relative importance of Fe sourced from aeolian and fluvial inputs for oceanic environments, but is likely to vary between environments (Bullard, 2017). However, as noted by Jickells et al. (2005), Fe supplied from glacial and fluvial inputs is likely to be restricted to coastal regions. These inputs

are also not at the surface of the ocean. The deposition of dust occurs at the surface, often 100s km's away from coastal regions.

For sediments at Markarfljotsandur, the potential impacts of these sediments may be greater due to the ultra-fine particle sizes as documented in Chapter 4. Fine sediments are unlikely to be immediately deposited, meaning their potential for providing nutrients in surface waters may be enhanced.

6.3 The relationship between soil texture, soil moisture and wind speed in driving dust emissions in Iceland

The results from this thesis indicate that the interlinking relationship between soil texture, soil moisture and wind speed drive dust concentrations in Iceland (Figure 6.2).

The relative importance of factors which provide moisture (e.g. precipitation, low evapotranspiration, relative humidity, groundwater etc.) are increased in the high latitudes (Einarsson, 1984) and therefore soil moisture often inhibits dust concentration by making sediments unavailable for transport (McKenna Neuman and Nickling, 1989; Ravi et al., 2006). Although soil moisture was not directly measured during the dust events presented in Chapter 4, it could be inferred that subtle increases in relative air humidity (%) and low intensity precipitation events can substantially reduce total concentrations of dust ($\mu\text{g m}^{-3}$) generated from Markarfljotsandur. Further work is required which measures PM10 concentrations and soil moisture content during dust events at source locations to fully understand this relationship (Mockford et al. 2018). In Chapter 5, an increase in relative humidity significantly decreased dust concentrations from two Icelandic dust sources, both of which have mixed sediment textures. These measurements agree with the findings of Belly (1964), Ravi et al., (2004, 2006) and McKenna Neuman (2008) who all found that an increased relative humidity increases the shear velocity required to entrain particles. This differs significantly from subtropical environments where, increases in soil moisture are removed quickly by high daytime temperatures and direct solar radiation (Ishizuka et al., 2008).

The retention rate of moisture is governed by soil texture. In Chapter 3, it was shown that the spatial variation in surface sediments varies considerably within a landscape unit. Observations also indicate that during field season two (May/June 2015), that the

sand-based dust source of Markarfljotsandur was considerably more active than the finer sediment-based source of the Markarfljot ephemeral channel system. This was related to inundation of glacio-fluvial meltwater. Surfaces where sand content dominates will retain considerably less soil water than surfaces dominated by silt/clay (McKenna Neuman and Nickling, 1989; Fécan et al., 1998). It will take the surfaces dominated by silt/clay significantly longer to remove soil water from surface sediments.

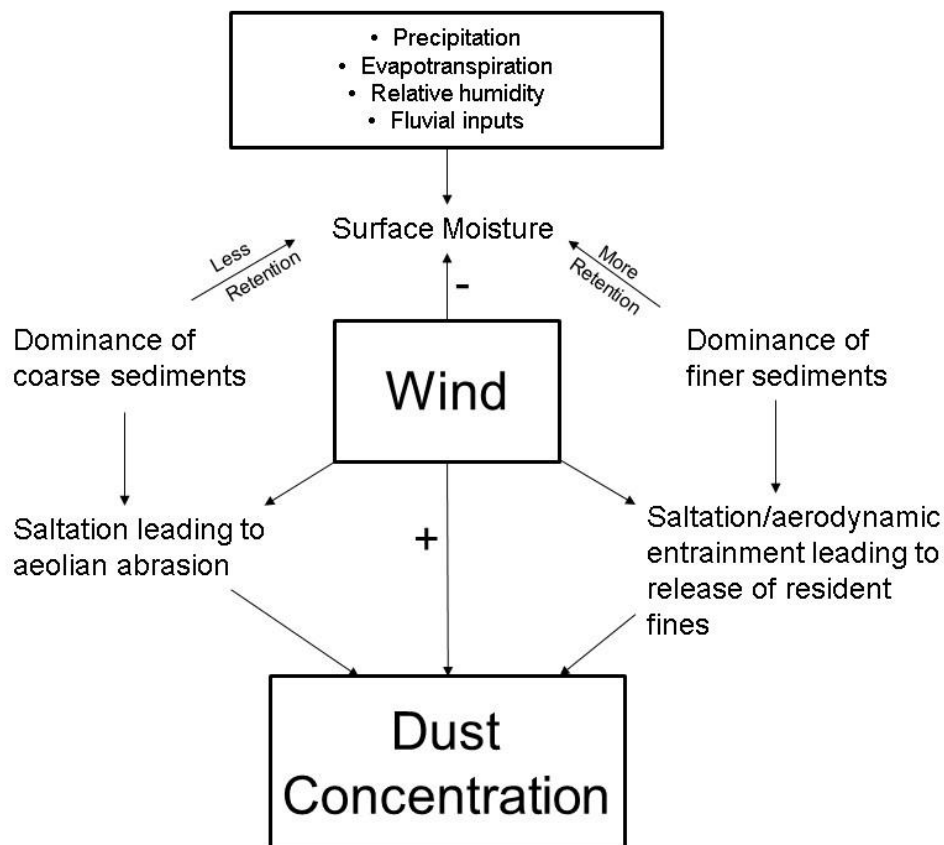


Figure 6.2: The interlinking relationship between wind speed, moisture and soil texture and how it impacts on dust emissions from the high latitudes

Soil texture controls dust particle properties. In Chapter 3, it was shown that the size of dust particles can be related to the size, shape and morphology of the surface sediments from where they are emitted. For surfaces where sand particles are dominant, saltation is likely to lead to the creation of dust sized particles via aeolian abrasion, with the size properties of the dust particles being related to the dominant abrasion process (Bullard et al., 2004). For surfaces where finer sediments dominate, saltation will lead to the release of resident fines which are already presented within the surface sediment matrix. Abrasion may occur in tandem and is likely to become

more prominent through time. These results are confirmed by experiments conducted in Chapter 5. As noted in Chapter 3, it could also be hypothesis that the dust emission process from surfaces where finer sediments dominate may not be driven by saltation, but particles are instead lifted by aerodynamic entrainment (Macpherson et al., 2008; Kloose et al., 2014). This requires further work on a variety of different surface types.

The primary control of dust concentration is wind speed. This is confirmed in Chapter 4 through the relationship between wind speed and dust concentration at source. As shown in Figure 6.2, dust concentration increases exponentially with shear velocity at the surface. However, as already noted, the shear velocity required for ejected particles will vary dependent on other factors. This was shown during dust events 1 and 5 in Chapter 4.

Events 1 and 5 also show the importance of surface wind in removing moisture from surface sediments. The time will be dependent on the percentage of surface sediment moisture and the relative sediment retention rate. In this thesis, dust concentration was shown to recover almost instantly following precipitation inputs during high wind speeds. However, entrainment did not occur at the Markarfljot ephemeral channel system during this time, indicating the complicated relationship between spatial differences in soil texture, soil moisture and wind speed in controlling dust concentrations.

The results from this study indicate that the role of these three factors are critical in understanding dust emissions in Iceland. Because Iceland is a good proxy for other high latitude dust systems, in terms of its sedimentology and meteorology, it could be suggested that this relationship will be important in all high latitude dust sources. However, current regional models estimating dust fluxes from the high latitudes have failed to recognise the importance of soil moisture in the high latitude aeolian system. Wittmann et al., (2017) and Groot Zwaaftink et al. (2017), both using the FLEXPART model (Stohl et al., 1995) to estimate vertical dust fluxes from Iceland, removed the soil moisture function within the model before running simulations. This will have likely caused the overestimation of dust event frequency and magnitudes in these analyses.

Further work in the form of field monitoring (as stated above) is required on a variety of surfaces to fully understand this interlinking relationship. Measurements taken could be refined and tuned in laboratory experiments (e.g. wind tunnels) to provide more

accurate mathematical expressions for these relationships which would significantly improve modelling attempts to calculate high latitude dust emissions.

6.4 The impact of temperature on dust production

Although changes in temperature are likely to be associated with changes in humidity, this thesis suggests that the role of temperature on total dust production may be of significance. Previous work by McKenna Neuman (1993; 2003; 2004) has shown decreases in temperature increase air density leading to a decrease in air viscosity and saturation evaporation pressure. This leads to alterations in the turbulent properties of air flow and causes increases in particle velocity during transport; increasing the magnitude of interparticle collisions (McKenna Neuman, 2003).

Much of the work associated with understanding the effect of temperature on aeolian transport rates has focussed solely on the transport of sand grains in saltation. However, this thesis has shown the importance of temperature in affecting the potential dust production of Icelandic sediments. Results from Chapter 5 indicate that for a decrease in temperature, potential dust production increases in the Markarfljotsandur sediments but decreases for both the Markarfljot ephemeral channel system and Mýrdalssandur sediments. The decreased rate of dust production for the Markarfljot ephemeral channel system and Mýrdalssandur sediments may be solely related to the impact relative humidity has on sediment matrices which have high proportions of silt and clay.

However, sediment matrices which are dominated by sand are likely to desiccate more efficiently following increases in surface soil moisture. In relation to chapter 5, an increase in humidity does not impact sediments and it could therefore be argued that temperature is the driving factor in increasing total dust production. Further work across a range of sedimentologies examining the relationship between dust concentration rates and temperature in an environment where humidity can be controlled.

6.5 High latitude dust in a warming earth?

The measurements from this thesis are valuable in understanding contemporary dust emissions from the high latitudes. However, they are also valuable in helping us understand the potential future impact of dust emissions from the high latitudes.

Landscapes in the high latitudes are rapidly changing (Stow et al., 2004; Hinzman et al., 2005; Anderson et al., 2017). These changes in the landscape are likely to have a significant impact on the frequency, magnitude and characteristics in the high latitudes. Anderson et al. (2017) suggested that by 2100, ice retreat will lead to the expansion of glacial outwash plains, which in turn, will lead to increased dune accretion and deflation of finer sediments as dust events. This will have a substantial effect on paraglacial ecosystems which are predominately nutrient limited (Mladenov et al., 2011; Anderson et al., 2017).

In Iceland, all glaciers have been retreating for over 25 years (Björnsson and Pálsson, 2008), and this is expected to continue as global temperatures continue to increase (Marcott et al., 2013). This trend is likely to expose new areas of sediment which might be available for the aeolian transport (Bullard et al., 2016).

However, this thesis has shown the importance of factors affecting sediment availability in suppressing dust emissions in high latitude environments. It could on one hand be suggested that because sediment volumes will likely increase with retreating glacier systems that dust emissions will increase in tandem. However, sediment supply is related to the glacio-fluvial system. If glacier retreat continues, landscape changes in the outwash channel networks may lead to the re-working of larger sediments to the surface therefore protecting finer surface sediments from entrainment (e.g. Nickling and McKenna Neuman, 1995) or elevated levels of moisture could persist within the landscape as increasing glacio-fluvial discharge levels persist for longer periods of the year.

It is expected that a short-term increase in dust emissions will increase due to increased sediment supply, however the long-term future of dust emissions from the high latitudes is unclear. It will likely be environment dependent and will depend on the colonisation of vegetation (Sturm et al., 2001) or the development of proglacial lakes. Both of which will severely affect sediment availability and sediment supply to the high latitude dust system.

6.6 Concluding remarks

The main aim of this thesis was to assess the sources, drivers and sedimentology of Icelandic dust events. Icelandic dust sources have been shown to vary

sedimentologically within a relative small unit of area. There is a strong relationship between parent soil sedimentology and the associated dust particle properties that a dust source unit emits. The relationship between parent soil texture, factors which dictate the spatial and temporal variations in sediment availability and variations in wind speed, control the relevant timings, intensities and magnitudes of dust storms at the event-scale in Iceland. Temperature is likely to play a key role in dust event magnitudes; however, the relative importance of temperature is likely related to how changes in temperature affect relative humidity, which in turn will depend on the surface parent sedimentology.

The results from this thesis are not just relevant to the Icelandic dust cycle but can be related to other high latitude dust systems. This is because the dominant geomorphological and sedimentological characteristics of source areas and the meteorological conditions which are associated with driving dust events are similar in most high latitude dust environments (with Patagonia being the exception). Iceland has received much greater attention as a dust source area because of the accessibility of source areas. It is therefore critical that active dust measurements in other high latitude dust sources are taken to improve our understanding of the contribution high latitude dust to the global atmospheric dust budget.

This thesis has provided the first active source measurements for multiple dust events at the high latitudes. However, continuous, all year-round measurements are required to capture the full seasonal variation in dust event magnitude, frequency and intensity. These measurements will help verify the seasonal patterns of dust emission. Long term continuous measurements at source, monitoring vertical dust fluxes and the associated meteorological and sedimentological variables on different surfaces are required to fully verify regional modelling outputs. The verification of regional modelling would allow for more realistic estimates of the total contribution of high latitude dust in the Earth's system.

References

- Ackerman, S.A., 1997. Remote sensing aerosols using satellite infrared observations. *Journal of Geophysical Research: Atmospheres*, 102(D14), pp.17069-17079.
- Achterberg, E.P., Moore, C.M., Henson, S.A., Steigenberger, S., Stohl, A., Eckhardt, S., Avendano, L.C., Cassidy, M., Hembury, D., Klar, J.K. and Lucas, M.I., 2013. Natural iron fertilization by the Eyjafjallajökull volcanic eruption. *Geophysical Research Letters*, 40(5), pp.921-926.
- Akhlaq, M., Sheltami, T.R. and Mouftah, H.T., 2012. A review of techniques and technologies for sand and dust storm detection. *Reviews in Environmental Science and Bio/Technology*, 11(3), pp.305-322.
- Albani, S., Mahowald, N.M., Delmonte, B., Maggi, V. and Winckler, G., 2012. Comparing modeled and observed changes in mineral dust transport and deposition to Antarctica between the Last Glacial Maximum and current climates. *Climate dynamics*, 38(9-10), pp.1731-1755.
- Alfaro, S.C., Gaudichet, A., Gomes, L. and Maillé, M., 1997. Modeling the size distribution of a soil aerosol produced by sandblasting. *Journal of Geophysical Research: Atmospheres*, 102(D10), pp.11239-11249.
- Alghamdi, M.A., Almazroui, M., Shamy, M., Redal, M.A., Alkhalaf, A.K., Hussein, M.A. and Khoder, M.I., 2015. Characterization and elemental composition of atmospheric aerosol loads during springtime dust storm in western Saudi Arabia. *Aerosol Air Quality Research*, 15(2), pp.440-453.
- Anderson, K. and Gaston, K.J., 2013. Lightweight unmanned aerial vehicles will revolutionize spatial ecology. *Frontiers in Ecology and the Environment*, 11(3), pp.138-146.

Anderson, R.S. and Haff, P.K., 1988. Simulation of eolian saltation. *Science*, 241(4867), pp.820-824.

Anderson, N.J., et al. 2017. The Arctic in the 21st century: Changing biogeochemical linkages across a paraglacial landscape of Greenland. *BioScience*, 67, pp.18–133

Anderson, G.E., 1926. Experiments on the rate of wear of sand grains. *The Journal of Geology*, 34(2), pp.144-158.

Arnalds, O., Gísladóttir, F.O. and Orradóttir, B., 2012. Determination of aeolian transport rates of volcanic soils in Iceland. *Geomorphology*, 167, pp.4-12.

Arnalds O. 2010. Dust sources and deposition of aeolian materials in Iceland. *Icelandic Agricultural Sciences*, 23, pp. 3–21.

Arnalds, O., Aradóttir, A.L. and Thorsteinsson, I., 1987. The nature and restoration of denuded areas in Iceland. *Arctic and Alpine Research*, pp.518-525.

Arnalds, O., Gísladóttir, F.O. and Sigurjonsson, H., 2001. Sandy deserts of Iceland: an overview. *Journal of Arid Environments*, 47(3), pp.359-371.

Arnalds, O., Thorarinsdóttir, E.F., Thorsson, J., Waldhauserova, P.D. and Agustsdóttir, A.M., 2013. An extreme wind erosion event of the fresh Eyjafjallajökull 2010 volcanic ash. *Scientific reports*, 3.

Arnalds, O., Olafsson, H. and Dagsson-Waldhauserova, P.D., 2014. Quantification of iron-rich volcanogenic dust emissions and deposition over the ocean from Icelandic dust sources. *Biogeosciences*, 11, pp. 6623-6632

Arnalds, O., Dagsson-Waldhauserova, P. and Olafsson, H., 2016. The Icelandic volcanic aeolian environment: Processes and impacts—A review. *Aeolian Research*, 20, pp.176-195.

Ashwell, I.Y., and F. G. Hannell., 1960. Wind and temperature variations at the edge of an ice cap. *Meteorological Magazine*, 89, pp. 17-24.

Ashwell, I.Y., 1966. Glacial control of wind and of soil erosion in Iceland. *Annals of the Association of American Geographers*, 56(3), pp.529-540.

Ashworth, P.J. and Ferguson, R.I., 1986. Interrelationships of channel processes, changes and sediments in a proglacial braided river. *Geografiska Annaler. Series A. Physical Geography*, pp.361-371.

Assallay, A.M., Rogers, C.D.F., Smalley, I.J. and Jefferson, I.F., 1998. Silt: 2–62 μm , 9–4 ϕ . *Earth-Science Reviews*, 45(1), pp.61-88.

Atkins, C.B., Barrett, P.J. and Hicock, S.R., 2002. Cold glaciers erode and deposit: Evidence from Allan Hills, Antarctica. *Geology*, 30(7), pp.659-662

Atkins, C.B. and Dunbar, G.B., 2009. Aeolian sediment flux from sea ice into Southern McMurdo Sound, Antarctica. *Global and Planetary Change*, 69(3), pp.133-141.

Ayling, B.F. and McGowan, H.A., 2006. Niveo-eolian sediment deposits in coastal South Victoria Land, Antarctica: indicators of regional variability in weather and climate. *Arctic, Antarctic, and Alpine Research*, 38(3), pp.313-324.

Baas, A.C. and Sherman, D.J., 2006. Spatiotemporal variability of aeolian sand transport in a coastal dune environment. *Journal of Coastal Research*, pp.1198-1205.

Bazhenova, O. and Tyumentseva, E., 2015. Contemporary aeolian morphogenesis in semiarid landscapes of the intermountain depressions of Southern Siberia. *Catena*, 134, pp.50-58.

Baddock, M.C., Bullard, J.E. and Bryant, R.G., 2009. Dust source identification using MODIS: a comparison of techniques applied to the Lake Eyre Basin, Australia. *Remote Sensing of Environment*, 113(7), pp.1511-1528.

Baddock, M., Boskovic, L., Strong, C., McTainsh, G., Bullard, J., Agranovski, I. and Cropp, R., 2013. Iron-rich nanoparticles formed by aeolian abrasion of desert dune sand. *Geochemistry, Geophysics, Geosystems*, 14(9), pp.3720-3729.

Baddock, M.C., Strong, C.L., Leys, J.F., Heidenreich, S.K., Tews, E.K. and McTainsh, G.H., 2014. A visibility and total suspended dust relationship. *Atmospheric Environment*, 89, pp.329-336.

Baddock, M.C., Ginoux, P., Bullard, J.E. and Gill, T.E., 2016. Do MODIS-defined dust sources have a geomorphological signature? *Geophysical Research Letters*, 43(6), pp.2606-2613.

Baddock, M.C., Mockford, T., Bullard, J.E. and Thorsteinsson, T., 2017. Pathways of high-latitude dust in the North Atlantic. *Earth and Planetary Science Letters*, 459, pp.170-182.

Bagnold, R.A., 1942. *Physics of Blown Sands and Desert Dunes*.

Baratoux, D., Mangold, N., Arnalds, O., Bardintzeff, J.M., Platevoet, B., Grégoire, M. and Pinet, P., 2011. Volcanic sands of Iceland-Diverse origins of aeolian sand deposits revealed at Dyngjusandur and Lambahraun. *Earth Surface Processes and Landforms*, 36(13), pp.1789-1808.

Barchyn, T.E. and Hugenholz, C.H., 2012. Winter variability of aeolian sediment transport threshold on a cold-climate dune. *Geomorphology*, 177, pp.38-50.

Barkan, J. and Alpert, P., 2010. Synoptic analysis of a rare event of Saharan dust reaching the Arctic region. *Weather*, 65(8), pp.208-211.

Basile, I., Grousset, F.E., Revel, M., Petit, J.R., Biscaye, P.E. and Barkov, N.I., 1997. Patagonian origin of glacial dust deposited in East Antarctica (Vostok and Dome C) during glacial stages 2, 4 and 6. *Earth and Planetary Science Letters*, 146(3-4), pp.573-589.

Bateman, M.D. and Murton, J.B., 2006. The chronostratigraphy of Late Pleistocene glacial and periglacial aeolian activity in the Tuktoyaktuk Coastlands, NWT, Canada. *Quaternary Science Reviews*, 25(19), pp.2552-2568.

Belly, P.Y., 1964. Sand movement by wind. TM No. 1. US Army Coastal Engineering Research Center.

Belnap, J. and Gardner, J.S., 1993. Soil microstructure in soils of the Colorado Plateau: the role of the cyanobacterium *Microcoleus vaginatus*. *The Great Basin Naturalist*, pp.40-47.

Belnap, J. and Gillette, D.A., 1997. Disturbance of biological soil crusts: impacts on potential wind erodibility of sandy desert soils in southeastern Utah. *Land Degradation & Development*, 8(4), pp.355-362.

Belnap, J. and Gillette, D.A., 1998. Vulnerability of desert biological soil crusts to wind erosion: the influences of crust development, soil texture, and disturbance. *Journal of arid environments*, 39(2), pp.133-142.

Bennett, M.R. and Bullard, J.E., 1991. Iceberg tool marks: an example from Heinabergsjökull, southeast Iceland. *Journal of Glaciology*, 37(125), pp.181-183.

Bergametti, G., Rajot, J.L., Pierre, C., Bouet, C. and Marticorena, B., 2016. How long does precipitation inhibit wind erosion in the Sahel? *Geophysical Research Letters*, 43(12), pp.6643-6649.

Bhattachan, A., D'Odorico, P., Baddock, M.C., Zobeck, T.M., Okin, G.S. and Cassar, N., 2012. The Southern Kalahari: a potential new dust source in the Southern Hemisphere? *Environmental Research Letters*, 7(2), p.024001.

Bhattachan, A., D'Odorico, P., Okin, G.S. and Dintwe, K., 2013. Potential dust emissions from the southern Kalahari's dunelands. *Journal of Geophysical Research: Earth Surface*, 118(1), pp.307-314.

Bhattachan, A., Wang, L., Miller, M.F., Licht, K.J. and D'Odorico, P., 2015. Antarctica's Dry Valleys: A potential source of soluble iron to the Southern Ocean? *Geophysical Research Letters*, 42(6), pp.1912-1918.

Björnsson, H. and Pálsson, F., 2008. Icelandic glaciers. *Jökull*, 58, pp.365-386.

Bluck, B.J., 1974. Structure and directional properties of some valley sandur deposits in southern Iceland. *Sedimentology*, 21(4), pp.533-554.

Bogen, J. 1980. 'The hysteresis effect of sediment transport systems', *Norsk Geogr. Tidsskr.*, 34, 45–54.

Boulton, G.S., 1979. Glacial history of the Spitsbergen archipelago and the problem of a Barents Shelf ice sheet. *Boreas*, 8(1), pp.31-57.

Boulton, G.S., 1996. The origin of till sequences by subglacial sediment deformation beneath mid-latitude ice sheets. *Annals of Glaciology*, 22(1), pp.75-84.

Breed, C.S., Grolier, M.J. and McCauley, J.F., 1979. Morphology and distribution of common 'sand'dunes on Mars: comparison with the Earth. *Journal of Geophysical Research: Solid Earth*, 84(B14), pp.8183-8204.

Bristow, C.S., Hudson-Edwards, K.A. and Chappell, A., 2010. Fertilizing the Amazon and equatorial Atlantic with West African dust. *Geophysical Research Letters*, 37(14).

Bristow, C.S. and Moller, T.H., 2017. Testing the auto-abrasion hypothesis for dust production using diatomite dune sediments from the Bodélé Depression in Chad. *Sedimentology*.

Brooks, N. and Legrand, M., 2000. Dust variability over northern Africa and rainfall in the Sahel. In *Linking climate change to land surface change* (pp. 1-25). Springer Netherlands.

Bryant, R.G., 2013. Recent advances in our understanding of dust source emission processes. *Progress in Physical Geography*, 37(3), pp.397-421.

Bullard, J.E., 2013. Contemporary glacial inputs to the dust cycle. *Earth Surface Processes and Landforms*, 38(1), pp.71-89.

Bullard, J.E., 2017. The distribution and biogeochemical importance of high-latitude dust in the Arctic and Southern Ocean-Antarctic regions. *Journal of Geophysical Research: Atmospheres*, 122(5), pp.3098-3103.

Bullard, J.E. and White, K., 2002. Quantifying iron oxide coatings on dune sands using spectrometric measurements: an example from the Simpson-Strzelecki Desert, Australia. *Journal of Geophysical Research: Solid Earth*, 107(B6).

Bullard, J.E. and McTainsh, G.H., 2003. Aeolian-fluvial interactions in dryland environments: examples, concepts and Australia case study. *Progress in Physical Geography*, 27(4), pp.471-501.

Bullard, J.E., McTainsh, G.H. and Pudmenzky, C., 2004. Aeolian abrasion and modes of fine particle production from natural red dune sands: an experimental study. *Sedimentology*, 51(5), pp.1103-1125.

Bullard, J.E. and White, K., 2005. Dust production and the release of iron oxides resulting from the aeolian abrasion of natural dune sands. *Earth Surface Processes and Landforms*, 30(1), pp.95-106.

Bullard, J.E., McTainsh, G.H. and Pudmenzky, C., 2007. Factors affecting the nature and rate of dust production from natural dune sands. *Sedimentology*, 54(1), pp.169-182.

Bullard, J., Baddock, M., McTainsh, G. and Leys, J., 2008. Sub-basin scale dust source geomorphology detected using MODIS. *Geophysical Research Letters*, 35(15).

Bullard, J.E., Harrison, S.P., Baddock, M.C., Drake, N., Gill, T.E., McTainsh, G. and Sun, Y., 2011. Preferential dust sources: A geomorphological classification designed for use in global dust-cycle models. *Journal of Geophysical Research: Earth Surface*, 116(F4).

Bullard, J.E. and Austin, M.J., 2011. Dust generation on a proglacial floodplain, West Greenland. *Aeolian Research*, 3(1), pp.43-54.

Bullard, J.E., Baddock, M., Bradwell, T., Crusius, J., Darlington, E., Gaiero, D., Gassó, S., Gisladóttir, G., Hodgkins, R., McCulloch, R., McKenna-Newman, C., Mockford, T., Stewart, H & Thorsteinsson, T. High-latitude dust in the Earth system. *Reviews of Geophysics*, 54(2), pp.447-485.

Bullard, J.E. and Mockford, T., 2018. Seasonal and decadal variability of dust observations in the Kangerlussuaq area, west Greenland. *Arctic, Antarctic, and Alpine Research*, 50(1).

Cahill, T.A., Gill, T.E., Reid, J.S., Gearhart, E.A. and Gillette, D.A., 1996. Saltating particles, playa crusts and dust aerosols at Owens (dry) Lake, California. *Earth Surface Processes and Landforms*, 21(7), pp.621-639.

Calderon-Garciduenas, L., Reed, W., Maronpot, R.R., Henriquez-Roldán, C., Delgado-Chavez, R., Calderon-Garciduenas, A.N.A., Dragustinovis, I., Franco-Lira, M., Aragón-Flores, M., Solt, A.C. and Altenburg, M., 2004. Brain inflammation and Alzheimer's-like pathology in individuals exposed to severe air pollution. *Toxicologic pathology*, 32(6), pp.650-658.

Cannone, N., Diolaiuti, G., Guglielmin, M. and Smiraglia, C., 2008. Accelerating climate change impacts on alpine glacier forefield ecosystems in the European Alps. *Ecological Applications*, 18(3), pp.637-648.

Carbonneau, P.E., Lane, S.N. and Bergeron, N.E., 2004. Catchment-scale mapping of surface grain size in gravel bed rivers using airborne digital imagery. *Water resources research*, 40(7).

Carbonneau, P.E. and Dietrich, J.T., 2017. Cost-effective non-metric photogrammetry from consumer-grade sUAS: implications for direct georeferencing of structure from motion photogrammetry. *Earth Surface Processes and Landforms*, 42(3), pp.473-486.

Carlson, T.N. and Prospero, J.M., 1972. The large-scale movement of Saharan air outbreaks over the northern equatorial Atlantic. *Journal of applied meteorology*, 11(2), pp.283-297.

Carlson, T.N., 1979. Atmospheric turbidity in Saharan dust outbreaks as determined by analyses of satellite brightness data. *Monthly Weather Review*, 107(3), pp.322-335.

Carlsen, H.K., Gislason, T., Forsberg, B., Meister, K., Thorsteinsson, T., Jóhannsson, T., Finnbjörnsdóttir, R. and Oudin, A., 2015. Emergency hospital visits in association with volcanic ash, dust storms and other sources of ambient particles: A time-series study in Reykjavík, Iceland. *International journal of environmental research and public health*, 12(4), pp.4047-4059.

Cassano, J.J., Uotila, P. and Lynch, A., 2006. Changes in synoptic weather patterns in the polar regions in the twentieth and twenty-first centuries, part 1: Arctic. *International Journal of Climatology*, 26(8), pp.1027-1049.

Chandler, D.G., Saxton, K.E., Kjelgaard, J. and Busacca, A.J., 2002. A technique to measure fine-dust emission potentials during wind erosion. *Soil Science Society of America Journal*, 66(4), pp.1127-1133.

Cheng, H., Zou, X.Y. and Zhang, C.L., 2006. Probability distribution functions for the initial liftoff velocities of saltating sand grains in air. *Journal of Geophysical Research: Atmospheres*, 111(D22).

Chepil, W.S., 1956. Influence of moisture on erodibility of soil by wind. *Soil Science Society of America Journal*, 20(2), pp.288-292.

Chewings, J.M., Atkins, C.B., Dunbar, G.B. and Golledge, N.R., 2014. Aeolian sediment transport and deposition in a modern high-latitude glacial marine environment. *Sedimentology*, 61(6), pp.1535-1557.

Chiang, K.W., Tsai, M.L. and Chu, C.H., 2012. The development of an UAV borne direct georeferenced photogrammetric platform for ground control point free applications. *Sensors*, 12(7), pp.9161-9180.

Church, M., 1972. Baffin Island sandurs: a study of Arctic fluvial processes. Ottawa Department of Energy Mines and Resources

Cooke, W.E., 1924. Fibrosis of the lungs due to the inhalation of asbestos dust. *British Medical Journal*, 2(3317), p.147.

Cornelis, W.M. and Gabriels, D., 2003. The effect of surface moisture on the entrainment of dune sand by wind: an evaluation of selected models. *Sedimentology*, 50(4), pp.771-790.

Costa, P.J.M., Andrade, C., Mahaney, W.C., Da Silva, F.M., Freire, P., Freitas, M.C., Janardo, C., Oliveira, M.A., Silva, T. and Lopes, V., 2013. Aeolian microtextures in silica spheres induced in a wind tunnel experiment: Comparison with aeolian quartz. *Geomorphology*, 180, pp.120-129.

Cowie, S.M., Knippertz, P. and Marsham, J.H., 2013. Are vegetation-related roughness changes the cause of the recent decrease in dust emission from the Sahel?. *Geophysical Research Letters*, 40(9), pp.1868-1872.

Crouvi, O., Amit, R., Enzel, Y., Porat, N. and Sandler, A., 2008. Sand dunes as a major proximal dust source for late Pleistocene loess in the Negev Desert, Israel. *Quaternary Research*, 70(2), pp.275-282.

Crouvi, O., Amit, R., Enzel, Y. and Gillespie, A.R., 2010. Active sand seas and the formation of desert loess. *Quaternary Science Reviews*, 29(17), pp.2087-2098.

Crouvi, O., Schepanski, K., Amit, R., Gillespie, A.R. and Enzel, Y., 2012. Multiple dust sources in the Sahara Desert: The importance of sand dunes. *Geophysical Research Letters*, 39(13).

Crusius, J., Schroth, A.W., Gasso, S., Moy, C.M., Levy, R.C. and Gatica, M., 2011. Glacial flour dust storms in the Gulf of Alaska: Hydrologic and meteorological controls and their importance as a source of bioavailable iron. *Geophysical Research Letters*, 38(6).

Cuffey, K.M., Conway, H., Gades, A.M., Hallet, B., Lorrain, R., Severinghaus, J.P., Steig, E.J., Vaughn, B. and White, J.W.C., 2000. Entrainment at cold glacier beds. *Geology*, 28(4), pp.351-354.

Dagsson-Waldhauserova, P., Arnalds, O. and Olafsson, H., 2013. Long-term frequency and characteristics of dust storm events in Northeast Iceland (1949–2011). *Atmospheric environment*, 77, pp.117-127.

Dagsson-Waldhauserova, P., Arnalds, O. and Ólafsson, H., 2014a. Long-term variability of dust events in Iceland (1949–2011). *Atmospheric Chemistry and Physics*, 14(24), pp.13411-13422.

Dagsson-Waldhauserova, P., Arnalds, O., Olafsson, H., Skrabalova, L., Sigurdardottir, G.M., Branis, M., Hladil, J., Skala, R., Navratil, T., Chadimova, L. and Jonsdottir, I., 2014b. Physical properties of suspended dust during moist and low-wind conditions in Iceland. *Icelandic Agricultural Science*, 27, pp.25-39.

Dagsson-Waldhauserova, P., Arnalds, O., Olafsson, H., Hladil, J., Skala, R., Navratil, T., Chadimova, L. and Meinander, O., 2015. Snow–dust storm: unique case study from Iceland, March 6–7, 2013. *Aeolian Research*, 16, pp.69-74.

Dall'Osto, M., Harrison, R.M., Highwood, E.J., O'Dowd, C., Ceburnis, D., Querol, X. and Achterberg, E.P., 2010. Variation of the mixing state of Saharan dust particles with atmospheric transport. *Atmospheric Environment*, 44(26), pp.3135-3146.

Davis, R.S., 1992. Equation for the determination of the density of moist air (1981/91). *Metrologia*, 29(1), p.67.

De Rose, R.C. and Basher, L.R., 2011. Measurement of river bank and cliff erosion from sequential LIDAR and historical aerial photography. *Geomorphology*, 126(1), pp.132-147.

Dellino, P., Gudmundsson, M.T., Larsen, G., Mele, D., Stevenson, J.A., Thordarson, T. and Zimanowski, B., 2012. Ash from the Eyjafjallajökull eruption (Iceland): Fragmentation processes and aerodynamic behavior. *Journal of Geophysical Research: Solid Earth*, 117(B9).

Delmonte, B., Andersson, P.S., Schöberg, H., Hansson, M., Petit, J.R., Delmas, R., Gaiero, D.M., Maggi, V. and Frezzotti, M., 2010. Geographic provenance of aeolian dust in East Antarctica during Pleistocene glaciations: preliminary results from Talos Dome and comparison with East Antarctic and new Andean ice core data. *Quaternary Science Reviews*, 29(1), pp.256-264.

DeMott, P.J., Sassen, K., Poellot, M.R., Baumgardner, D., Rogers, D.C., Brooks, S.D., Prenni, A.J. and Kreidenweis, S.M., 2003. African dust aerosols as atmospheric ice nuclei. *Geophysical Research Letters*, 30(14).

Desboeufs, K.V., Sofikitis, A., Losno, R., Colin, J.L. and Ausset, P., 2005. Dissolution and solubility of trace metals from natural and anthropogenic aerosol particulate matter. *Chemosphere*, 58(2), pp.195-203.

Dijkmans, J.W. and Törnqvist, T.E., 1991. Modern periglacial eolian deposits and landforms in the Søndre Strømfjord area, West Greenland and their palaeoenvironmental implications. *Meddelelser om Grønland. Geoscience*, 25, pp.3-39.

Di Mauro, B., Fava, F., Ferrero, L., Garzonio, R., Baccolo, G., Delmonte, B. and Colombo, R., 2015. Mineral dust impact on snow radiative properties in the European Alps combining ground, UAV, and satellite observations. *Journal of Geophysical Research: Atmospheres*, 120(12), pp.6080-6097.

Doran, P.T., Priscu, J.C., Lyons, W.B., Walsh, J.E., Fountain, A.G., McKnight, D.M., Moorhead, D.L., Virginia, R.A., Wall, D.H., Clow, G.D. and Fritsen, C.H., 2002. Antarctic climate cooling and terrestrial ecosystem response. *Nature*, 415(6871), pp.517-520.

Dowdeswell, J.A., 1982. Relative dating of late Quaternary deposits using cluster and discriminant analysis, Audubon Cirque, Mt. Audubon, Colorado Front Range. *Boreas*, 11(2), pp.151-161.

Drab, E., Gaudichet, A., Jaffrezo, J.L. and Colin, J.L., 2002. Mineral particles content in recent snow at Summit (Greenland). *Atmospheric Environment*, 36(34), pp.5365-5376.

Dragosics, M., Meinander, O., Jónsdóttir, T., Dürig, T., De Leeuw, G., Pálsson, F., Dagsson-Waldhauserová, P. and Thorsteinsson, T., 2016. Insulation effects of Icelandic dust and volcanic ash on snow and ice. *Arabian Journal of Geosciences*, 9(2), p.126.

Draxler, R.R. and Hess, G.D., 1997. Description of the HYSPLIT4 modeling system

Draxler, R.R. and Hess, G.D., 1998. An overview of the HYSPLIT_4 modelling system for trajectories. *Australian meteorological magazine*, 47(4), pp.295-308.

Draxler, R.R., Gillette, D.A., Kirkpatrick, J.S. and Heller, J., 2001. Estimating PM 10 air concentrations from dust storms in Iraq, Kuwait and Saudi Arabia. *Atmospheric Environment*, 35(25), pp.4315-4330.

Draxler, R.R. and Rolph, G.D., 2003. HYSPLIT (HYbrid Single-Particle Lagrangian Integrated Trajectory). NOAA Air Resources Laboratory, Silver Spring, MD. Model access via NOAA ARL READY Website.

Draxler, R.R., 1999. HYSPLIT. US Department of Commerce, National Oceanic and Atmospheric Administration, Environmental Research Laboratories, Air Resources Laboratory.

Dubovik, O., Holben, B., Eck, T.F., Smirnov, A., Kaufman, Y.J., King, M.D., Tanré, D. and Slutsker, I., 2002. Variability of absorption and optical properties of key aerosol types observed in worldwide locations. *Journal of the Atmospheric Sciences*, 59(3), pp.590-608.

Dugmore, A.J., Gísladóttir, G., Simpson, I.A. and Newton, A., 2009. Conceptual model's of 1200 years of Icelandic soil erosion reconstructed using tephrochronology. *Journal of the North Atlantic*, 2(1), pp.1-18.

Dunion, J.P. and Velden, C.S., 2004. The impact of the Saharan air layer on Atlantic tropical cyclone activity. *Bulletin of the American Meteorological Society*, 85(3), pp.353-365.

Dunning, S.A., Large, A.R., Russell, A.J., Roberts, M.J., Duller, R., Woodward, J., Mériaux, A.S., Tweed, F.S. and Lim, M., 2013. The role of multiple glacier outburst floods in proglacial landscape evolution: The 2010 Eyjafjallajökull eruption, Iceland. *Geology*, 41(10), pp.1123-1126.

Dvorkin, J. and Nur, A., 1996. Elasticity of high-porosity sandstones: Theory for two North Sea data sets. *Geophysics*, 61(5), pp.1363-1370.

Edlund, S.A. and Woo, M.K., 1992. Eolian deposition on western Fosheim Peninsula, Ellesmere Island, Northwest Territories during the winter of 1990-91. *Current Research, Part B, Geological Survey of Canada, Paper*, pp.91-96.

Einarsson, M.A., 1984. Climate of Iceland. H. van Loon (Ed.), *World Survey of Climatology: 15: Climates of the Oceans*, Elsevier, Amsterdam (1984), pp. 673-697

Ely, J.C., Graham, C., Barr, I.D., Rea, B.R., Spagnolo, M. and Evans, J., 2017. Using UAV acquired photography and structure from motion techniques for studying glacier landforms: application to the glacial flutes at Isfallsglaciären. *Earth Surface Processes and Landforms*, 42(6), pp.877-888.

Engelstaedter, S., Kohfeld, K.E., Tegen, I. and Harrison, S.P., 2003. Controls of dust emissions by vegetation and topographic depressions: An evaluation using dust storm frequency data. *Geophysical Research Letters*, 30(6).

Evan, A.T., Dunion, J., Foley, J.A., Heidinger, A.K. and Velden, C.S., 2006. New evidence for a relationship between Atlantic tropical cyclone activity and African dust outbreaks. *Geophysical Research Letters*, 33(19).

Evans, J.E. and Tokar Jr, F.J., 2000. Use of SEM/EDS and X-ray diffraction analyses for sand transport studies, Lake Erie, Ohio. *Journal of Coastal Research*, pp.926-933.

Fécan, F., Marticorena, B. and Bergametti, G., 1998, December. Parametrization of the increase of the aeolian erosion threshold wind friction velocity due to soil moisture for arid and semi-arid areas. In *Annales Geophysicae* (Vol. 17, No. 1, pp. 149-157). Springer-Verlag

Flower, V.J. and Kahn, R.A., 2017. Distinguishing Remobilized Ash From Erupted Volcanic Plumes Using Space-Borne Multiangle Imaging. *Geophysical Research Letters*, 44(20).

Fountain, A.G., 1996. Effect of snow and firn hydrology on the physical and chemical characteristics of glacial runoff. *Hydrological Processes*, 10(4), pp.509-521.

Fryrear, D.W., 1986. A field dust sampler. *Journal of Soil and Water Conservation*, 41(2), pp.117-120.

Gaiero, D.M., 2007. Dust provenance in Antarctic ice during glacial periods: From where in southern South America? *Geophysical Research Letters*, 34(17).

Gaiero, D.M., Depetris, P.J., Probst, J.L., Bidart, S.M. and Leleyter, L., 2004. The signature of river-and wind-borne materials exported from Patagonia to the southern latitudes: a view from REEs and implications for paleoclimatic interpretations. *Earth and Planetary Science Letters*, 219(3), pp.357-376.

Gaiero, D.M., Brunet, F., Probst, J.L. and Depetris, P.J., 2007. A uniform isotopic and chemical signature of dust exported from Patagonia: Rock sources and occurrence in southern environments. *Chemical Geology*, 238(1), pp.107-120.

Gaiero, D.M., Simonella, L., Gassó, S., Gili, S., Stein, A.F., Sosa, P., Becchio, R., Arce, J. and Marelli, H., 2013. Ground/satellite observations and atmospheric modeling of dust storms originating in the high Puna-Altiplano deserts (South America): Implications for the interpretation of paleo-climatic archives. *Journal of Geophysical Research: Atmospheres*, 118(9), pp.3817-3831

Gassó, S. and Stein, A.F., 2007. Does dust from Patagonia reach the sub-Antarctic Atlantic Ocean? *Geophysical Research Letters*, 34(1).

Gassó, S., Stein, A., Marino, F., Castellano, E., Udisti, R. and Ceratto, J., 2010. A combined observational and modeling approach to study modern dust transport from the Patagonia desert to East Antarctica. *Atmospheric Chemistry and Physics*, 10(17), p.8287.

Gaudichel, A., De Angelis, M., Joussaume, S., Petit, J.R., Korotkevitch, Y.S. and Petrov, V.N., 1992. Comments on the origin of dust in East Antarctica for present and ice age conditions. *Journal of atmospheric chemistry*, 14(1-4), pp.129-142.

Gherboudj, I., Beegum, S.N., Marticorena, B. and Ghedira, H., 2015. Dust emission parameterization scheme over the MENA region: Sensitivity analysis to soil moisture and soil texture. *Journal of Geophysical Research: Atmospheres*, 120(20).

Gill, T.E., Zobeck, T.M. and Stout, J.E., 2006. Technologies for laboratory generation of dust from geological materials. *Journal of Hazardous Materials*, 132(1), pp.1-13.

Gill, T.E., Zobeck, T.M., Stout, J.E. and Gregory, J.M., 1999. Fugitive dust generation in the laboratory. In *Proceedings of the Wind erosion International Symposium-Workshop USDA-ARS Wind Erosion Research Unit, Kansas State University, Manhattan, Kansas*.

Gillette, D.A. and Walker, T.R., 1977. Characteristics of airborne particles produced by wind erosion of sandy soil, High Plains of west Texas. *Soil Science*, 123(2), pp.97-110.

Gillette, D., 1978. A wind tunnel simulation of the erosion of soil: Effect of soil texture, sandblasting, wind speed, and soil consolidation on dust production. *Atmospheric Environment* (1967), 12(8), pp.1735-1743.

Gillette, D.A., Fryrear, D.W., Xiao, J.B., Stockton, P., Ono, D., Helm, P.J., Gill, T.E. and Ley, T., 1997. Large-scale variability of wind erosion mass flux rates at Owens Lake: 1. Vertical profiles of horizontal mass fluxes of wind-eroded particles with diameter greater than 50 μm . *Journal of Geophysical Research: Atmospheres*, 102(D22), pp.25977-25987.

Gillies, J.A., Nickling, W.G. and Tilson, M., 2013. Frequency, magnitude, and characteristics of aeolian sediment transport: McMurdo Dry Valleys, Antarctica. *Journal of Geophysical Research: Earth Surface*, 118(2), pp.461-479.

Ginoux, P., Chin, M., Tegen, I., Prospero, J.M., Holben, B., Dubovik, O. and Lin, S.J., 2001. Sources and distributions of dust aerosols simulated with the GOCART model. *Journal of Geophysical Research: Atmospheres*, 106(D17), pp.20255-20273.

Ginoux, P., Prospero, J.M., Gill, T.E., Hsu, N.C. and Zhao, M., 2012. Global-scale attribution of anthropogenic and natural dust sources and their emission rates based on MODIS Deep Blue aerosol products. *Reviews of Geophysics*, 50(3).

Gísladóttir, F.O., Arnalds, O. and Gísladóttir, G., 2005. The effect of landscape and retreating glaciers on wind erosion in south Iceland. *Land degradation & development*, 16(2), pp.177-187.

Gísladóttir, G., Erlendsson, E., Lal, R. and Bigham, J., 2010. Erosional effects on terrestrial resources over the last millennium in Reykjanes, southwest Iceland. *Quaternary Research*, 73(1), pp.20-32.

Gomes, L., Bergametti, G., Coudé-Gaussen, G. and Rognon, P., 1990. Submicron desert dusts: A sandblasting process. *Journal of Geophysical Research: Atmospheres*, 95(D9), pp.13927-13935.

Gomez, B., Smith, L.C., Magilligan, F.J., Mertes, L.A.K. and Smith, N.D., 2000. Glacier outburst floods and outwash plain development: Skeiðarársandur, Iceland. *Terra Nova*, 12(3), pp.126-131.

Goossens, D., Gross, J. and Spaan, W., 2001. Aeolian dust dynamics in agricultural land areas in lower Saxony, Germany. *Earth Surface Processes and Landforms*, 26(7), pp.701-720.

Goossens, D. and Buck, B.J., 2012. Can BSNE (Big Spring Number Eight) samplers be used to measure PM₁₀, respirable dust, PM_{2.5} and PM₁₀. *Aeolian Research*, 5, pp.43-49.

Goossens, D., Offer, Z. and London, G., 2000. Wind tunnel and field calibration of five aeolian sand traps. *Geomorphology*, 35(3), pp.233-252.

Goudie, A.S. and Watson, A., 1981. Shape of desert sand dune grains. *Journal of Arid Environments*.

Goudie, A. and Viles, H.A., 1997. *Salt weathering hazard*. Wiley

Graham, D.J., Rice, S.P. and Reid, I., 2005. A transferable method for the automated grain sizing of river gravels. *Water Resources Research*, 41(7).

Graham, D.J., Reid, I. and Rice, S.P., 2005. Automated sizing of coarse-grained sediments: image-processing procedures. *Mathematical Geology*, 37(1), pp.1-28.

Griffin, D.W. and Kellogg, C.A., 2004. Dust storms and their impact on ocean and human health: dust in Earth's atmosphere. *EcoHealth*, 1(3), pp.284-295.

Griffin, D.W., 2007. Atmospheric movement of microorganisms in clouds of desert dust and implications for human health. *Clinical microbiology reviews*, 20(3), pp.459-477.

Grini, A., Zender, C.S. and Colarco, P.R., 2002. Saltation sandblasting behavior during mineral dust aerosol production. *Geophysical Research Letters*, 29(18).

Grini, A. and Zender, C.S., 2004. Roles of saltation, sandblasting, and wind speed variability on mineral dust aerosol size distribution during the Puerto Rican Dust Experiment (PRIDE). *Journal of Geophysical Research: Atmospheres*, 109(D7).

Grini, A., Myhre, G., Zender, C.S. and Isaksen, I.S., 2005. Model simulations of dust sources and transport in the global atmosphere: Effects of soil erodibility and wind speed variability. *Journal of Geophysical Research: Atmospheres*, 110(D2).

Groot Zwaftink, C.D., Grythe, H., Skov, H. and Stohl, A., 2016. Substantial contribution of northern high-latitude sources to mineral dust in the Arctic. *Journal of Geophysical Research: Atmospheres*.

Groot Zwaftink, C.D., Arnalds, Ó., Dagsson-Waldhauserova, P., Eckhardt, S., Prospero, J.M. and Stohl, A., 2017. Temporal and spatial variability of Icelandic dust emissions and atmospheric transport. *Atmospheric Chemistry and Physics*, 17(17), pp.10865-10878.

Gautam, R., Liu, Z., Singh, R.P. and Hsu, N.C., 2009. Two contrasting dust-dominant periods over India observed from MODIS and CALIPSO data. *Geophysical Research Letters*, 36(6).

Gudmundsson, G., 2011. Respiratory health effects of volcanic ash with special reference to Iceland. A review. *The Clinical Respiratory Journal*, 5(1), pp.2-9.

Gunnarsson, T.G., Arnalds, O., Appleton, G., Méndez, V. and Gill, J.A., 2015. Ecosystem recharge by volcanic dust drives broad-scale variation in bird abundance. *Ecology and evolution*, 5(12), pp.2386-2396.

Gurnell, A., Hannah, D. and Lawler, D., 1996. Suspended sediment yield from glacier basins. IAHS Publications-Series of Proceedings and Reports-Intern Assoc Hydrological Sciences, 236, pp.97-104.

Haff, P.K. and Anderson, R.S., 1993. Grain scale simulations of loose sedimentary beds: The example of grain-bed impacts in aeolian saltation. *Sedimentology*, 40(2), pp.175-198.

Harris, J.M., Draxler, R.R. and Oltmans, S.J., 2005. Trajectory model sensitivity to differences in input data and vertical transport method. *Journal of Geophysical Research: Atmospheres*, 110(D14).

Harvey, K.R. and Hill, G.J.E., 2001. Vegetation mapping of a tropical freshwater swamp in the Northern Territory, Australia: a comparison of aerial photography, Landsat TM and SPOT satellite imagery. *International Journal of Remote Sensing*, 22(15), pp.2911-2925.

Hedegaard, K., 1982. Wind vector and extreme wind statistics in Greenland. Danish Meteorological Institute, Weather Service Report No. 1, Copenhagen

Helland, P.E. and Holmes, M.A., 1997. Surface textural analysis of quartz sand grains from ODP Site 918 off the southeast coast of Greenland suggests glaciation of southern Greenland at 11 Ma. *Palaeogeography, Palaeoclimatology, Palaeoecology*, 135(1), pp.109-121.

Herut, B., Collier, R. and Krom, M.D., 2002. The role of dust in supplying nitrogen and phosphorus to the Southeast Mediterranean. *Limnology and Oceanography*, 47(3), pp.870-878.

Hine, A.C. and Boothroyd, J.C., 1978. Morphology, processes, and recent sedimentary history of a glacial-outwash plain shoreline, southern Iceland. *Journal of Sedimentary Research*, 48(3).

Hinzman, L.D., Bettez, N.D., Bolton, W.R., Chapin, F.S., Dyurgerov, M.B., Fastie, C.L., Griffith, B., Hollister, R.D., Hope, A., Huntington, H.P. and Jensen, A.M., 2005. Evidence and implications of recent climate change in northern Alaska and other arctic regions. *Climatic Change*, 72(3), pp.251-298.

Hobbs, W.H., 1931. Loess, pebble bands, and boulders from glacial outwash of the Greenland continental glacier. *The Journal of Geology*, 39(4), pp.381-385.

Hobbs, W.H., 1942. Wind: the dominant transportation agent within extramarginal zones to continental glaciers. *The Journal of Geology*, 50(5), pp.556-559.

Hodgkins, R., 1996. Seasonal trend in suspended-sediment transport from an Arctic glacier, and implications for drainage-system structure. *Annals of Glaciology*, 22(1), pp.147-151.

Hodgkins, R., 1999. Controls on suspended-sediment transfer at a High-Arctic glacier, determined from statistical modelling. *Earth Surface Processes and Landforms*, 24(1), pp.1-21.

Hodgkins, R., Cooper, R., Wadham, J. and Tranter, M., 2003. Suspended sediment fluxes in a high-Arctic glacierised catchment: implications for fluvial sediment storage. *Sedimentary Geology*, 162(1), pp.105-117.

Hodson, A.J. and Ferguson, R.I., 1999. Fluvial suspended sediment transport from cold and warm-based glaciers in Svalbard. *Earth Surface Processes and Landforms*, 24(11), pp.957-974.

Hope, A.S., Fleming, J.B., Stow, D.A. and Aguado, E., 1991. Tussock tundra albedos on the north slope of Alaska: effects of illumination, vegetation composition, and dust deposition. *Journal of Applied Meteorology*, 30(8), pp.1200-1206.

House, W.A. and Warwick, M.S., 1998. Hysteresis of the solute concentration/discharge relationship in rivers during storms. *Water Research*, 32(8), pp.2279-2290.

Houser, C.A. and Nickling, W.G., 2001. The emission and vertical flux of particulate matter < 10 µm from a disturbed clay-crust surface. *Sedimentology*, 48(2), pp.255-267.

Huang, J., Minnis, P., Yi, Y., Tang, Q., Wang, X., Hu, Y., Liu, Z., Ayers, K., Trepte, C. and Winker, D., 2007. Summer dust aerosols detected from CALIPSO over the Tibetan Plateau. *Geophysical Research Letters*, 34(18).

Hugenholtz, C.H. and Wolfe, S.A., 2006. Morphodynamics and climate controls of two aeolian blowouts on the northern Great Plains, Canada. *Earth Surface Processes and Landforms*, 31(12), pp.1540-1557.

Hugenholtz, C.H., Wolfe, S.A., Walker, I.J. and Moorman, B.J., 2009. Spatial and temporal patterns of aeolian sediment transport on an inland parabolic dune, Bigstick Sand Hills, Saskatchewan, Canada. *Geomorphology*, 105(1), pp.158-170.

Ishizuka, M., Mikami, M., Leys, J., Yamada, Y., Heidenreich, S., Shao, Y. and McTainsh, G.H., 2008. Effects of soil moisture and dried raindroplet crust on saltation and dust emission. *Journal of Geophysical Research: Atmospheres*, 113(D24).

Iversen, J.D. and White, B.R., 1982. Saltation threshold on earth, mars and venus. *Sedimentology*, 29(1), pp.111-119.

Iverson, N.R. and Semmens, D.J., 1995. Intrusion of ice into porous media by regelation: A mechanism of sediment entrainment by glaciers. *Journal of Geophysical Research: Solid Earth*, 100(B6), pp.10219-10230.

Iwasaka, Y., Minoura, H. and Nagaya, K., 1983. The transport and spacial scale of Asian dust-storm clouds: a case study of the dust-storm event of April 1979. *Tellus B: Chemical and Physical Meteorology*, 35(3), pp.189-196.

Jackson, M.L., Tyler, S.A., Willis, A.L., Bourbeau, G.A. and Pennington, R.P., 1948. Weathering sequence of clay-size minerals in soils and sediments. I. Fundamental generalizations. *The Journal of Physical Chemistry*, 52(7), pp.1237-1260.

Jackson, M.G., Oskarsson, N., Trønnnes, R.G., McManus, J.F., Oppo, D.W., Grönvold, K., Hart, S.R. and Sachs, J.P., 2005. Holocene loess deposition in Iceland: Evidence for millennial-scale atmosphere-ocean coupling in the North Atlantic. *Geology*, 33(6), pp.509-512.

Jacoby, M., Dvorkin, J. and Liu, X., 1996. Elasticity of partially saturated frozen sand. *Geophysics*, 61(1), pp.288-293.

James, M.R. and Robson, S., 2014. Mitigating systematic error in topographic models derived from UAV and ground-based image networks. *Earth Surface Processes and Landforms*, 39(10), pp.1413-1420.

Jickells, T.D., An, Z.S., Andersen, K.K., Baker, A.R., Bergametti, G., Brooks, N., Cao, J.J., Boyd, P.W., Duce, R.A., Hunter, K.A. and Kawahata, H., 2005. Global iron connections between desert dust, ocean biogeochemistry, and climate. *science*, 308(5718), pp.67-71.

Johnsson, M.J. and Meade, R.H., 1990. Chemical weathering of fluvial sediments during alluvial storage: The Macuapanim Island point bar, Solimoes River, Brazil. *Journal of Sedimentary Research*, 60(6).

Kalashnikova, O.V. and Sokolik, I.N., 2002. Importance of shapes and compositions of wind-blown dust particles for remote sensing at solar wavelengths. *Geophysical Research Letters*, 29(10).

Kaufman, Y.J., Koren, I., Remer, L.A., Tanré, D., Ginoux, P. and Fan, S., 2005. Dust transport and deposition observed from the Terra-Moderate Resolution Imaging Spectroradiometer (MODIS) spacecraft over the Atlantic Ocean. *Journal of Geophysical Research: Atmospheres*, 110(D10).

Kim, D.S., Cho, G.H. and White, B.R., 2000. A wind-tunnel study of atmospheric boundary-layer flow over vegetated surfaces to suppress PM10 emission on Owens (dry) Lake. *Boundary-layer meteorology*, 97(2), pp.309-329.

Kimura, R. and Shinoda, M., 2010. Spatial distribution of threshold wind speeds for dust outbreaks in northeast Asia. *Geomorphology*, 114(3), pp.319-325.

Kjær, K.H., Sultan, L., Krüger, J. and Schomacker, A., 2004. Architecture and sedimentation of outwash fans in front of the Mýrdalsjökull ice cap, Iceland. *Sedimentary Geology*, 172(1), pp.139-163.

Klose, M. and Shao, Y., 2012. Stochastic parameterization of dust emission and application to convective atmospheric conditions. *Atmospheric Chemistry and Physics*, 12(16), p.7309.

Klose, M., Shao, Y., Li, X., Zhang, H., Ishizuka, M., Mikami, M. and Leys, J.F., 2014. Further development of a parameterization for convective turbulent dust emission and evaluation based on field observations. *Journal of Geophysical Research: Atmospheres*, 119(17), pp.10441-10457.

Klose, M., Gill, T.E., Webb, N.P. and Van Zee, J.W., 2017. Field sampling of loose erodible material: A new system to consider the full particle-size spectrum. *Aeolian Research*, 28, pp.83-90.

Knight, S.H., 1924. Eolian abrasion of quartz grains. *Geological Society of American Bulletin*, 35, pp. 107–108.

Kocurek, G., 1998. Aeolian system response to external forcing factors – a sequence stratigraphic view of the Sahara region. In: *Quaternary Deserts and Climatic Change* (Ed. by K.W. Glennie), pp. 327–337. A.A. Balkema, Rotterdam.

Kocurek, G. and Lancaster, N., 1999. Aeolian system sediment state: theory and Mojave Desert Kelso dune field example. *Sedimentology*, 46(3), pp.505-515.

Kok, J.F., 2010. An improved parameterization of wind-blown sand flux on Mars that includes the effect of hysteresis. *Geophysical Research Letters*, 37(12).

Kok, J.F., 2011. A scaling theory for the size distribution of emitted dust aerosols suggests climate models underestimate the size of the global dust cycle. *Proceedings of the National Academy of Sciences*, 108(3), pp.1016-1021.

Kok, J.F., Parteli, E.J., Michaels, T.I. and Karam, D.B., 2012. The physics of wind-blown sand and dust. *Reports on Progress in Physics*, 75(10), p.106901.

Krigström, A., 1962. Geomorphological studies of sandur plains and their braided rivers in Iceland. *Geografiska Annaler*, 44(3/4), pp.328-346.

Krinsley, D.H. and Doornkamp, J.C., 1973. *Atlas of Sand Grain Surface Textures*.

Kruger, J., 1997. Development of minor outwash fans at Kötlujökull, Iceland. *Quaternary Science Reviews*, 16(7), pp.649-659.

Kuenen, P.H., 1960. Experimental abrasion 4: eolian action. *The Journal of Geology*, 68(4), pp.427-449.

LaChapelle, E., 1962. Assessing glacier mass budgets by reconnaissance aerial photography. *Journal of Glaciology*, 4(33), pp.290-297.

Lambert, F., Delmonte, B., Petit, J.R., Bigler, M., Kaufmann, P.R., Hutterli, M.A., Stocker, T.F., Ruth, U., Steffensen, J.P. and Maggi, V., 2008. Dust-climate couplings over the past 800,000 years from the EPICA Dome C ice core. *Nature*, 452(7187), pp.616-619.

Lancaster, N., 2002. Flux of eolian sediment in the McMurdo Dry Valleys, Antarctica: a preliminary assessment. *Arctic, Antarctic, and Alpine Research*, pp.318-323.

Lancaster, N., 2004. Relations between aerodynamic and surface roughness in a hyper-arid cold desert: McMurdo Dry Valleys, Antarctica. *Earth Surface Processes and Landforms*, 29(7), pp.853-867.

Lancaster, N. and Baas, A., 1998. Influence of vegetation cover on sand transport by wind: field studies at Owens Lake, California. *Earth Surface Processes and Landforms*, 23(1), pp.69-82.

Lancaster, N., Nickling, W.G. and Gillies, J.A., 2010. Sand transport by wind on complex surfaces: Field studies in the McMurdo Dry Valleys, Antarctica. *Journal of Geophysical Research: Earth Surface*, 115(F3).

Lässig, J.L., Cogliati, M.G., Bastanski, M.A. and Palese, C., 1999. Wind characteristics in Neuquen, North Patagonia, Argentina. *Journal of Wind Engineering and Industrial Aerodynamics*, 79(1), pp.183-199.

Leadbetter, S.J., Hort, M.C., Löwis, S., Weber, K. and Witham, C.S., 2012. Modeling the resuspension of ash deposited during the eruption of Eyjafjallajökull in spring 2010. *Journal of Geophysical Research: Atmospheres*, 117(D20).

Lee, J.A., Gill, T.E., Mulligan, K.R., Acosta, M.D. and Perez, A.E., 2009. Land use/land cover and point sources of the 15 December 2003 dust storm in southwestern North America. *Geomorphology*, 105(1), pp.18-27.

Lee, J.A., Baddock, M.C., Mbuh, M.J. and Gill, T.E., 2012. Geomorphic and land cover characteristics of aeolian dust sources in West Texas and eastern New Mexico, USA. *Aeolian Research*, 3(4), pp.459-466.

Li, F., Ginoux, P. and Ramaswamy, V., 2008. Distribution, transport, and deposition of mineral dust in the Southern Ocean and Antarctica: Contribution of major sources. *Journal of Geophysical Research: Atmospheres*, 113(D10).

Li, X. and Zhang, H., 2011. Research on threshold friction velocities during dust events over the Gobi Desert in northwest China. *Journal of Geophysical Research: Atmospheres*, 116(D20).

Licciardi, J.M., Kurz, M.D. and Curtice, J.M., 2006. Cosmogenic ^3He production rates from Holocene lava flows in Iceland. *Earth and Planetary Science Letters*, 246(3), pp.251-264.

Lipponen, A., Mielonen, T., Pitkänen, M.R., Levy, R.C., Sawyer, V.R., Romakkaniemi, S., Kolehmainen, V. and Arola, A., Bayesian Dark Target Algorithm for MODIS AOD retrieval over land. *Atmospheric Measurement Techniques Discussions*

Littmann, T., 1991. Dust storm frequency in Asia: climatic control and variability. *International Journal of Climatology*, 11(4), pp.393-412.

Liu, D., Wang, Z., Liu, Z., Winker, D. and Trepte, C., 2008. A height resolved global view of dust aerosols from the first year CALIPSO lidar measurements. *Journal of Geophysical Research: Atmospheres*, 113(D16).

Liu, X., Huneeus, N., Schulz, M., Balkanski, Y., Griesfeller, J., Prospero, J., Kinne, S., Bauer, S., Boucher, O., Chin, M. and Dentener, F., 2011. Global dust model intercomparison in AeroCom phase I. *Atmospheric Chemistry and Physics*, 11(15), p.7781.

Liu, Z., Liu, D., Huang, J., Vaughan, M., Uno, I., Sugimoto, N., Kittaka, C., Trepte, C., Wang, Z., Hostetler, C. and Winker, D., 2008. Airborne dust distributions over the Tibetan Plateau and surrounding areas derived from the first year of CALIPSO lidar observations. *Atmospheric Chemistry and Physics*, 8(16), pp.5045-5060.

Logie, M., 1982. Influence of roughness elements and soil moisture on the resistance of sand to wind erosion. In *Acidic soils and geomorphic processes: proceedings of the International Conference of the International Society of Soil Science*, Jerusalem, Israel, March 19-April 4, 1981/DH Yaalon, ed. Cremlingen [W. Ger.]: Catena Verlag, 1982.

Loosmore, G.A. and Hunt, J.R., 2000. Dust resuspension without saltation. *Journal of Geophysical Research: Atmospheres*, 105(D16), pp.20663-20671.

Lu, H. and Shao, Y., 1999. A new model for dust emission by saltation bombardment. *Journal of Geophysical Research: Atmospheres*, 104(D14), pp.16827-16842.

Lynch, A., Uotila, P. and Cassano, J.J., 2006. Changes in synoptic weather patterns in the polar regions in the twentieth and twenty-first centuries, part 2: Antarctic. *International Journal of Climatology*, 26(9), pp.1181-1199.

Macpherson, T., Nickling, W.G., Gillies, J.A. and Etyemezian, V., 2008. Dust emissions from undisturbed and disturbed supply-limited desert surfaces. *Journal of Geophysical Research: Earth Surface*, 113(F2).

Madden, N.M., Southard, R.J. and Mitchell, J.P., 2010. Soil water and particle size distribution influence laboratory-generated PM 10. *Atmospheric Environment*, 44(6), pp.745-752.

Magilligan, F.J., Gomez, B., Mertes, L.A.K., Smith, L.C., Smith, N.D., Finnegan, D. and Garvin, J.B., 2002. Geomorphic effectiveness, sandur development, and the pattern of landscape response during jökulhlaups: Skeiðarársandur, southeastern Iceland. *Geomorphology*, 44(1), pp.95-113.

Mahaney, W.C., 2002. *Atlas of sand grain surface textures and applications*. Oxford University Press, USA.

Mahaney, W.C., Stewart, A. and Kalm, V., 2001. Quantification of SEM microtextures useful in sedimentary environmental discrimination. *Boreas*, 30(2), pp.165-171.

Mahowald, N., Kohfeld, K., Hansson, M., Balkanski, Y., Harrison, S.P., Prentice, I.C., Schulz, M. and Rodhe, H., 1999. Dust sources and deposition during the last glacial maximum and current climate: A comparison of model results with paleodata from ice cores and marine sediments. *Journal of Geophysical Research: Atmospheres*, 104(D13), pp.15895-15916.

Mahowald, N.M., Baker, A.R., Bergametti, G., Brooks, N., Duce, R.A., Jickells, T.D., Kubilay, N., Prospero, J.M. and Tegen, I., 2005. Atmospheric global dust cycle and iron inputs to the ocean. *Global Biogeochemical Cycles*, 19(4).

Maizels, J., 1989. Sedimentology, paleoflow dynamics and flood history of jökulhlaup deposits: paleohydrology of Holocene sediment sequences in southern Iceland sandur deposits. *Journal of Sedimentary Research*, 59(2).

Maizels, J., 1991. The origin and evolution of Holocene sandur deposits in areas of jökulhlaup drainage, Iceland. In *Environmental change in Iceland: Past and present* (pp. 267-302). Springer, Dordrecht.

Maizels, J., 1993. Lithofacies variations within sandur deposits: the role of runoff regime, flow dynamics and sediment supply characteristics. *Sedimentary geology*, 85(1), pp.299-325.

Maizels, J., 1997. Jökulhlaup deposits in proglacial areas. *Quaternary Science Reviews*, 16(7), pp.793-819.

Marcott, S.A., Shakun, J.D., Clark, P.U. and Mix, A.C., 2013. A reconstruction of regional and global temperature for the past 11,300 years. *Science*, 339(6124), pp.1198-1201.

Marren, P.M., Russell, A.J. and Rushmer, E.L., 2009. Sedimentology of a sandur formed by multiple jökulhlaups, Kverkfjöll, Iceland. *Sedimentary Geology*, 213(3), pp.77-88.

Marshall, J.R., Bull, P.A. and Morgan, R.M., 2012. Energy regimes for aeolian sand grain surface textures. *Sedimentary Geology*, 253, pp.17-24.

Martcorena, B. and Bergametti, G., 1995. Modelling the atmospheric dust cycle: 1. Design of a soil-derived dust emission scheme. *Journal of Geophysical Research: Atmospheres*, 100(D8), pp.16415-16430.

Marticorena, B., Bergametti, G., Aumont, B., Callot, Y., N'doumé, C. and Legrand, M., 1997. Modeling the atmospheric dust cycle: 2. Simulation of Saharan dust sources. *Journal of Geophysical Research: Atmospheres*, 102(D4), pp.4387-4404.

Marx, S.K., Kamber, B.S. and McGowan, H.A., 2005. Provenance of long-travelled dust determined with ultra-trace-element composition: a pilot study with samples from New Zealand glaciers. *Earth Surface Processes and Landforms*, 30(6), pp.699-716.

Marx, S.K. and McGowan, H.A., 2005. Dust transportation and deposition in a superhumid environment, West Coast, South Island, New Zealand. *Catena*, 59(2), pp.147-171.

Marx, S.K., McGowan, H.A., Kamber, B.S., Knight, J.M., Denholm, J. and Zawadzki, A., 2014. Unprecedented wind erosion and perturbation of surface geochemistry marks the Anthropocene in Australia. *Journal of Geophysical Research: Earth Surface*, 119(1), pp.45-61.

Mayaud, J.R., Bailey, R.M. and Wiggs, G.F., 2017. A coupled vegetation/sediment transport model for dryland environments. *Journal of Geophysical Research: Earth Surface*, 122(4), pp.875-900.

McConnell, J.R., Aristarain, A.J., Banta, J.R., Edwards, P.R. and Simões, J.C., 2007. 20th-Century doubling in dust archived in an Antarctic Peninsula ice core parallels climate change and desertification in South America. *Proceedings of the National Academy of Sciences*, 104(14), pp.5743-5748.

McGowan, H.A., 1997. Meteorological controls on wind erosion during foehn wind events in the eastern Southern Alps, New Zealand. *Canadian Journal of Earth Sciences*, 34(11), pp.1477-1485.

McGowan, H.A. and Sturman, A.P., 1996. Interacting multi-scale wind systems within an alpine basin, Lake Tekapo, New Zealand. *Meteorology and Atmospheric Physics*, 58(1), pp.165-177.

McGowan, H.A., Sturman, A.P. and Owens, I.F., 1996. Aeolian dust transport and deposition by foehn winds in an alpine environment, Lake Tekapo, New Zealand. *Geomorphology*, 15(2), pp.135-146.

McGowan, H. and Clark, A., 2008. Identification of dust transport pathways from Lake Eyre, Australia using Hysplit. *Atmospheric Environment*, 42(29), pp.6915-6925

McKenna Neuman, C., 1993. A review of aeolian transport processes in cold environments. *Progress in physical Geography*, 17(2), pp.137-155.

McKenna Neuman, C., 2003. Effects of temperature and humidity upon the entrainment of sedimentary particles by wind. *Boundary-Layer Meteorology*, 108(1), pp.61-89.

McKenna Neuman, C., 2004. Effects of temperature and humidity upon the transport of sedimentary particles by wind. *Sedimentology*, 51(1), pp.1-17.

McKenna-Neuman, C. Boulton, J.W. and Sanderson, S., 2009. Wind tunnel simulation of environmental controls on fugitive dust emissions from mine tailings. *Atmospheric Environment*, 43(3), pp.520-529.

McKenna Neuman, C. and Langston, G., 2006. Measurement of water content as a control of particle entrainment by wind. *Earth Surface Processes and Landforms*, 31(3), pp.303-317.

McKenna-Neuman, C. and Nickling, W.G., 1989. A theoretical and wind tunnel investigation of the effect of capillary water on the entrainment of sediment by wind. *Canadian Journal of Soil Science*, 69(1), pp.79-96.

McKenna Neuman, C. and Sanderson, S., 2008. Humidity control of particle emissions in aeolian systems. *Journal of Geophysical Research: Earth Surface*, 113(F2).

McTainsh, G., Duhaylungsod, N.C. and Lynch, A.W., 1988. A modified laboratory method for soil and sediment particle-size analysis. Division of Australian Environmental Studies, Griffith University.

McTainsh, G., Chan, Y.C., McGowan, H., Leys, J. and Tews, K., 2005. The 23rd October 2002 dust storm in eastern Australia: characteristics and meteorological conditions. *Atmospheric Environment*, 39(7), pp.1227-1236.

McTainsh, G. and Strong, C., 2007. The role of aeolian dust in ecosystems. *Geomorphology*, 89(1), pp.39-54.

Meinander, O., Dagsson-Waldhauserova, P. and Arnalds, O., 2016. Icelandic volcanic dust can have a significant influence on the cryosphere in Greenland and elsewhere. *Polar Research*, 35.

Meloni, D., Di Sarra, A., Monteleone, F., Pace, G., Piacentino, S. and Sferlazzo, D.M., 2008. Seasonal transport patterns of intense Saharan dust events at the Mediterranean island of Lampedusa. *Atmospheric Research*, 88(2), pp.134-148.

Mendez, M.J., Funk, R. and Buschiazzo, D.E., 2011. Field wind erosion measurements with big spring number eight (BSNE) and modified wilson and cook (MWAC) samplers. *Geomorphology*, 129(1), pp.43-48.

Meng, Z. and Lu, B., 2007. Dust events as a risk factor for daily hospitalization for respiratory and cardiovascular diseases in Minqin, China. *Atmospheric Environment*, 41(33), pp.7048-7058.

Mernild, S.H. and Hasholt, B., 2009. Observed runoff, jökulhlaups and suspended sediment load from the Greenland ice sheet at Kangerlussuaq, West Greenland, 2007 and 2008. *Journal of Glaciology*, 55(193), pp.855-858.

Meskhidze, N., Nenes, A., Chameides, W.L., Luo, C. and Mahowald, N., 2007. Atlantic Southern Ocean productivity: Fertilization from above or below?. *Global Biogeochemical Cycles*, 21(2).

Middleton, N.J., 1985. Effect of drought on dust production in the Sahel. *Nature*, 316(6027), pp.431-434.

Miller, R.L., Tegen, I. and Perlwitz, J., 2004. Surface radiative forcing by soil dust aerosols and the hydrologic cycle. *Journal of Geophysical Research: Atmospheres*, 109(D4).

Miller, S.D., 2003. A consolidated technique for enhancing desert dust storms with MODIS. *Geophysical Research Letters*, 30(20).

Mishchenko, M.I., Lacis, A.A., Carlson, B.E. and Travis, L.D., 1995. Nonsphericity of dust-like tropospheric aerosols: Implications for aerosol remote sensing and climate modeling. *Geophysical Research Letters*, 22(9), pp.1077-1080.

Mitchell, T.D., Carter, T.R., Jones, P.D., Hulme, M. and New, M., 2004. A comprehensive set of high-resolution grids of monthly climate for Europe and the globe: the observed record (1901–2000) and 16 scenarios (2001–2100). *Tyndall centre for climate change research working paper*, 55(0), p.25.

Mladenov, N., Sommaruga, R., Morales-Baquero, R., Laurion, I., Camarero, L., Dieguez, M.C., Camacho, A., Delgado, A., Torres, O., Chen, Z. and Felip, M., 2011. Dust inputs and bacteria influence dissolved organic matter in clear alpine lakes. *Nature Communications*, 2, p.405.

Mockford, T., 2013. Effect of soil texture and calcium carbonate on laboratory-generated dust emissions from SW North America (MS dissertation). Texas Tech University 2012.

Mockford, T., Bullard, J.E. and Thorsteinsson, T., 2018. The dynamic effects of sediment availability on the relationship between wind speed and dust concentration. *Earth Surface Processes and Landforms*.

Montreuil, A.L., Bullard, J. and Chandler, J., 2013. Detecting seasonal variations in embryo dune morphology using a terrestrial laser scanner. *Journal of Coastal Research*, 65(sp2), pp.1313-1318.

Mossman, B.T., Costa, D.L., Donaldson, K., Borm, P.J., Kleeberger, S.R. and Castranova, V., 2007. Mechanisms of action of inhaled fibers, particles and nanoparticles in lung and cardiovascular diseases. *Particle and Fibre Toxicology*, 4(1), p.4.

Moulin, C., Lambert, C.E., Dulac, F. and Dayan, U., 1997. Control of atmospheric export of dust from North Africa by the North Atlantic Oscillation. *Nature*, 387(6634), pp.691-694.

Mountney, N.P. and Russell, A.J., 2004. Sedimentology of cold-climate aeolian sandsheet deposits in the Askja region of northeast Iceland. *Sedimentary Geology*, 166(3), pp.223-244.

Muhs, D.R., Bush, C.A., Stewart, K.C., Rowland, T.R. and Crittenden, R.C., 1990. Geochemical evidence of Saharan dust parent material for soils developed on Quaternary limestones of Caribbean and western Atlantic islands. *Quaternary Research*, 33(2), pp.157-177.

Muhs, D.R., Budahn, J.R., McGeehin, J.P., Bettis, E.A., Skipp, G., Paces, J.B. and Wheeler, E.A., 2013. Loess origin, transport, and deposition over the past 10,000 years, Wrangell-St. Elias National Park, Alaska. *Aeolian Research*, 11, pp.85-99.

Muhs, D.R., Budahn, J.R., Skipp, G.L. and McGeehin, J.P., 2016. Geochemical evidence for seasonal controls on the transportation of Holocene loess, Matanuska Valley, southern Alaska, USA. *Aeolian Research*, 21, pp.61-73.

Munson, S.M., Belnap, J. and Okin, G.S., 2011. Responses of wind erosion to climate-induced vegetation changes on the Colorado Plateau. *Proceedings of the National Academy of Sciences*, 108(10), pp.3854-3859.

Murayama, T., Sugimoto, N., Uno, I., Kinoshita, K., Aoki, K., Hagiwara, N., Liu, Z., Matsui, I., Sakai, T., Shibata, T. and Arao, K., 2001. Ground-based network observation of Asian dust events of April 1998 in east Asia. *Journal of Geophysical Research: Atmospheres*, 106(D16), pp.18345-18359.

Nahon, D. and Trompette, R., 1982. Origin of siltstones: glacial grinding versus weathering. *Sedimentology*, 29(1), pp.25-35.

Namikas, S.L. and Sherman, D.J., 1995. A review of the effects of surface moisture content on aeolian sand transport. In *Desert aeolian processes* (pp. 269-293). Springer, Dordrecht.

NASA 2014. Surface meteorology and Solar Energy (SSE) Release 6.0 Methodology Version 3.1.2 May 6, 2014

Neff, P.D. and Bertler, N.A., 2015. Trajectory modeling of modern dust transport to the Southern Ocean and Antarctica. *Journal of Geophysical Research: Atmospheres*, 120(18), pp.9303-9322.

Nickling, W.G., 1978. Eolian sediment transport during dust storms: Slims River valley, Yukon Territory. *Canadian Journal of Earth Sciences*, 15(7), pp.1069-1084.

Nickling, W.G. and Neuman, C.M., 1995. Development of deflation lag surfaces. *Sedimentology*, 42(3), pp.403-414.

Nield, J.M., King, J., Wiggs, G.F., Leyland, J., Bryant, R.G., Chiverrell, R.C., Darby, S.E., Eckardt, F.D., Thomas, D.S., Vircavs, L.H. and Washington, R., 2013. Estimating aerodynamic roughness over complex surface terrain. *Journal of Geophysical Research: Atmospheres*, 118(23).

Nield, J.M., King, J. and Jacobs, B., 2014. Detecting surface moisture in aeolian environments using terrestrial laser scanning. *Aeolian Research*, 12, pp.9-17.

Nielsen, D.R.J.W., Biggar, J.W. and Erh, K.T., 1973. Spatial variability of field-measured soil-water properties. *California Agriculture*, 42(7), pp.215-259.

Niethammer, U., James, M.R., Rothmund, S., Travelletti, J. and Joswig, M., 2012. UAV-based remote sensing of the Super-Sauze landslide: Evaluation and results. *Engineering Geology*, 128, pp.2-11.

Obanawa, H. and Hayakawa, Y.S., 2015. High-resolutional topographic survey using small UAV and SfM-MVS technologies in hardly accessible area. In *The International Symposium on Cartography in Internet and Ubiquitous Environment 2015 C (Vol. 4)*.

Oerlemans, J., 2001. *Glaciers and climate change*. CRC Press.

Oerlemans, J., Anderson, B., Hubbard, A., Huybrechts, P., Johannesson, T., Knap, W.H., Schmeits, M., Stroeven, A.P., Van de Wal, R.S.W., Wallinga, J. and Zuo, Z., 1998. Modelling the response of glaciers to climate warming. *Climate dynamics*, 14(4), pp.267-274.

Okin, G.S. and Gillette, D.A., 2001. Distribution of vegetation in wind-dominated landscapes: Implications for wind erosion modeling and landscape processes. *Journal of Geophysical Research: Atmospheres*, 106(D9), pp.9673-9683.

Okin, G.S., Roberts, D.A., Murray, B. and Okin, W.J., 2001. Practical limits on hyperspectral vegetation discrimination in arid and semiarid environments. *Remote Sensing of Environment*, 77(2), pp.212-225.

Okin, G.S. and Gillette, D.A., 2004. Modelling wind erosion and dust emission on vegetated surfaces. *Spatial Modeling of the Terrestrial Environment*, pp.137-156.

Okin, G.S., Mahowald, N., Chadwick, O.A. and Artaxo, P., 2004. Impact of desert dust on the biogeochemistry of phosphorus in terrestrial ecosystems. *Global Biogeochemical Cycles*, 18(2).

Okin, G.S., Gillette, D.A. and Herrick, J.E., 2006. Multi-scale controls on and consequences of aeolian processes in landscape change in arid and semi-arid environments. *Journal of Arid Environments*, 65(2), pp.253-275.

Okin, G.S., 2008. A new model of wind erosion in the presence of vegetation. *Journal of Geophysical Research: Earth Surface*, 113(F2).

Okin, G.S., Baker, A.R., Tegen, I., Mahowald, N.M., Dentener, F.J., Duce, R.A., Galloway, J.N., Hunter, K., Kanakidou, M., Kubilay, N. and Prospero, J.M., 2011. Impacts of atmospheric nutrient deposition on marine productivity: Roles of nitrogen, phosphorus, and iron. *Global Biogeochemical Cycles*, 25(2).

Ólafsson, H., Furger, M. and Brummer, B., 2007. The weather and climate of Iceland. *Meteorologische Zeitschrift*, 16(1), pp.5-8.

Old, G.H., Lawler, D.M. and Snorrason, Á., 2005. Discharge and suspended sediment dynamics during two jökulhlaups in the Skaftá river, Iceland. *Earth Surface Processes and Landforms*, 30(11), pp.1441-1460.

O'Loingsigh, T., McTainsh, G.H., Tews, E.K., Strong, C.L., Leys, J.F., Shinkfield, P. and Tapper, N.J., 2014. The Dust Storm Index (DSI): a method for monitoring broadscale wind erosion using meteorological records. *Aeolian Research*, 12, pp.29-40.

O'Loingsigh, T., Chubb, T., Baddock, M., Kelly, T., Tapper, N.J., De Deckker, P. and McTainsh, G., 2017. Sources and pathways of dust during the Australian "Millennium Drought" decade. *Journal of Geophysical Research: Atmospheres*, 122(2), pp.1246-1260.

Orwin, J.F. and Smart, C.C., 2004. Short-term spatial and temporal patterns of suspended sediment transfer in proglacial channels, Small River Glacier, Canada. *Hydrological Processes*, 18(9), pp.1521-1542.

Pagli, C. and Sigmundsson, F., 2008. Will present day glacier retreat increase volcanic activity? Stress induced by recent glacier retreat and its effect on magmatism at the Vatnajökull ice cap, Iceland. *Geophysical Research Letters*, 35(9).

Painter, T.H., Skiles, S.M., Deems, J.S., Bryant, A.C. and Landry, C.C., 2012. Dust radiative forcing in snow of the Upper Colorado River Basin: 1. A 6 year record of energy balance, radiation, and dust concentrations. *Water Resources Research*, 48(7).

Pandolfi, M., Tobias, A., Alastuey, A., Sunyer, J., Schwartz, J., Lorente, J., Pey, J. and Querol, X., 2014. Effect of atmospheric mixing layer depth variations on urban air quality and daily mortality during Saharan dust outbreaks. *Science of the Total Environment*, 494, pp.283-289.

Parajuli, S.P. and Zender, C.S., 2017. Connecting geomorphology to dust emission through high-resolution mapping of global land cover and sediment supply. *Aeolian Research*, 27, pp.47-65.

Parajuli, S.P., Zobeck, T.M., Kocurek, G., Yang, Z.L. and Stenchikov, G.L., 2016. New insights into the wind-dust relationship in sandblasting and direct aerodynamic entrainment from wind tunnel experiments. *Journal of Geophysical Research: Atmospheres*, 121(4), pp.1776-1792.

Parish, T.R. and Cassano, J.J., 2003. The role of katabatic winds on the Antarctic surface wind regime. *Monthly Weather Review*, 131(2), pp.317-333.

Parish, T.R., 1984. A numerical study of strong katabatic winds over Antarctica. *Monthly weather review*, 112(3), pp.545-554.

Pascoe, K.J., 1961. *An Introduction to the Properties of Engineering Materials*. Blackie, London

Pell, S.D. and Chivas, A.R., 1995. Surface features of sand grains from the Australian Continental Dunefield. *Palaeogeography, Palaeoclimatology, Palaeoecology*, 113(1), pp.119-132.

Pérez, C., Nickovic, S., Pejanovic, G., Baldasano, J.M. and Özsoy, E., 2006. Interactive dust-radiation modeling: A step to improve weather forecasts. *Journal of Geophysical Research: Atmospheres*, 111(D16).

Périard, C. and Pettré, P., 1993. Some aspects of the climatology of dumont D'Irville, adélie land, Antarctica. *International Journal of Climatology*, 13(3), pp.313-328.

Péwé, T.L., 1951. An observation on wind-blown silt. *The Journal of Geology*, 59(4), pp.399-401.

Pieri, D., Ma, C., Simpson, J.J., Hufford, G., Grindle, T. and Grove, C., 2002. Analyses of in-situ airborne volcanic ash from the February 2000 eruption of Hekla volcano, Iceland. *Geophysical Research Letters*, 29(16).

Prospero, J.M., 1999. Assessing the impact of advected African dust on air quality and health in the eastern United States. *Human and Ecological Risk Assessment: An International Journal*, 5(3), pp.471-479.

Prospero, J.M. and Carlson, T.N., 1972. Vertical and areal distribution of Saharan dust over the western equatorial North Atlantic Ocean. *Journal of Geophysical Research*, 77(27), pp.5255-5265.

Prospero, J.M., Barrett, K., Church, T., Dentener, F., Duce, R.A., Galloway, J.N., Levy, H., Moody, J. and Quinn, P., 1996. Atmospheric deposition of nutrients to the North Atlantic Basin. *Biogeochemistry*, 35(1), pp.27-73.

Prospero, J.M., Ginoux, P., Torres, O., Nicholson, S.E. and Gill, T.E., 2002. Environmental characterization of global sources of atmospheric soil dust identified with the Nimbus 7 Total Ozone Mapping Spectrometer (TOMS) absorbing aerosol product. *Reviews of Geophysics*, 40(1).

Prospero, J.M. and Lamb, P.J., 2003. African droughts and dust transport to the Caribbean: Climate change implications. *Science*, 302(5647), pp.1024-1027.

Prospero, J.M., Bullard, J.E. and Hodgkins, R., 2012. High-latitude dust over the North Atlantic: inputs from Icelandic proglacial dust storms. *Science*, 335(6072), pp.1078-1082.

Pye, K. and Tsoar, H., 2008. *Aeolian sand and sand dunes*. Springer Science & Business Media.

Pye, K., 2015. *Aeolian dust and dust deposits*. Elsevier.

Ramanathan, V., 2006. Western Pacific Autonomous UAV campaign: aerosol-dust-cloud interactions and climate effects. Scripps Institution of Oceanography, University of California, San Diego, White Paper, 28.

Raupach, M., 1992. Drag and drag partition on rough surfaces. *Boundary-Layer Meteorology*, 60(4), pp.375-395.

Ravi, S., D'Odorico, P., Over, T.M. and Zobeck, T.M., 2004. On the effect of air humidity on soil susceptibility to wind erosion: The case of air-dry soils. *Geophysical Research Letters*, 31(9).

Ravi, S., Zobeck, T.M., Over, T.M., Okin, G.S. and D'odorico, P., 2006. On the effect of moisture bonding forces in air-dry soils on threshold friction velocity of wind erosion. *Sedimentology*, 53(3), pp.597-609.

Ravi, S., D'odorico, P., Breshears, D.D., Field, J.P., Goudie, A.S., Huxman, T.E., Li, J., Okin, G.S., Swap, R.J., Thomas, A.D. and Van Pelt, S., 2011. Aeolian processes and the biosphere. *Reviews of Geophysics*, 49(3).

Rawls, W.J., Brakensiek, D.L. and Saxtonn, K.E., 1982. Estimation of soil water properties. *Transactions of the ASAE*, 25(5), pp.1316-1320.

Reheis, M.C. and Kihl, R., 1995. Dust deposition in southern Nevada and California, 1984–1989: Relations to climate, source area, and source lithology. *Journal of Geophysical Research: Atmospheres*, 100(D5), pp.8893-8918.

Reheis, M.C. and Urban, F.E., 2011. Regional and climatic controls on seasonal dust deposition in the southwestern US. *Aeolian Research*, 3(1), pp.3-21.

Reijmer, C.H., Knap, W.H. and Oerlemans, J., 1999. The surface albedo of the Vatnajökull ice cap, Iceland: a comparison between satellite-derived and ground-based measurements. *Boundary-layer meteorology*, 92(1), pp.123-143.

Retelle, M.J. and Child, J.K., 1996. Suspended sediment transport and deposition in a high arctic meromictic lake. *Journal of Paleolimnology*, 16(2), pp.151-167.

Revel-Rolland, M., De Deckker, P., Delmonte, B., Hesse, P.P., Magee, J.W., Basile-Doelsch, I., Grousset, F. and Bosch, D., 2006. Eastern Australia: a possible source of dust in East Antarctica interglacial ice. *Earth and Planetary Science Letters*, 249(1), pp.1-13.

Reynolds, R.L., Yount, J.C., Reheis, M., Goldstein, H., Chavez, P., Fulton, R., Whitney, J., Fuller, C. and Forester, R.M., 2007. Dust emission from wet and dry playas in the Mojave Desert, USA. *Earth Surface Processes and Landforms*, 32(12), pp.1811-1827.

Rice, M.A., Willetts, B.B. and McEwan, I.K., 1995. An experimental study of multiple grain-size ejecta produced by collisions of saltating grains with a flat bed. *Sedimentology*, 42(4), pp.695-706.

Richards, K., 1984. Some observations on suspended sediment dynamics in Storbregrova, Jotunheimen. *Earth Surface Processes and Landforms*, 9(2), pp.101-112.

Ries, J.B. and Marzloff, I., 2003. Monitoring of gully erosion in the Central Ebro Basin by large-scale aerial photography taken from a remotely controlled blimp. *Catena*, 50(2), pp.309-328.

Romm, J., 2011. Desertification: The next dust bowl. *Nature*, 478(7370), pp.450-451.

Rosenfeld, D., Rudich, Y. and Lahav, R., 2001. Desert dust suppressing precipitation: A possible desertification feedback loop. *Proceedings of the National Academy of Sciences*, 98(11), pp.5975-5980.

Roskovensky, J.K. and Liou, K.N., 2003. Detection of thin cirrus from 1.38 μm /0.65 μm reflectance ratio combined with 8.6–11 μm brightness temperature difference. *Geophysical research letters*, 30(19).

Ruckley, V.A., Gauld, S.J., Chapman, J.S., Davis, J.M., Douglas, A.N., Fernie, J.M., Jacobsen, M. and Lamb, D., 1984. Emphysema and dust exposure in a group of coal workers. *The American review of respiratory disease*, 129(4), pp.528-532.

Russell, A.J., 1993. Obstacle marks produced by flow around stranded ice blocks during a glacier outburst flood (jökulhlaup) in west Greenland. *Sedimentology*, 40(6), pp.1091-1111.

Russell, A.J., Knudsen, O., Fay, H., Marren, P.M., Heinz, J. and Tronicke, J., 2001. Morphology and sedimentology of a giant supraglacial, ice-walled, jökulhlaup channel, Skeiðarárjökull, Iceland: implications for esker genesis. *Global and Planetary Change*, 28(1), pp.193-216.

Russell, A.J., 2007. Controls on the sedimentology of an ice-contact jökulhlaup-dominated delta, Kangerlussuaq, west Greenland. *Sedimentary Geology*, 193(1), pp.131-148.

Ryan, J.C., Hubbard, A.L., Todd, J., Carr, J.R., Box, J.E., Christoffersen, P., Holt, T.O. and Snooke, N., 2014. Repeat UAV photogrammetry to assess calving front dynamics at a large outlet glacier draining the Greenland Ice Sheet. *The Cryosphere*, 8(2), pp.2243-2275.

Salama, R.B., Tapley, I., Ishii, T. and Hawkes, G., 1994. Identification of areas of recharge and discharge using Landsat-TM satellite imagery and aerial photography mapping techniques. *Journal of Hydrology*, 162(1-2), pp.119-141.

Satheesh, S.K. and Moorthy, K.K., 2005. Radiative effects of natural aerosols: A review. *Atmospheric Environment*, 39(11), pp.2089-2110.

Schepanski, K., Tegen, I., Laurent, B., Heinold, B. and Macke, A., 2007. A new Saharan dust source activation frequency map derived from MSG-SEVIRI IR-channels. *Geophysical Research Letters*, 34(18).

Schroth, A.W., Crusius, J., Sholkovitz, E.R. and Bostick, B.C., 2009. Iron solubility driven by speciation in dust sources to the ocean. *Nature Geoscience*, 2(5), pp.337-340.

Schroth, A.W., Crusius, J., Chever, F., Bostick, B.C. and Rouxel, O.J., 2011. Glacial influence on the geochemistry of riverine iron fluxes to the Gulf of Alaska and effects of deglaciation. *Geophysical Research Letters*, 38(16)

Schroth, A.W., Crusius, J., Gassó, S., Moy, C.M., Buck, N.J., Resing, J.A. and Campbell, R.W., 2017. Atmospheric deposition of glacial iron in the Gulf of Alaska impacted by the position of the Aleutian Low. *Geophysical Research Letters*, 44, pp.5053-5061.

Selby, M.J., 1974. Dominant geomorphic events in landform evolution. *Bulletin of Engineering Geology and the Environment*, 9(1), pp.85-89.

Serreze, M.C., Carse, F., Barry, R.G. and Rogers, J.C., 1997. Icelandic low cyclone activity: Climatological features, linkages with the NAO, and relationships with recent changes in the Northern Hemisphere circulation. *Journal of Climate*, 10(3), pp.453-464.

Serreze, M.C. and Hurst, C.M., 2000. Representation of mean Arctic precipitation from NCEP–NCAR and ERA reanalyses. *Journal of Climate*, 13(1), pp.182-201.

Shao, Y., 2001. A model for mineral dust emission. *Journal of Geophysical Research: Atmospheres*, 106(D17), pp.20239-20254.

Shao, Y., 2004. Simplification of a dust emission scheme and comparison with data. *Journal of Geophysical Research: Atmospheres*, 109(D10).

Shao, Y., 2008. *Physics and modelling of wind erosion* (Vol. 37). Springer Science & Business Media.

Shao, Y. and Raupach, M.R., 1992. The overshoot and equilibration of saltation. *Journal of Geophysical Research: Atmospheres*, 97(D18), pp.20559-20564.

Shao, Y., Raupach, M.R. and Findlater, P.A., 1993. Effect of saltation bombardment on the entrainment of dust by wind. *Journal of Geophysical Research: Atmospheres*, 98(D7), pp.12719-12726.

Shao, Y. and Lu, H., 2000. A simple expression for wind erosion threshold friction velocity. *Journal of Geophysical Research: Atmospheres*, 105(D17), pp.22437-22443.

Shao, Y., Wyrwoll, K.H., Chappell, A., Huang, J., Lin, Z., McTainsh, G.H., Mikami, M., Tanaka, T.Y., Wang, X. and Yoon, S., 2011. Dust cycle: An emerging core theme in Earth system science. *Aeolian Research*, 2(4), pp.181-204.

Sharratt, B., Feng, G. and Wendling, L., 2007. Loss of soil and PM10 from agricultural fields associated with high winds on the Columbia Plateau. *Earth Surface Processes and Landforms*, 32(4), pp.621-630.

Sieberth, T., Wackrow, R. and Chandler, J.H., 2014. Motion blur disturbs—the influence of motion-blurred images in photogrammetry. *The Photogrammetric Record*, 29(148), pp.434-453.

Singer, A., Zobeck, T., Poberezsky, L. and Argaman, E., 2003. The PM10 and PM2.5 dust generation potential of soils/sediments in the Southern Aral Sea Basin, Uzbekistan. *Journal of Arid Environments*, 54(4), pp.705-728.

Skiles, S.M., Painter, T.H., Deems, J.S., Bryant, A.C. and Landry, C.C., 2012. Dust radiative forcing in snow of the Upper Colorado River Basin: 2. Interannual variability in radiative forcing and snowmelt rates. *Water Resources Research*, 48(7).

Smalley, I.J., 1966. The properties of glacial loess and the formation of loess deposits. *Journal of Sedimentary Research*, 36(3).

Smalley, I., 1995. Making the material: the formation of silt sized primary mineral particles for loess deposits. *Quaternary Science Reviews*, 14(7-8), pp.645-651.

Smalley, I.J. and Glendinning, S., 1991. Two distinct particle types in the Lanzhou loess. *Naturwissenschaften*, 78(4), pp.167-167.

Smalley, I.J., Jefferson, I.F., Dijkstra, T.A. and Derbyshire, E., 2001. Some major events in the development of the scientific study of loess. *Earth-Science Reviews*, 54(1), pp.5-18.

Smalley, I.J. and Vita-Finzi, C., 1968. The formation of fine particles in sandy deserts and the nature of 'desert' loess. *Journal of Sedimentary Research*, 38(3).

Smith, B.J., Wright, J.S. and Whalley, W.B., 1991. Simulated aeolian abrasion of Pannonian sands and its implications for the origins of Hungarian loess. *Earth Surface Processes and Landforms*, 16(8), pp.745-752.

Smith, B.J., Wright, J.S. and Whalley, W.B., 2002. Sources of non-glacial, loess-size quartz silt and the origins of "desert loess". *Earth-Science Reviews*, 59(1), pp.1-26.

Sokolik, I.N. and Toon, O.B., 1996. Direct radiative forcing by anthropogenic airborne mineral aerosols. *Nature*, 381(6584), pp.681-683.

Stein, A.F., Draxler, R.R., Rolph, G.D., Stunder, B.J., Cohen, M.D. and Ngan, F., 2015. NOAA's HYSPLIT atmospheric transport and dispersion modeling system. *Bulletin of the American Meteorological Society*, 96(12), pp.2059-2077.

Stockton, P.H. and Gillette, D.A., 1990. Field measurement of the sheltering effect of vegetation on erodible land surfaces. *Land Degradation & Development*, 2(2), pp.77-85.

Stohl, A., Wotawa, G., Seibert, P. and Kromp-Kolb, H., 1995. Interpolation errors in wind fields as a function of spatial and temporal resolution and their impact on different types of kinematic trajectories. *Journal of Applied Meteorology*, 34(10), pp.2149-2165.

Stohl, A., 1998. Evaluation of trajectories calculated from ECMWF data against constant volume balloon flights during ETEX. *Atmospheric Environment*, 32(24), pp.4151-4156.

Stott, T.A. and Grove, J.R., 2001. Short-term discharge and suspended sediment fluctuations in the proglacial Skeldal River, north-east Greenland. *Hydrological Processes*, 15(3), pp.407-423.

Stout, J.E., Warren, A. and Gill, T.E., 2009. Publication trends in aeolian research: An analysis of the Bibliography of Aeolian Research. *Geomorphology*, 105(1), pp.6-17.

Stout, J.E., 2001. Dust and environment in the southern high plains of North America. *Journal of Arid Environments*, 47(4), pp.425-441.

Stout, J.E., 2010. Diurnal patterns of blowing sand. *Earth Surface Processes and Landforms*, 35(3), pp.314-318.

Stout, J.E., 2015. Diurnal patterns of blowing dust on the Llano Estacado. *Journal of Arid Environments*, 122, pp.85-92

Stow, D.A., Hope, A., McGuire, D., Verbyla, D., Gamon, J., Huemmrich, F., Houston, S., Racine, C., Sturm, M., Tape, K. and Hinzman, L., 2004. Remote sensing of vegetation and land-cover change in Arctic Tundra Ecosystems. *Remote sensing of environment*, 89(3), pp.281-308.

Strong, C.L., Bullard, J.E., Dubois, C., McTainsh, G.H. and Baddock, M.C., 2010. Impact of wildfire on interdune ecology and sediments: An example from the Simpson Desert, Australia. *Journal of Arid Environments*, 74(11), pp.1577-1581.

Sturm, M., Racine, C. and Tape, K., 2001. Climate change: increasing shrub abundance in the Arctic. *Nature*, 411(6837), pp.546-547.

Sugden, D.E., McCulloch, R.D., Bory, A.J.M. and Hein, A.S., 2009. Influence of Patagonian glaciers on Antarctic dust deposition during the last glacial period. *Nature Geoscience*, 2(4), pp.281-285.

Sutton, S.L.F. and McKenna Neuman, C., 2008. Sediment entrainment to the lee of roughness elements: effects of vortical structures. *Journal of Geophysical Research: Earth Surface*, 113(F2).

Sweeney, M., Etyemezian, V., Macpherson, T., Nickling, W., Gillies, J., Nikolich, G. and McDonald, E., 2008. Comparison of PI-SWERL with dust emission measurements from a straight-line field wind tunnel. *Journal of Geophysical Research: Earth Surface*, 113(F1).

Swift, D.A., Nienow, P.W. and Hoey, T.B., 2005. Basal sediment evacuation by subglacial meltwater: suspended sediment transport from Haut Glacier d'Arolla, Switzerland. *Earth Surface Processes and Landforms*, 30(7), pp.867-883.

Takamura, T., Sasano, Y. and Hayasaka, T., 1994. Tropospheric aerosol optical properties derived from lidar, sun photometer, and optical particle counter measurements. *Applied Optics*, 33(30), pp.7132-7140.

Takemura, T., Okamoto, H., Maruyama, Y., Numaguti, A., Higurashi, A. and Nakajima, T., 2000. Global three-dimensional simulation of aerosol optical thickness distribution of various origins. *Journal of Geophysical Research: Atmospheres*, 105(D14), pp.17853-17873.

Tarr, R.S. and Martin, L., 1913. Glacial deposits of the continental type in Alaska. *The Journal of Geology*, 21(4), pp.289-300.

Tegen, I., 2003. Modeling the mineral dust aerosol cycle in the climate system. *Quaternary Science Reviews*, 22(18), pp.1821-1834.

Tegen, I. and Lacis, A.A., 1996. Modeling of particle size distribution and its influence on the radiative properties of mineral dust aerosol. *Journal of Geophysical Research: Atmospheres*, 101(D14), pp.19237-19244.

Tegen, I., Lacis, A.A. and Fung, I., 1996. The influence on climate forcing of mineral aerosols from disturbed soils. *Nature*, 380(6573), pp.419-422.

Tegen, I., Harrison, S.P., Kohfeld, K., Prentice, I.C., Coe, M. and Heimann, M., 2002. Impact of vegetation and preferential source areas on global dust aerosol: Results from a model study. *Journal of Geophysical Research: Atmospheres*, 107(D21).

Tegen, I., Werner, M., Harrison, S.P. and Kohfeld, K.E., 2004. Relative importance of climate and land use in determining present and future global soil dust emission. *Geophysical Research Letters*, 31(5).

Thomas, D.S.G., 1987. Discrimination of depositional environments using sedimentary characteristics in the Mega Kalahari, central southern Africa. *Geological Society, London, Special Publications*, 35(1), pp.293-306.

Thorarinsdottir, E.F. and Arnalds, O., 2012. Wind erosion of volcanic materials in the Hekla area, South Iceland. *Aeolian Research*, 4, pp.39-50.

Thorsteinsson, T., Gísladóttir, G., Bullard, J. and McTainsh, G., 2011. Dust storm contributions to airborne particulate matter in Reykjavík, Iceland. *Atmospheric environment*, 45(32), pp.5924-5933.

Thorsteinsson, T., Jóhannsson, T., Stohl, A. and Kristiansen, N.I., 2012. High levels of particulate matter in Iceland due to direct ash emissions by the Eyjafjallajökull eruption and resuspension of deposited ash. *Journal of Geophysical Research: Solid Earth*, 117(B9).

Tonkin, T.N., Midgley, N.G., Graham, D.J. and Labadz, J.C., 2014. The potential of small unmanned aircraft systems and structure-from-motion for topographic surveys: A test of emerging integrated approaches at Cwm Idwal, North Wales. *Geomorphology*, 226, pp.35-43.

Torres, O., Bhartia, P.K., Herman, J.R., Ahmad, Z. and Gleason, J., 1998. Derivation of aerosol properties from satellite measurements of backscattered ultraviolet radiation: Theoretical basis. *Journal of Geophysical Research: Atmospheres*, 103(D14), pp.17099-17110.

Tozer, P. and Leys, J., 2013. Dust storms—what do they really cost? *The Rangeland Journal*, 35(2), pp.131-142.

Tsoar, H. and Pye, K., 1987. Dust transport and the question of desert loess formation. *Sedimentology*, 34(1), pp.139-153.

Tuck, R., 1938. The loess of the Matanuska valley, Alaska. *The Journal of Geology*, 46(4), pp.647-653.

Turner, D., Lucieer, A. and Wallace, L., 2014. Direct georeferencing of ultrahigh-resolution UAV imagery. *IEEE Transactions on Geoscience and Remote Sensing*, 52(5), pp.2738-2745.

Tweed, F.S. and Russell, A.J., 1999. Controls on the formation and sudden drainage of glacier-impounded lakes: implications for jökulhlaup characteristics. *Progress in Physical Geography*, 23(1), pp.79-110.

van der Does, M., Korte, L.F., Munday, C.I., Brummer, G.J.A. and Stuut, J.B.W., 2016. Particle size traces modern Saharan dust transport and deposition across the equatorial North Atlantic. *Atmospheric Chemistry and Physics*, 16(21), p.13697.

Vos, K., Vandenberghe, N. and Elsen, J., 2014. Surface textural analysis of quartz grains by scanning electron microscopy (SEM): From sample preparation to environmental interpretation. *Earth-Science Reviews*, 128, pp.93-104.

Wackrow, R. and Chandler, J.H., 2008. A convergent image configuration for DEM extraction that minimises the systematic effects caused by an inaccurate lens model. *The Photogrammetric Record*, 23(121), pp.6-18.

Wackrow, R. and Chandler, J.H., 2011. Minimising systematic error surfaces in digital elevation models using oblique convergent imagery. *The Photogrammetric Record*, 26(133), pp.16-31.

Wainwright, J., Parsons, A.J., Cooper, J.R., Gao, P., Gillies, J.A., Mao, L., Orford, J.D. and Knight, P.G., 2015. The concept of transport capacity in geomorphology. *Reviews of Geophysics*, 53(4), pp.1155-1202.

Waller, R.I., 2001. The influence of basal processes on the dynamic behaviour of cold-based glaciers. *Quaternary International*, 86(1), pp.117-128.

Walvoord, M.A. and Striegl, R.G., 2007. Increased groundwater to stream discharge from permafrost thawing in the Yukon River basin: Potential impacts on lateral export of carbon and nitrogen. *Geophysical Research Letters*, 34(12).

Wang, Y., Stein, A.F., Draxler, R.R., Jesús, D. and Zhang, X., 2011. Global sand and dust storms in 2008: Observation and HYSPLIT model verification. *Atmospheric Environment*, 45(35), pp.6368-6381.

Warren, A., Chappell, A., Todd, M.C., Bristow, C., Drake, N., Engelstaedter, S., Martins, V., M'bainayel, S. and Washington, R., 2007. Dust-raising in the dustiest place on earth. *Geomorphology*, 92(1), pp.25-37.

Washington, R., Todd, M., Middleton, N.J. and Goudie, A.S., 2003. Dust-storm source areas determined by the total ozone monitoring spectrometer and surface observations. *Annals of the Association of American Geographers*, 93(2), pp.297-313.

Webb, N.P., Okin, G.S. and Brown, S., 2014. The effect of roughness elements on wind erosion: The importance of surface shear stress distribution. *Journal of Geophysical Research: Atmospheres*, 119(10), pp.6066-6084.

Webb, N.P., Herrick, J.E., Van Zee, J.W., Courtright, E.M., Hugenholtz, C.H., Zobeck, T.M., Okin, G.S., Barchyn, T.E., Billings, B.J., Boyd, R. and Clingan, S.D., 2016. The National Wind Erosion Research Network: Building a standardized long-term data resource for aeolian research, modelling and land management. *Aeolian Research*, 22, pp.23-36.

Weber, M.E., Kuhn, G., Sprenk, D., Rolf, C., Ohlwein, C. and Ricken, W., 2012. Dust transport from Patagonia to Antarctica—a new stratigraphic approach from the Scotia Sea and its implications for the last glacial cycle. *Quaternary Science Reviews*, 36, pp.177-188.

Wentworth, C.K., 1922. A scale of grade and class terms for clastic sediments. *The Journal of Geology*, 30(5), pp.377-392.

Werner, M., Tegen, I., Harrison, S.P., Kohfeld, K.E., Prentice, I.C., Balkanski, Y., Rodhe, H. and Roelandt, C., 2002. Seasonal and interannual variability of the mineral dust cycle under present and glacial climate conditions. *Journal of Geophysical Research: Atmospheres*, 107(D24).

Westoby, M.J., Dunning, S.A., Woodward, J., Hein, A.S., Marrero, S.M., Winter, K. and Sugden, D.E., 2015. Sedimentological characterization of Antarctic moraines using UAVs and Structure-from-Motion photogrammetry. *Journal of Glaciology*, 61(230), pp.1088-1102.

Whalley, W.B., Smith, B.J., McAlister, J.J. and Edwards, A.J., 1987. Aeolian abrasion of quartz particles and the production of silt-size fragments: preliminary results. *Geological Society, London, Special Publications*, 35(1), pp.129-138.

Wick, P., Malek, A., Manser, P., Meili, D., Maeder-Althaus, X., Diener, L., Diener, P.A., Zisch, A., Krug, H.F. and von Mandach, U., 2010. Barrier capacity of human placenta for nanosized materials. *Environmental health perspectives*, 118(3), p.432.

Wiggs, G.F.S., Livingstone, I., Thomas, D.S.G. and Bullard, J.E., 1994. Effect of vegetation removal on airflow patterns and dune dynamics in the southwest Kalahari Desert. *Land Degradation & Development*, 5(1), pp.13-24.

Wiggs, G.F.S., Baird, A.J. and Atherton, R.J., 2004. The dynamic effects of moisture on the entrainment and transport of sand by wind. *Geomorphology*, 59(1), pp.13-30.

Winker, D.M., Vaughan, M.A., Omar, A., Hu, Y., Powell, K.A., Liu, Z., Hunt, W.H. and Young, S.A., 2009. Overview of the CALIPSO mission and CALIOP data processing algorithms. *Journal of Atmospheric and Oceanic Technology*, 26(11), pp.2310-2323.

Winterbottom, S.J. and Gilvear, D.J., 1997. Quantification of channel bed morphology in gravel-bed rivers using airborne multispectral imagery and aerial photography. *River Research and Applications*, 13(6), pp.489-499.

Winker, D.M., Pelon, J. and McCormick, M.P., 2003, March. The CALIPSO mission: Spaceborne lidar for observation of aerosols and clouds. In *Proc. Spie* (Vol. 4893, No. 1, pp. 1-11).

Wittmann, M., Zwaafink, C.D.G., Schmidt, L.S., Guðmundsson, S., Pálsson, F., Arnalds, O., Björnsson, H., Thorsteinsson, T. and Stohl, A., 2017. Impact of dust deposition on the albedo of Vatnajökull ice cap, Iceland. *The Cryosphere*, 11(2), p.741.

Wolfe, S.A. and Nickling, W.G., 1993. The protective role of sparse vegetation in wind erosion. *Progress in physical geography*, 17(1), pp.50-68.

Wolfe, S.A. and Nickling, W.G., 1996. Shear stress partitioning in sparsely vegetated desert canopies. *Earth Surface Processes and Landforms*, 21(7), pp.607-619.

Wolfe, S.A., 2013. Cold-climate aeolian environments. *Treatise on Geomorphology*, 11, pp.375-394.

Wolff, E.W., Fischer, H., Fundel, F., Ruth, U., Twarloh, B., Littot, G.C., Mulvaney, R., Röthlisberger, R., De Angelis, M., Boutron, C.F. and Hansson, M., 2006. Southern Ocean sea-ice extent, productivity and iron flux over the past eight glacial cycles. *Nature*, 440(7083), pp.491-496.

Woodget, A.S., Fyffe, C. and Carbonneau, P.E., 2017. From manned to unmanned aircraft: Adapting airborne particle size mapping methodologies to the characteristics of sUAS and SfM. *Earth Surface Processes and Landforms*.

Woodward, S., Roberts, D.L. and Betts, R.A., 2005. A simulation of the effect of climate change–induced desertification on mineral dust aerosol. *Geophysical Research Letters*, 32(18).

Wopfner, H. and Twidale, C.R., 1988. Formation and age of desert dunes in the Lake Eyre depocenters in central Australia. *Geologische Rundschau*, 77(3), pp.815-834.

Wopfner, H. and Twidale, C.R., 2001. Australian desert dunes: wind rift or depositional origin? *Australian Journal of Earth Sciences*, 48(2), pp.239-244.

Wright, J.S., 1993. Non-glacial origins of loess-sized quartz silt (Doctoral dissertation, Queen's University of Belfast).

Wright, J.S., 1995. Glacial comminution of quartz sand grains and the production of loessic silt: a simulation study. *Quaternary Science Reviews*, 14(7), pp.669-680.

Wright, J., 2001. Making loess-sized quartz silt: data from laboratory simulations and implications for sediment transport pathways and the formation of desert loess deposits associated with the Sahara. *Quaternary International*, 76, pp.7-19.

Wright, J., Smith, B. and Whalley, B., 1998. Mechanisms of loess-sized quartz silt production and their relative effectiveness: laboratory simulations. *Geomorphology*, 23(1), pp.15-34.

Xuan, J., Sokolik, I.N., Hao, J., Guo, F., Mao, H. and Yang, G., 2004. Identification and characterization of sources of atmospheric mineral dust in East Asia. *Atmospheric Environment*, 38(36), pp.6239-6252.

Yoshioka, M., Mahowald, N.M., Conley, A.J., Collins, W.D., Fillmore, D.W., Zender, C.S. and Coleman, D.B., 2007. Impact of desert dust radiative forcing on Sahel precipitation: Relative importance of dust compared to sea surface temperature variations, vegetation changes, and greenhouse gas warming. *Journal of Climate*, 20(8), pp.1445-1467.

Zdanowicz, C.M., Zielinski, G.A., Wake, C.P., Fisher, D.A. and Koerner, R.M., 2000. A Holocene record of atmospheric dust deposition on the Penny Ice Cap, Baffin Island, Canada. *Quaternary Research*, 53(1), pp.62-69.

Zender, C.S., Miller, R.L.R.L. and Tegen, I., 2004. Quantifying mineral dust mass budgets: Terminology, constraints, and current estimates. *Eos, Transactions American Geophysical Union*, 85(48), pp.509-512.

Zender, C.S. and Kwon, E.Y., 2005. Regional contrasts in dust emission responses to climate. *Journal of Geophysical Research: Atmospheres*, 110(D13).

Zhang, X.Y., Arimoto, R. and An, Z.S., 1999. Glacial and interglacial patterns for Asian dust transport. *Quaternary Science Reviews*, 18(6), pp.811-819.

Zobeck, T.M., Gill, T.E. and Popham, T.W., 1999. A two-parameter Weibull function to describe airborne dust particle size distributions. *Earth Surface Processes and Landforms*, 24(10), pp.943-955.

Zobeck, T.M., Sterk, G., Funk, R., Rajot, J.L., Stout, J.E. and Van Pelt, R.S., 2003. Measurement and data analysis methods for field-scale wind erosion studies and model validation. *Earth Surface Processes and Landforms*, 28(11), pp.1163-1188.

Zou, X.Y., Wang, Z.L., Hao, Q.Z., Zhang, C.L., Liu, Y.Z. and Dong, G.R., 2001. The distribution of velocity and energy of saltating sand grains in a wind tunnel. *Geomorphology*, 36(3), pp.155-165.